NON-CARBOCYCLIC LIGANDS IN ORGANOTHORIUM CHEMISTRY

RIGID NON-CARBOCYCLIC ANCILLARY LIGANDS

IN

ORGANOTHORIUM CHEMISTRY

By

CARLOS A. CRUZ, B.Sc.

A Thesis

Submitted to the School of Graduate Studies

in Partial Fulfillment of the Requirements

for the Degree

Doctor of Philosophy

McMaster University

DOCTOR OF PHILOSOPHY (2010)
(Chemistry)

McMaster University
Hamilton, Ontario

TITLE: Rigid Non-Carbocyclic Ancillary Ligands in Organothorium Chemistry

AUTHOR: Carlos A. Cruz, B.Sc. (McMaster University)

SUPERVISOR: Dr. David J. H. Emslie

NUMBER OF PAGES: xxxii, 239

Abstract

A new rigid, dianionic ligand, 4,5-bis(2,6-diisopropylanilido)-2,7-di-*tert*-butyl-9,9-dimethylxanthene {[XA_2]}, has been designed for use in the chemistry of the actinides. Pro-ligand $H_2[XA_2]$ (**1**) was synthesized by the Hartwig-Buchwald coupling of 4,5-dibromo-2,7-di-*tert*-butyl-9,9-dimethylxanthene with 2,6-diisopropylaniline.

Stable alkali metal salts of the [XA_2] ligand, $K_2(dme)_2[XA_2]$ (**2**) and $Na_2[XA_2]$ (**3**), were accessible by deprotonation of $H_2[XA_2]$ with KH or NaH in dme or toluene, respectively. The thermally unstable lithium salt of McConville's 2,6-bis(2,6-diisopropylanilidomethyl)pyridine {Li_2[BDPP], **4**} was isolated by deprotonation of pro-ligand H_2[BDPP] with *n*BuLi or $LiCH_2SiMe_3$ in hexanes at low temperature. Reaction of $[ThCl_4(dme)_2]$ with Li_2[BDPP] or $M_2(dme)_n[XA_2]$ (M = K, n = 2; M = Na, n = 0) resulted in the formation of pentagonal bipyramidal $[LThCl_2(dme)]$ complexes {L = [BDPP], **5**; [XA_2], **6**}. Subsequent reaction of the dichloride complexes with $LiCH_2SiMe_3$ gave base- and salt-free dialkyl complexes $[LTh(CH_2SiMe_3)_2]$ {L = [BDPP], **9**; [XA_2], **10**}, which are stable for days in solution at 90 and 70 °C, respectively. Reaction of **5** with $LiNEt_2$ or **10** with H_2NPh provided $[(BDPP)Th(NEt_2)_2]$ (**11**) and $[(XA_2)Th(NHPh)_2]$ (**28**), respectively.

An alternative route to $[(BDPP)ThCl_2(dme)]$ (**5**) and $[LTh(CH_2SiMe_3)_2]$ (**9** and **10**) involved combination of two or four equivalents of $LiCH_2SiMe_3$ with $[ThCl_4(dme)_2]$, followed by addition of H_2L. These reactions likely proceed by alkane elimination from dialkyl or tetraalkyl thorium intermediates. The solid-state structure of $[(BDPP)Th(CH_2SiMe_3)_2]$ (**9**) suggests the presence of α-agostic C–H–Th interactions for

both alkyl groups. In solution, **9** and **10** exhibit temperature-dependent $^1J_{C\text{-}H}$ coupling constants for Th*C*H_2, consistent with an equilibrium between products participating in α-agostic C–H–Th bonding to a greater or lesser extent, with more agostic products favored at lower temperatures. Reaction of Li_2[BDPP] (**4**) with [(BDPP)$ThCl_2$(dme)] (**5**) at 0 °C, or the reaction of [(BDPP)Th(CH_2SiMe_3)$_2$] (**9**) with H_2[BDPP] at 100 °C resulted in the formation of extremely sterically encumbered [Th(BDPP)$_2$] (**8**), which adopts a highly distorted six-coordinate geometry with the four anilido groups arranged in an approximate tetrahedron around thorium. A bis-ligand complex was not accessible with the [XA_2] ancillary ligand, presumably due to increased ligand rigidity.

Addition of two equivalents of $PhCH_2MgCl$ to [L$ThCl_2$(dme)] yielded solvent-free [LTh(CH_2Ph)$_2$] {L = [XA_2] (**12**) and [BDPP] (**13**)]. The $^1J_{C\text{-}H}$ coupling constants in both complexes {120 and 139 Hz for **12**; 127 and 138 Hz for **13**} are indicative of η^1- and η^2- or η^3-coordinated benzyl ligands in solution; polyhapto benzyl coordination was also observed in the solid state.

Reaction of [L$ThCl_2$(dme)] with two equivalents of *n*BuLi provided highly soluble [LTh(*n*Bu)$_2$] {L = [BDPP] (**14**), [XA_2] (**15**)]. These β-hydrogen-containing compounds are remarkably thermally stable, showing no sign of decomposition after days at 60 and 80 °C, respectively. Combination of [(BDPP)$ThCl_2$(dme)] (**5**) with three equivalents of MeLi yielded the thorium trimethyl 'ate' complex [(BDPP)$ThMe_3${Li(dme)}] (**16**), which underwent thermal decomposition over 3 days at room temperature to produce the metalated complex [(BDPP*)Th(μ-Me)$_2$Li(dme)] (**17**) {BDPP* = 2,6-{$\underline{N}C_5H_3$($CH_3\underline{N}$Ar)($CH_2\underline{N}${C_6H_3*i*Pr($\underline{C}Me_2$)-2,6})}; Ar = 2,6-

diisopropylphenyl; donor atoms in BDPP* are underlined}. Reaction of two equivalents of complex **16** with one equivalent of [(BDPP)$ThCl_2$(dme)] (**5**) yielded the dimethyl complex [(BDPP)$ThMe_2$] (**18**) which decomposes rapidly at room temperature to form a mixture of unidentified products. Labeling studies using $^{13}CD_3$ groups revealed that thermal decomposition of **16** and **18** occurs via a straightforward σ-bond metathesis pathway.

Reaction of [L$ThCl_2$(dme)] with Grignard reagents {MeMgBr, L = [BDPP]; $PhCH_2MgCl$, L = [XA_2]} resulted, under certain conditions, in halide exhange and adduct formation as evidenced by the solid state structure of [{Th(BDPP)Br(μ-Br)$_2$Mg(μ-Me)(OEt_2)}$_2$] (**19**), or ancillary ligand transfer to magnesium to produce [(XA_2)Mg(dme)] (**20**). Complex **19** provides insight into the type of intermediates likely involved in undesired halide exchange reactions between d- or f-element halide complexes and Grignard reagents.

Reaction of [(XA_2)Th(CH_2Ph)$_2$] (**12**) with either one or two equivalents of $B(C_6F_5)_3$ afforded the first non-carbocyclic actinide alkyl cation, [(XA_2)Th(CH_2Ph)][$PhCH_2B(C_6F_5)_3$] (**21**), and a rare example of an actinide dication, [(XA_2)Th][$PhCH_2B(C_6F_5)_3$]$_2$ (**27**). In both **21** and **27** the $PhCH_2B(C_6F_5)_3^-$ anion is η^6-coordinated to thorium. Reaction of neutral dialkyl complex [(XA_2)Th(CH_2SiMe_3)$_2$] (**9**) with [Ph_3C][$B(C_6F_5)_4$] in benzene or toluene at room temperature resulted in the formation of [(XA_2)Th(CH_2SiMe_3)(η^6-arene)][$B(C_6F_5)_4$] (arene = C_6H_6, **22**; arene = C_7H_8, **23**). These complexes were characterized in solution by NMR spectroscopy (**21**, **22** and **23**) and/or in the solid state by X-ray crystallography (**22** and **27**). In close

analogy, $[(XA_2)Th(CH_2Ph)_2]$ (**12**) reacted with $[Ph_3C][B(C_6F_5)_4]$ in toluene at room temperature to form $[(XA_2)Th(\eta^2\text{-}CH_2Ph)(\eta^6\text{-}C_7H_8)][B(C_6F_5)_4]$ (**24**). In contrast, related $[(BDPP)Th(CH_2Ph)_2]$ (**13**) reacted with $[Ph_3C][B(C_6F_5)_4]$ to precipitate a mixture of mononuclear and a dinuclear cations; the dinuclear cation was identified as $[(BDPP)Th(\eta^2\text{-}CH_2Ph)(\mu\text{-}\eta^1\text{:}\eta^6\text{-}CH_2Ph)Th(\eta^1\text{-}CH_2Ph)(BDPP)][B(C_6F_5)_4]$ (**25**) by X-ray crystallography. Complexes **22**, **23**, and **24** are rare examples of arene solvent-separated ion pairs, while complex **21** exists as a tight contact ion pair, and dinuclear **25** exhibits a unique benzyl ligand bridging mode. Cations **21** - **25** and **27** highlight a pronounced tendency for these systems to engage in arene π-coordination.

Preliminary reaction studies with both neutral and cationic thorium complexes supported by the [BDPP] and $[XA_2]$ ancillary ligands demonstrated significant activity for olefin polymerization and hydroamination catalysis. Reactions of **9** and **10** with 4 atm. of hydrogen also suggest that the [BDPP] and $[XA_2]$ ligand frameworks may be suitable for the stabilization of thorium hydride complexes.

Acknowledgements

I would like to express my deepest gratitude to my supervisor, Dr. David J. H. Emslie for sharing with me his scientific knowledge and experience, and for providing an outstanding scientific environment in which I could mature as a chemist. I have always found his ability to constantly infect students with his enthusiasm for chemistry fascinating, and exposure to him over the course of this degree has heightened my appreciation for science. His scientific ingenuity, integrity and efficiency have been an inspiration. I feel priviledged to have had the chance to work with him, and to be a graduate from his laboratory. This thesis would not have been possible without you boss. Thank you.

I owe a debt of gratitude to Dr. Jason Traer for helping me keep in both physical and mental shape during the course of my graduate career, and to both him and Simon Oakley for their continual friendship and support throughout the years.

I would also like to thank the many people I have had the pleasure of working with in the Emslie lab over the years, especially: Dr. Bala Vidjayacoumar, Dr. Sougandi Ilango, Brad Cowie, Kelly Motolko, Kris Kolpin, Terry Chu, Jordan Thompson, Matthew Ray, Kyle Parker, Rachelle Kleinberger and Natalie Huk.

I thank Drs. Gary Schrobilgen and Ignacio Vargas-Baca for their invaluable input and suggestions throughout the course of this research, as well as countless reference letters sent on my behalf. My gratitude is also extended to Drs. William Evans, Jack Rosenfeld and Mark Hatton for being members of my Candidacy Committee.

This work was supported directly and indirectly by the help of the superb support staff at the McMaster University Chemistry Department. Special thanks go to Mrs. Lynda Fraser, Mrs. Karen Neumann, Mrs. Angela Vanderlaan, Mrs. Tammy Feher, Ms. Christine Cosgrove, and Ms. Connie Carrabs for their assistance throughout the years. I thank Drs. James Britten, Laura Harrington, Craig Robertson and Hilary Jenkins for their expertise in X-ray crystallography, Drs. Donald Hughes and Bob Berno for their assistance with NMR spectroscopy and Dr. Steve Kornic for help with elemental analysis.

I would like to thank McMaster University, the Department of Chemistry, the Natural Sciences and Engineering Research Council of Canada and the Government of Ontario for their generous financial support in the form of teaching assistanships and numerous scholarships awarded to me throughout my graduate career.

Finally I would like express my profound gratitude to my parents, Carlos and Carmen Cruz, my sister, Carmen, my aunts Ana Maria and Mercedes, and my wife Grace for their unwavering support throughout the years. Your love is the cornerstone upon which everything I do is built upon, and one of the few non-scientific constants in my universe.

I dedicate the following to my loving wife Grace, without whose infallible love and support none of this would have been possible.

Table of Contents

List of Compounds

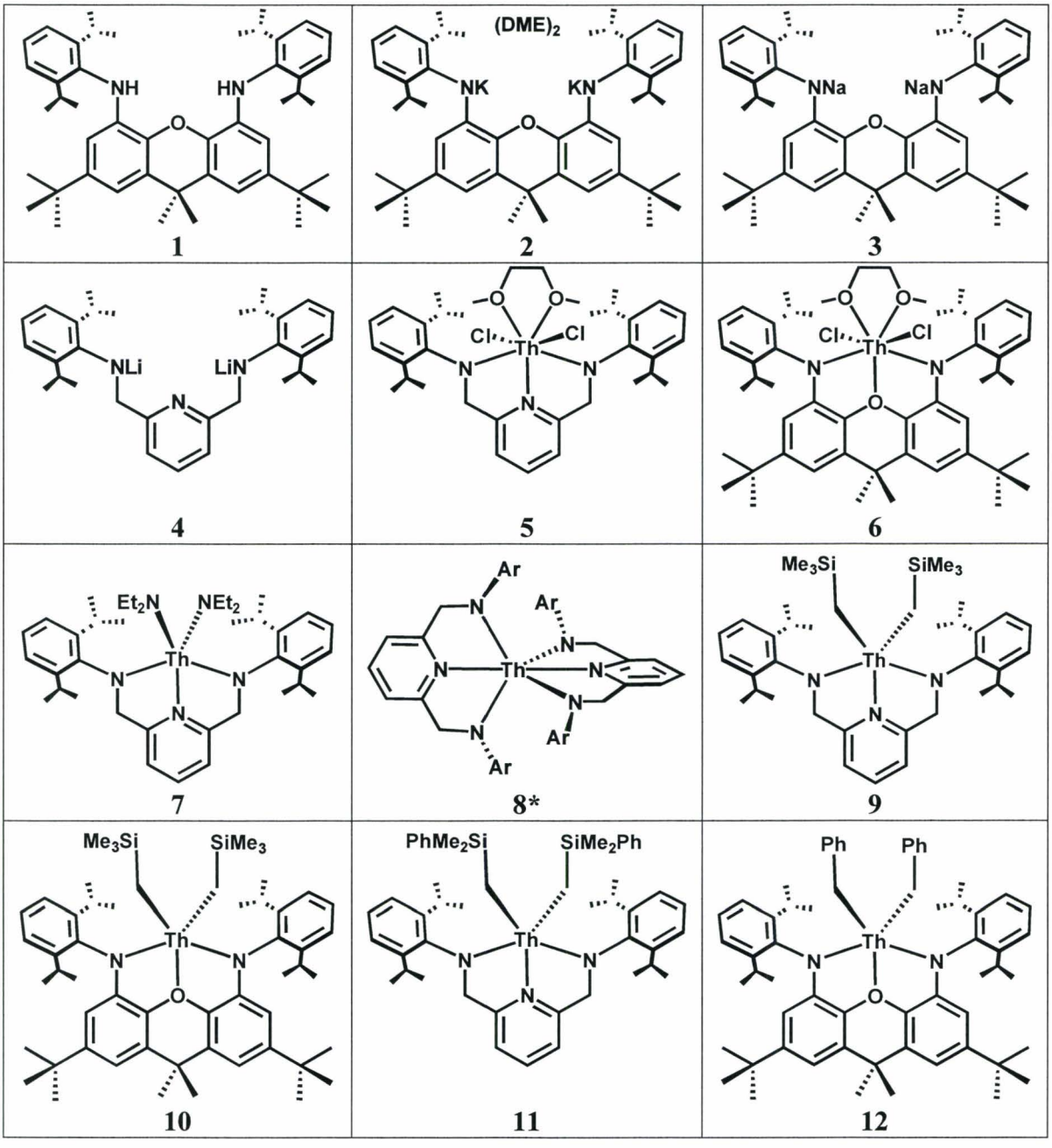

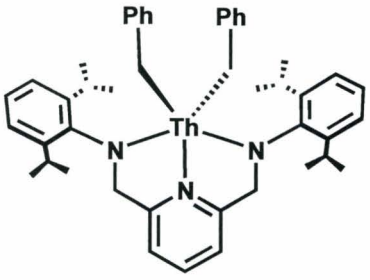

13

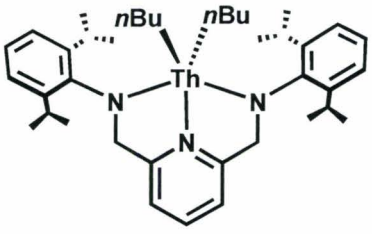

14

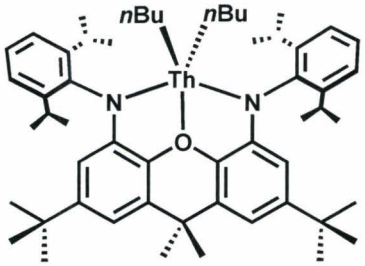

15

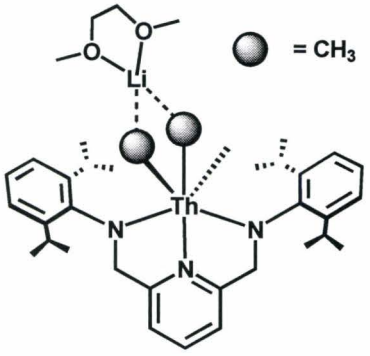

16

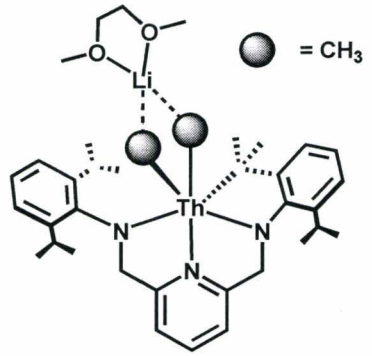

17

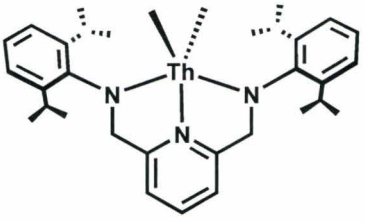

18

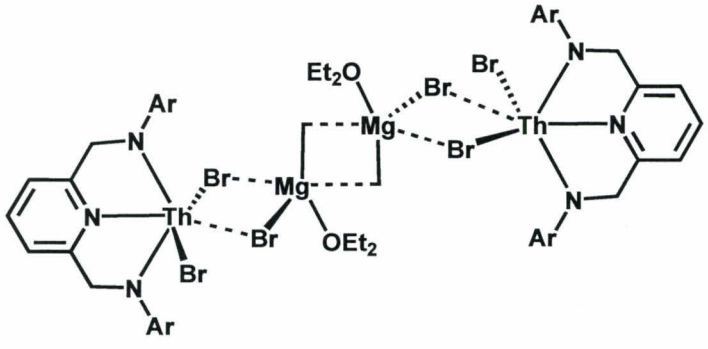

19*

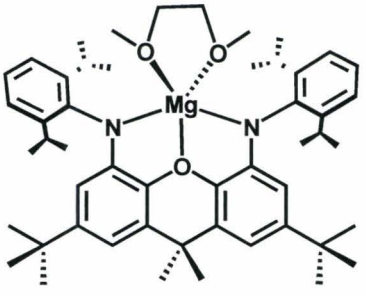

20

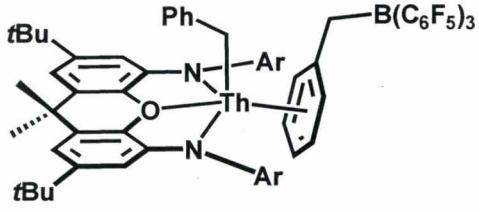

21*

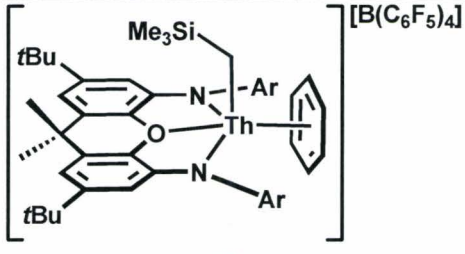

22*

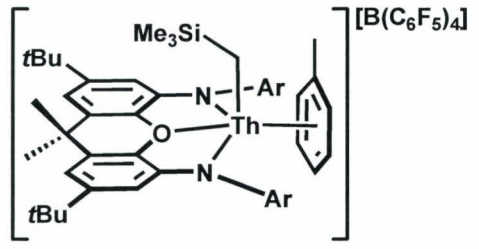

23*

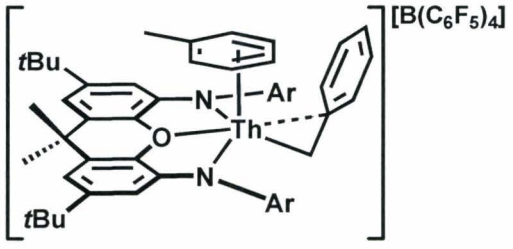

24*

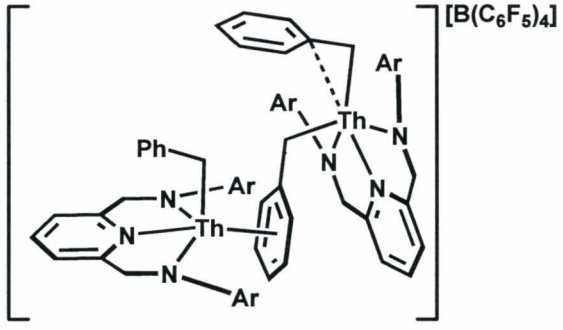

25*

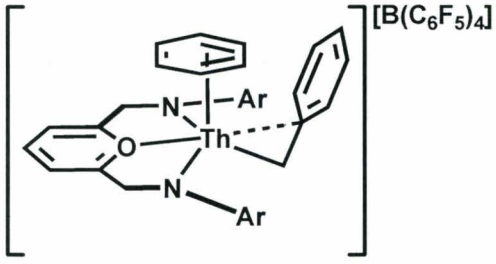

26*

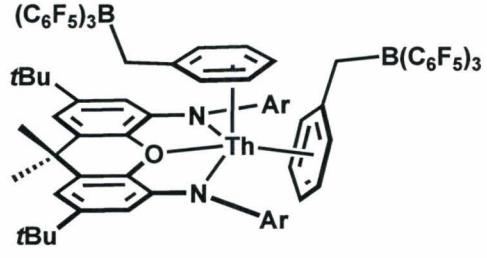

27*

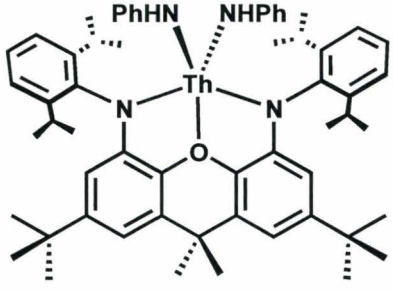

28

*Ar = 2,6-diisopropylphenyl

List of Tables

List of Figures

List of Schemes

List of Abbreviations and Symbols

Å	Angstrom
An	actinide
Anal. Calcd.	calculated (elemental) analysis
Ar	aryl
br	broad
Bz	benzyl
C	Celcius
COSY	correlation spectroscopy
Cp	cyclopentadienyl
Cp*	pentamethylcyclopentadienyl
d	doublet
dme	1,2-dimethoxyethane
dmf	dimethylformamide
dmpe	1,2-dimethylphosphinoethane
Et	ethyl
EXSY	exchange spectroscopy
g	gram(s)
h	hour(s)
hmpa	hexamethylphosphoamide
HSQC	heteronuclear single quantum coherence
Hz	hertz

*i*Pr	*iso*propyl
J	symbol for coupling constant
K	Kelvin
Ln	lanthanide
M	molarity (mol L^{-1})
m	multiplet
MAO	methylaluminoxane
Me	methyl
MHz	megahertz
min	minute(s)
mL	milliliter(s)
mmol	millimole(s)
NMR	nuclear magnetic resonance
NOESY	nuclear Overhauser effect spectroscopy
OTf	trifluoromethanesulfonate
Ph	phenyl
ppm	parts per million
py	pyridine
q	quartet
R	alkyl or aryl group (unless otherwise specified)
ROESY	rotating frame Overhauser effect spectroscopy
s	singlet

sept	septet
SSIP	solvent separated ion-pair
t	triplet
*t*Bu	*tertiary* butyl
THF	tetrahydrofuran
tol	toluene
TM	transition metal
Tp	hydrotris(pyrazolyl)borate
UV	ultraviolet
δ	chemical shift (parts per million)
^{o}	degree(s)
$^{1}J_{X\text{-}Y}$	one bond coupling constant between X and Y
$^{2}J_{X\text{-}Y}$	two bond coupling constant between X and Y
$^{3}J_{X\text{-}Y}$	three bond coupling constant between X and Y
1D	one dimensional
2D	two dimensional
$\{^{1}H\}$	proton decoupled
λ	wavelength

Chapter 1:

Introduction

1.1 – General Actinide Introduction

The "actinide" label refers to the fourteen elements that occupy the row of the periodic table in which the 5f shell is filled with electrons (Figure 1.1). Over the past 70 years, the focus of study of these 5f elements has shifted dramatically from the search for stable, volatile compounds for isotopic separation and enrichment via gaseous diffusion, towards the preparation of actinide compounds exhibiting novel structural features and divergent reactivity from their transition metal and lanthanide counterparts. While actinide metals and their complexes have been developed to play a major role in nuclear energy generation, and have been used as heterogeneous catalysts, much of their organometallic chemistry remains largely unexplored.

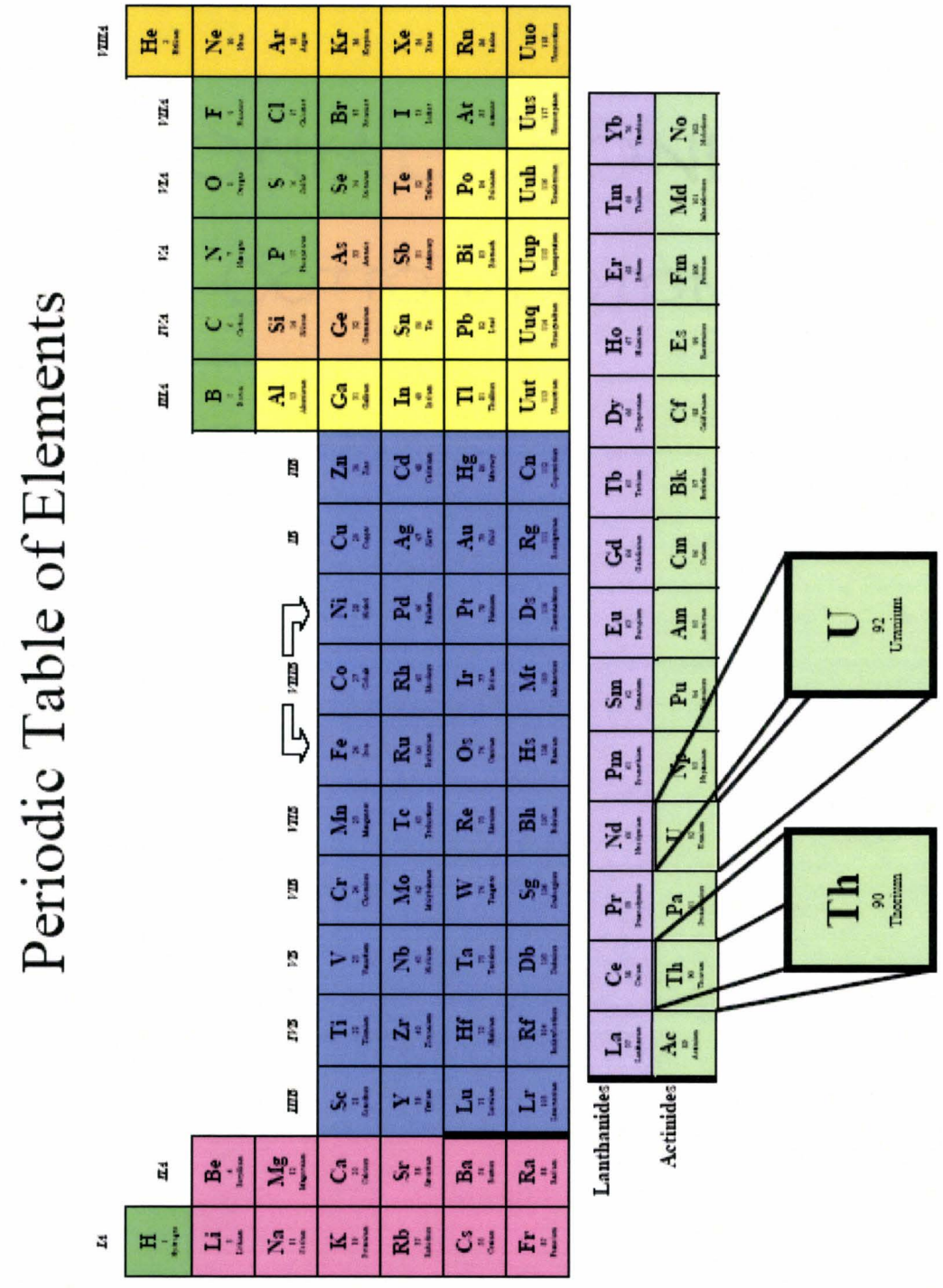

Figure 1.1: Periodic table of the elements highlighting the position of thorium and uranium.

1.1.1 – Thorium and Uranium Natural Abundance and Regulations

Of the fourteen 5f elements, only thorium, protactinium and uranium are naturally occurring.[1] Protactinium is a decay product of ^{235}U (*vide infra*) and as such, is only found in the environment in minute quantities. Uranium was first found in the mineral known as pitchblende, which consists partly of UO_2 (also known as uraninite), and U_3O_8. Aside from pitchblende, uranium is also found in numerous other minerals, such as carnotite, autunite, tobernite, uranophane, studtite and davidite, as well as in phosphate rock and monazite sands. The largest deposits of uranium are found in Canada, New Mexico, Colorado and Utah. In the earth's crust, uranium is present in 2 to 4 parts per million, making it approximately 40 times more abundant than silver, and it can reach levels of up to 11 parts per million in soil.

Thorium is also readily found in the earth's crust. It is three to four times more abundant than uranium, three times as abundant as tin, twice as abundant as arsenic, and nearly as abundant as lead. Unlike uranium, which may be found in two oxidations states (+4 and +6) in nature, thorium occurs almost exclusively in the +4 oxidation state. In nature, thorium occurs in thorite ($ThSiO_4$) and thorianite (ThO_2/UO_2) and is frequently associated with trivalent rare earth elements that have similar ionic radii, as well as U(IV), Zr(IV), Hf(IV) and Ce(IV). The largest deposits of thorium can be found in New England, in the United States.

The large amounts of naturally occurring thorium and uranium on earth and their low radioactivity preclude strict regulations regarding their sale, distribution and use. Thorium and natural abundance uranium are readily available for purchase from chemical

companies as their nitrate or oxide compounds, and research into their coordination and organometallic chemistry may be performed without external regulations or precautions beyond those typically associated with the chemistry of heavy metals.

1.1.2 – Non-Nuclear Applications of Thorium and Uranium

As far back as the time of the Roman Empire, uranium containing compounds had been employed in several trades, for example as colorants for ceramics and glasses.[2] Other non-military applications have included the use of uranium in photographic toner, lamp filaments and as stains for transmission electron microscopy. Aside from nuclear energy generation (*vide infra*), other military applications of uranium have included its use in high density missiles, where alloys containing depleted uranium are used to penetrate heavily armored vehicles. Depleted uranium is also used as a shielding material for transport and storage of radioactive materials.

In contrast to uranium which has been known and utilized widely for centuries, no use was found for thorium until 1885, with the invention of the incandescent gas mantle (99 % ThO_2 / 1 % CeO_2). Thorium metal is also employed as an alloying element with magnesium and to coat tungsten wires used in electronic equipment. However, the majority of the uses of thorium rely on thorium oxide, which is used as a regulator to control the grain-size of tungsten used in electric lamps, in high-quality lenses for cameras and scientific equipment (to impart high refractive index and low dispersion properties), and as a catalyst for petroleum cracking, sulfuric acid production, and the conversion of ammonia to nitric acid.[3]

1.1.3 – Thorium and Uranium Isotopes, Radioactive Decay Series and Uses in Energy Production

Decay series including ^{238}U, ^{235}U and ^{232}Th can be seen in Figures 1.2, 1.3 and 1.4, respectively. Naturally abundant uranium consists of a mixture of three isotopes: ^{238}U, ^{235}U and ^{234}U, with relative natural abundances of 99.27 %, 0.72 % and 0.006 % respectively. The isotope ^{238}U is the parent of ^{234}U by radioactive decay (Figure 1.2), while ^{235}U is of independent origin. The three isotopes of uranium are α-particle emitters. ^{238}U emits α-particles of 4.196 MeV, has a half-life of 4.468 $x10^9$ years and is the longest lived isotope. ^{235}U α-particles are marginally higher in energy at 4.397 MeV, and while the isotope has a shorter half-life than ^{238}U at 7.038 $x10^8$ years, the shortest half-life belongs to ^{234}U, having a half-life of 2.455 x 10^5 years, and emitting the strongest α-particles at 4.777 MeV.

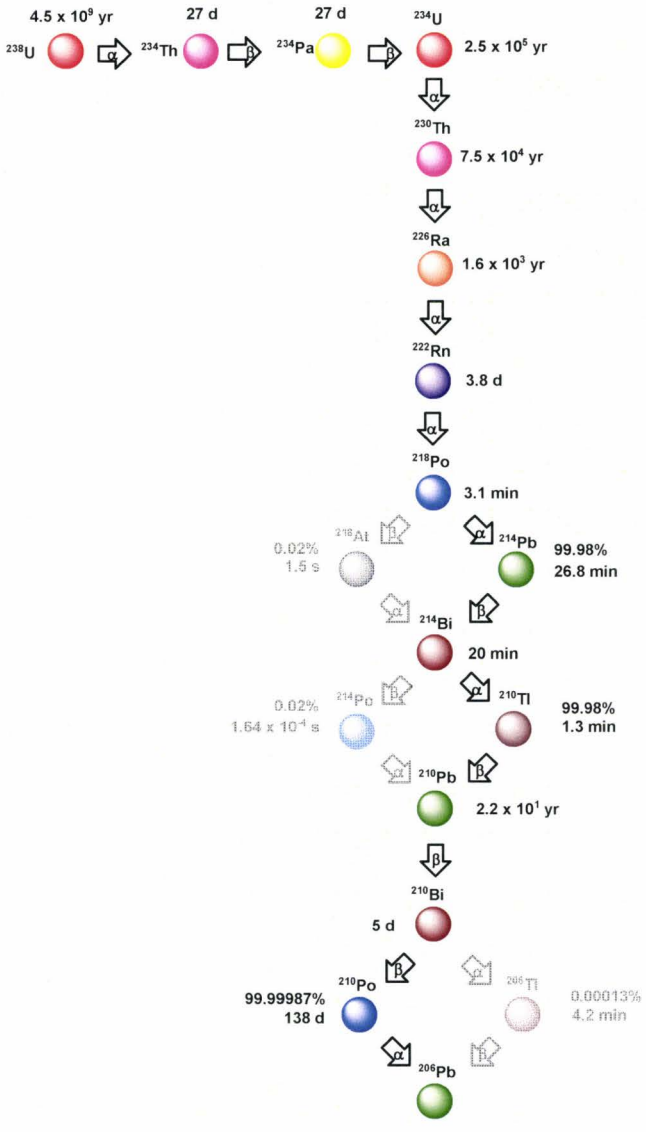

Figure 1.2: Decay series including ^{238}U yielding non-radioactive ^{206}Pb as the final decay product. This series is known as the "Uranium Series" or the "Radium Series."

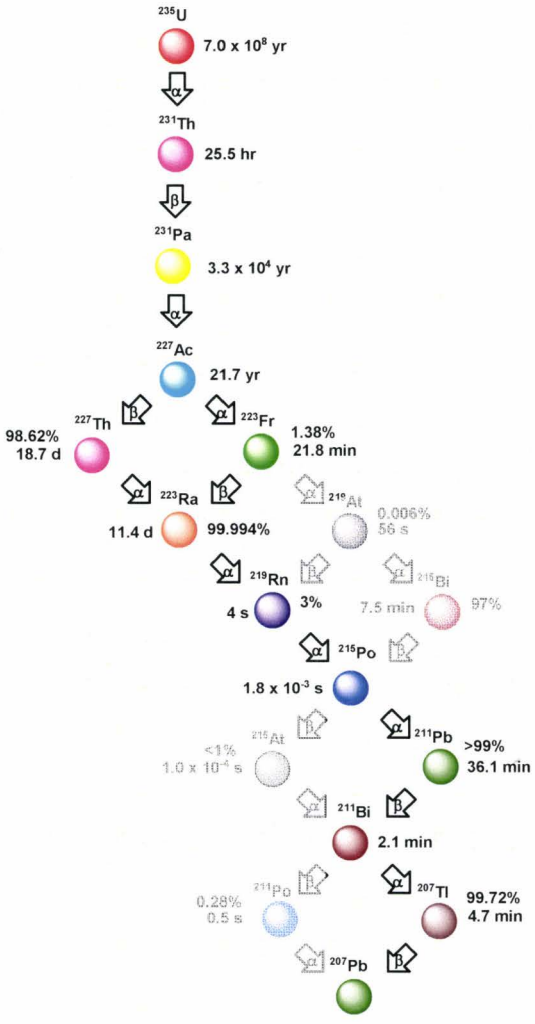

Figure 1.3: Decay series including ^{235}U yielding non-radioactive ^{207}Pb as the final decay product. This series is known as the "Actinium Series."

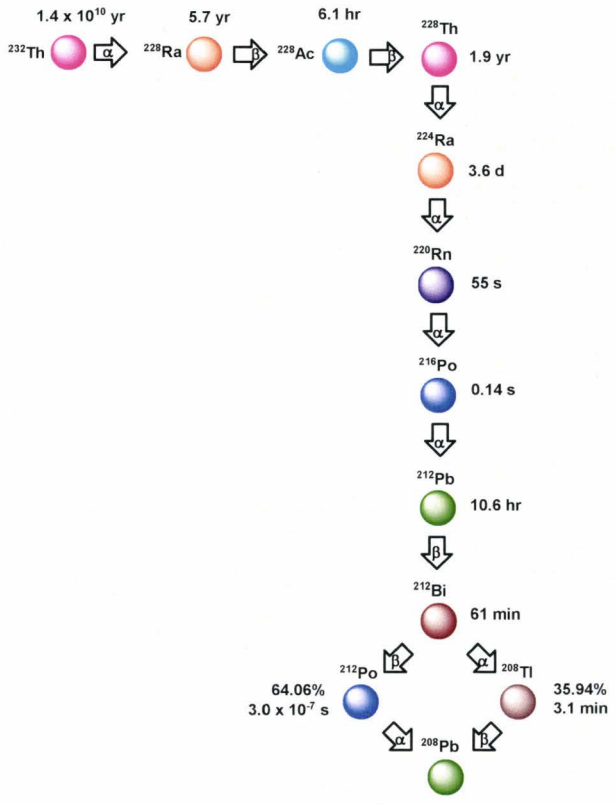

Figure 1.4: Decay series including ^{232}Th yielding non-radioactive ^{208}Pb as the final decay product. This series is known as the "Thorium Series."

The notoriety of the actinides amongst the general population may be largely attributed to uranium's use in both nuclear reactors and nuclear weapons. The crucial importance of uranium, and by relation the actinides, was discovered in 1938 when the process of nuclear fission was first observed.[4] Of the three naturally occurring isotopes, ^{235}U is the most important in energy production. ^{238}U alone may not be used for energy production, as neutrons generated by fission of ^{238}U lack the required energy (~1 MeV) to cause this uranium isotope to continue undergoing chain fission events. Fission events involving ^{238}U are responsible for less than 10 % of the energy produced in a nuclear reactor. Therefore, for practical reasons arising from the relatively high natural

abundance of ^{235}U compared to ^{234}U, ^{235}U is the fissile isotope enriched for use in nuclear energy and weapon production.

When a neutron is absorbed by a fissile isotope, energy, decay products and several neutrons are ejected. For ^{235}U, slow neutron (energies of c.a. 25 meV) absorption yields ^{236}U which ejects neutrons, energy and produces a statistical mixture of fission products, of which there are hundreds of possible combinations (some examples are given in equations 1.1 to 1.3). The free neutrons produced, if found in the presence of further amounts of fissile material and a moderator (e.g., D_2O, H_2O or graphite to slow the neutron down through multiple collisions), may be absorbed, propagating the reaction. Nuclear fission is therefore a self sustaining cycle of fission events, which may be exploited for the large amounts of energy produced. Theoretically, complete self-sustained fission of ^{235}U produces approximately 2.0 $x10^{10}$ kWh of energy per kilogram of ^{235}U employed (enough to power two million average North American homes for one year).

$$\mathbf{^{235}U + n \longrightarrow {}^{236}U \longrightarrow 3\,n + {}^{94}Zr + {}^{139}Te + 197\ MeV} \qquad \mathbf{(1.1)}$$

$$\mathbf{^{236}U \longrightarrow 3\,n + {}^{92}Kr + {}^{141}Ba + 170\ MeV} \qquad \mathbf{(1.2)}$$

$$\mathbf{^{236}U \longrightarrow 3\,n + {}^{89}Kr + {}^{144}Ba + 177\ MeV} \qquad \mathbf{(1.3)}$$

Naturally abundant thorium is radioactive, with ^{232}Th (100 % abundant) having a half-life of 1.405 x 10^{10} years, and emitting α-particles (4.016 MeV). While thorium is not directly involved in nuclear energy generation processes, it does have the potential to

play an important part in nuclear energy generation due to its ability to be converted by slow neutrons to the non-naturally occurring, fissionable uranium isotope, ^{233}U.

$$^{232}Th(n,\gamma) \longrightarrow {}^{233}Th \xrightarrow{-\beta} {}^{233}Pa \xrightarrow{-\beta} {}^{233}U \qquad (1.4)$$

^{233}U also provides the neutrons necessary to commence the cycle again. The process is therefore known as the thorium cycle. The greatest advantage of this cycle is the possibility it opens up to produce large amounts of slow neutron fissile materials, especially when considering the high natural abundance of ^{232}Th when compared to the low natural abundance of ^{235}U. Several advantages also exist in thorium-based nuclear fuels, which include the higher neutron yield of ^{233}U relative to ^{235}U, the ability to mix ^{233}U with ^{238}U to prevent its use in weapon manufacturing, and increased reactor core safety and performance. Unfortunately, the refinement and reprocessing costs of ^{233}U are higher than those for ^{235}U based fuels, so have been deemed impractical thus far.[5]

1.1.4 – General Properties of the Actinides Focused on Thorium and Uranium

The early actinide elements are endowed with a unique combination of properties by virtue of their special position in the periodic table. Key properties of the early actinide elements relevant to their chemical behavior are:

- The relatively large size of the actinides when compared to members of the transition series, which allow access to particularly high coordination numbers.

- The potential for significant covalency and availability of the f-orbitals for bonding. This endows the actinides with chemical distinction over the lanthanides and transition metals.
- The highly electropositive nature of the actinides.
- In the case of uranium, neptunium and plutonium, and to a lesser extent protactinium and americium, the availability of a wide range of oxidation states (e.g. U^{3+} to U^{6+}).
- Resistance to M–M bond formation.

The first four attributes in the list merit further discussion, and are described in more detail below.

1.1.4.1 – Ionic and Covalent Radii

The actinides are amongst the largest elements in the periodic table, with atomic radii similar to those of lanthanides (Table 1.1). Furthermore, the ionic radii of the early actinides match or surpass those of the lanthanides in similar oxidation states due to less concentrated 5f-orbitals as evident by the comparison of ionic radii for trivalent Ac^{3+} and U^{3+} versus La^{3+}, Ce^{3+} and Nd^{3+} (1.12 and 1.03 Å versus 1.03, 1.01 and 0.98 Å respectively) and for tetravalent Th^{4+} and U^{4+} versus Ce^{4+} (0.94 and 0.89 Å versus 0.87 Å; Table 1.2).

Table 1.1: Atomic radii for selected actinide, lanthanide and transition metals[6]

E	Atomic Radii / Å
Ac	1.95
Th	1.80
U	1.75
La	1.95
Ce	1.85
Nd	1.85
Lu	1.75
Hf	1.55
W	1.35
Ti	1.40
V	1.35
Cr	1.40

E = element

Table 1.2: Ionic radii for selected actinide, lanthanide and transition metal ions with a coordination number of six[7]

E^{x+}	Ionic Radii / Å
Ac^{3+}	1.12
U^{3+}	1.03
La^{3+}	1.03
Ce^{3+}	1.01
Nd^{3+}	0.98
Lu^{3+}	0.86
Th^{4+}	0.94
U^{4+}	0.89
Ce^{4+}	0.87
Hf^{4+}	0.71
Ti^{4+}	0.61
U^{5+}	0.76
Ta^{5+}	0.64
V^{5+}	0.54
U^{6+}	0.73
W^{6+}	0.60
Cr^{6+}	0.44

E = element

In higher oxidation states (M^{5+}, M^{6+}), comparisons with the lanthanide elements are not possible, and comparison with group 5 and group 6 transition metals are appropriate. From Table 1.2, it can be seen that actinide elements in +5 and +6 oxidation states are significantly larger than their transition metal analogues.[8]

The large size of the actinides allows the formation of complexes with higher coordination numbers than in compounds of the transition metals. As such, a larger number of reactive species can potentially be coordinated and maintained in spatially unusual orientations. In the presence of ligands with high steric demands, the large size of the actinides can also result in complexes that are considerably less coordinatively saturated than their transition metal counterparts.

1.1.4.2 – f-Orbitals and Covalency

1.1.4.2.1 – General

One of the most appealing features of the actinides is the potential of their coordination and organometallic compounds to exhibit considerable metal-ligand orbital overlap, or covalency. The availability of the 5f valence orbitals (Figure 1.5) to participate in bonding is a distinctive feature of the early actinide ions. By contrast, the 4f-orbitals in the lanthanides are highly contracted and typically unavailable for bonding, and the 5f-orbitals of the heavier actinides are similarly reduced in availability due to increasing effective nuclear charge and poor shielding by the 5f-electrons.

Of particular interest in the chemistry of the actinides is the study of orbital overlap as a function of actinide ion and ligand identity, the role that covalency plays in molecular structure and reactivity, and comparison of metal-ligand bonding with related d-element systems. Both experimental and theoretical efforts have been undertaken to elucidate the nature of bonding in actinide systems and to determine the degree of covalency present in actinide coordination and organometallic compounds. It is expected that f-orbital participation may result in new bonding possibilities that are not observed with the transition metals, given the dissimilar symmetry properties when compared to d-orbitals, and smaller expected ligand field stabilization energies.[9]

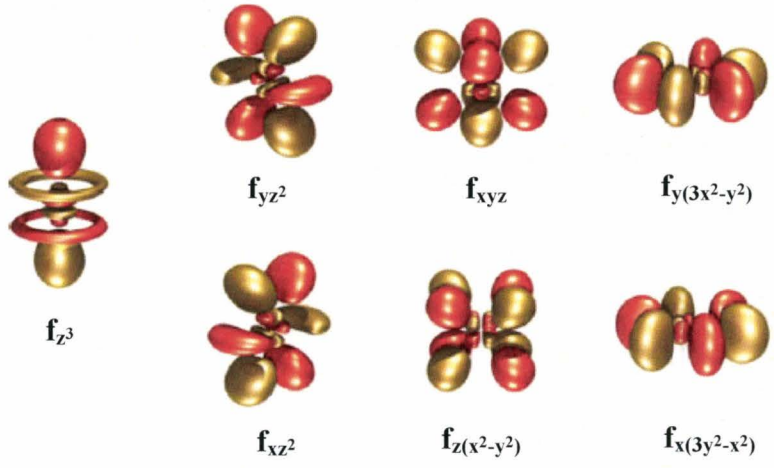

Figure 1.5: Graphical representation of the 5f-orbitals.[10]

1.1.4.2.2 – Theoretical Methods

Organoactinide complexes supported by cyclopentadienyl ligands have been investigated by numerous theoretical methods in order to elucidate the nature of the

metal-ligand bonding, in particular the extent to which the f-orbitals participate in bonding interactions.[9] While it is non-trivial to quantify the degree of covalency and ionicity of cyclopentadienylactinide complexes, and exact values are not available, it is believed that the predominant character in early actinide metal-ligand bonding is ionic. However, cyclopentadienyl complexes do typically show evidence for a significant covalent contribution to actinide-ligand bonding, although it is often unclear whether these covalent contributions arise from 6d or 5f orbital participation.[11]

Similarly to actinide cyclopentadienyl complexes, sandwich complexes of the cyclooctatetraenyl ligand $[An(C_8H_8)_2]$ (An = Th, U, Pa, Np, Pu; Figure 1.6), have also been investigated extensively. In general, the large size of the actinide ion allows for high coordination numbers, and in agreement with studies performed on cyclopentadienyl actinide systems, cyclooctatetraenyl supported actinide complexes exhibit a large ionic contribution to bonding. However, in this case, a greater covalent contribution due to overlap between 5f and 6d orbitals on the metal and the ligand orbitals is observed.[9, 12] *Ab initio* calculations on uranocene $\{[U(C_8H_8)_2]\}$ in particular, incorporating relativistic core potentials and spin-orbit configuration interaction calculations, suggest that the 6d orbitals play a primary role in metal-ligand bonding, and that 5f orbital involvement is secondary.[13]

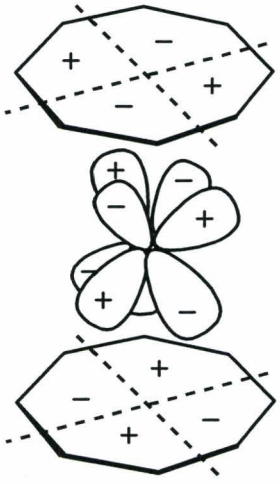

Figure 1.6: Metal-ligand orbital interaction in uranocene [$U(C_8H_8)_2$] between highest occupied $C_8H_8^{2-}$ orbital and actinide f_{xzy} or $f_{z(x^2-y^2)}$ orbitals.

Recent studies have also demonstrated stronger metal–ligand bonding in octahedral actinide(III) [$M\{\kappa^2 EE\text{-}(EPR_2)_2N\}_3$] (M = U, Pu; E = S, Se, Te; R = Ph, *i*Pr)[14] and pentagonal bipyramidal [$Cp^*U(\kappa^2 NS\text{-}SBT)_3]^-$ (SBT = 2-mercapto-benzothiazolate)[15] complexes than in isostructural trivalent lanthanide (*e.g.* La, Ce) complexes. Computational studies highlight increased f-orbital participation as the major factor responsible for stronger An–L bonding. However, for both lanthanides and actinides, they also point towards increasing metal d-orbital participation in metal-chalcogen bonding as group 16 is descended. Stronger metal-ligand bonding for the An(III) complexes with heavier chalcogen or pnictogen elements is consistent with the observed preference of ligands containing such elements to bind with An(III) over Ln(III) elements in nuclear fuel reprocessing (*vide infra*).

1.1.4.2.3 – Physical Properties and Reactivity of Actinide Complexes

Volatility: Some of the simplest examples depicting the increased covalency of the actinides when compared to the lanthanides are compounds of uranium, such as UF_6 and $U(BH_4)_4$ which due to low lattice energies (a trait seldom observed in ionic compounds), may be readily volatilized. Large scale synthesis of UF_6 involves the reaction of UF_4 with F_2 or ClF_3.[16] This white, volatile solid sublimes at 57 °C, and at room temperature, has a vapor pressure of about 0.14 atm, which increases to 13.6 atm at 150 °C. Uranium borohydride may be obtained by the reaction of UF_4 with two equivalents of $Al(BH_4)_3$ or from UCl_4 with four equivalents of $LiBH_4$, and has an a vapor pressure of 0.01 atm at 60 °C.[17]

*Soft-Donor Ligand Coordination:*The effect of substitution of hard oxygen and nitrogen donors for heavier chalcogen or pnictogen elements is of importance for the development of new strategies for non-aqueous lanthanide/actinide separation in nuclear fuel reprocessing.[18] One important advance in this field involves the separation of Ln(III) and An(III) through the use of soft donor containing ligands to selectively bind with the actinide over the lanthanide ions. This effect has been attributed to increased covalency in actinide–ligand bonding compared to the lanthanides.[19] Soft donor ligands of current importance for trivalent lanthanide/actinide separation in nuclear fuel reprocessing include dithiophosphinic acids [e.g. $(t\text{BuCH}_2\text{CHMeCH}_2)_2\text{P(S)SH}$; bis(2,4,4-trimethylpentyl)dithiophosphinic acid; HC301], poly-aza compounds [e.g. 2,6-bis(1,2,4-triazin-3-yl)pyridines; BTP ligands], and thiocyanate.[20]

Reactivity: Unlike similar cyclopentadienyl complexes of the lanthanides and Group 3 metals, the uranium chloride complex [Cp_3UCl] decomposes relatively slowly in water, and does not react with $FeCl_2$ to produce ferrocene {[Cp_2Fe]}. The above evidence supports the postulated increased covalency in actinide complexes when compared to lanthanide or Group 3 metal compounds. However actinide complexes in general are still believed to be considerably more ionic than the majority of similarly ligated transition metal complexes.[21]

1.1.4.3 – Electropositivity

The early actinides are amongst the most electropositive elements in the periodic table. Pauling electronegativity[22] values for selected main group, transition metal, lanthanide and actinide elements can be found in Figure 1.7; these electronegativity data are inversely related to the electropositivity of an element. As such, it is evident that the actinide elements Th, Pa and U have electropositivities most similar to magnesium and elements in groups 3 and 4, and slightly lower than the lanthanide elements.

IA	*IIA*									*IIIA*
Li 1.0	**Be** 1.6									**B** 2.0
Na 0.9	**Mg** 1.3	*IIIB*	*IVB*	*VB*	*VIB*	*VIIB*	*VIIIB*		*IIB*	**Al** 1.6
K 0.8	**Ca** 1.0	**Sc** 1.4	**Ti** 1.5	**V** 1.6	**Cr** 1.6	**Mn** 1.6	**Fe** 1.8	...	**Zn** 1.6	**Ga** 1.8
Rb 0.8	**Sr** 1.0	**Y** 1.2	**Zr** 1.3	**Nb** 1.6	**Mo** 2.1	**Tc** 1.9	**Ru** 2.2	...	**Cd** 1.7	**In** 1.8
Cs 0.7	**Ba** 0.9	**Lu** 1.3	**Hf** 1.3	**Ta** 1.5	**W** 2.4	**Re** 1.9	**Os** 2.2	...	**Hg** 2.0	**Tl** 1.6
Fr 0.7	**Ra** 0.9	**Lr** -								

Lanthanides	**La** 1.1	**Ce** 1.1	**Pr** 1.1	**Nd** 1.1	**Pm** 1.1	**Sm** 1.2	**Eu** 1.2	**Gd** 1.2	**Tb** 1.1	...	**Yb** 1.2
Actinides	**Ac** 1.1	**Th** 1.3	**Pa** 1.5	**U** 1.4	**Np** 1.3	**Pu** 1.3	**Am** 1.1	**Cm** 1.3	**Bk** 1.3	...	**No** 1.5

Figure 1.7: Pauling electronegativity values for selected alkali metal, alkaline earth, triel, transition metal, lanthanide and actinide elements.

1.1.4.4 – Oxidation States

A summary of accessible oxidation states for the actinides is presented in Table 1.3.[23] The highest possible oxidation state of the early actinides reflects the total number of electrons that may be removed from their outer shell. The elements with the widest range of commonly observed oxidation states are uranium, neptunium and plutonium, which readily span between the +3 and +6 or +7 oxidation state. However, increasing effective nuclear charge across the period begins to limit the number of readily achievable

oxidation states, and beyond americium the actinide elements, like the lanthanides, are commonly observed in just one or two oxidation states. The preference of most late actinide elements for the +3 oxidation state is a trait that these elements share with the lanthanides. Furthermore, the preference of nobelium for the +2 oxidation state mirrors the relative ease with which the +2 oxidation state is accessible in the lanthanide series; Yb (directly above No) is the lanthanide element with the greatest propensity to form divalent complexes, resulting in a favorable f^{14} electronic configuration.

Table 1.3: Table of reported oxidation states of the actinide elements. Blue = commonly observed; Red = known

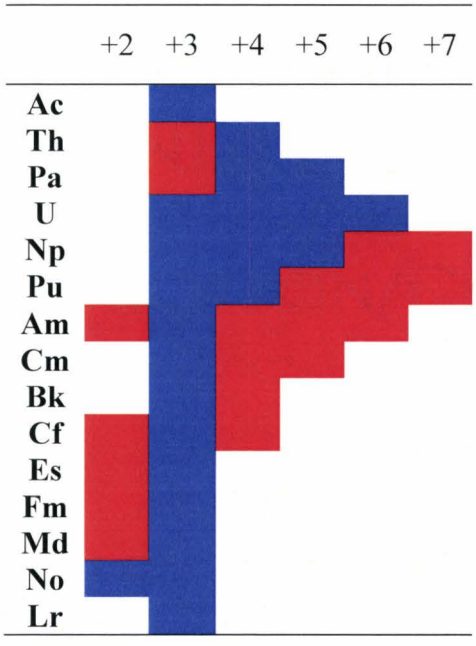

Progress in the field of organoactinide chemistry has centered largely on the use of thorium and uranium. One of the most interesting traits of uranium is its ability to access a range of oxidation states, which spans from +3 to +6 in non-aqueous solvents. This trait endows uranium with greater flexibility in the types of complexes accessible

when compared to thorium. However, predominance of the tetravalent state for thorium can be advantageous in that it leads to more predictable reactivity and diamagnetic compounds, which are amenable to straightforward NMR characterization, unlike complexes of tetravalent uranium.

1.1.4.4.1 – Low Valent Thorium Chemistry

As highlighted in Table 1.3, a wide variety of uranium(III) complexes are quite readily accessible, but thorium has great difficulty accessing the trivalent oxidation state. The first reported synthesis of a trivalent thorium molecular complex, $[(C_5H_5)_3Th]$, was reported in 1974 by chemical reduction of $[(C_5H_5)_3ThCl]$ with sodium-potassium alloy.[24] Later, Marks and co-workers reported an alternative photochemical route to this and a related complex, starting from $[(C_5H_4R)_3Th(i\text{Pr})]$ (R = H, Me) to yield $[(C_5H_4R)_3Th]$, as well as propane and propene.[25, 26] The production of propene is likely to proceed via the generation of a thorium(IV) hydride complex, $[(C_5H_4R)_3ThH]$, though no direct evidence of hydride complex formation was observed.

The first structurally characterized thorium(III) complex was reported in 1986 by Blake *et al.* and was obtained via reaction of $[Cp''_2ThCl_2]$ {$Cp'' = C_5H_3(SiMe_3)_2$-1,3} with sodium-potassium alloy in toluene to produce $[Cp''_3Th]$ with concurrent deposition of thorium metal.[27] Hursthouse and Cloke later reported the first synthesis of a Th(III) sandwich compound, $[Th\{COT^{TBS2}\}_2][K(dme)_2]$, from the reduction of $[Th\{COT^{TBS2}\}_2]$ {$COT^{TBS2} = 1,4\text{-}(t\text{BuMe}_2\text{Si})_2C_8H_6$} with potassium metal.[28]

The difficulty of accessing Th(III) complexes is largely attributed to the position of thorium in the actinide series. The 5f-orbitals of actinium and thorium have the highest energy of all of the actinides due to the lowering of the orbital energies with increased effective nuclear charge as the actinide series is traversed.[29] As such, it is believed that Th(III) complexes, such as $[(C_5H_5)_3Th]$[24-26] may have a $6d^1$ ground state; a hypothesis which has some spectroscopic support.[30]

Divalent thorium compounds are extremely rare, and those reported, such as ThI_2, are considered divalent only from the perspective of formula, since the valence electrons are located in a type of conduction band. However, the inaccessibility of divalent actinide compounds may be circumvented through the use of thorium(II) synthetic equivalents or 'synthons,' such as $[\{(L)Th\}\{K(dme)\}(\eta^4\text{-}C_{10}H_8)][Li(dme)_3]$ {L = Et_8-calix[4]tetrapyrrole} which was isolated as one of three products from the reaction of $[(L)Th(\mu\text{-}Cl)]_2[K(dme)]_2$ with two equivalents of lithium or potassium naphthalenide. Structural properties and diamagnetism suggest that the metal is in the formal +4 oxidation state. However, this complex behaves as a Th(II) synthon, reacting with two equivalents of Me_3SiN_3 to yield $[(L)Th\{N(SiMe_3)_2\}][Li(dme)_3]$. This reaction likely proceeds via a two step mechanism; (1) reaction with trimethylsilyl azide to liberate nitrogen gas and form a thorium-imido complex, and (2) reaction of this unobserved imido complex with a second equivalent of azide to abstract a Me_3Si group and eliminate KN_3, which is an observed byproduct of the reaction.[31]

A remarkable series of polypnictide complexes (Figure 1.8, top) have also been prepared by reaction of P_4 and As_4 with $[(1,3\text{-}t\text{Bu}_2C_5H_3)_2Th(\eta^4\text{-}C_4H_6)]$.[32] In these

reactions, the [(1,3-tBu$_2$C$_5$H$_3$)$_2$Th(η^4-C$_4$H$_6$)] precursor also acts as a thorium(II) synthetic equivalent, losing neutral butadiene during the reaction. In the presence of magnesium chloride, formation of these hexapnictide complexes was not observed, and while the reaction with arsenic gave rise to an intractable mixture of products, the reaction with P_4 resulted in the formation of [(1,3-tBu$_2$C$_5$H$_3$)$_2$Th](μ:η^3-P$_3$)[Th(Cl)(1,3-tBu$_2$C$_5$H$_3$)$_2$] (Figure 1.8, bottom).

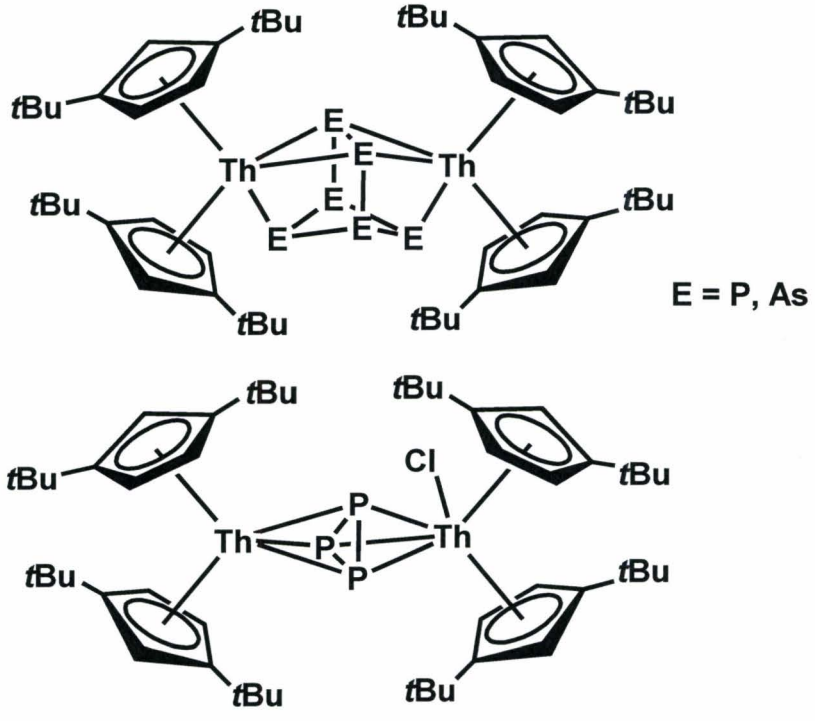

Figure 1.8: Polypnictide complexes of thorium generated via reaction of [($C_5H_3tBu_2$-1,3)$_2$Th(η^4-C_4H_6)] with, Top: E_4 (E = P, As); Bottom: P_4 in the presences of $MgCl_2$.

1.2 – Organoactinide Chemistry

1.2.1 – Homoleptic and Related Polyalkyl Derivatives

Interest in the development of homoleptic actinide alkyl complexes dates back to the Manhattan project in the 1940s, [33, 34] where the search for stable and readily volatilized compounds for isotope separation resulted in numerous attempted syntheses of σ-bonded uranium alkyl compounds. However, these efforts proved unsuccessful due to thermal instability which prevented isolation of these peralkyl species. This thermal instability was attributed to coordinative unsaturation of the metal,[35] and while it precluded the use of actinide peralkyl compounds for isotope separation, they remain of potential importance as convenient precursors to new organoactinide complexes via alkane elimination (*vide infra*).

Several researchers, having recognized the problems associated with actinide peralkyl syntheses, proceeded to employ excess amounts of alkyl lithium reagents to produce kinetically stabilized 'ate' compounds of the type $[Li(S)_4]_2[UR_6]$ {S = THF, Et_2O; R = CH_3, C_6H_5, CH_2SiMe_3},[11] and $[Li(S')]_3[Th(CH_3)_7]$ {S′ = TMEDA},[36] and $[Li_2(py)_3][U(fc)_3]$[37] (fc = 1,1′-ferrocenyl). Homoleptic actinide alkyl compounds may also be accessed via phenoxide-to-alkyl exchange. For example, the 5 coordinate $[Li_{14}(O\textit{t}Bu)_{12}Cl][U(CH_2SiMe_3)_5]$ may be isolated in low yield by reaction of $[Li(THF)]_2[U(O\textit{t}Bu)_6]$ with 4.5 equivalents of $LiCH_2SiMe_3$.[38] This compound is thermally stable in the solid state, showing no sign of decomposition after days at room temperature, although it does undergo rapid decomposition in benzene solution.

However, anionic polyalkyl derivatives are in general poorly suited as starting materials for the synthesis of neutral alkyl derivatives.

Neutral actinide alkyl compounds are extremely rare. The reaction of benzyllithium with thorium tetrachloride is claimed to yield $Th(CH_2Ph)_4$, but the validity of this result is unknown; the only characterization provided is IR data.[39] However, the more sterically protected tetrabenzyl derivative {$[Th(CH_2C_6H_3Me_2\text{-}3,5)_4]$, synthesized by the reaction of thorium tetrachloride with $LiCH_2C_6H_3Me_2$-3,5 in THF, has been thoroughly characterized via NMR spectroscopy and elemental analysis.[40] Base-stabilized tetralkyl compounds may be accessed via the reaction of $[(dmpe)_2AnCl_4]$ (An = Th, U) with four equivalents of methyllithium[41] or benzyllithium[42] to produce $(dmpe)_xAnR_4$ {R = CH_3, x = 2; R = CH_2Ph, x = 1}. These compounds have been characterized by elemental analysis and subsequent reactivity with phenol to yield the corresponding $[(dmpe)An(OPh)_4]$ compound. Mixed methyl/benzyl containing derivative, $[(dmpe)An(CH_2Ph)_3Me]$ may also be obtained by reaction of a mixture of three molar equivalents of $PhCH_2Li$ and MeLi with $[(dmpe)_2AnCl_4]$.[42] Related $[U(CH_2Ph)_4(MgCl_2)]$ was also reported to form from reaction of $UCl_4(THF)_3$ with $Mg(CH_2Ph)_2$, and was characterized by elemental analysis.[43]

Homoleptic actinide allyl complexes are closely related to actinide alkyl complexes. The presence of an anionic charge and three π-delocalized carbon atoms allows allyl ligands to coordinate in an η^1-fashion like alkyl ligands, or alternatively they may coordinate in an η^3-fashion depending on the requirements of the metal center. The first example of a homoleptic actinide allyl complex, $[Th(C_3H_5)_4]$ was reported by Wilke

in 1966.[44] This complex readily decomposes at 0 °C and is best handled at temperatures of –20 °C or lower. Almost 40 years later, sterically stabilized analogues of this compound were reported by Hanusa and Brennessel,[45] who increased the stability of the original $[Th(C_3H_5)_4]$ by increasing the steric properties of the allyl ligands through single or double $SiMe_3$ substitution. By reaction of $K[1,3\text{-}(SiMe_3)_2C_3H_3]$ or $K[1\text{-}(SiMe_3)C_3H_4]$ with $[ThBr_4(thf)_4]$ they were able to isolate the complexes $[\{1,3\text{-}(SiMe_3)_2C_3H_3\}_4Th]$ and $[\{1\text{-}(SiMe_3)C_3H_4\}_4Th]$. In contrast with $[Th(C_3H_5)_4]$, the two new homoleptic allyl complexes are remarkably thermally robust, melting without decomposition at temperatures of 124 °C and 90 °C, respectively.

An analogous homoleptic uranium allyl complex, $[U(C_3H_5)_4]$ was prepared by the reaction of UCl_4 with C_3H_5MgBr at –30 °C.[46] Thermal instability similar to the thorium analogue was reported, with the complex decomposing above –20 °C. Despite the thermal instability of $[U(C_3H_5)_4]$, reaction with two equivalents of *t*BuOH at –20 °C yielded $[(t\text{BuO})_2U(C_3H_5)_2]$.[47] A second example of a homoleptic uranium allyl, $[U(C_3H_4Me\text{-}2)_4]$, was also reported by reaction of UCl_4 with $(C_3H_4Me\text{-}2)MgCl$ at –30 °C, and was studied by ^1H NMR and IR spectroscopy.[48]

The above mentioned actinide 'ate' complexes, base stabilized $[(dmpe)_xAnR_4]$ or sterically-hindered allyl complexes demonstrate that with a judicious amount coordinative saturation, 'homoleptic hydrocarbyl' complexes of the actinides may be isolated. However, it is important to note that while several of the compounds in this section have been shown to undergo alkane or alkene elimination with highly acidic proton sources,

they have not yet been utilized as starting materials of any broad utility for the synthesis of new organometallic derivatives.

1.2.2 – Carbocyclic Ligands in Actinide Chemistry

Ancillary ligands modulate the steric and electronic environment of a coordinated metal and play a vital role in controlling the stability and reactivity of coordination and organometallic complexes. To date, organoactinide chemistry has largely focused on the use of carbocyclic ancillaries such as cyclopentadienyl ($C_5R_5^-$) and related systems,[49-53] the tetramethylphospholyl anion,[54] dianionic $C_8R_8^{2-}$ or pentalene ligands,[55] carboranes,[56] arenes[57] and the cycloheptatrienyl trianion (Figure 1.9).[58]

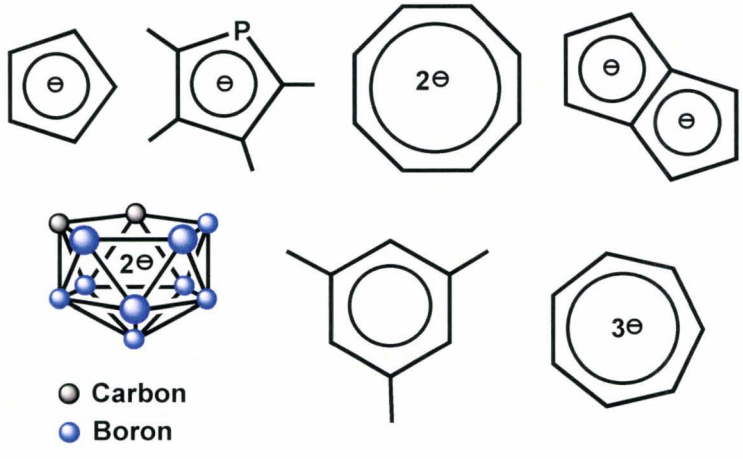

Figure 1.9: Carbocyclic ligands in actinide chemistry. From left to right: (Top) cyclopentadienyl anion, tetramethylphospholyl anion, cyclooctatetraenyl dianion, pentalenyl dianion; (Bottom) *nido*-1,2-*ortho*-carborane dianion, mesitylene, cycloheptatrienyl trianion.

Amongst these, the most robust and versatile ligand system in organoactinide chemistry is the ubiquitous cyclopentadienyl ($C_5R_5^-$; Cp = $C_5H_5^-$; Cp* = $C_5Me_5^-$) ligand, and as in the chemistry of the transition metals, the $C_5R_5^-$ ligand has dominated the field of organoactinide chemistry since its inception. This cyclic, aromatic organic molecule contains a delocalized π-system and may bond to metal centers in an η^1-, η^3- or η^5-bonding mode (with η^5-coordination being the most common). Covalent bonding interactions are dictated by the available group orbitals derived from the π-orbitals of the $C_5R_5^-$ ring since the nodal behavior of the ligand group orbitals must be preserved in the molecular orbitals resulting from interaction of the ligand with a metal center (e.g. 2-node group orbitals must interact with a 2-node metal orbital and produce a 2-node molecular orbital). The strongest bonding interactions occur between group and metal orbitals of similar size and energy.

An interesting feature of the cyclopentadienyl ligand system that highlights its flexibility as a supporting ancillary is the possibility of forming mono-, bis-, tris- and tetrakis-ligand actinide complexes with thorium and uranium. Characteristic examples of these types of complexes will be further described in the following sections to grant insight into the advantages and disadvantages of coordination by varying numbers of carbocyclic ancillaries and the effects of altering the steric environment at an actinide metal center.

1.2.2.1 – Cyclopentadienyl Actinide Chemistry: Tris(cyclopentadienyl) Complexes

In the mid 1950s, Birmingham and Wilkinson were the first to employ the cyclopentadienyl ligand to prepare $[(C_5H_5)_3M]$ compounds of lanthanide elements.[59] Their results strongly suggested that Cp ligands would be suitable to the synthesis of various organoactinide complexes due to similarities in the size of lanthanide and actinide elements. Isolation of $[(C_5H_5)_3UCl]$ (Figure 1.10), the first reported organoactinide complex, as a red-black crystalline solid followed soon thereafter.[60] The synthesis of $[(C_5H_5)_3UCl]$ was achieved by the reaction of UCl_4 with the sodium salt of the cyclopentadienyl anion.[61]

$$UCl_4 + 3\ Na[C_5H_5] \longrightarrow [(C_5H_5)_3UCl] + 3\ NaCl \qquad (1.5)$$

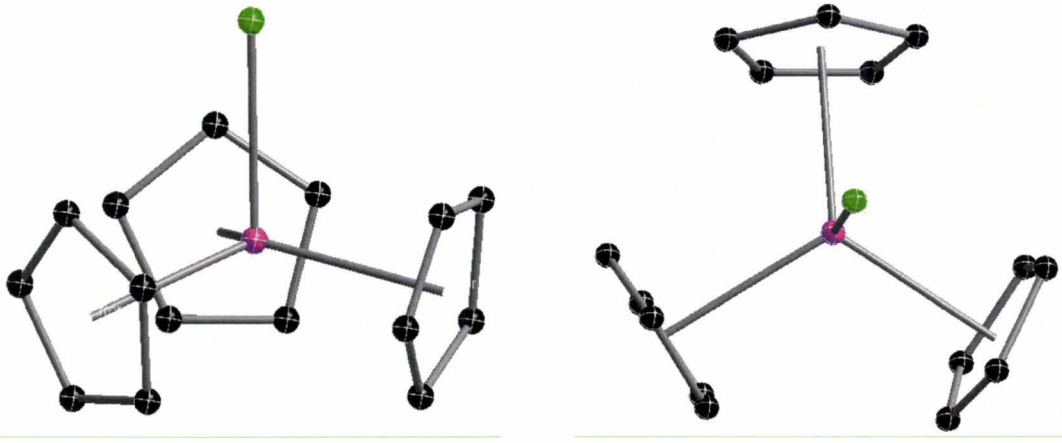

Figure 1.10: X-ray structure of $[(C_5H_5)_3UCl]$. Hydrogen atoms are omitted for clarity.

Tetravalent actinide compounds bearing three cyclopentadienyl or indenyl ligands make up an extensive class of organoactinide complexes, and halide derivatives can be accessed via reaction of actinide tetrachloride starting materials with stoichiometric amounts of the sodium or potassium salts of the desired $C_5R_5^-$ ligand.[62]

Further derivatization of $[(C_5H_5)_3AnX]$ complexes may be readily accomplished through salt metathesis and protonation routes starting from tetravalent complexes to yield compounds containing alkyl, aryl, allyl, cyanide, alkoxide, amide, phosphide and thiolate ligands.[63-66]

$$[(C_5H_5)_3AnX] + LiR \longrightarrow [(C_5H_5)_3AnR] + LiX \quad (1.6)$$

$$[(C_5H_5)_3AnX] + NaSR \longrightarrow [(C_5H_5)_3AnSR] + NaX \quad (1,7)$$

$$[(C_5H_5)_3AnX] + LiNEt_2 \longrightarrow [(C_5H_5)_3AnNEt_2] + LiX \quad (1.8)$$

$$[(C_5H_5)_3AnR] + HCN \longrightarrow [(C_5H_5)_3AnCN] + HR \quad (1.9)$$

$$[(C_5H_5)_3AnR] + HOR \longrightarrow [(C_5H_5)_3AnOR] + HR \quad (1.10)$$

$$[(C_5H_5)_3AnR] + HPR_2 \longrightarrow [(C_5H_5)_3AnPR_2] + HR \quad (1.11)$$

(An =Th or U; X = halide; R = alkyl, aryl or allyl)

X-ray diffraction studies of several tris-cyclopentadienyl actinide halide complexes show that they share a similar structure, with the halide residing on a threefold axis of symmetry, and very similar An–C bond lengths regardless of the nature of halide. However, when comparing thorium and uranium complexes, it is evident that the larger ionic radius of thorium leads to longer M–C and M–X bond lengths (Table 1.4).

The extent to which the three cyclopentadienyl anions saturate the coordination environment around the metal center is clearly illustrated in the following examples: (a) Addition of large excesses of alkyl lithium (LiR) reagents to [Cp_3AnR] complexes does not result in formation of [$Cp_3AnR_2]^-$ derivatives,[66] and (b) In [$(C_5H_5)_3U(C_3H_5)$] the allyl ligand is η^1-coordinated in the solid state,[67] and η^1-coordination is maintained in solution, although at room temperature exchange of the α and γ allyl carbon atoms is observed; a phenomena that presumably occurs via an η^3-coordinated intermediate.

Table 1.4: M–$C_{centroid}$ and An–X bond distances for complexes of type [L_3AnX] (L = C_5R_5; An = Th, U; X = Cl, Br, I)[68-73]

Complex	M-$C_{centroid}$ / Å	M-X / Å	Ref.
{[$(Me_3Si)_2C_5H_3]_3$**Th**Cl}	2.84(1)	2.651(2)	69
{[$(Me_3Si)_2C_5H_3]_2[C_5Me_5]$**Th**Cl}	2.84(2)	2.657(5)	69
{[$(Me_2tBuSi)_2C_5H_3]_3$**Th**Cl}	2.85(1)	2.648(2)	69
{[{$(Me_3Si)_2CH$}$C_5H_4]_3$**Th**Cl}	2.83(1)	2.664(2)	69
{[$(Me_3Si)_2C_5H_3]_3$**U**Cl}	2.77(1)	2.614(2)	69
[$(C_5H_5)_3$**U**Cl]	2.74	2.559(16)	70
[$(C_5H_5)_3$**U**Br]	2.72(1)	2.820(2)	71
[$(C_5H_5)_3$**U**I]	2.73(3)	3.059(2)	72
[$(PhCH_2C_5H_4)_3$**U**Cl]	2.733(1)	2.627(2)	73

Another effect of substantial steric protection is a high degree of thermal stability. For example, the primary, β-hydrogen containing alkyl complex [$(C_5H_5)_3U(n$Bu)] and tertiary β-H containing [$(C_5H_5)_3U(t$Bu)] are only 50 % decomposed after heating at 97 °C for 47 days and 11 days, respectively. Thermal decomposition in these types of complexes is presumed to occur via σ-bond homolysis based on the nature of the volatile byproducts, rather than β-H elimination, although no metal containing byproducts have been identified.

1.2.2.2 – Cyclopentadienyl Actinide Chemistry: Tetrakis(cyclopentadienyl) Complexes

Some of the earliest successes in the field of organoactinide chemistry involved the synthesis of homoleptic tetrakis(cyclopentadienyl) complexes, $[(C_5H_5)_4An]$, which have been prepared for thorium,[74] uranium,[75] protactinium[76] and neptunium.[77] From a combination of infrared and powder X-ray data, all four complexes were confirmed to be pseudo-tetrahedral. Related thorium and uranium complexes bearing indenyl ($C_9H_7^-$) ancillaries have also been prepared by salt metathesis (*vide infra*) using $K(C_9H_7)$ to react with $ThCl_4$ and UCl_4 in tetrahydrofuran (THF). However, while conceptually similar to Cp complexes, they differ in their η^3-coordination mode and longer M–C bond lengths as a result of increased steric crowding.[78] While structurally remarkable, the lack of any readily accessible reactive valences on homoleptic tetrakis-cyclopentadienyl actinide complexes limits the scope of any subsequent reactivity.

1.2.2.3 – Cyclopentadienyl Actinide Chemistry: Mono(cyclopentadienyl) Complexes

Complexes of the general formula $[(C_5R_5)AnX_3L_x]$ (L = neutral donor ligand) employing a single cyclopentadienyl ligand are quite rare. The synthesis of $[(C_5H_5)UCl_3(dme)]$ was first described in 1972 via the reaction of UCl_4 with the thallium cyclopentadienyl salt in 1,2-dimethoxyethane (dme).[79] In this complex and in other mono-cyclopentadienyl or mono-indenyl derivatives, the low level of steric protection at the metal center requires coordination of external neutral bases (e.g. thf, dme) to yield isolable and stable metal complexes.[80, 81]

$$AnX_4 + Tl(C_5H_5) \xrightarrow{THF} [(C_5H_5)AnX_3(THF)_2] + TlX \qquad (1.12)$$

Various substituted cyclopentadienyl ligands have been investigated for the synthesis of mono-cyclopentadienyl actinide complexes in order to impart greater stability to the resulting complexes, and have met with some success.[82] For example, a single bulky tris-trimethylsilyl substituted cyclopentadienyl ligand {Cp″ = 1,2,4-$(Me_3Si)_3C_5H_2$} may be coordinated to uranium through the reaction of UCl_4 with LiCp″ in the presence of thf, leading to the formation of a mononuclear uranate complex (Figure 1.11).[83,84] However, formation of the analogous thorium complex was not observed; reaction of $ThCl_4$ with NaCp″ in diethyl ether resulted in the formation of a tetrametallic cluster consisting of two $[(Cp''ThCl_2)_2(\mu\text{-}Cl)_3]^-$ units bridged by $Na^+(OEt_2)$ cations (Figure 1.12).

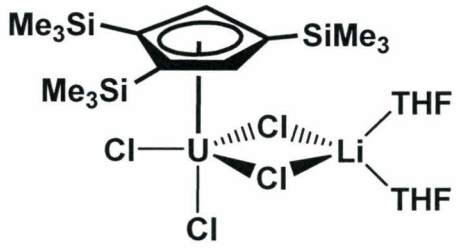

Figure 1.11: Uranate complex [{1,2,4-$(Me_3Si)_3C_5H_2$}$UCl_2(\mu\text{-}Cl)_2Li(THF)_2$].

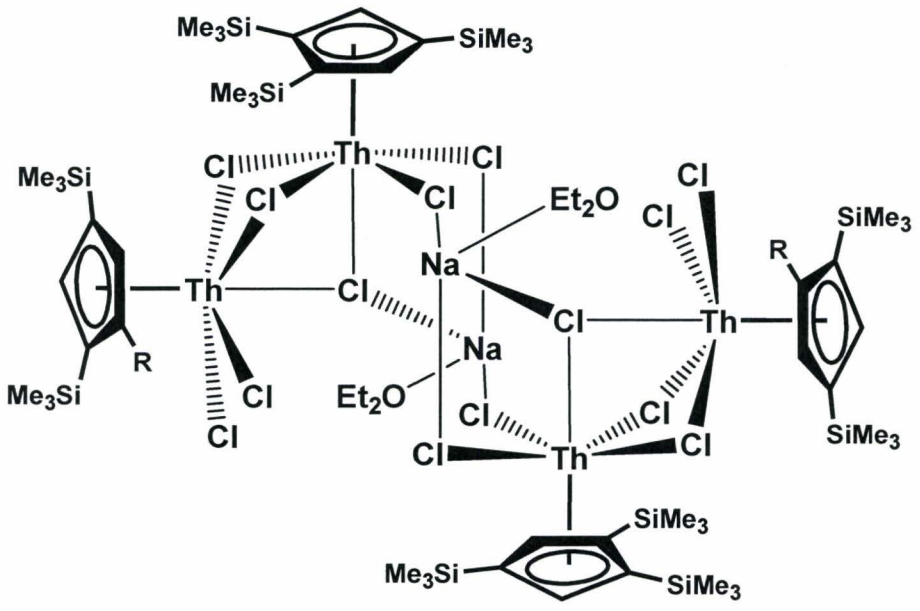

Figure 1.12: Thorium-ate complex $[\{(Me_3Si)_3C_5H_2\}ThCl_2(\mu\text{-}Cl)_2(\mu_3\text{-}Cl)\{(Me_3Si)_3C_5H_2\}Th(\mu\text{-}Cl)_2Na(OEt_2)]_2$; (R = $SiMe_3$).

The chemistry of the actinides involving the pentamethylcyclopentadienyl ligand (Cp*), first reported in the late 1970s and early 1980s by Marks and coworkers,[90,91] offers significant advantages relative to chemistries involving the unsubstituted cyclopentadienyl ligand. Base stabilized actinide complexes supported by a single Cp* ancillary, $[(C_5Me_5)AnX_3(THF)]$,[85,86] may be accessed through reaction of the corresponding metal tetrachloride salt with $(C_5Me_5)MgCl$. Furthermore, these compounds may be alkylated to produce rare examples of stable trialkyl actinide complexes, $[(C_5Me_5)AnR_3]$ (An = Th; R = C_3H_5, $CH_2C_6H_5$, *o*-$C_6H_4NMe_2$. An = U; R = C_3H_5, 2-methylallyl, $CH_2C_6H_5$).[49, 85, 87]

1.2.2.4 – Cyclopentadienyl Actinide Chemistry: Bis(cyclopentadienyl) Complexes

Tetravalent organoactinide complexes of the general formula $[(C_5H_5)_2AnX_2]$ initially proved difficult to synthesize due to instability of the metallocene complex with respect to ligand redistribution to yield mono- and tris-ligand species.[88] For example, the first reported synthesis of $[(C_5H_5)_2UCl_2]$ by reaction of two equivalents of $Tl(C_5H_5)$ with UCl_4 in 1971 was later shown to actually yield a mixture of $[(C_5H_5)_3UCl]$ and $[(C_5H_5)UCl_3(dme)]$.[81]

However, complexes supported by the sterically undemanding cyclopentadienyl ancillaries can be stabilized by the coordination of strong Lewis bases such as dmpe.[89]

$$\mathbf{[(C_5H_5)_2ThCl_2(dmpe)] + 2\ LiR \longrightarrow [(C_5H_5)_2ThR_2(dmpe)]} \qquad \mathbf{(1.13)}$$

$$\mathbf{R = CH_3,\ CH_2C_6H_5}$$

An alternative strategy for the synthesis of stable $[(C_5R_5)_2AnX_2]$ complexes is the use of the pentamethylcyclopentadienyl (Cp*) ligand.[90,91] This ligand has since become one of the most widely employed ancillaries in organoactinide chemistry, typically yielding complexes that exhibit high thermal stability, solubility in a variety of solvents, and appreciable crystallinity. Complexes of the form $[(C_5Me_5)_2AnCl_2]$ (An = Th, U) are thermally robust and monomeric, with pseudo-tetrahedral, bent-metallocene geometries.[92] These complexes are also readily amenable to alkylation, typically by treatment with two equivalents of an alkyl lithium reagent.

$$\mathbf{[(C_5Me_5)_2AnX_2] + 2\ LiR \longrightarrow [(C_5Me_5)_2AnR_2] + 2\ LiX} \qquad \mathbf{(1.14)}$$

$$\mathbf{An = Th,\ U}$$
$$\mathbf{R = CH_3,\ CH_2SiMe_3,\ CH_2CMe_3,\ C_6H_5,\ CH_2C_6H_5}$$

Other substituted cyclopentadienyl ligand sets have also had various degrees of success for the stabilization of tetravalent metallocenes. Some of the most successful examples are the $[1,3\text{-}(Me_3Si)_2C_5H_3]^-$ and $[1,3\text{-}(Me_3C)_2C_5H_3]^-$ anions, which have allowed the synthesis of monomeric $[(C_5R_5)_2UX_2]$ (X = Me) and related coordination complexes (X = BH_4, I, Br, Cl, F).[93] Furthermore, $[(Me_4C_5)_2SiMe_2]^{2-}$ dianions have proven suitable for the synthesis of *ansa* actinide metallocenes (*e.g.* $[\{(Me_4C_5)_2SiMe_2\}ThCl_2]$) with particularly acute centroid–metal–centroid angles (~115° versus ~140° in unlinked metallocenes). This in turn results in a more open metal coordination environment yielding complexes capable of accommodating more than two equatorial ligands, and increasing the accessibility of substrates to the metal center for potential reactivity.[94] *Ansa*-metallocenes have also been employed successfully for the formation and isolation of organoactinide dialkyl complexes bearing CH_2SiMe_3, CH_2CMe_3, C_6H_5, *n*-butyl, and benzyl ligands.[53]

1.2.2.5 – Thermal Stability of $[(Cp)_xAn(R)_y]$ Complexes

The thermal stability of carbocyclic thorium(IV) alkyl complexes is not commonly identified and reported in most literature sources. However, a compilation of reported thermal decomposition times and temperatures can be found in Table 1.5. Bis-cyclopentadienyl alkyl complexes of sufficient steric bulk are generally robust and thermally stable, and require elevated temperatures (80–110 °C) to undergo decomposition.[65,95] The highest thermal stability for a dialkyl actinide complex was

observed for [$Cp^*_2ThMe_2$], which after heating for 1 week at 100 °C, was only 50 % decomposed. Remarkably, tris-cyclopentadienyl complexes [$(Cp)_3ThR$] {R = *n*-butyl, *iso*-propyl, C_3H_5, $CH_2C(CH_3)_3$} demonstrate even greater thermal stability, in some cases showing no sign of decomposition after months at 167 °C.[96]

Table 1.5: Reported thermal decomposition temperatures for ancillary ligand supported thorium alkyl complexes

Complex	Decomposition T / °C	Time / hr	Ref.
$[(OC_6H_3tBu_2\text{-}2,6)_2Th(CH_2SiMe_3)_2]$	60	36	97
$[(Cp^*)Th(OC_6H_3tBu_2\text{-}2,6)(CH_2SiMe_3)_2]$	60	12	98
$[(Cp^*)_2Th(CH_2SiMe_3)_2]$	85	36	99
$[\{Me_2Si(C_5Me_4)_2\}Th(CH_2SiMe_3)_2]$	60	n.a.	100
$[(Cp^*)_2ThMe_2]$	100	> 168	101
$[(Cp)_3Th(n\text{Bu})]$	167	192	96
$[(Cp)_3Th(i\text{Pr})]$	167	14	96
$[(Cp)_3Th(C_3H_5)]$	167	>566	96
$[(Cp)_3Th\{CH_2C(CH_3)_3\}]$	167	>7500	96

Detailed description of the thermodynamics of actinide-alkyl bonding can be used to gain insights into some of the properties of these molecules. Bond disruption enthalpies (BDE) for complexes of the type $[(Cp^*)_2ThR_2]$ (R = alkyl, aryl) have been acquired through the exploitation of the propensity of organoactinide compounds of this type to undergo rapid, sequential and quantitative protonolysis; a process that is highly exothermic. In this manner, using anhydrous *tert*-butylalcohol (*t*BuOH), the Th–R bond disruption energies were probed, and a summary of the first and second BDE for selected compounds can be found in Table 1.6.[102]

Table 1.6: Selected first and second bond disruption enthalpies for selected thorium dialkyl complexes

Compound	1st BDE / kcal mol^{-1}	2nd BDE / kcal mol^{-1}
$[(Cp^*)_2Th(Me)_2]$	81.2(0.8)	83.6(0.9)
$[(Cp^*)_2Th(Et)_2]$	73.5(1.6)	76.3(1.6)
$[(Cp^*)_2Th(n\text{Bu})_2]$	71.6(1.0)	73.6(3.4)
$[(Cp^*)_2Th(CH_2CMe_3)_2]$	72.3(3.8)	76.9(3.7)
$[(Cp^*)_2Th(CH_2SiMe_3)_2]$	80.0(3.1)	82.2(3.1)
$[(Cp^*)_2Th\{(CH_2)_2CMe_2\}]$	65.3(2.3)	78.6(2.6)
$[(Cp^*)_2Th\{(CH_2)_2SiMe_2\}]$	75.5(3.2)	83.0(3.4)

These BDE values suggest that thorium alkyl bonds are particularly strong, especially for alkyl ligands with low steric demands. For comparison, early to mid transition metal alkyl complexes have lower M–C bond disruption energies. For example, a BDE of ca. 60 kcal mol^{-1} was reported for homoleptic $TiMe_4$, and BDEs of 70 kcal mol^{-1} and 65 kcal mol^{-1} were reported for $ZrMe_4$ and for $[(Cp)_2Ti(Ph)_2]$ respectively.[102] Metal-alkyl BDEs also decrease rapidly across the periodic table, for example, $Mn(CO)_5R$ complexes exhibit BDEs ranging from 21 kcal mol^{-1} when R = Me up to 41 kcal mol^{-1} when R = CF_3,[103] and $[(Cp)_2WMe_2]$[104] has a W–Me BDE of 43 kcal mol^{-1}.

The high strength of actinide–carbon bonds relative to transition metal–carbon bonds leads to various deviations in actinide and transition metal organometallic reactivity. Particularly, notable examples are: (1) the pronounced resistance of many β-H containing actinide alkyl complexes towards β-H elimination, and (2) the ability of actinide-hydride complexes to engage in 1,1-insertion reactions with CO.

1.2.2.6 – Cyclopentadienyl Actinide Hydride Complexes

Exposure of several dialkyl complexes [$Cp^*_2AnR_2$] (An = Th, U; R = CH_3, CH_2SiMe_3) to four atmosphere of hydrogen gas resulted in hydrogenolysis to yield dimeric dihydride complexes.[105] Single crystal neutron diffraction studies support the dimeric formulation in the solid state (Figure 1.13), while variable temperature ^1H nuclear magnetic resonance (NMR) experiments shows that the terminal and bridging hydrogen atoms undergo rapid exchange down to –85 °C in solution.

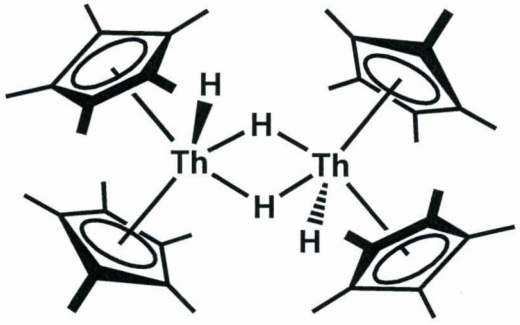

Figure 1.13: Structure of [$(C_5Me_5)_2Th(\mu\text{-}H)H]_2$.

Dialkyl complexes of the type [{$(C_5Me_4)_2(\mu\text{-}SiMe_2)$}$AnR_2$] (R = CH_2SiMe_3, CH_2CMe_3, C_6H_5, *n*Bu, CH_2Ph) also undergo rapid hydrogenolysis when exposed to an atmosphere of hydrogen gas to yield the light-sensitive dimeric dihydride complex [{$(C_5Me_4)_2(\mu\text{-}SiMe_2)$}$ThH_2]_2$, which was investigated by solution NMR spectroscopy and X-ray diffraction experiments. In the absence of a neutron diffraction structure, determination of the exact nature and position of the hydrogen atoms present in the molecule (bridging or terminal) was not possible. However, the short Th–Th distance of

3.632(2) Å and single Th–H stretch in the IR spectrum suggest that the four hydrogen atoms are equivalent, and bridging between the two thorium atoms.[53]

A compilation of reported homonuclear actinide(IV) hydride complexes with ^{1}H NMR data corresponding to the hydride ligand (when available), can be found in Table 1.7. Actinide hydride complexes have been reported to be capable of participating in insertion reactions with unsaturated C–C bonds (hydrogenation, olefin polymerization) and protonation reactions with acidic substrates.[17]

Table 1.7: Compilation of homonuclear actinide(IV) hydride complexes with ^{1}H NMR chemical shift data

Complex	Hydride ^{1}H NMR data / ppm	Ref.
$[(Me_3Si)_2N]_3ThH$	0.63[a]	106
$[(Me_3Si)_2N]_3UH$	not observed	103
$[(2,6\text{-}^tBu_2C_6H_3O)_2ThH_2]_3$	20.54[a]	107
$[(Cp^*)(2,6\text{-}^tBu_2C_6H_3O)ThH_2]_3$	18.54[a]	86
$[(Cp^*)(COT)ThH]_x$	not observed	108
$[(Cp^*)_2ThH_2]_2$	19.2[a]	102
$[(Cp^*)_2UH_2]_2$	316.8[a]	109
$[\{(C_5Me_4)_2(\mu\text{-}SiMe_2)\}ThH_2]_2$	18.36[a]	92
$[(Cp^*)_2Th(O^tBu)H]$	17.4[a]	107
$[(Cp^*)_2Th(OCH^tBu_2)H]$	17.1[b]	110
$[(Cp^*)_2Th(O\text{-}2,6\text{-}^tBu_2C_6H_3)H]$	19.1[a]	86
$[(Cp^*)_2Th(OSiMe_2{}^tBu)H]$	18.0[a]	111
[(Cp*)$_2$Th{(1,S)-*endo*-bornoxide}H]	17.7[a]	112
$[(Cp^*)_2U(O^tBu)H]$	267.1[a]	109
$[(Cp^*)_2U(OCH^tBu_2)H]$	276.7[a]	86
$[(Cp^*)_2U(OSiMe_2{}^tBu)H]$	not observed	113
[(Cp*)$_2$U{(R)-2-butoxide}H]	265.9[a]	109
[(Cp*)$_2$U{(1R,2S,5R)-menthoxide}H]	267.9[a]	109
[(Cp*)$_2$U{(1,S)-*endo*-bornoxide}H]	269.6[a]	109
[(Cp*)$_2$U{(1R,2S,5R)-neomenthoxide}H]	269.2[a]	109
$[(Cp^*)_2Th(Cl)H]$	19.0[a]	107
$[(Cp^*)_2ThH][Co(B_9C_2H_{11})_2]$	19.04[a]	114
$[(C_5H_4{}^tBu)_3UH]$	276.1[b]	115
$[(C_5H_4SiMe_3)_3UH]$	290.5[b]	112
$[(C_5H_4SiMe_3)_3ThH]$	12.94[a]	116
$[(C_5H_4PPh_2)_3UH]$	305[a]	117
$[(C_9H_6SiMe_3)_3ThH]$	14.73[b]	113
$[(C_4Me_4P)_3UH]$	333.4[b]	118
$[Na(THF)_2][\{(Cp)_3U\}_2(\mu\text{-}H)]$	293[c]	119
$[Na(THF)_2][\{(C_5H_4Me)_3U\}_2(\mu\text{-}H)]$	302.2[c]	116
$[Na(18\text{-crown-}6)][\{(C_5H_4SiMe_3)_3U\}_2(\mu\text{-}H)]$	319.2[c]	116

[a] ^{1}H NMR data in C_6D_6. [b] ^{1}H NMR data in C_7D_8. [c] ^{1}H NMR data in THF-d_8.

1.2.2.7 – Cationic Organoactinide Complexes and Applications in Olefin Polymerization

Similar to actinide hydride compounds, actinide alkyl cations are rare. In fact, all base-free mononuclear actinide alkyl cations have been developed by Marks and coworkers, and exist in the form $[(C_5Me_5)_2ThR]_x[A]$ (R = CH_3, CH_2SiMe_3, $CH_2C_6H_5$, C_3H_6 and H; x = 1 or 2) where A is either a weakly-coordinating borate anion or $[M(B_9C_2H_{11})_2]^{y-}$ (M = Co, y = 1; M = Fe, y = 2; Figure 1.14).[114, 120-123] The synthesis of derivatives differing in the nature of the counter anion is of interest due to the ability of such changes to alter the cation's solubility and crystallinity, as well as their interaction with the cationic metal center to affect catalytic activity.

Complexes of this type are of particular interest as catalysts for olefin polymerization, but activity for ethylene polymerization has been reported only for methyl complexes paired with borate anions, with the highest ethylene polymerization activity belonging to $[Cp^*_2ThMe][t BuCH_2CH\{B(C_6F_5)_2\}_2H]$, which exhibits polymerization activity of 5.8 x 10^6 g(PE) $mol^{-1}h^{-1}atm^{-1}$ (product M_w = 2.8 x 10^5, M_n = 1.2 x 10^5).[122] However, ethylene polymerization catalysts prepared from $[\{Me_2Si(indenyl)_2\}AnMe_2]$ as well as $[Cp^*_2AnMe_2]$ (An = Th or U) are mentioned in several T. J. Marks patents.[124] In addition, The Dow Chemical Company has also patented a variety of pentaalkylcyclopentadienyl actinide polymerization catalysts, including those formed from $[Cp^*_2AnX_2]$ and $[Cp^*AnX_3]$ (An = Th and U; X = Cl, Me, or CH_2SiMe_3) in combination with activators such as MAO (*vide infra*).[125] Furthermore, Marks and coworkers reported highly active heterogeneous olefin polymerization

catalysts, which are similar in nature to $[Cp^*_2ThR][A]$, but are formed by reaction of thorium and/or uranium polyalkyl complexes with dehydroxylated γ-alumina or $MgCl_2$.[126]

Other actinide alkyl cations are polynuclear or base-stabilized, and include $[(Cp^*_2ThMe)_2(\mu\text{-}Me)][B(C_6F_5)_4]$[114, 120] which exists in equilibrium with $[Cp^*_2ThMe_2]$ and $[Cp^*_2ThMe][B(C_6F_5)_4]$ in solution, $[Cp^*_2ThMe(L)_x][A]$ (L = THF or NR_3; x = 1-3),[122] $[Cp^*_2UMe(THF)][MeBPh_3]$,[127] and $[LU(CH_2Ph)(OEt_2)][BPh_4]$ $\{L = Fe(C_5H_4NSi^tBuMe_2)_2\}$.[128] A comprehensive graphical list of reported alkyl cations can be found in Figure 1.14.

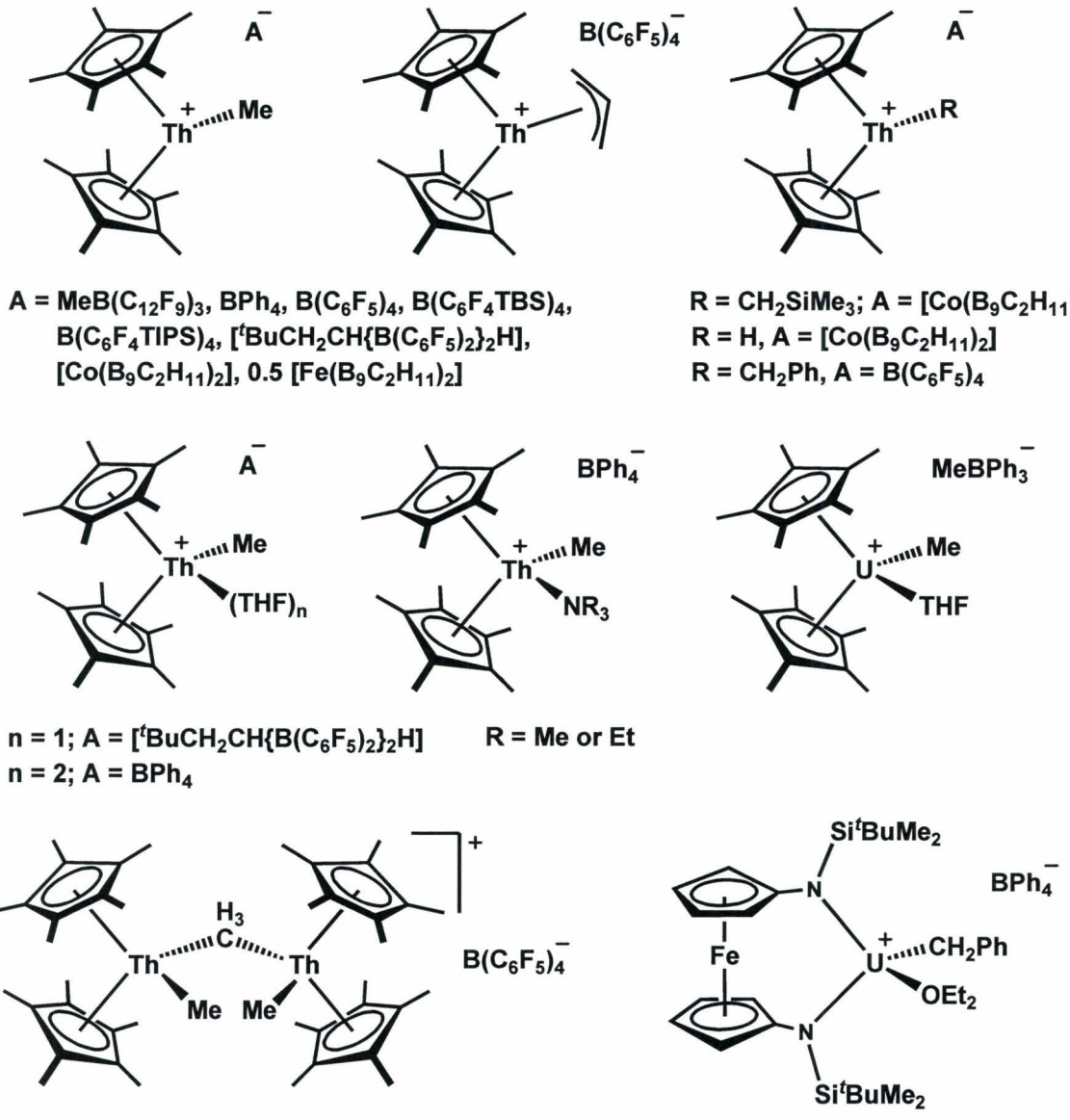

Figure 1.14: Comprehensive list of literature examples of cationic thorium and uranium alkyl complexes.

Several cationic actinide aryl, alkynyl, and borohydride complexes have also been reported. The cationic borohydride complex $[(COT)U(BH_4)(THF)_2][BPh_4]$ was prepared from $[(COT)U(BH_4)_2(THF)]$ by reaction with $[NEt_3H][BPh_4]$, and the adducts $[(COT)U(BH_4)L_3][BPh_4]$ (L = HMPA and $OPPh_3$) were prepared by subsequent reaction

with three equivalents of Lewis base. Related $[(\eta^5:\eta^1\text{-}C_5Me_4\text{-pyridyl-}o)_2U(BH_4)][BPh_4]$ has also been reported to be isolable from the reaction of $[(\eta^5:\eta^1\text{-}C_5Me_4\text{-pyridyl-}o)U(BH_4)_2]$ with $[NEt_3H][BPh_4]$.[129,130] Moreover, cationic aryl and alkynyl complexes have been reported; $[Cp^*_2Th(\kappa^2\text{-}C_6H_4CH_2NMe_2\text{-}o)][BPh_4]$ was prepared by reaction of $[Cp^*_2Th(\kappa^2\text{-}C_6H_4CH_2NMe_2\text{-}o)Me]$ with $[NEt_3H][BPh_4]$,[131] while $[(Et_2N)_2U(C_2{}^t\text{Bu})(HC_2{}^t\text{Bu})][BPh_4]$ was isolated from the reaction of $[(Et_2N)_3U][BPh_4]$ with two equivalents of *tert*-butyl acetylene.[132]

1.2.3 – Neutral Non-Cyclopentadienyl Hydrocarbyl Actinide Complexes

In stark contrast to the actinide chemistry of cyclopentadienyl and other carbocyclic ancillary ligands, non-cyclopentadienyl organometallic actinide(IV) chemistry is particularly underdeveloped. Most examples reported to date rely heavily on the coordination of monoanionic ancillaries such as alkoxy and aryloxy,[47,97,133,134] amidinate,[135] and tris(pyrazolyl)borate ligands (Figure 1.15).[136]

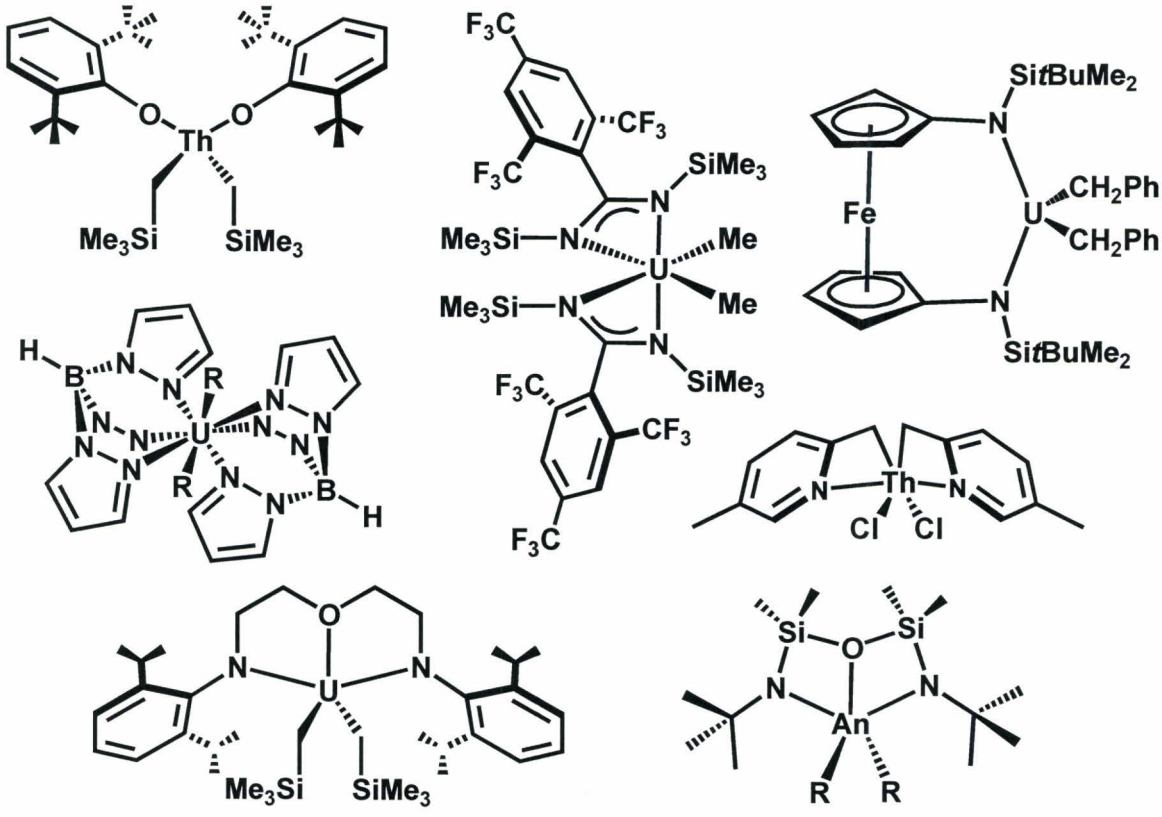

Figure 1.15: Representative examples of non-cyclopentadienyl ancillaries in actinide(IV) alkyl chemistry including aryloxy, amidinate, tris(pyrazolyl)borate, 1,1′-bis(amido)ferrocene, 2-methylpyridine and diamidoether ligands.

Table 1.8: Compilation of reported actinide(IV) alkyl complexes* supported by non-carbocyclic ancillary ligands.[47,97,128,133-138]

Complex	Nature of Variable
$[(ArO)_2Th(CH_2SiMe_3)_2]$	Ar = 2,6-tBu$_2$C$_6$H$_3$
$[(ArO)_2Th(CH_2SiMe_3)\{OC(NR)CH_2SiMe_3\}]$	Ar = 2,6-tBu$_2$C$_6$H$_3$; R = 2,6-Me$_2$C$_6$H$_3$
$[(R_3CO)_2U(C_3H_5)_2]$	R = tBu
$[(R_3CO)_2U(CH_2Ph)_2]$	R = tBu
$[(RO)_2U(C_3H_5)_2]$	R = Et, iPr, tBu
$[ThCl_2(CH_2\text{-}5\text{-}MePy)_2]$	
$[(ArO)_2Th(CH_2\text{-}5\text{-}MePy)_2]$	Ar = 2,6-tBu$_2$C$_6$H$_3$
$[\{(3,5\text{-}Me_2pz)_3BH\}UCl_2\{CH(SiMe_3)_2\}]$	
$[\{(3,5\text{-}Me_2pz)_3BH\}UCl_{3-x}(CH_2SiMe_3)_x]$	x = 1 - 3
$[\{HB(pz)_3\}_2UClR]$	R = Me, CH_2SiMe_3, C_6H_4-o-CH_2NMe_2
$[\{HB(pz)_3\}_2UR_2]$	R = Me, CH_2SiMe_3
$[\{B(pz)_4\}_2UClMe]$	pz = pyrazolyl
$[fc(NSi$$t$$BuMe_2)U(CH_2Ph)_2]$	
$[fc(NSi$$t$$BuMe_2)U(CH_2Ph)(OEt_2)][BPh_4]$	fc = $Fe(C_5H_4)_2$
$[\{4\text{-}MeC_6H_4C(NSiMe_3)_2\}_3UMe]$	
$[\{4\text{-}(CF_3)C_6H_4C(NSiMe_3)_2\}_2UMe_2]$	
$[\{PhC(NSiMe_3)_2\}_3UMe$	
$[(^{DIIP}NCOCN)U(CH_2SiMe_3)_2]$	^{DIIP}NCOCN = O(CH$_2$CH$_2$NAr)$_2$ Ar = 2,6-diisopropylphenyl
$[(^{tBu}NON)Th(R)_2]$	R = C_3H_5, CH_2SiMe_3
$[(^{tBu}NON)U(R)_2]$	R = C_3H_5, CH_2SiMe_3

*This list does not include tetraalkyl complexes described in Section 1.2.1 or cyclometallated compounds.

All complexes in Table 1.8 were synthesized by reaction of RLi, RK or RMgBr reagent with an appropriate non-Cp actinide halide complex. Of the non-Cp alkyl complexes in Table 1.8, the only dialkyl actinide(IV) complexes bearing a single dianionic, non-carbocyclic supporting ancillary are $[(^{DIIP}NCOCN)U(CH_2SiMe_3)_2]$ {^{DIIP}NCOCN = O(CH$_2$CH$_2$NAr)$_2$; Ar = 2,6-diisopropylphenyl}, $[(^{tBu}NON)M(R)_2]$ {^{tBu}NON = O(SiMe$_2$NtBu)$_2$; M = Th or U; R = C_3H_5 or CH_2SiMe_3} and

[fc(NSi*t*BuMe$_2$)U(CH$_2$Ph)$_2$] {fc = Fe(C$_5$H$_4$)}, which were reported during the course of this work.[137,138]

1.3 – Thesis Goals

Organometallic actinide complexes are of particular interest due to their potential as catalysts for organic transformations such as olefin polymerization, hydrogenation, hydrosilylation and hydroamination. To date, the most prominent role in these studies has been played by carbocyclic ligands, providing a suitably well defined and robust platform for these metal centers. However, as highlighted above, very little work has been carried out to explore the effects of non-carbocyclic ancillaries in actinide organometallic chemistry. In fact, at the outset of this work, alkyl or hydride complexes supported by a single dianionic, non-cyclopentadienyl ancillary ligand remained unknown, and non-cyclopentadienyl actinide alkyl cations were also undiscovered.

We are interested in the preparation of non-carbocyclic organoactinide complexes to explore the structure and thermal stability of such complexes, and as a result of their largely untapped potential in both stoichiometric and catalytic organometallic reactivity. Of particular interest are neutral and cationic thorium(IV) alkyl and hydride complexes.

Chapter 2:

Non-Carbocyclic Ancillary Ligand Synthesis and Thorium(IV) Coordination Complexes

2.1 – Introduction to Chapter 2

2.1.1 – Non-Carbocyclic Ligand Design Criteria for Use in Actinide Chemistry

2.1.1.1 – General Considerations in Ligand Design

The development of well-designed and thermally stable actinide complexes mandates the careful design of ancillary ligands. Since thorium exists almost exclusively in the +4 oxidation state,[78] the option exists to use one, two or three valences for the supporting ligand framework, depending on the desired number of remaining reactive valences. Much of traditional organometallic reactivity requires two reactive valences, thus dianionic ancillary ligands are desirable (Figure 2.1). These ligands must also place sufficient steric demands on the metal complex to protect against undesirable aggregation, Lewis base ligation and ligand redistribution reactions without substantially diminishing the reactivity of the ensuing complexes.

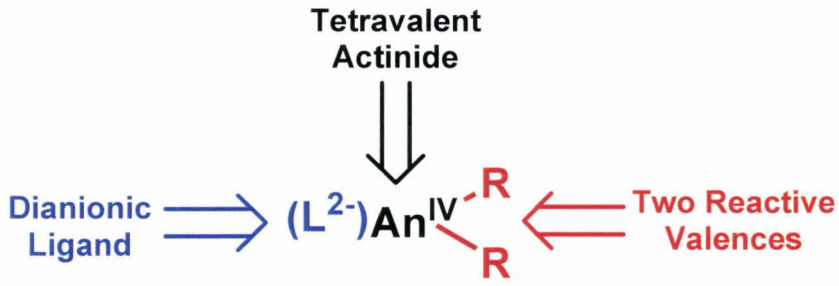

Figure 2.1: Desired composition of target non-cyclopentadienyl thorium complexes.

2.1.2 – Application of Common Non-cyclopentadienyl Ligands in Actinide Chemistry; The β-Diketiminate Anion as a Case Study

In the chemistry of the early transition metals, a wide variety of non-cyclopentadienyl alternatives exist.[139] A frequently encountered example is the β-diketiminato anion (nacnac), which has been coupled successfully with the majority of elements across the periodic table.[140] However, in the case of the actinide metals, its success has been severely limited, giving rise to undesired reactions and proving ineffective in its ability to provide an appropriately sized binding pocket for the metal center (Scheme 2.1).[141,142] For example, in the reaction of UCl_4 with the lithiated nacnac ligand, Li[(Me$_3$Si)NC(Ph)CHC(Ph)N(SiMe$_3$)], a dinuclear, dicationic U(VI) complex, with two U(V) counterions was formed through ligand degradation, redistribution and redox reactions. This reaction was also accompanied by the production of various uncharacterized organic byproducts. Reaction of $UI_3(THF)_4$ with two equivalents of K[(Ar)NC(Me)CHC(Me)N(Ar)] (Ar = 2,6-dimethylphenyl) also did not yield the expected structure. Instead, [(κ^2*NN*-nacnac)(η^3*NCC'*-nacnac)UI] was formed featuring one β-diketiminate ligand bound to uranium(III) in an unusual η^3*NCC'*-1-azaallyl mode.

This example highlights the reluctance of the nacnac ligand to enforce its typical coordination mode on uranium. By contrast, the reaction of $ThCl_4$ with $K[(Me_3Si)NC(Ph)CHC(Ph)N(SiMe_3)]$ did yield a bis-ligand complex with the nacnac ligand in its normal coordination mode. However, an actinide complex bearing a single nacnac ligand has not yet been reported, perhaps due to insufficient steric demands of the nacnac ligands employed thus far.

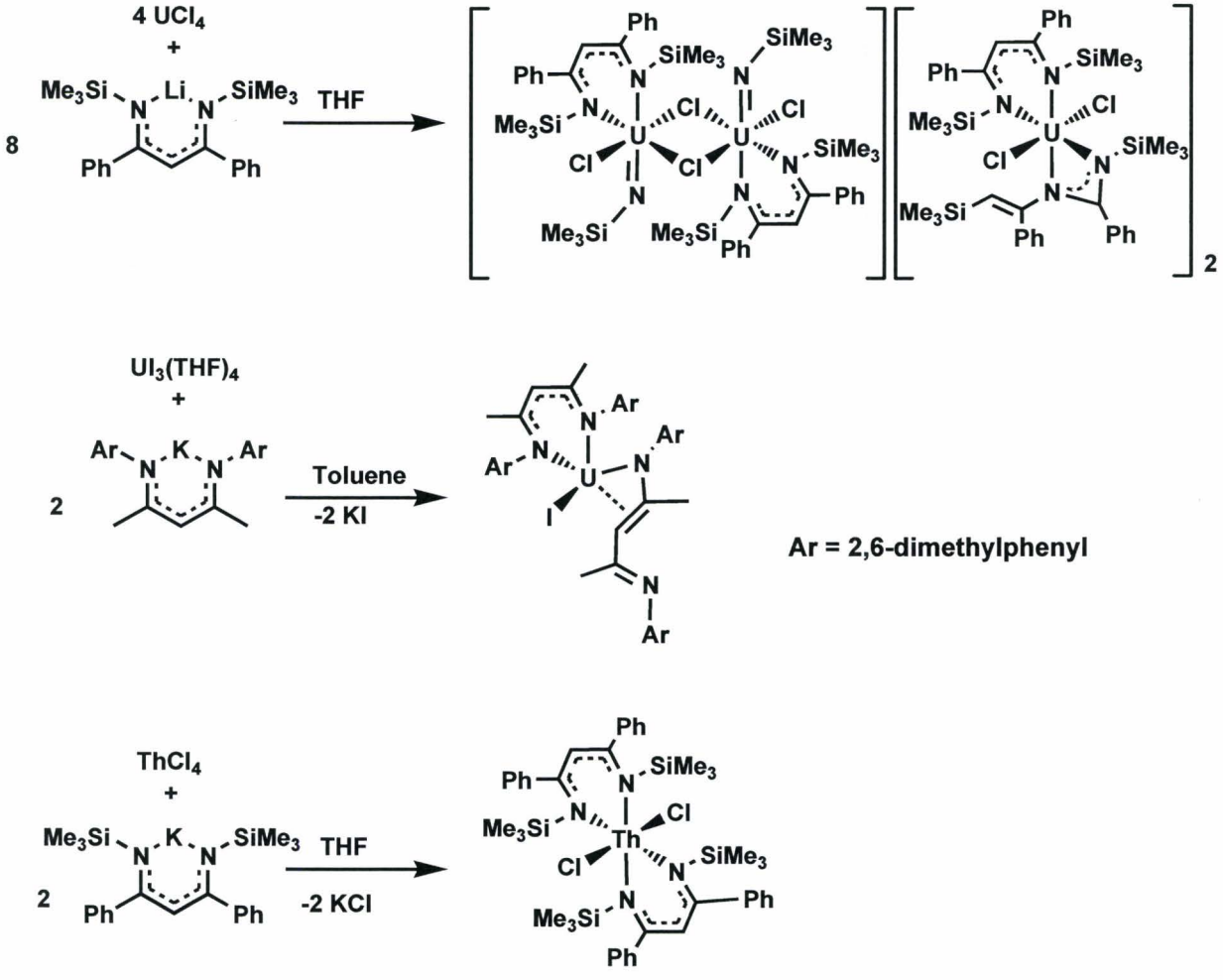

Scheme 2.1: Examples of uranium and thorium complexes formed by reaction with β-diketiminato ligand salts.

With these and related examples in mind[47,97,133-136,141,143,144] it was decided that the 2,6-bis(2,6-diisopropylanilidomethyl)pyridine {[BDPP]} dianion, previously employed in the chemistry of titanium, zirconium and tantalum (and more recently Y, La and Lu),[145-148] could potentially prove advantageous in the synthesis of highly stable, well defined thorium(IV) coordination and organometallic complexes.

2.1.3 – The [BDPP] Ligand

The [BDPP] ligand (Figure 2.2) is expected to be particularly suitable for thorium(IV) chemistry since it is tridentate, rigid, and planar. It also provides a binding pocket of suitable size to accommodate a large actinide metal, and contains only robust structural elements (*e.g.*, avoidance of isolated imine groups).[149,150] Our preference for rigid ligands stems from the expectation that they will (a) allow access to coordination environments that are dictated by design rather than the preferences of the central metal and/or co-ligands and (b) ensure that well-intentioned steric bulk is not positioned in such a way as to significantly limit its effectiveness. As a result, various modes of decomposition are expected to become less favorable, especially those involving sterically hindered transition states or the formation of dinuclear or bis-ligand complexes. Rigid ligands are also expected to be more amenable to steric tuning since the effects of steric bulk are not easily mitigated by alterations in the ligand geometry or hapticity and are, therefore, more predictable.

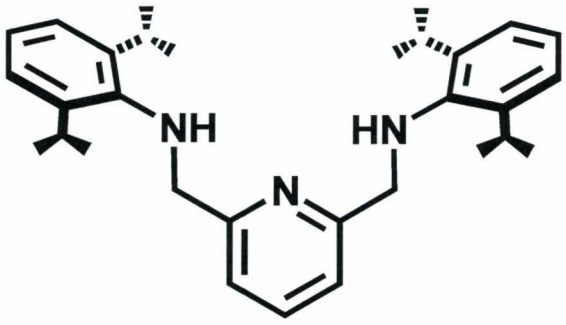

Figure 2.2: Pro-ligand H_2[BDPP].

The [BDPP] ligand has been shown to stabilize five-coordinate complexes of tantalum and titanium, and coordinates exclusively in a meridional fashion via the neutral pyridine donor between two anionic aryl amides. In the case of [(BDPP)$ZrMe_2$] (*vide infra*) when compared to [Cp_2ZrMe_2],[147,151] the coordination sphere of the compounds share many similar properties. In fact, comparable bond lengths (e.g., Zr–N_{amido}, Zr–Cent, Zr–Me; Cent = Cp centroid) and bond angles {N_{amido}–Zr–N_{amido} = 139.6(2)°, Cent–Zr–Cent = 132.5°; (BDEP): Me–Zr–Me = 102.4(3)°, (Cp_2): Me–Zr–Me = 95.6(12)°; Figure 2.3} suggest that the pyridine diamide ligand system may be considered as an electron deficient (6 electron donor) bis-cyclopentadienyl equivalent.

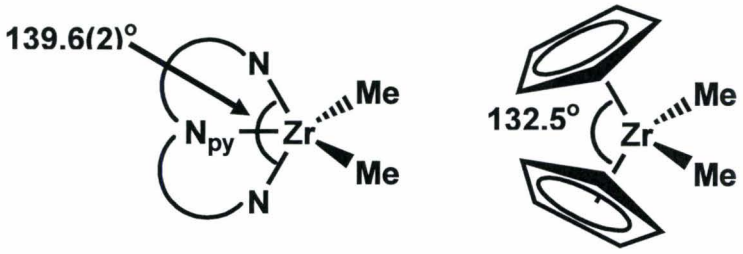

Figure 2.3: N_{amido}–Zr–N_{amido} and Cent–Zr–Cent angles in [(BDPP)$ZrMe_2$] and [Cp_2ZrMe_2].

A considerable advantage of this tridentate, dianionic ligand system versus carbocyclic ancillaries is the ease of manipulation of its steric properties. Several analogues may be accessed in a similar fashion to [BDPP], by reaction of 2 equivalents of LiNHR {R = 2,6-diethylphenyl, 2,6-dimethylphenyl} with 2,6-bis(bromomethyl)pyridine to yield the corresponding pro-ligands as viscous oils in multi-gram quantities, and at yields of greater than 50 % (Scheme 2.2).

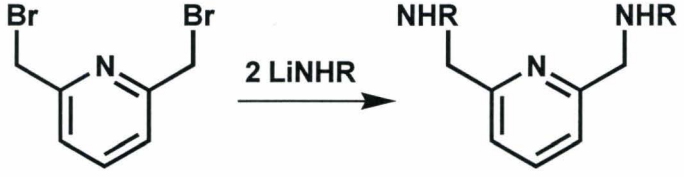

(BDPP) R = 2,6-$^{i}Pr_2$-C_6H_3
(BDEP) R = 2,6-Et_2-C_6H_3
(BDMP) R = 2,6-Me_2-C_6H_3

Scheme 2.2: Synthesis of bis-amino pyridine pro-ligands.

Extended Hückel molecular orbital calculations have been performed by McConville *et al.* on an idealized model of C_{2v} symmetry (Figure 2.4) for a

2,6-bis(amidomethyl)pyridine Zr fragment (NN_2Zr). The frontier orbitals were then compared with those reported for the bis-cyclopentadienyl zirconium analogue (Cp_2Zr).[152] The NN_2Zr 'd_{xz}' orbital ($5b_2$) has a comparable energy to the 'd_{xz}' in Cp_2Zr as a result of limited π-donation from the backbone pyridine to the metal. However, σ-donation from the pyridine donor in NN_2Zr does have a significant effect, raising the 'd_{z^2}'orbital ($12a_1$) in NN_2Zr to higher energy relative to the corresponding ($1a_1$) orbital of Cp_2Zr. The same phenomenon causes the increase in energy of the '$d_{x^2+y^2}$' orbital ($13a_1$) in the NN_2Zr fragment, but to a lesser degree.

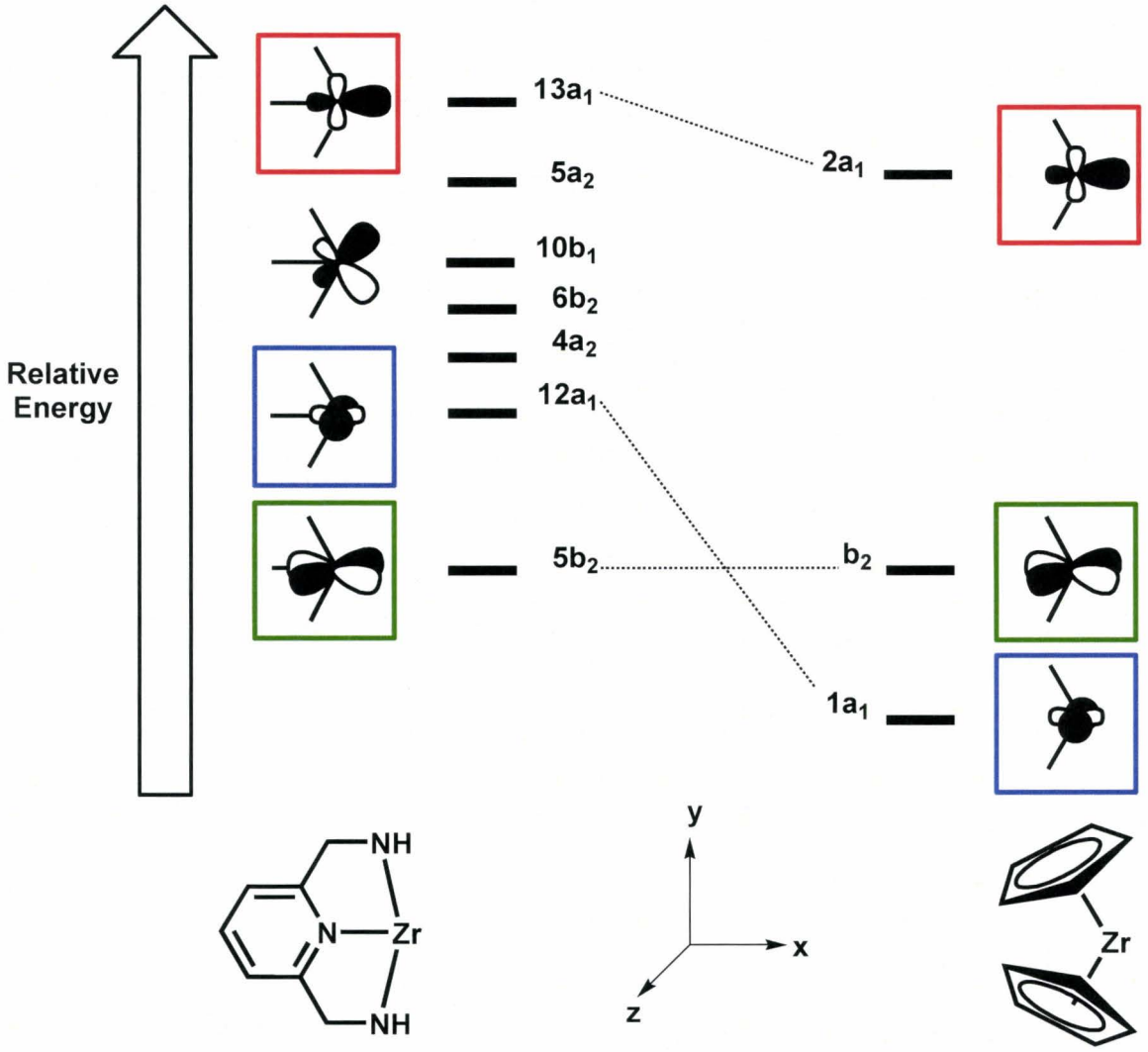

Figure 2.4: Frontier orbital comparison between an idealized 2,6-bis(amidomethyl)pyridine zirconium complex and a bis-cyclopentadienyl zirconium complex.[147]

2.1.4 – The [XA_2] Ligand

As an alternative to the [BDPP] ligand, the previously unknown 4,5-bis(2,6-diisopropylanilido)-2,7-di-*tert*-butyl-9,9-dimethylxanthene {[XA_2], Figure 2.5} ligand

was chosen. This ligand is considered a suitable candidate for actinide complex formation due to two main factors:

(1) Structural similarities with the [BDPP] ligand; [XA_2] is tridentate, dianionic and contains a neutral donor in a bridging position between two hard amido donors. Donor groups in the [XA_2] and [BDPP] ligands also occupy similar positions in the ligand framework.

(2) Increased ligand rigidity relative to [BDPP]. This is due to the tricyclic xanthene backbone, which enforces a more consistent metal binding environment when compared to the 2,6-dimethylpyridine backbone in [BDPP].

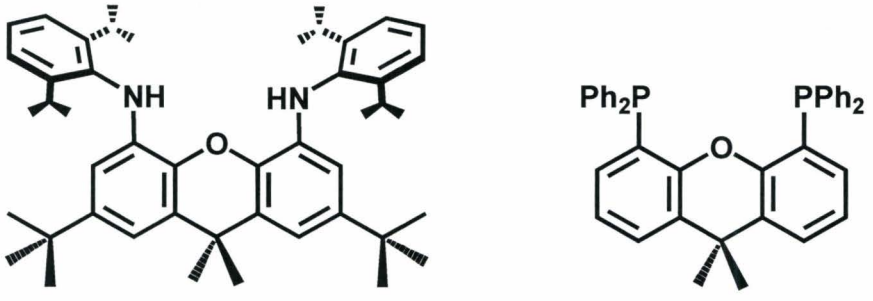

Figure 2.5: Structure of the $H_2[XA_2]$ pro-ligand (left) and the structurally related, neutral xantphos ligand (right).

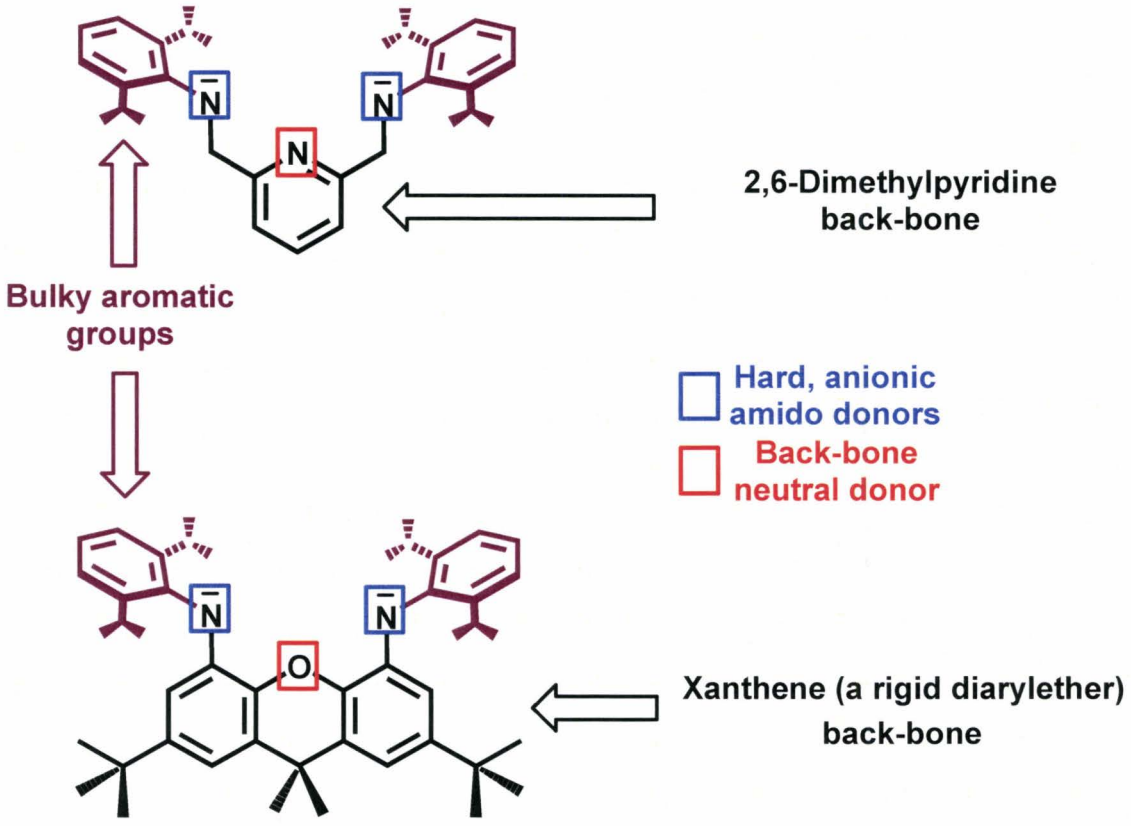

Figure 2.6: Comparison of the [BDPP] (top) and [XA_2] (bottom) ligands.

2.1.4.1 – The Xanthene Backbone as a Ligand Structural Motif

The xanthene back-bone has previously been utilized in neutral bis-phosphine ligands such as the xantphos ligand (Figure 2.5). This type of ligand enforces a large P–M–P bite angle, modulating the reactivity of transition metal centers by enforcing a constrained coordination geometry. The special structure of the xantphos ligand is responsible for the production of highly selective and active catalysts for hydroformylation, amination of aryl halides, and hydrocyanation.[153-155]

The vast majority of xantphos ligand complexes are κ^2-coordinated, and in the solid state, twisting of the xanthene backbone into a butterfly conformation occurs.[153] However, a planar xanthene backbone is observed in cationic complexes where κ^3*POP*-coordination is favored.[155,156]

At the outset of this work (2004), anionic ligands based on similar structural motifs to the xantphos ligand had not been reported, but have since become the subject of increased interest. During the course of this work (2006), Danopoulos reported the synthesis of *N*-cyclohexyl- and *N*-mesityl-substituted 4,5-bis-amidoxanthene ligands, which were used to synthesize dibenzyl and bis-dimethylamido titanium complexes. The authors of this work reported an inability to obtain alkali metal ligand salts, and thus work was limited to metal coordination through amine elimination.[100]

A 4,5-di-*tert*-butylphosphidoxanthene ligand was also reported recently (2007) and used to isolate a mononuclear zirconium amido complex and a heteronuclear zirconium-rhodium complex.[157]

2.1.5 – Tridentate and Potentially Planar Ligand Dianions in Actinide Chemistry

Both the $[BDPP]^{2-}$ and $[XA_2]^{2-}$ ligands are structurally related to the diamidoamine ligand $[(Me_3SiN(CH_2CH_2NSiMe_3)_2]^{2-}$ previously employed by Cloke *et al.* for the synthesis of dichloro and bis(ligand) thorium(IV) complexes.[158] During the course of this work, Leznoff and coworkers also developed the flexible dianionic NON-donor ligands $[O(CH_2CH_2NAr)_2]^{2-}$ {Ar = 2,6-diisopropylphenyl} and $[O(SiMe_2NtBu)_2]^{2-}$, and coupled them with thorium and uranium to make halide and alkyl complexes. However,

the rigidity of the ligand backbone increases dramatically in the order $[Me_3SiN(CH_2CH_2NSiMe_3)_2]^{2-}$ ~ $[O(CH_2CH_2NAr)_2]^{2-}$ {Ar = 2,6-diisopropylphenyl} < $[O(Me_2SiNtBu)_2]^{2-}$ < $[BDPP]^{2-}$ < $[XA_2]^{2-}$. As a result, significant differences in reactivity, complex nuclearity, and thermal stability can be expected in the chemistry of [BDPP] and $[XA_2]$.

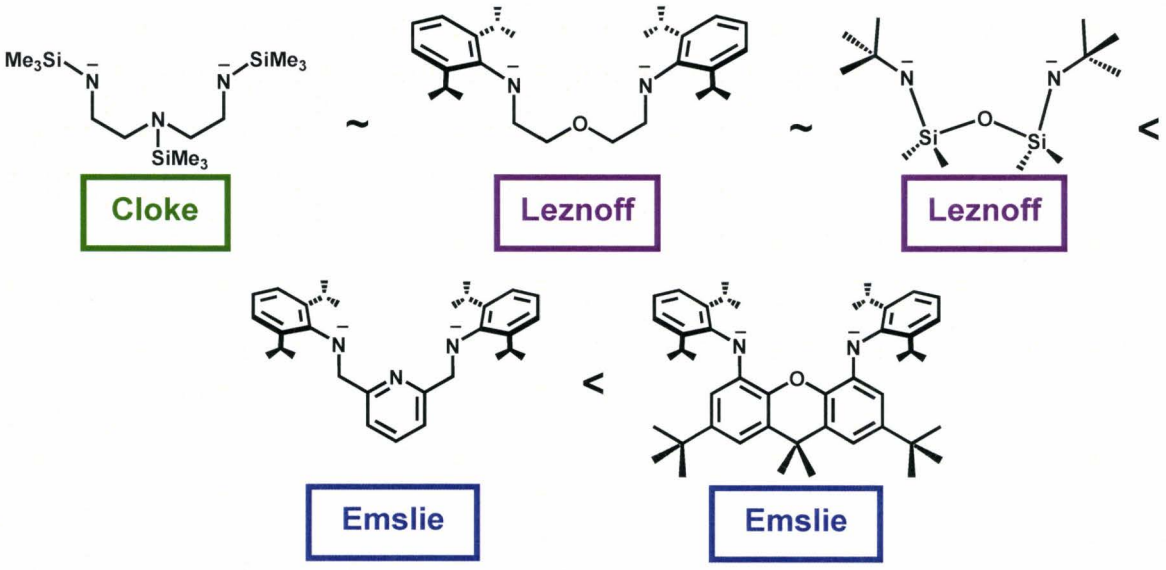

Figure 2.7: Planar, tridentate and dianionic non-carbocyclic ancillaries in the chemistry of thorium and uranium. Ligands are arranged in order of increasing rigidity. Names indicate the research groups responsible for investigation of each ligand in actinide chemistry.

2.1.6 – Ligand Attachment Protocols

Prior to the discussion of [BDPP] and $[XA_2]$ thorium complex formation, it is important to consider suitable methods for ligand attachment. There are three commonly

utilized methods for ligand attachment to a metal center: salt metathesis, amine elimination and alkane elimination. The first is the most versatile and involves the reaction of a metal halide precursor with an alkali metal salt of the ligand, eliminating an insoluble inorganic salt and yielding a metal halide species (equation 2.1). Amine elimination involves the reaction of a homoleptic metal amido compound $[M(NR_2)_y]$ with proteo ligand, giving rise to a metal amido complex and amine byproducts (equation 2.2). Alkane elimination is analogous to amine elimination, but with the proteo ligand $H_2[L]$ reacting with a homoleptic alkyl compound $[MR_x]$ to yield a metal alkyl complex and produce alkane byproducts (equation 2.3).

$$\mathbf{[ThCl_4(dme)_2] + Li_2[L] \longrightarrow [(L)ThCl_2(dme)] + 2\ LiCl + dme} \qquad \mathbf{(2.1)}$$

$$\mathbf{[Th(NR_2)_4] + H_2[L] \longrightarrow [(L)Th(NR_2)_2] + 2\ HNR_2} \qquad \mathbf{(2.2)}$$

$$\mathbf{[ThR_4] + H_2[L] \longrightarrow [(L)ThR_2] + 2\ HR} \qquad \mathbf{(2.3)}$$

A less common ligand attachment procedure involves the elimination of trimethylsilylchloride. In this approach, the bis-trimethylsilyl ligand derivative $[(Me_3Si)_2L]$ is reacted with the metal chloride salt, producing a ligated metal chloride compound and eliminating Me_3SiCl. However, this reaction often requires highly forcing conditions which may result in unacceptable levels of decomposition.

$$\mathbf{[ThCl_4] + [(Me_3Si)_2L] \longrightarrow [(L)ThCl_2] + 2\ Me_3SiCl} \qquad \mathbf{(2.4)}$$

The advantage of salt metathesis for ligand attachment is that it provides metal halides rather than amido or alkyl complexes, allowing subsequent conversion to a variety

of different organometallic or coordination compounds via standard techniques. The target compounds in this work are metal alkyl complexes, therefore, amine elimination is of limited use as a ligand attachment protocol. It is also important to note that for thorium in particular, the lack of thermally robust and appropriately substituted thorium tetraalkyl reagents contributes to the appeal of salt metathesis as the premier method for the production of new thorium complexes.

2.1.7 – Thorium Halide Starting Materials

For thorium, the base-stabilized tetrachloride, $[ThCl_4(dme)_2]$, is the most readily accessible anhydrous tetrahalide. $[ThCl_4(H_2O)_x]$ is first synthesized from hydrated thorium nitrate by reaction with refluxing, concentrated hydrochloric acid. After the evolution of NO_2 has ceased, solvent (concentrated HCl) is removed *in vacuo*. It is important at this stage to maintain the temperature well below 100 ^{o}C to avoid the formation of unwanted oxide/chloride and hydroxide/chloride species.[159] This step therefore takes several days when the reaction is performed on a 25 g scale. Coordinated water is then eliminated by refluxing in neat thionyl chloride yielding $[ThCl_4(OSCl_2)_x]$ from which coordinated $SOCl_2$ cannot be removed *in vacuo* at ambient or elevated temperatures. However, thionyl chloride may be displaced by Soxhlet extraction with dme to yield $[ThCl_4(dme)_2]$ in 52 % yield.

2.2 – Results and Discussion

2.2.1 – Synthesis of Pro-Ligands $H_2[XA_2]$ and $H_2[BDPP]$

The new NON-donor proligand $H_2[XA_2]$ (**1**) was synthesized in 86 % isolated yield by Hartwig-Buchwald coupling of 4,5-dibromo-2,7-di-*tert*-butyl-9,9-dimethyl-xanthene with 2,6-diisopropylaniline (Scheme 2.3).

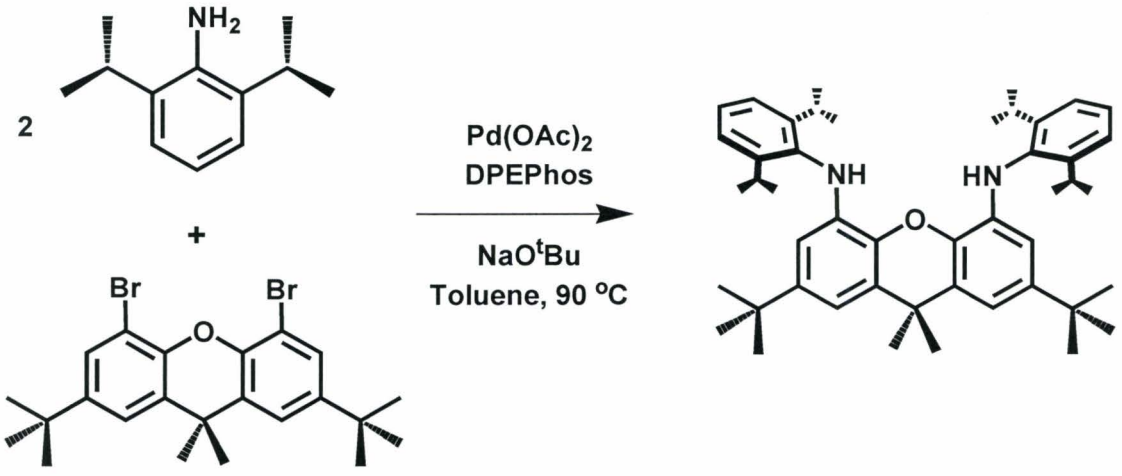

Scheme 2.3: Synthesis of pro-ligand $H_2[XA_2]$ (1).

2.2.2 – Synthesis of Alkali Metal $[XA_2]$ and [BDPP] Salts

Stirring $H_2[XA_2]$ with excess KH in 1,2-dimethoxyethane (dme) at room temperature for 5 hours gave base-stabilized $K_2(dme)_2[XA_2]$ (**2**) in 81 % yield. Alternatively, base-free $Na_2[XA_2]$ (**3**) was accessible by refluxing $H_2[XA_2]$ with excess NaH in toluene for several days (Scheme 2.4).

The NNN-donor ligand H_2[BDPP] was prepared as reported by McConville *et al.* (Scheme 2.2). The ligand synthesis is simple and readily scalable, allowing for production of multi-gram quantities of ligand.

An alkali or alkaline earth metal salt of the [BDPP] dianion, which would allow direct access to chloro complexes by salt metathesis, had not been reported. However, it was determined that reaction of H_2[BDPP] with 2 equivalents of an alkyl lithium reagent ($LiCH_2SiMe_3$ or *n*BuLi) in hexanes at –78 °C resulted in precipitation of base-free Li_2[BDPP] (**4**), which was isolated in 87 % yield as a bright yellow solid (Scheme 2.4). This compound is unusually temperature sensitive, decomposing in minutes upon dissolution in benzene or THF at room temperature, and is even less stable in toluene, where decomposition occurs rapidly at temperatures as low as –30 °C. The thermal decomposition of Li_2[BDPP] in benzene yields a mixture of unidentified, air-sensitive products. Solid **4** is substantially more stable, and although it does undergo significant decomposition over several hours at room temperature, it may be stored for weeks without appreciable decomposition at –30 °C.

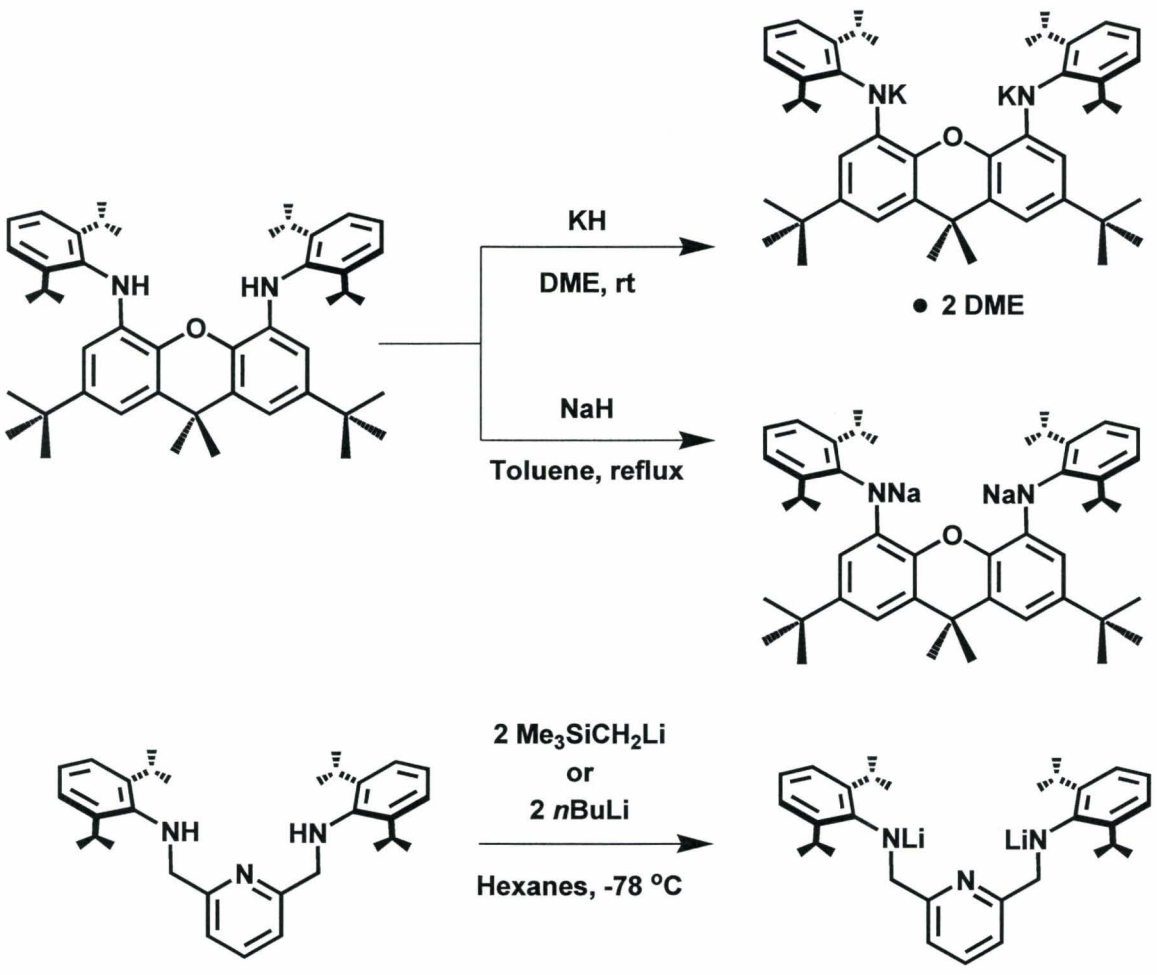

Scheme 2.4: Preparation of alkali metal salts of the [XA_2] (2 and 3; top) and [BDPP] (4; bottom) dianions.

2.2.3 – Dichloride Complexes [(L)$ThCl_2$(dme)], (L = [BDPP], [XA_2])

Reaction of 1 equivalent of Li_2[BDPP] (**4**) with [$ThCl_4(dme)_2$] in benzene at 0 °C produced [(BDPP)$ThCl_2$(dme)] (**5**) as an off-white solid in 51 % yield. Similarly, [(XA_2)$ThCl_2$(dme)] (**6**) was isolated in a 69 % yield by reaction of Na_2[XA_2] (**3**) with

$[ThCl_4(dme)_2]$ in toluene at room temperature (Scheme 2.5). In contrast to the observed reactivity of the base-free ligand sodium salt (**3**), base-coordinated $K_2(dme)_2[XA_2]$ (**2**) is considerably less reactive, despite similar solubilities of the two $[XA_2]$ salts in benzene and toluene; the reaction between **2** and $[ThCl_4(dme)]$ is complete only after refluxing in toluene for 12 hours.

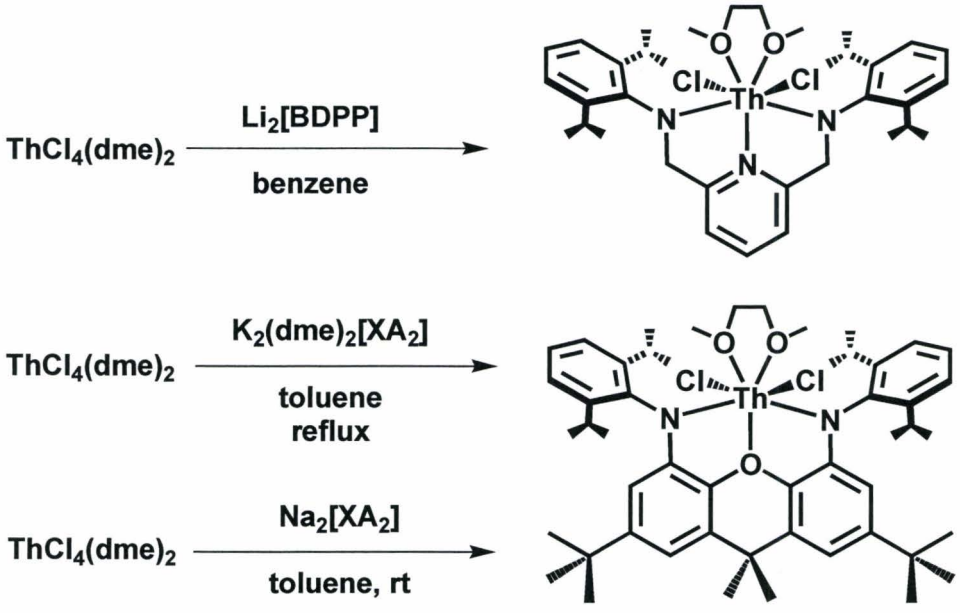

Scheme 2.5: Synthesis of Dichloro Complexes 5 (top) and 6 (bottom).

An alternative route to [BDPP] complex **5** involves the reaction of 2 equivalents of $LiCH_2SiMe_3$ with $[ThCl_4(dme)_2]$ for 1 hour at 0 °C, followed by cooling to –78 °C and addition of $H_2[BDPP]$. In this case, ligand attachment likely proceeds by alkane elimination from a source of "$ThCl_2(CH_2SiMe_3)_2$". However, the reaction of $LiCH_2SiMe_3$ (2 equivalents) with $[ThCl_4(dme)_2]$ formed a mixture of products in solution,

the nature of which was not determined (Scheme 2.6). Nevertheless, this is the preferred route for the synthesis of **5** due to the greater simplicity and improved yield (85 %). By contrast, attempts to prepare **6** by this method gave solutions containing $H_2[XA_2]$ and $SiMe_4$ as the only soluble products, presumably due to thermal decomposition of the alkyl thorium precursor in preference to reaction with the rigid $H_2[XA_2]$ pro-ligand.

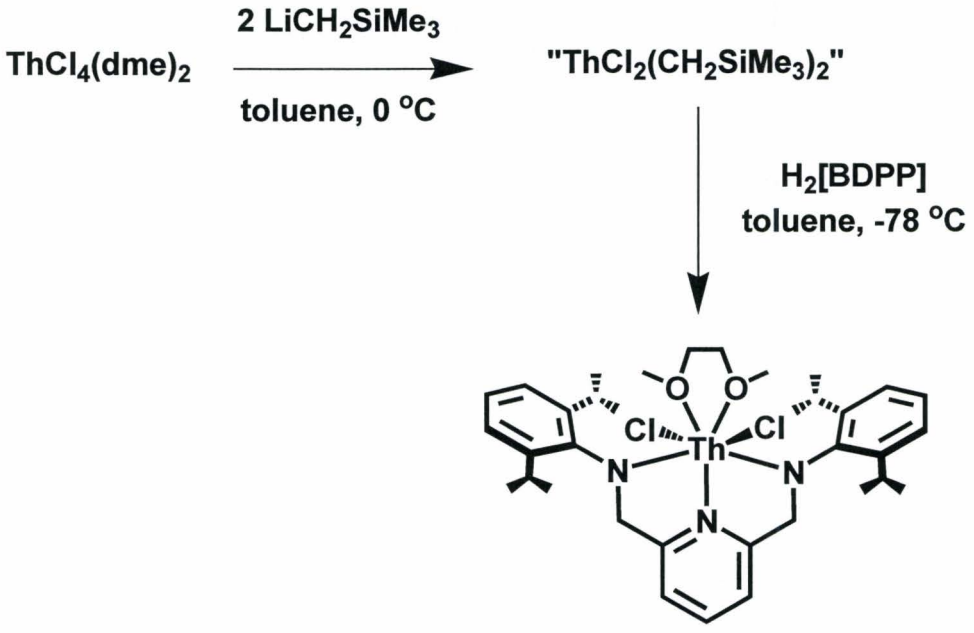

Scheme 2.6: Alternative route for the synthesis of 5 via "$ThCl_2(CH_2SiMe_3)_2$".

^{1}H NMR spectra of **5** and **6** between 20 and –90 °C show the presence of one molecule of symmetrically coordinated dme and a lone C*H*Me_2 signal, consistent with C_{2v} symmetric, pentagonal bipyramidal products. The isopropyl methyl groups of the arene group in both **5** and **6** are diastereotopic, due to restricted rotation about the N–C_{ipso} bond, yielding two doublets in the ^{1}H NMR spectrum. Single crystals of

[(BDPP)$ThCl_2$(dme)]•2toluene were grown by slow diffusion of hexanes into a toluene solution of **5** at –30 °C. The X-ray crystal structure of **5•2toluene** (Figure 2.8, Table 2.1) confirms a distorted pentagonal bipyramidal geometry with the two chloride anions occupying apical positions [Cl(1)–Th–Cl(2) = 156.38(10)°; Th–Cl = 2.698(3) and 2.686(3) Å]. As anticipated, the [BDPP] ligand is approximately planar and binds thorium via short Th-$N_{anilido}$ contacts [2.305(9) and 2.321(8) Å] and a longer Th–N_{py} bond [2.568(9) Å]. However, while N(1), N(3), O(1), O(2), and Th lie in a plane, the metal is located 0.33(1) Å above the N(1)–N(2)–N(3) plane of the [BDPP] ligand. In this way, only one chloro ligand, Cl(1), is positioned directly between the bulky isopropyl groups, while the other, Cl(2), is located in a more open region of the thorium coordination sphere. Furthermore, to minimize unfavorable steric interactions with Cl(1), the 2,6-diisopropylphenyl rings rotate to give C(14)•••C(26) = 6.35(2) Å and C(17)•••C(29) = 7.26(2) Å.

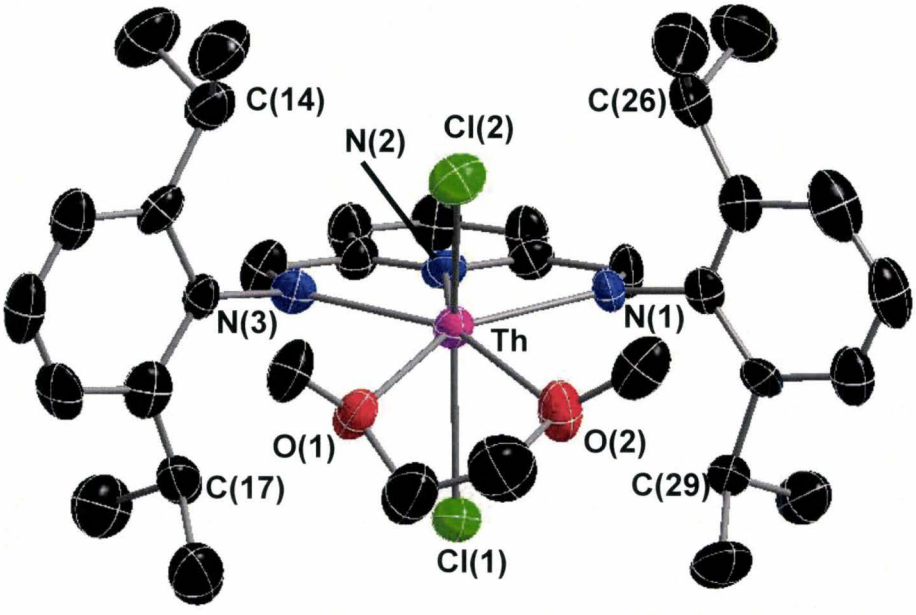

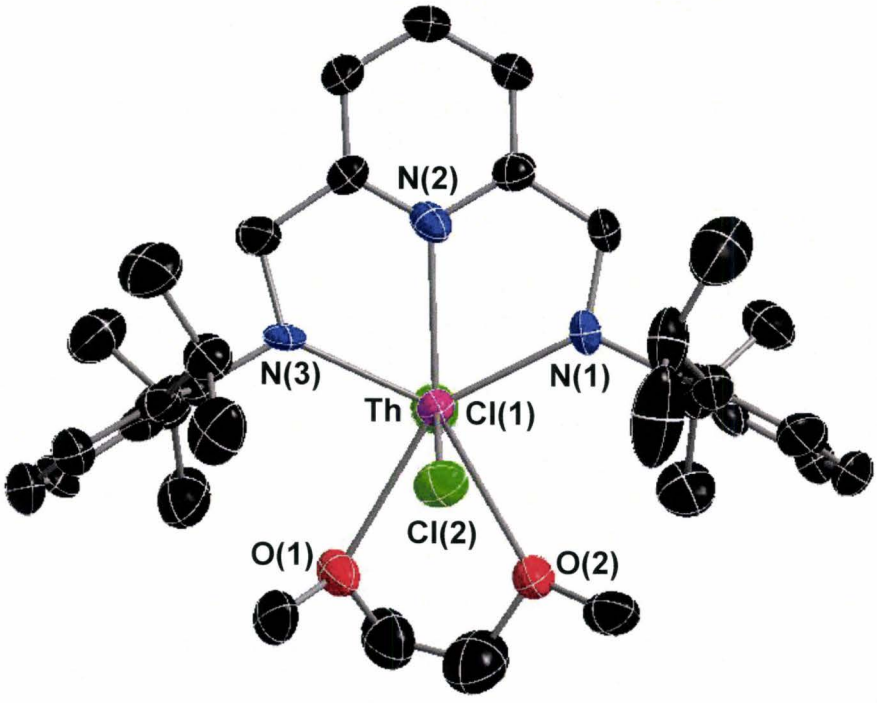

Figure 2.8: Molecular structure of 5•2toluene. Thermal ellipsoids at the 50 % probability level. Hydrogen atoms and non-coordinated solvent omitted for clarity.

The dme molecule in **5** is κ^2-coordinated in the pentagonal plane and is bound via long and unequal Th–O contacts {Th–O(1) = 2.674(8) Å and Th–O(2) = 2.724(8) Å}, likely due to steric pressure at the metal; cf. Th–O distances of 2.564(8)-2.620(8) Å in $[ThBr_4(\kappa^2\text{-dme})_2]$,[160] 2.620(5) Å in $[LTh(NH_2)(\kappa^1\text{-dme})]^-$ and 2.613(3) Å in $[LThCl(\kappa^1\text{-dme})]^-$ {L = 2,2′-methylenebis(6-*tert*-butyl-4-methylphenolate)}.[161] In contrast, the Th–N_{py} bond {2.568(9) Å} is atypically short. For example, Th–N is 2.72(1)-2.80(1) Å in [Th(quinolinolate)$_4$(dmf)],[162] 2.730(6) Å in $[\{Th(OCHEt_2)_3(\mu\text{-}OCHEt_2)(py)\}_2]$, 2.752(7) Å in *cis*-$[Th(O\textit{t}Bu)_4(Py)_2]$,[163] and 2.662(8), 2.696(8) in *cis*-$[Th(OC_6H_3Me_2\text{-}2,6)_4(py)_2]$.[164] The only Th–$NC_5R_5$ bonds of comparable length are found in $[Th(OC_6H_3\textit{t}Bu_2\text{-}$

2,6)$_2$(κ^2*CN*-2,6-lutidinyl)$_2$] {2.61(1) Å}[134] which is a special case since significant delocalization of negative charge to the N-donor can occur. Therefore, the short Th–N_{py} bond lengths observed in complex **5** (and other thorium [BDPP] complexes in this work) are likely a result of incorporation of the pyridine unit into a rigid ligand framework, perhaps augmented by the enhanced donor properties of N_{py} in [BDPP] (relative to an unsubstituted pyridine) as a result of 2,6-dialkyl substitution. All other metal-ligand bonds are in the usual range. For comparison, Th–$N_{anilido}$ distances are 2.327(6)-2.378(7) Å in $[L_2ThCl]^-$ {L = 1,3-bis(2,6-diisopropylanilido)propane}[165] and 2.299(7), 2.304(6) Å in [Th{N(SiMe$_3$)$_2$}$_2$(NMePh)$_2$],[166] while Th–Cl is 2.620(6)-2.697(1) Å in [L_2ThCl_2] {L = Tp, ArC(NSiMe$_3$)$_2$, and HC(CPhNSiMe$_3$)$_2$; Ar = $C_6H_2(CF_3)_3$-2,4,6}[167] and 2.673(1), 2.721(2) Å in [L′ThCl(THF)] {L′ = Me$_3$SiN(C$_2$H$_4$NSiMe$_3$)$_2$}.[158]

2.2.4 – Synthesis of [(BDPP)Th(NEt$_2$)$_2$]

The reactivity of dichloride [(BDPP)$ThCl_2$(dme)] (**5**) was assessed initially by reaction with two equivalents of $LiNEt_2$, yielding bis-amido complex [(BDPP)Th(NEt$_2$)$_2$] (**7**) in 64 % yield (Scheme 2.7). This complex is highly soluble in hydrocarbon solvents including hexanes and hexamethyldisiloxane; a trait that may be responsible for the moderate isolated yield, despite quantitative formation by NMR spectroscopy.

In solution (22 to –80 °C), complex **7** exhibits top-bottom and side-side symmetry by ^{1}H and ^{13}C NMR spectroscopy. A single set of C*H*Me$_2$ and py-C*H*$_2$ signals are visible at 3.70 and 5.17 ppm respectively, and the CH*Me*$_2$ signals are observed as doublets at 1.42 and 1.30 ppm in the ^{1}H NMR spectrum. The diethyl amido groups are

indistinguishable by NMR spectroscopy at room temperature, and remain equivalent upon cooling of the solution to –80 °C, giving rise to a quartet and a triplet for the NCH_2 and NCH_2CH_3 protons at 3.00 and 0.87 ppm respectively.

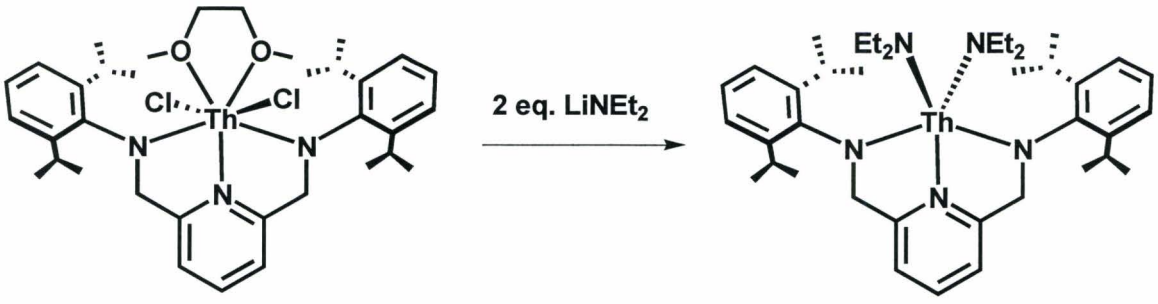

Scheme 2.7: Synthesis of bis-amido complex [(BDPP)Th(NEt_2)$_2$] (7).

Table 2.1: Crystallographic data collection and refinement parameters and selected bond distances for complexes 5•2toluene and 8

	5•2toluene	**8**
Formula	$C_{91}H_{126}Cl_4N_6O_4Th_2$	$C_{62}H_{82}N_6Th$
fw	1973.86	1143.38
Cryst. Syst.	Monoclinic	Monoclinic
Space group	*C2/c*	*C2/c*
a(Å)	28.7133(8)	14.901(15)
b(Å)	15.8253(5)	17.895(17)
c(Å)	21.3589(7)	21.354(16
α(deg)	90	90
β(deg)	107.398(2)	106.72(3)
γ(deg)	90	90
Volume(Å^3)	9261.4(5)	5453(9)
Z	4	4
Density(calcd; mg/m^3)	1.449	1.393
μ(mm^{-1})	3.374	2.779
F(000)	4074	2344
Cryst size (mm^3)	0.22 x 0.22 x 0.18	0.12 x 0.10 x 0.03
θ range for collection(deg)	1.49 to 27.54	1.83 to 25.50
No. of reflns. collected	40126	20838
No. of indep. reflns.	10567	5071
Completeness to θ_{max}	98.9 %	100.0 %
Max. and min. transmn.	0.55 and 0.455	0.920 and 0.711
GOF on F^2	1.003	1.100
Final R_1 [$I > 2\sigma(I)$]	R1 = 0.0665	R1 = 0.0702
	wR2 = 0.1313	wR2 = 0.1140
R indices (all data)	R1 = 0.1685	R1 = 0.0963
	wR2 = 0.1654	wR2 = 0.1198
Th–N_{amido}	2.305(9), 2.321(8)	2.373(7), 2.488(7)
Th–N_{py}	2.568(9)	2.614(7)
Th–Cl	2.686(3), 2.698(3)	n.a.
Th–O_{dme}	2.674(8), 2.724(8)	n.a.

For **5•2toluene** and **8**: T = 173(2) K, wavelength = 0.71073 Å, absorption correction = semiempirical from equivalents, and refinement method = full-matrix least-squares on F^2.

2.2.5 – Bis-ligand Complexes

The bis-ligand complex $[(BDPP)_2Th]$ (**8**) was accessed in 73 % yield by addition of benzene to 2 equivalents of $Li_2[BDPP]$ (**4**) and $[ThCl_4(dme)_2]$ at –78 °C, followed by warming to room temperature. Alternatively, addition of 1 equivalent of $H_2[BDPP]$ to a solution of $[(BDPP)Th(CH_2SiMe_3)_2]$ (**9**, *vide infra*) followed by heating to 100 °C for 24 hours in a sealed reaction vessel resulted in $SiMe_4$ elimination to form the bis-ligand complex $[Th(BDPP)_2]$ (**8**) as a pale greenish-yellow solid in 37 % isolated yield (Scheme 2.8).

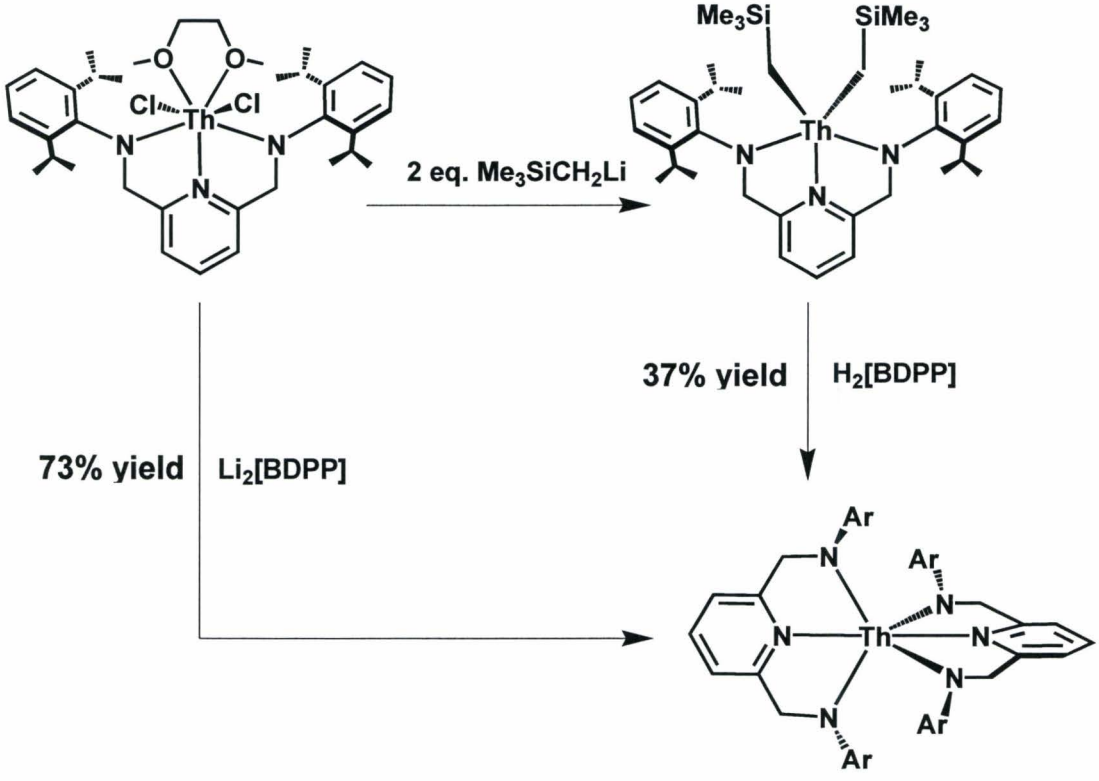

Scheme 2.8: Bis-ligand complex (8) formation by salt metathesis or alkane elimination.

Solution NMR spectra of **8** between 20 and –35 °C (in d_5-bromobenzene) are consistent with a highly symmetrical product containing a single C*H*Me$_2$ environment. Crystals of **8** suitable for X-ray diffraction were grown by cooling a saturated toluene solution of **8** from room temperature to –30 °C (Figure 2.9, Table 2.1). Complex **8** adopts an unusual six-coordinate geometry in which the four amido donors form a distorted tetrahedron around thorium (see red N–Th bonds in Figure 2.9) while the pyridine units are directed toward two of the edges {N(2)•••N(3) and N(2)′•••N(3)′} of the tetrahedron but offset toward the center of the two smaller faces {N(1) is offset toward the N(3), N(3)′, N(2) face and N(1)′ is offset toward the N(3), N(3)′, N(2)′ face}. Above each of the two larger faces, which are defined by N(2), N(2)′ and X, where X is N(3) or N(3)′ of the tetrahedron, are three of the eight isopropyl groups (Figure 2.9). In order to adopt such a distorted geometry, the two identical [BDPP] ligands are considerably twisted away from planarity and the C(4)–N(1)–Th angle is far from linear at 165°. This situation likely arises due to severe steric crowding at the metal, resulting in a geometry influenced more strongly by the anionic N_{amido} donors than the neutral pyridine units. Steric pressure at the metal center is also considered to be responsible for the significant differences in Th–$N_{anilido}$ bond lengths {Th–N(3) = 2.368(7) Å and Th–N(2) = 2.488(6) Å}, as well as Th–$N_{anilido}$ and Th–N_{py} bonds {Th–N_{py} = 2.615(6) Å} which are considerably longer than those observed in the structure of the dichloro [BDPP] complex **5** {and dialkyl [BDPP] complexes **9** and **11**; *vide infra*}.

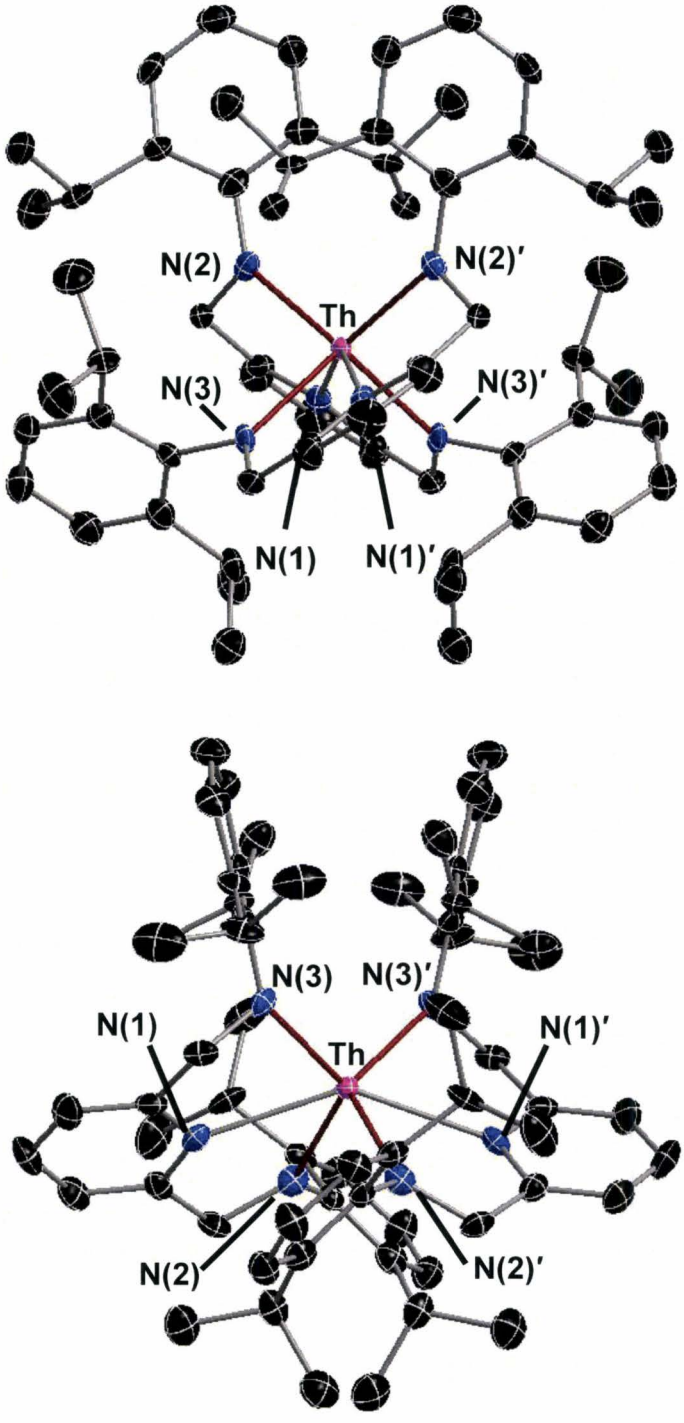

Figure 2.9: Molecular structure of bis-ligand complex 8. Thermal ellipsoids at the 50% probability level. Hydrogen atoms and non-coordinated solvent are omitted for clarity.

Attempts to prepare the analogous $[Th(XA_2)_2]$ complex by either salt metathesis or alkane elimination were unsuccessful: $[(XA_2)ThCl_2(dme)]$ (**6**) failed to react with $K_2(dme)_2[XA_2]$ (**2**) or $Na_2[XA_2]$ (**3**) at temperatures up to 110 °C, and $[(XA_2)Th(CH_2SiMe_3)_2]$ (**10**, *vide infra*) did not react with $H_2[XA_2]$ (**1**) at temperatures below the onset of thermal decomposition (80 °C). A lack of reactivity was also observed in attempts to prepare the mixed ligand derivative $[Th(BDPP)(XA_2)]$ by salt metathesis {$[(BDPP)ThCl_2(dme)]$ + $Na_2[XA_2]$ up to 110 °C} or alkane elimination {$[(BDPP)Th(CH_2SiMe_3)_2$ + $H_2[XA_2]$ up to 110 °C} in toluene.

The marked difference in [BDPP] and $[XA_2]$ ligand reactivity presumably stems from the enhanced rigidity of κ^3-coordinated $[XA_2]$, which does not permit the type of ligand twisting observed in $[Th(BDPP)_2]$ (**8**). As a result, $[XA_2]$ ligand coordination (κ^3*NON*- or even κ^2*NN*-donation, which would likely allow the xanthene backbone of $[XA_2]$ to adopt a butterfly conformation) to form $[ThL(XA_2)]$ {L = [BDPP] or $[XA_2]$} must be rendered sterically inaccessible. Given that alkyl complex decomposition by ligand redistribution requires the formation of bis-ligand complexes (*e.g.* $L_2ThR_2 \rightarrow ThR_4 + ThL_2$) the ability of the $[XA_2]$ ligand to prevent $[Th(XA_2)_2]$ formation may be expected to result in enhanced thermal stability of organothorium $[XA_2]$ derivatives, certainly with respect to this particular decomposition pathway.

2.3 – Conclusions

In summary, a rigid, dianionic ligand based on the xanthene back-bone has been designed for application in the coordination and organometallic chemistry of the

actinides. The new [XA_2] ligand, along with the previously reported [BDPP] ligand, have been used successfully for the synthesis and isolation of stable and well defined thorium coordination complexes. Ligand attachment was achieved through salt metathesis by reaction of sodium or potassium salts of [XA_2] or the lithium salt of [BDPP] with [$ThCl_4(dme)_2$]. Alternatively, alkane elimination was employed to affect ligand attachment by reaction of "$Th(CH_2SiMe_3)_2Cl_2$" with H_2[BDPP]. The effect of varying structural rigidity between the [XA_2] and [BDPP] ligands is illustrated by the ability of the [BDPP] dianion to form a highly strained bis-ligand complex; a feat that could not be imitated by the [XA_2] dianion. The synthesis of organothorium [BDPP] and [XA_2] complexes, in particular neutral and cationic alkyl derivatives will be described in the following chapters of this thesis.

Chapter 3:

Synthesis and Characterization of Neutral and Anionic Thorium(IV) Alkyl Complexes

3.1 – Introduction to Chapter 3

3.1.1 – Actinide Alkyl Complexes

Initial interest in organoactinide chemistry, especially in homopleptic alkyl and borohydride complexes, stemmed from potential applications in uranium isotope separation processes. However, low thermal stability prevented significant progress in this area (see section 1.2.1).[33,168] More recently, the scope of potential applications involving the actinides has expanded to include stoichiometric and catalytic reactivity. Of particular interest are reaction types which differ from those performed by transition metal and lanthanide complexes, and studies to probe the role of the 5f and 6d orbitals in actinide–ligand bonding.

Non-cyclopentadienyl actinide(IV) bis-hydrocarbyl (alkyl, allyl, or aryl) complexes are particularly rare and generally rely on the coordination of monoanionic anicillaries such as alkoxy or aryloxy,[47,97,133,134] amidinate,[135] and tris(pyrazolyl)borate[136,143] ligands (see section 1.2.3). The only other dialkyl actinide(IV) complexes bearing a single dianionic, non-carbocyclic supporting ligand are $[(^{DIIP}NCOCN)U(CH_2SiMe_3)_2]$ {$^{DIIP}NCOCN$ = $O(CH_2CH_2NAr)_2$; Ar = 2,6-diisopropylphenyl}, $[(^{tBu}NON)M(R)_2]$ {M = Th or U; R = C_3H_5 or CH_2SiMe_3; ^{tBu}NON =

$O(SiMe_2NtBu)_2\}$[137,138] and $[\{fc(NSitBuMe_2)_2\}U(CH_2Ph)_2]$ $\{fc = Fe(C_5H_4)_2^{2-}\}$,[128] which were reported during the course of this work (Figure 3.1).

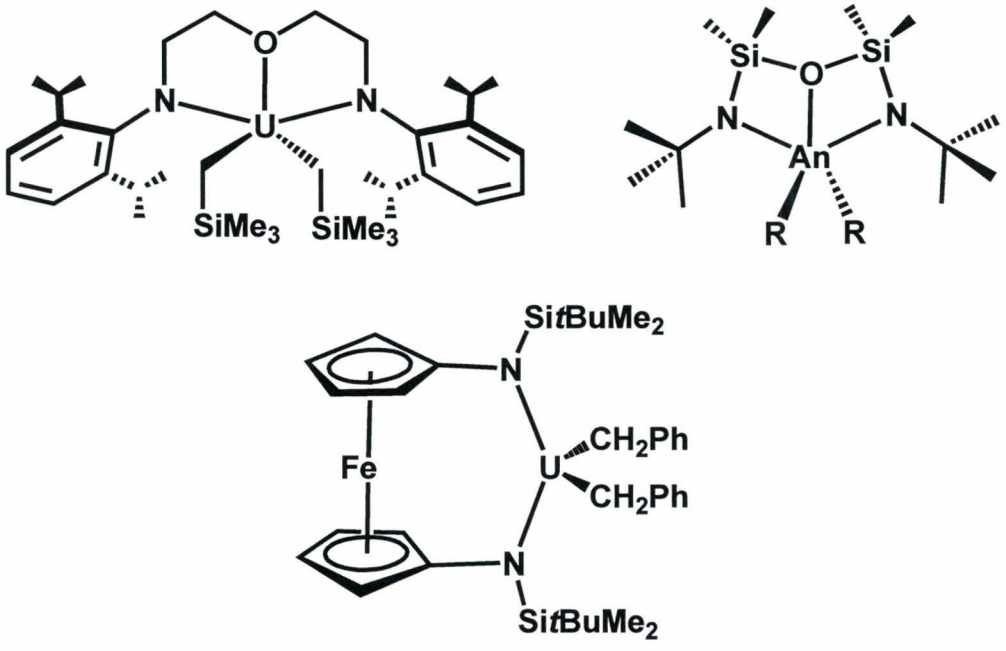

Figure 3.1: Dialkyl actinide complexes bearing a single, dianionic, non-carbocyclic ligand reported during the course of this work. An = Th or U; R = C_3H_5 or CH_2SiMe_3.

In this chapter, the synthesis and properties of $[XA_2]$ and [BDPP] thorium(IV) trimethylsilylmethyl (CH_2SiMe_3), benzyl (CH_2Ph), *n*-butyl (*n*Bu) and methyl (CH_3) complexes are discussed. Reactions of thorium(IV) chloro complexes with alkyl Grignard reagents resulting in unexpected halogen exchange or ancillary ligand transfer reactivity are also included.

3.2 – Results and Discussion

3.2.1 – Thorium(IV) Bis-trimethylsilylmethyl Complexes and $[Th(CH_2SiR_3)_4(dme)_n]$ Precursors

Reaction of dichlorides **5** and **6** with 2 equivalents of $LiCH_2SiMe_3$ gave the base- and salt-free dialkyl complexes $[LTh(CH_2SiMe_3)_2]$ {L = [BDPP] (**9**) and $[XA_2]$ (**10**)} in quantitative yields by ^1H NMR spectroscopy (68 % and 63 % isolated yields, respectively; Scheme 3.1).

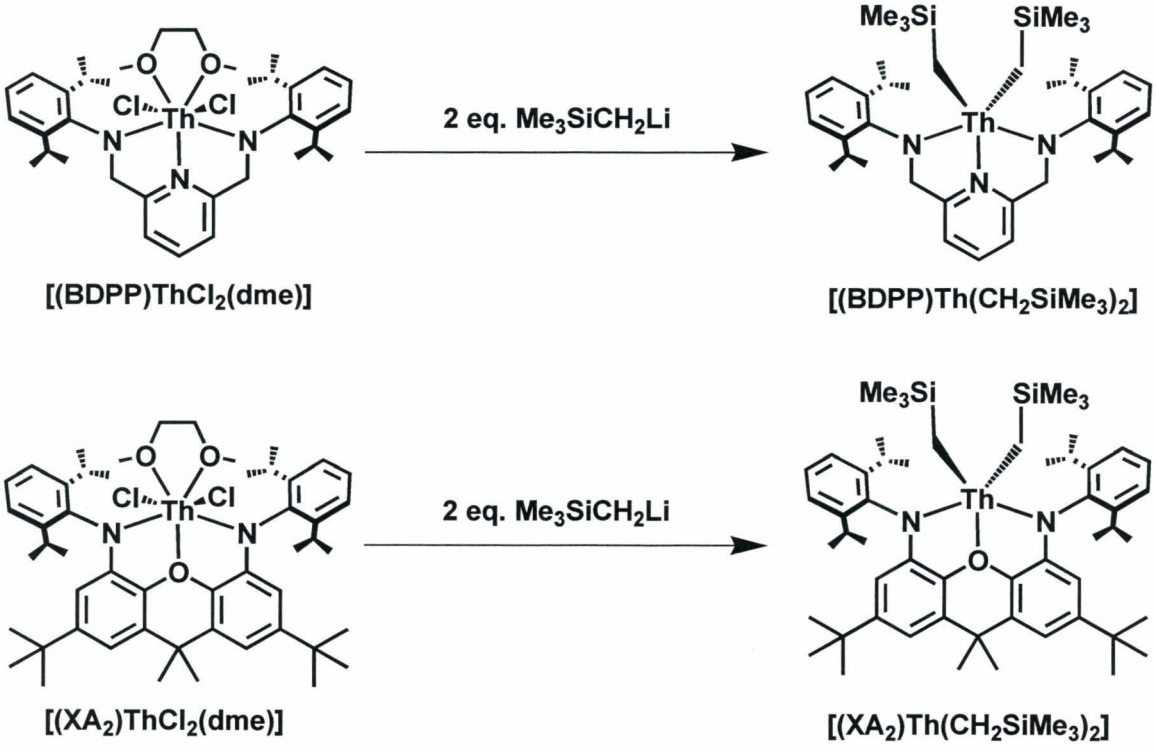

Scheme 3.1: Synthesis of dialkyl complexes $[(BDPP)Th(CH_2SiMe_3)_2]$ (9) and $[(XA_2)Th(CH_2SiMe_3)_2]$ (10).

However, a more straightforward route to these complexes involved reaction of $[ThCl_4(dme)_2]$ with 4 equivalents of $LiCH_2SiMe_3$ at –78 °C for one hour, then warming the reaction mixture to 0 °C for one hour, re-cooling to –78 °C, and the addition of $H_2[BDPP]$ or $H_2[XA_2]$. Using this method, which likely proceeds by alkane elimination from a source of "$Th(CH_2SiMe_3)_4(dme)_n$", tan **9** and white **10** were isolated in 82 % and 49 % yield respectively.

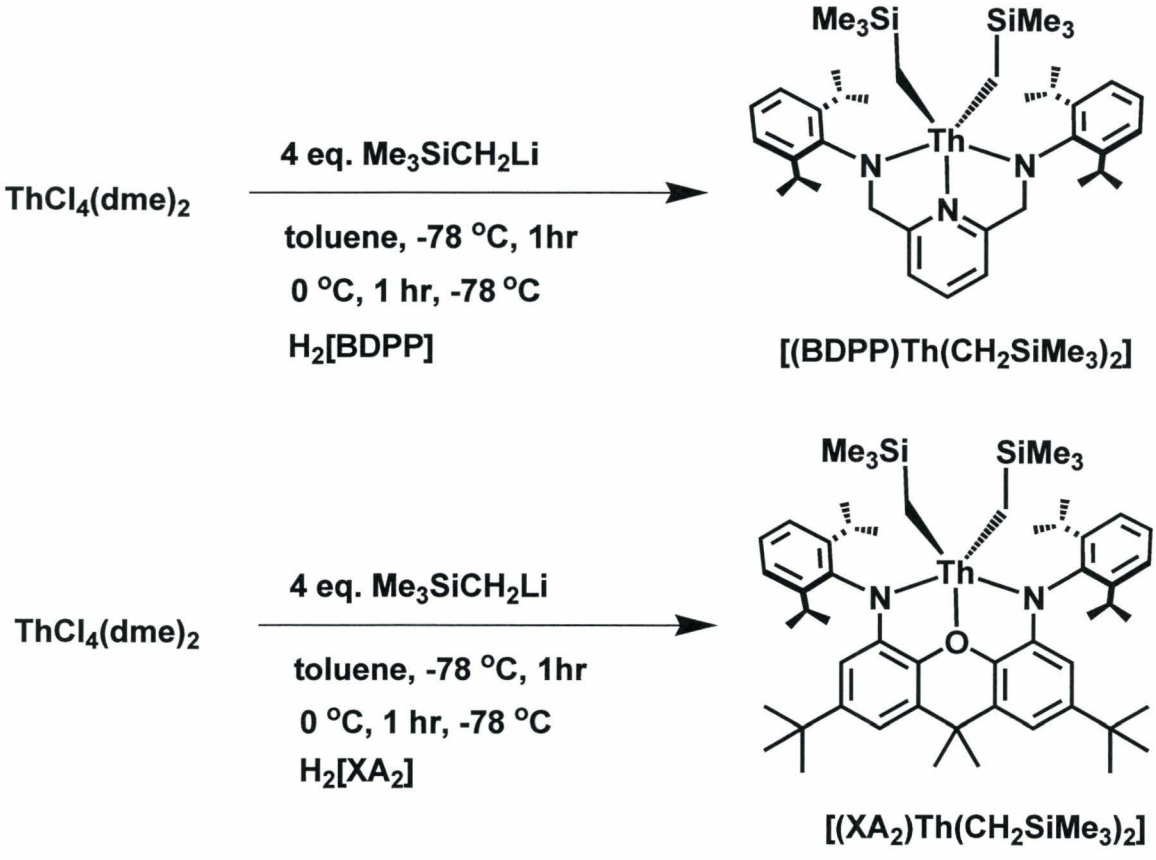

Scheme 3.2: Alternative synthesis of compounds 9 and 10 by alkane elimination from "$Th(CH_2SiMe_3)_4(dme)_n$".

The initial reaction between $[ThCl_4(dme)_2]$ and $LiCH_2SiMe_3$ proceeded cleanly and reproducibly to form a product or mixture of products giving rise to a single set of

O*Me*, O*CH*$_2$, Si*Me*$_3$, and C*H*$_2$SiMe$_3$ signals in the ^{1}H NMR spectrum at 20 °C (Figure 3.2), with no change down to –90 °C. Unfortunately, the oily nature and thermal instability (decomposition was complete after 1.5 hours at 20 °C) of this material precluded its isolation. The syntheses of related complexes bearing bulkier CH_2SiMe_2Ph and $CH_2SiMePh_2$ alkyl groups was also investigated in attempts to obtain products with higher thermal stability and crystallinity. However, the reaction of four equivalents of $LiCH_2SiMe_2Ph$ or $(dme)LiCH_2SiMePh_2$ with $[ThCl_4(dme)_2]$ under analogous conditions, yielded similar results to the $LiCH_2SiMe_3$ reaction, producing only oily compounds of low thermal stability that lacked any appreciable crystallinity. The product of the reaction between $[ThCl_4(dme)_2]$ with $LiCH_2SiMe_2Ph$, presumably "$Th(CH_2SiMe_2Ph)_4(dme)_n$" was further reacted with H_2[BDPP] to yield dialkyl complex [(BDPP)Th($CH_2SiMe_2Ph)_2$] (**11**). This complex was investigated by ^{1}H and ^{13}C NMR spectroscopy between 20 and –90 °C. However, due to substantial similarities between **9** and **11**, this chemistry was not pursued further.

The formation of a tetraalkyl derivative[40-43,45,48,169,170] in the reactions described above seems likely given that $[Th(CH_3)_4(dmpe)_2]$,[41,42] $[Th(CH_2Ph)_4]$,[170] $[Th(CH_2C_6H_3Me_2\text{-}3,5)_4]$[40] and $[Th(C_3H_5)_4]$[40] are formed in related reactions of $[ThCl_4L_x]$ {L_x = $(dmpe)_2$ or $(THF)_3$} with 4 equivalents of LiR at temperatures below 0 °C. That said, the involvement of 'ate'-complexes structurally related to [MeTh(μ-Me)$_6${Li(TMEDA)}][36] and $[UR_6Li_2S_x]$ (S = THF),[35] or *in-situ* H_2[L] {L = [BDPP] or $[XA_2]$} ligand deprotonation by remaining $LiCH_2SiMe_3$ cannot be ruled out.

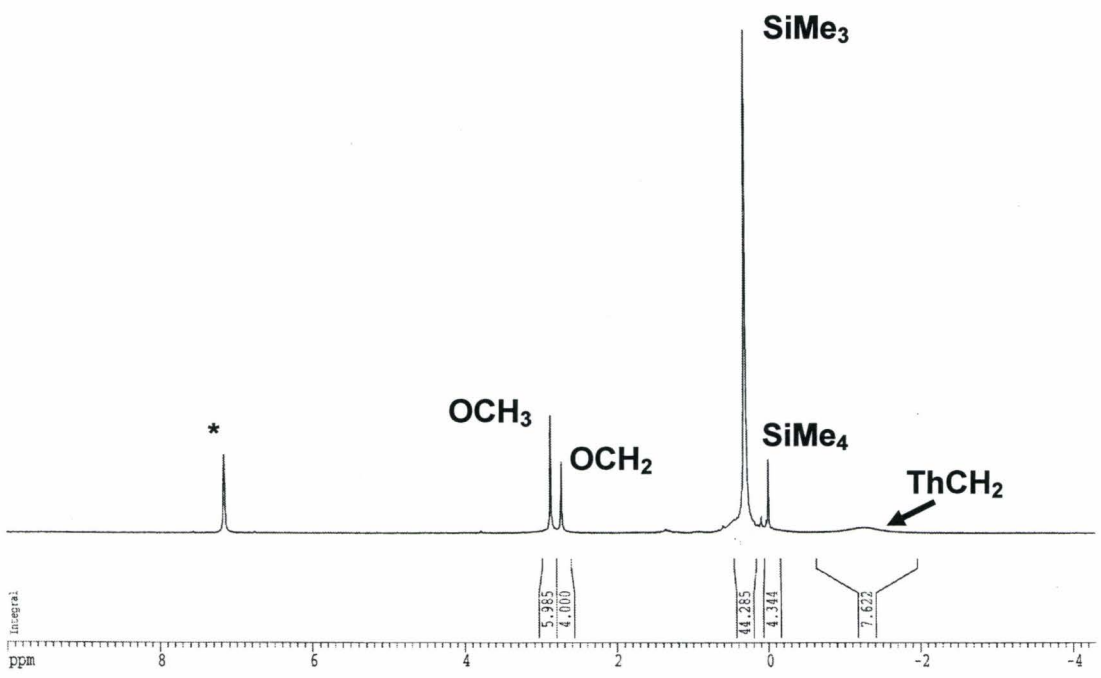

Figure 3.2: ^{1}H NMR spectrum of "Th(CH_2SiMe_3)$_4$(dme)" (* = benzene) in C_6D_6 at room temperature.

At 60 °C (d_8-toluene), the ^{1}H and ^{13}C NMR spectra for 5-coordinate compounds **9** and **10** are consistent with C_{2v} symmetry. For example, complexes **9** and **10** exhibit a single set of ThCH_2 and CHMe$_2$ resonances; the ThCH_2 resonance is located at –0.32 (**9**) or –0.17 (**10**) ppm in the ^{1}H NMR and 89 (**9**) or 97 (**10**) ppm in the ^{13}C NMR. However, upon cooling to –80 °C, the ^{1}H and ^{13}C NMR spectra of both complexes show two distinct CH_2SiMe_3 groups, two CHMe$_2$ signals, and ligand backbone resonances consistent a C_s symmetric product as observed in the solid state (*vide infra*). The Th–CH_2 resonances are located at 0.31 and –0.70 (**9**) or 0.52 and –0.68 (**10**) ppm in the ^{1}H NMR and 78 and 98 (**9**) or 90 and 103 (**10**) ppm in the ^{13}C NMR (Figure 3.3). This fluxional behavior requires exchange between apical and in-plane CH_2SiMe_3 groups in the

molecule, coupled with adjustment of the ligand backbone to accommodate the changing steric demands imposed by the alkyl subsitutents.

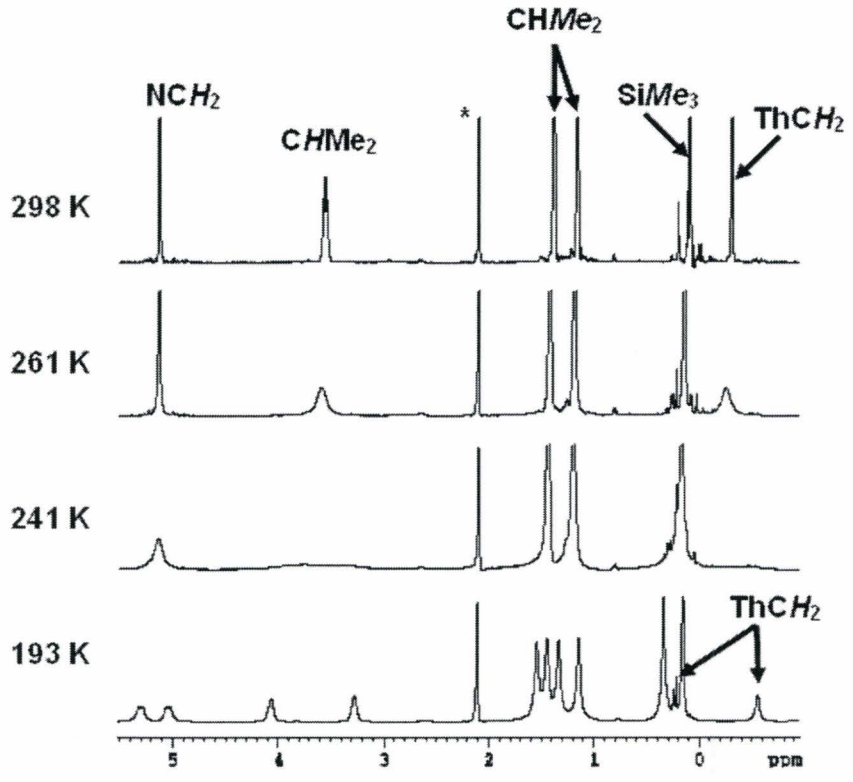

Figure 3.3: Variable-temperature ^{1}H NMR spectra of 9 in d_8-toluene (* = toluene).

The loss of symmetry in **9** is evidence of top-bottom asymmetry, which may be visualized as the inability of the molecule to reflect the same structural features on both sides of a hypothetical horizontal mirror plane through the NNN-ligand donors as depicted in Figure 3.4 (top). In this diagram, an imaginary horizontal mirror plane is placed in the plane of the back-bone pyridine donor in the [BDPP] ligand, with C1 to C8, N1 and N2 and Th lying in the plane. When a molecule has top-bottom symmetry, the atoms above and below the horizontal mirror plane are equivalent. Any coordination

change that disrupts this mirrored behavior between atoms above and below the plane results in a molecule having top-bottom asymmetry. Practically, the number of NMR signals of a complex that loses top-bottom symmetry increases compared to its more symmetric predecessor, and when a molecule loses top-bottom or side-side symmetry (Figure 3.4, bottom), the number of signals increases further.

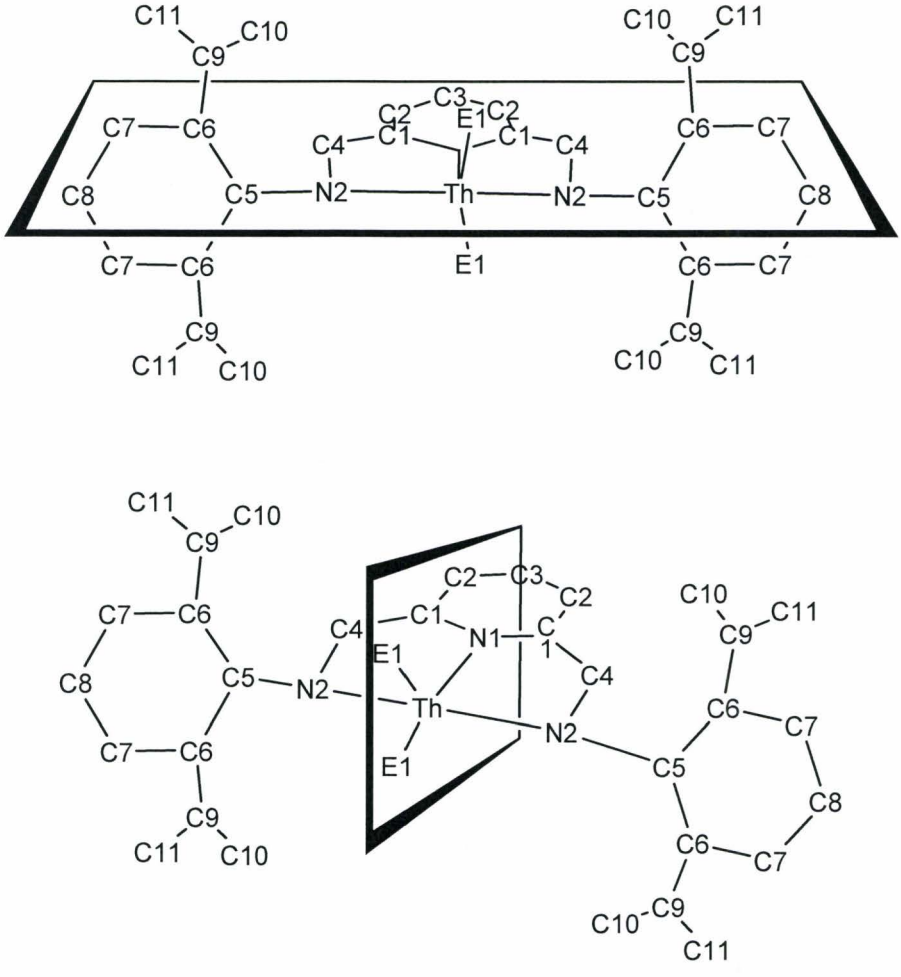

Figure 3.4: Top-bottom and side-side symmetric [(BDPP)ThE$_2$]. (Top) Mirror plane reflecting top-bottom sides of [(BDPP)ThE$_2$]; N1 (pyridine nitrogen) omitted for clarity. (Bottom) Mirror plane reflecting right-left sides of [(BDPP)ThE$_2$].

X-ray quality single crystals of $[(XA_2)Th(CH_2SiMe_3)_2]$•toluene were grown by cooling a saturated toluene solution of **10** from room temperature to –30 °C; complex **10** is the first example of a structurally characterized thorium dialkyl complex supported by a multidentate, non-carbocyclic ancillary. In the solid state (Figure 3.5,Table 3.1), **10** is pentacoordinate and adopts a square pyramidal geometry that is strongly distorted in the square plane as a result of $[XA_2]$ ligand rigidity. The $[XA_2]$ ligand backbone is approximately planar, but thorium is located 0.475(6) Å above the NON ligand plane. Consistent with the low-temperature ^1H and ^{13}C NMR spectra of **10**, the two alkyl groups are distinct, with one located approximately in the NON plane, while the other is located directly above the plane. This arrangement, in conjunction with rotation of the two 2,6-diisopropylphenyl groups to give C(34)•••C(44) = 7.514(9) and C(30)•••C(48) = 4.995(9) Å, is adopted in order to minimize unfavorable steric interactions between metal-alkyl and ligand-isopropyl groups (Figure 3.5, Table 3.1). Similar behavior has been observed in other dialkyl complexes in which a metal is flanked by bulky 2,6-diisopropylphenyl substituents.[145,150,171]

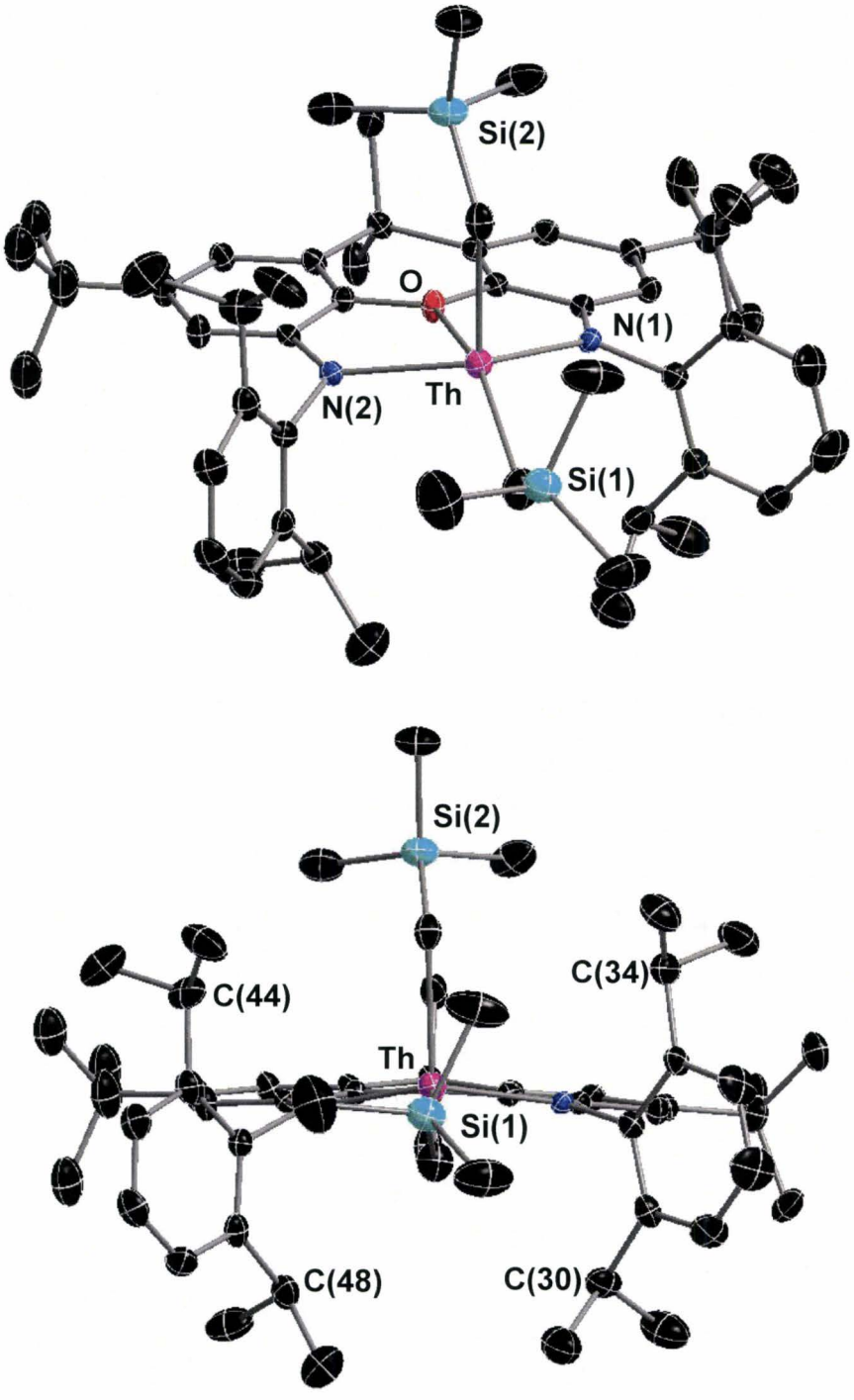

Figure 3.5: Molecular structure of $[(XA_2)Th(CH_2SiMe_3)_2]$•toluene (10•toluene). Thermal ellipsoids at the 50 % probability level. Hydrogen atoms and solvent are omitted for clarity.

The Th–$N_{anilido}$ bond lengths {2.292(4), 2.312(4) Å} in **10** are similar to those observed in [(BDPP)$ThCl_2$(dme)] (**5**), and the Th–C {2.468(6), 2.485(6) Å} bond lengths fall within the range observed for the other crystallographically characterized thorium(IV) trimethylsilylmethyl or related neopentyl complexes: 2.48(2) and 2.54(2) Å in [{$Me_2Si(C_5Me_4)_2$}ThR_2],[172] 2.47(3) Å in [Cp*$_2$Th(CH_2tBu)$_2$],[99] 2.438(16) and 2.485(18) Å in [(2,6-tBu$_2H_3C_6O$)$_2$$ThR_2$],[97] and 2.488(2) and 2.460(9) Å in [Cp*(2,6-tBu$_2H_3C_6O$)ThR_2][86] (R = CH_2SiMe_3). Structurally characterized thorium diaryl ether or aryl ether complexes have not been previously reported. However, the Th-O bond length in **10** {2.534(3) Å} is similar to those observed for coordinated dme {2.564(8)–2.620(8) Å} in [(L)ThCl(κ^1-dme){K(dme)$_2$}] {L = 2,2′-methylenebis(4-methyl-6-$t$butyl)phenolate}[160,161] or THF {e.g., 2.53(1), 2.58(1) Å in [(COT)$ThCl_2$(THF)][173] and 2.520(7), 2.526(7) Å in [Cp*$_2$Th(NXyl)(THF)]}.[174] This is surprising since a diaryl ether should be a considerably less effective donor than dme or THF. However, a short bond between thorium and the neutral donor of the ligand backbone is also observed in dichloride **5**, and this feature is likely a consequence of tridentate binding and ligand rigidity.

Of particular note are the Th–C–Si bond angles in [XA_2] complex **10** {127.6(3)° and 126.8(3)°}, which are both significantly larger than is typically observed for an sp^3-hybridized carbon atom. Similar increases in M–C–Si or M–C–C (M = Th or U) bond angles have been observed in other trimethylsilymethyl or neopentyl complexes and are attributed to α-agostic C–H–Th interactions.[41,86,99,172] Further evidence for the presence of agostic interactions is provided by a $^1J_{C\text{-}H}$ coupling of 102 Hz for the rapidly exchanging

CH_2SiMe_3 groups in the ^{1}H-coupled ^{13}C NMR spectrum of **10** in d_8-toluene at 60 °C. This value is significantly lower than typically observed for an sp^3-hybridized carbon atom (~125 Hz) and compares well with literature values for related complexes: 104 Hz in Leznoff's [($^{t\text{Bu}}$NON)ThR$_2$],[137] 100 Hz in [Cp*(2,6-tBu$_2$H$_3$C$_6$O)ThR$_2$],[86] 99 Hz in [{Me$_2$Si(C$_5$Me$_4$)$_2$}ThR$_2$],[172] and 98 Hz in [(2,6-tBu$_2$H$_3$C$_6$O)$_2$ThR$_2$][97] (R = CH_2SiMe_3). A similarly low $^1J_{C\text{-}H}$ value of 103 Hz was also observed for the CH_2SiMe_3 groups in **9** (60 °C, C_7D_8).

Interestingly, upon lowering the temperature to –80 °C, separate $^1J_{C\text{-}H}$ coupling constants for each CH_2SiMe_3 group in **9** and **10** were observed by fully coupled HSQC NMR. These values (88 and 91 Hz for **9** and 81 and 88 Hz for **10**) are considerably reduced relative to those obtained at 60 °C and suggest that for both complexes in solution, an equilibrium exists between products participating in α-agostic C–H–Th bonding to a greater or lesser extent (up to four α-agostic interactions[99] could occur in either **9** or **10**) and that entropy favors less agostic products. Consequently, as the temperature is lowered, the equilibrium shifts toward more agostic products, resulting in a decrease in the average $^1J_{C\text{-}H}$ coupling constant. The alternative explanation in which the strength of the E–H–M interactions are strongly affected by temperature has been determined not to be responsible for the temperature-dependent $^1J_{E\text{-}H}$ coupling constants in Ti and Nb complexes displaying a similar phenomenon (*vide infra*).[175]

The weak and nonstatic nature of α-agostic interactions has been previously discussed,[99,176] and temperature-dependent $^1J_{E\text{-}H}$ coupling constants as a result of an equilibrium between an agostic and non-agostic isomer have been reported for several

transition metal organometallic complexes. For example, $^1J_{C\text{-}H}$ for Nb*CH*R_2 in [(κ^3-Tp′)NbCl(cyclopropyl)(C_2Me_2)] varies from 102 Hz at 20 °C to 93 Hz at –80 °C,[177] and $^1J_{Si\text{-}H}$ in [Cp_2Ti(*t*BuC_2SiHMe_2)] varies from 123 Hz at 30 °C to 93 Hz at –80 °C.[176] A temperature-dependent $^1J_{C\text{-}H}$ constant was also observed for Ta*C*H_2Me in [(P_2N_2)Ta(Et)(C_2H_4)] (123 Hz at 77 °C and 134 Hz at –40 °C), but in this case, it is due to a greater contribution from a β-agostic structure (versus an α-agostic structure) at lower temperature.[178]

Dialkyls **9** and **10** both exhibit remarkable thermal stability; [(BDPP)Th(CH_2SiMe_3)$_2$] (**9**) is stable for days in toluene at 90 °C and is only fully decomposed after 3 days at 110 °C, while [(XA_2)Th(CH_2SiMe_3)$_2$] (**10**) is stable at 70 °C but decomposes over several hours at 90 °C. Tetramethylsilane was the only soluble product observed when the thermal decomposition of **9** or **10** was monitored by ^{1}H NMR spectroscopy. The greater stability of **9** could be a result of decreased ligand rigidity, allowing the ligand to form a more optimal metal binding pocket. However, Th–N_{amido} bond lengths in **10** are very similar to those observed in the dichloro [BDPP] complex **5**, and in both cases, the ligand is approximately planar. Therefore, the greater stability of **9** is more likely due to improved donor properties of a pyridine versus a diaryl ether neutral donor, leading to increased electronic saturation at the metal center.

The stability of **9** is particularly remarkable and highlights the suitability of rigid tridentate ligands such as [BDPP] for the stabilization of organoactinide complexes. The thermal stability of most other non-cyclopentadienyl thorium(IV) dialkyl complexes has not been reported. However, for comparison, [Th(OC_6H_3tBu$_2$-2,6)$_2$(CH_2SiMe_3)$_2$]

decomposes over 36 hours at 60 °C,[97] [Cp*Th($OC_6H_3tBu_2$-2,6)$_2$(CH_2SiMe_3)$_2$] decomposes over 12 hours at 60 °C,[97] [Cp*$_2$Th(CH_2SiMe_3)$_2$] decomposes over 36 hours at 85 °C,[99] and [{$Me_2Si(C_5Me_4)_2$}Th(CH_2SiMe_3)$_2$] decomposes at 60 °C.[100] The only thorium dialkyl complex of similar stability is [Cp*$_2$ThMe_2], being 50 % decomposed after 1 week at 100 °C.[101] In addition, while [(C_5R_5)$_2$ThR_2] complexes are reported to be extremely air sensitive,[109] exposure of toluene solutions of **9** to air for 5 minutes resulted in only 20-30 % decomposition. By contrast, solid samples of **9** and **10** are more sensitive, being entirely decomposed after 5 minutes of exposure to air.

3.2.2 – Thorium(IV) Dibenzyl Complexes

Reaction of [(XA_2)ThCl_2(dme)] (**6**) with 2 equivalents of benzyl magnesium chloride resulted in the formation of base free [(XA_2)Th(CH_2Ph)$_2$] (**12**) as a hexane-soluble light yellow solid in 56 % yield. At 50 °C, the ^{1}H NMR spectrum of **12** is suggestive of C_{2v} symmetry. However, at temperatures below –40 °C, the ^{1}H NMR spectrum exhibits ThCH_2 signals at 1.34 and 1.26 ppm, and ^{13}C NMR signals for the carbon atoms bearing these protons are observed at 90.9 and 93.4 ppm. These data are consistent with a C_s-symmetric complex lacking top-bottom symmetry, and containing two distinct benzyl groups. The $^1J_{C\text{-}H}$ coupling constants of 120 and 139 Hz for CH_2Ph indicate that one benzyl group is η^1-coordinated, while the other adopts an η^2- or η^3-coordination mode ($^1J_{C\text{-}H}$ coupling constants in the range of 120 to 130 Hz are indicative of η^1-coordination, while $^1J_{C\text{-}H}$ coupling constants greater than 130 Hz are indicative of η^2- or η^3-coordination).[179-181]

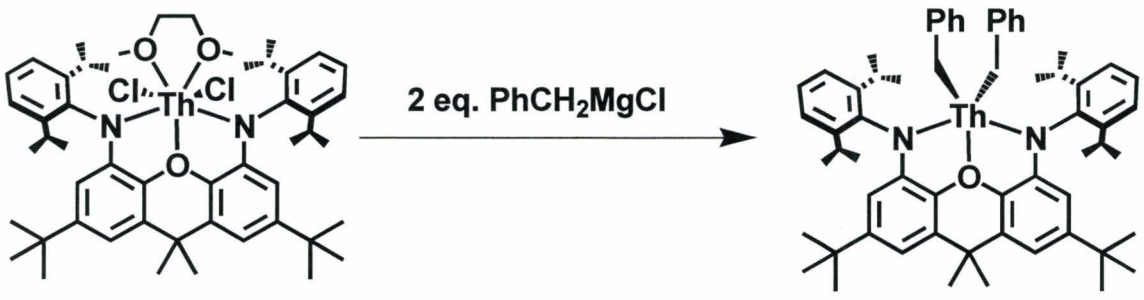

Scheme 3.3: Synthesis of [(XA_2)Th(CH_2Ph)$_2$] (12).

X-ray quality crystals of [(XA_2)Th(CH_2Ph)$_2$] (**12**) were grown from a saturated solution of hexanes at –30 °C. The unit cell contains two distinct molecules of **12**, with Th-CH_2 bond lengths between 2.503(3) and 2.545(3) Å, and in both molecules, one benzyl group is located in the ligand plane, while the other occupies an apical site (Figure 3.6, Table 3.1). For both molecules, the in-plane benzyl group adopts a bonding mode intermediate between η^2- and η^3-coordination, with Th–CH_2–C_{ipso} angles of 85.6(2)° and 87.5(2)°. Distances between thorium and the ring carbons of the in-plane benzyl group differ slightly between the two molecules {Th(1)–C_{ortho} = 3.191(3) and 3.510(3) Å; Th(2)–C_{ortho} = 3.126(4) and 3.647(4) Å}. By contrast, the apical benzyl group is η^1-coordinated in one molecule [Th(1)–CH_2–C_{ipso} = 115.1(2)°; Th(1)–C_{ipso} = 3.402(3) Å], but approaches η^2-coordination in the other [Th(2)–CH_2–C_{ipso} = 96.1(2)°; Th(2)–C_{ipso} = 3.058(3) Å].

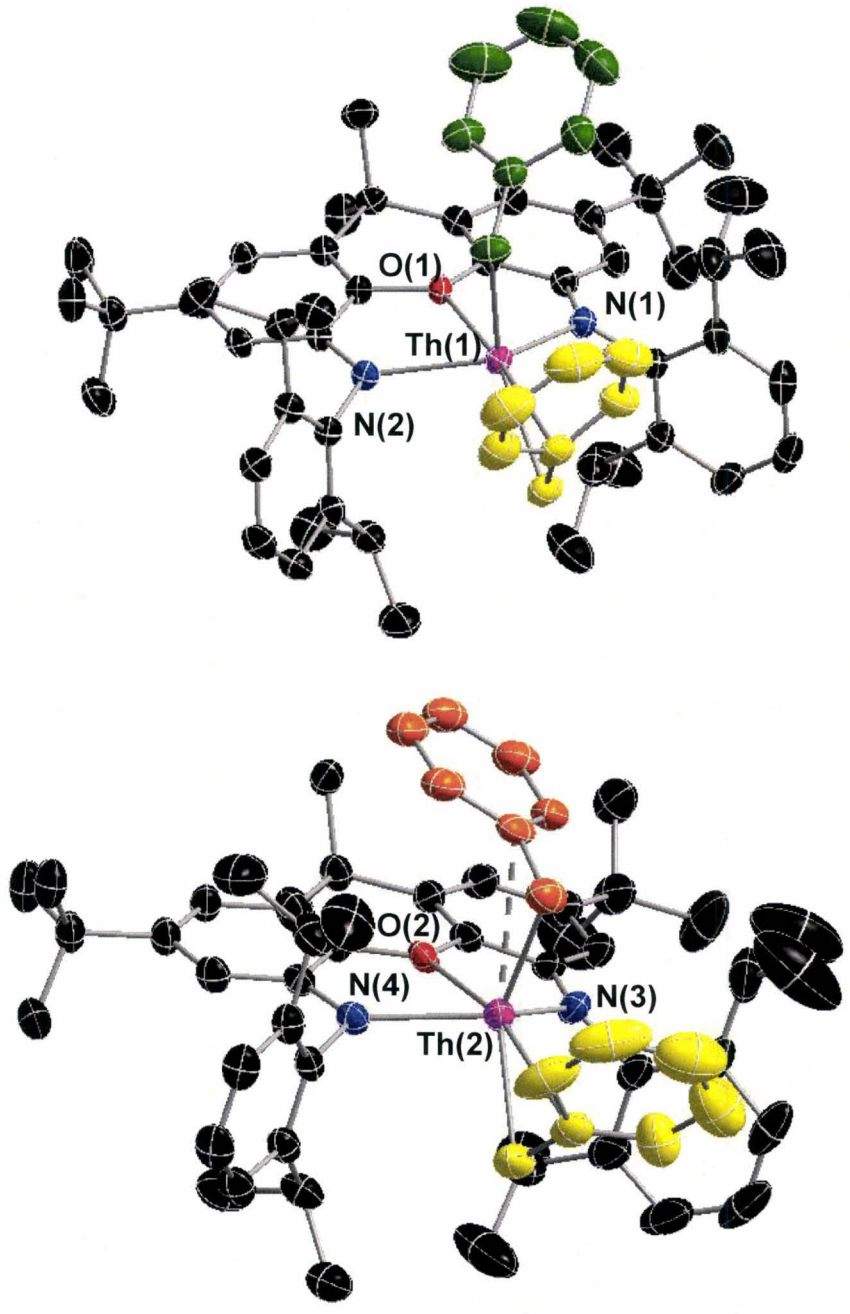

Figure 3.6: Solid state structures for the two molecules of $[(XA_2)Th(CH_2Ph)_2]$ (12) in the unit cell. Yellow = carbon atoms belong to the in plane η^2- to η^3-coordinated CH_2Ph; Green (top) = carbon atoms belong to the apical η^1-coordinated CH_2Ph; Orange (bottom) = carbon atoms belong to the apical η^1- to η^2-coordinated CH_2Ph. Thermal ellipsoids at the 50 % probability level. Hydrogen atoms are omitted for clarity.

Dibenzyl complex [(BDPP)Th(CH_2Ph)$_2$] (**13**) was accessible in a similar fashion to the [XA_2] supported dibenzyl complex, via the reaction of **5** with $PhCH_2MgCl$ or KCH_2Ph. Room temperature NMR spectra show both benzyl ligands and the four isopropyl groups to be equivalent due to fluxional behavior in solution, and raising the temperature to 80 °C was insufficient to obtain a sharp averaged ^{1}H NMR spectrum. However, at –35 °C in d_8-toluene, two distinct benzyl groups were observed by both ^{1}H and ^{13}C NMR spectroscopy. These data indicate top-bottom asymmetry in the molecule, consistent with one benzyl group in an axial position and one in the ligand plane. The $^1J_{C\text{-}H}$ coupling constants of 138 and 127 Hz for Th–CH_2 are suggestive of bonding approaching either η^2- or η^3-coordination and η^1-coordination respectively.[179, 181]

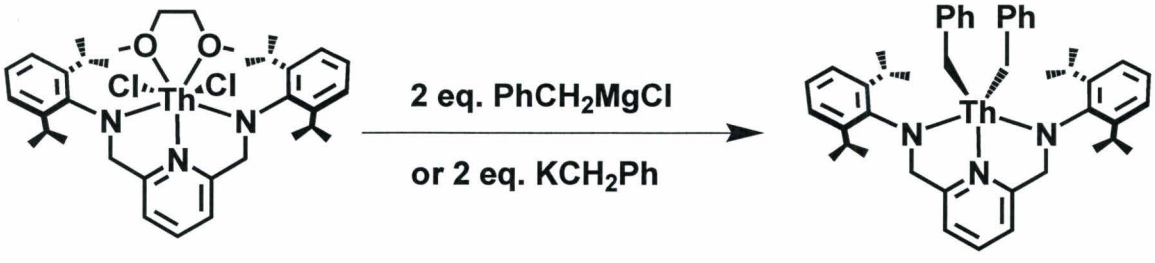

Scheme 3.4: Synthesis of [(BDPP)Th(CH_2Ph)$_2$] (13).

X-ray quality crystals of **13•0.5hexane** were grown from a mixture of toluene and hexanes at –30 °C. In the solid state (Figure 3.7, Table 3.1), one benzyl group is η^3-coordinated in the plane of the ligand [Th–C(32)–C(33) = 84.6(3)°; Th–C(32) = 2.576(6) Å; Th–C(33) = 2.836(5) Å; Th–C(34) = 3.095(6) Å], while the other occupies an apical site and adopts a coordination mode intermediate between η^1- and η^2-coordination [Th–

C(39)–C(40) = 96.7(4)°; Th–C(39) = 2.454(6) Å; Th–C(40) = 3.087(6) Å]. These benzyl group hapticities differ from those observed in solution, and illustrate the nonstatic nature of polyhapto-benzyl coordination.

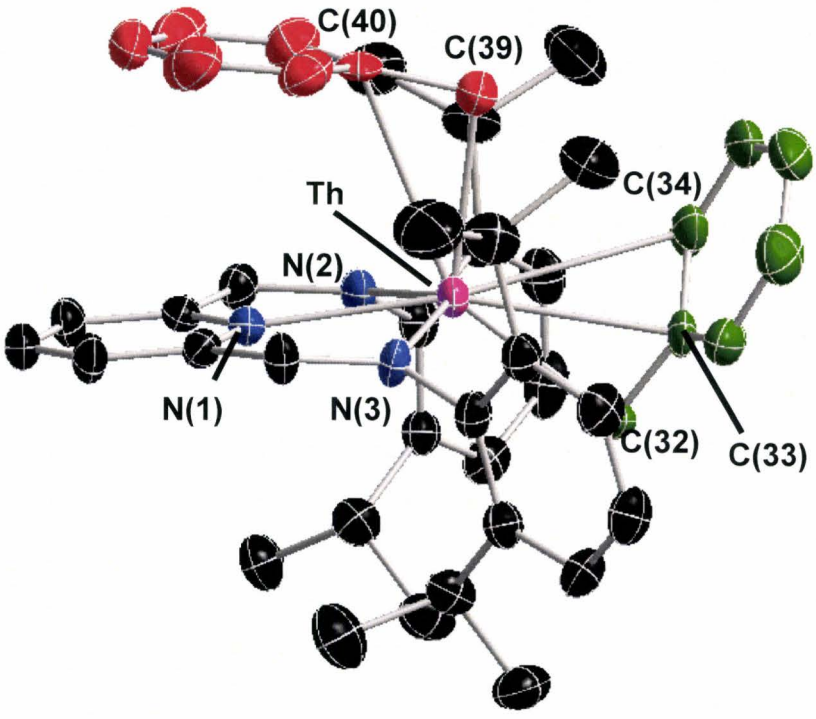

Figure 3.7: Molecular structure of [(BDPP)Th(CH_2Ph)$_2$]•0.5hexane (13•0.5hexane). Red = carbon atoms belong to the axial η^1- to η^2-coordinated CH_2Ph group; Green = carbon atoms belong to the in-plane η^3-coordinated CH_2Ph group. Thermal ellipsoids at the 50 % probability level. Hydrogen atoms and solvent are omitted for clarity.

Table 3.1: Crystallographic data collection and refinement parameters and selected bond distances for complexes 10, 12 and 13•0.5hexane

	10	**12**	**13•0.5hexane**
Formula	$C_{62}H_{90}N_2OSi_2Th$	$C_{61}H_{76}N_2OTh$	$C_{48}H_{62}N_3Th$
Fw	1167.58	1085.28	913.05
Cryst. Syst.	Monoclinic	Monoclinic	Triclinic
Space Group	P2(1)/*n*	P2(1)/*n*	P-1
a(Å)	16.6445(5)	11.3511(3)	10.5942(8)
b(Å)	22.5599(7)	26.3640(7)	12.7271(10)
c(Å)	16.8509(5)	36.2376(9)	17.1177(13)
α(deg)	90	90	104.4660(10)
β(deg)	107.928(2)	98.7360(10)	104.553(2)
γ(deg)	90	90	96.002(2)
Volume(Å^3)	6020.2(3)	10718.7(5)	2128.4(3)
Z	4	8	2
Density(calcd; mg/m^3)	1.288	1.345	1.425
μ(mm^{-1})	2.555	2.823	3.538
F(000)	2408	4432	922
Cryst size (mm^3)	0.10 x 0.08 x 0.01	0.40 x 0.40 x 0.30	0.30 x 0.20 x 0.10
θ range for collection(deg)	1.50 to 27.49	1.87 to 36.40	1.28 to 26.49
No. of reflns. collected	32615	300903	24864
No. of indep. reflns.	13480	51324	8721
Completeness to θ_{max}	97.5 %	98.3 %	98.9 %
Transmn. ratio	0.8367	0.717	0.640
GOF on F^2	0.996	1.124	0.996
Final R_1 [$I > 2\sigma(I)$]	R1 = 0.0566	R1 = 0.0459	R1 = 0.0437
	wR2 = 0.0891	wR2 = 0.0918	wR2 = 0.0873
R indices (all data)	R1 = 0.1169	R1 = 0.1006	R1 = 0.0668
	wR2 = 0.1031	wR2 = 0.1067	wR2 = 0.1008
Th–N_{amido}	2.293(4), 2.312(4)	2.318(2), 2.332(2)	2.273(5), 2.300(5)
Th–CH_2R	2.468(6), 2.486(6)	2.503(3), 2.545(3)	2.576(6), 2.545(6)
Th–O	2.534(3)	2.5263(17)	n.a.
Th–$N_{pyridine}$	n.a.	n.a.	2.545(4)
Th–C_{ipso}	n.a.	2.826(3)	2.836(5), 3.087(6)

For **10**, **12**, and **13**•0.5hexane: *T* = 173(2) K, wavelength = 0.71073 Å, absorption correction = semiempirical from equivalents, and refinement method = full-matrix least-squares on F^2.

3.2.3 – Thorium(IV) Di-*n*-butyl Complexes

Reaction of [(BDPP)$ThCl_2$(dme)] (**5**) with 2 equivalents of *n*BuLi resulted in the formation of [(BDPP)Th(*n*Bu)$_2$] (**14**) as an off-white solid in 57 % isolated yield (Scheme 3.5). Complex **14** is highly soluble in ethereal, arene and hydrocarbon solvents, a property responsible for the low isolated yield. Surprisingly, compound **14** is extremely thermally stable, exhibiting no signs of thermal decomposition after several hours at 60 °C in benzene. However, at 80 °C, thermal decomposition was observed over a period of 12 hours, resulting in the formation of an intractable mixture of products.

While the solid state structure of **14** was not obtained, despite numerous crystallization attempts employing a variety of solvent systems and conditions, it is likely that the structure of this complex is distorted square pyramidal, analogous to that of [(XA_2)Th(CH_2SiMe_3)$_2$] (**10**) and [(BDPP)Th(CH_2Ph)$_2$] (**13**). However, NMR spectra of **14** show a single *n*-butyl environment at room temperature, with ThCH_2 ^{1}H and ^{13}C NMR signals at 0.35 and 87.7 ppm and a $^1J_{C\text{-}H}$ value of 118 Hz. Qualitative features of the spectra persist upon cooling to –90 °C, likely due to limited steric demands of the *n*-butyl groups. By contrast the low temperature NMR spectra for [(L)Th(CH_2SiMe_3)$_2$] {L = [BDPP], **9**; [XA_2], **10**} revealed top-bottom asymmetry, with two different alkyl group environments.

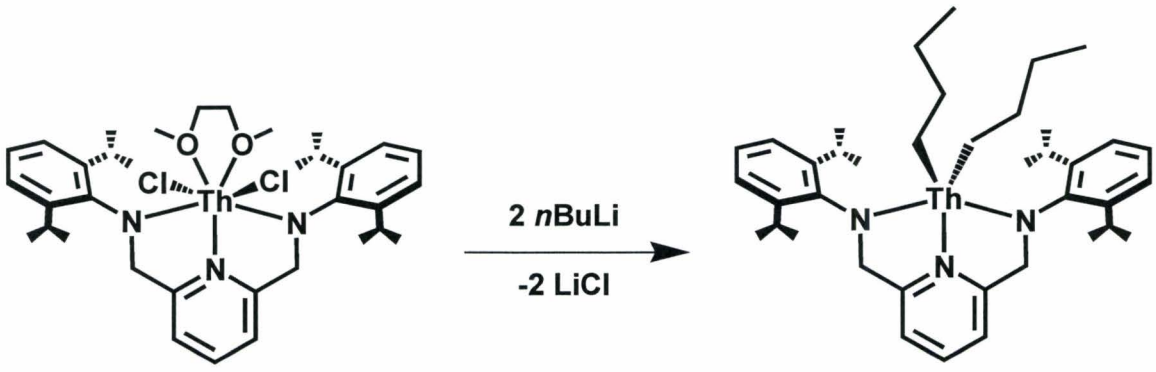

Scheme 3.5: Synthesis of di-*n*-butyl complex [(BDPP)Th(*n*Bu)$_2$] (14).

In a reaction analogous to that used to prepare the [BDPP] di-*n*butyl complex **14**, treatment of [(XA$_2$)ThCl$_2$(dme)] (**6**) with 2 equivalents of *n*BuLi resulted in the formation of [(XA$_2$)Th(*n*Bu)$_2$] (**15**) as an off-white solid in 57 % isolated yield (Scheme 3.6). Complex **15** is also highly soluble common ethereal, arene and hydrocarbon solvents, and shows a single *n*-butyl environment by ^{1}H NMR spectroscopy between room temperature and –90 °C. The thermal stability of compound **15** surpasses that of its [BDPP] analogue, with no sign of thermal decomposition observed after days at 80 °C in benzene.

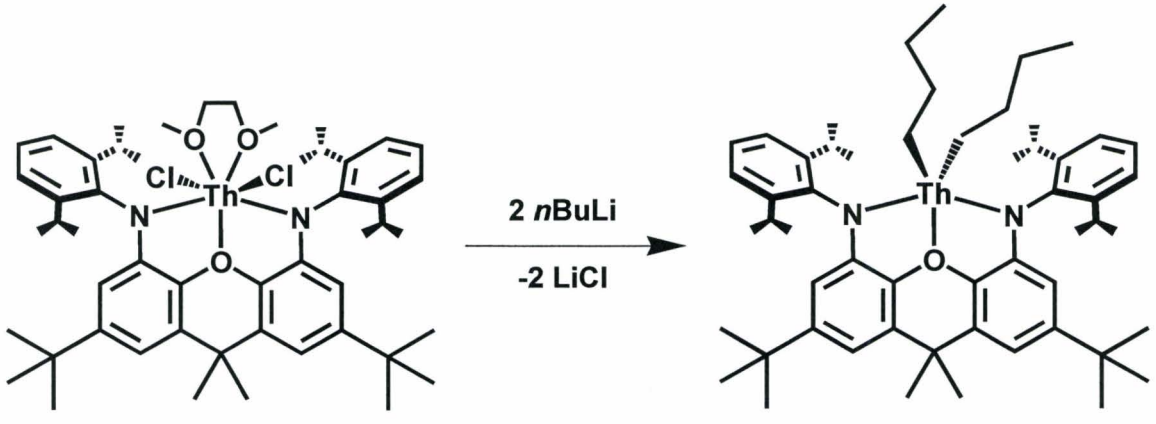

Scheme 3.6: Synthesis of di-*n*-butyl complex [(XA$_2$)Th(*n*Bu)$_2$] (15).

3.2.4 – Thorium(IV) Methyl Complexes

Bearing in mind the high degree of thermal stability observed in complexes **9**, **10**, **14** and **15**, it was deemed likely that organoactinide dialkyl complexes bearing methyl ligands would be accessible.

Initial attempts to produce [(BDPP)$ThMe_2$] by reaction of dichloride [(BDPP)$ThCl_2$(dme)] (**5**) with two equivalents of methyl lithium at room temperature proved ineffective, yielding a complex mixture of reaction products {these products do not match those formed via thermal decomposition of [(BDPP)$ThMe_2$] (**18**); *vide infra*}. However, reaction of [(BDPP)$ThCl_2$(dme)] (**5**) with three equivalents of MeLi in toluene resulted in the formation of the trimethyl 'ate' complex [(BDPP)$ThMe_3${Li(dme)}] (**16**), in 74 % isolated yield (Scheme 3.7). The room temperature ^{1}H NMR spectrum of **16** shows a single Th-*Me* peak at δ 0.02 ppm, and only one C*H*Me_2 peak was observed arising from the [BDPP] ligand. At –70 °C in d_8-toluene, several [BDPP] signals began to de-coalesce, but were not resolved even at temperatures as low as –90 °C (solvent limited temperature). Explanation of this data requires rapid exchange of the in-plane and axial methyl groups in **16**, as well as rapid transfer of the $Li(dme)^+$ moiety between methyl ligands. The involvement of methyllithium dissociation in this process is highly unlikely since thorium-methyl groups in **16** do not undergo exchange with $LiCD_3$/LiI in toluene after several hours at room temperature. Similar dynamic behaviour was reported for [ThMe{(μ-Me)$_2$Li(tmeda)}$_3$] in which all thorium methyl groups are equivalent (^{1}H NMR δ 0.02 ppm) on the NMR timescale at –90 °C.[36]

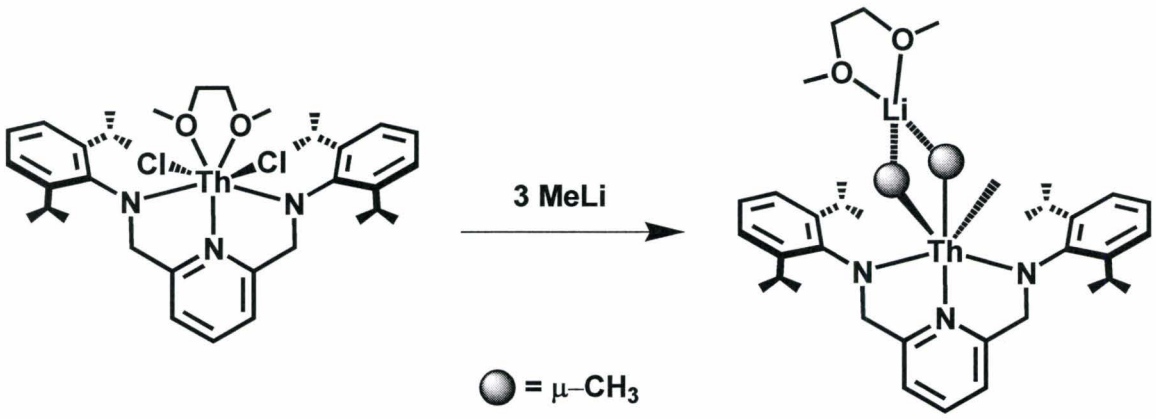

Scheme 3.7: Synthesis of [(BDPP)ThMe$_3${Li(dme)}] (16).

Compound **16** is stable as a solid for extended periods of time at room temperature. However, solutions of **16** in toluene or benzene began to show signs of decomposition after 8 hours, and decomposed over several days to form orange-brown [(BDPP*)Th(μ-Me)$_2$Li(dme)] {**17**; BDPP* = 2,6-$\underline{N}C_5H_3(CH_3\underline{N}Ar)$-($CH_2\underline{N}${$C_6H_3{}^{i}Pr(\underline{C}Me_2)$-2,6}); Ar = 2,6-diisopropylphenyl; donor atoms in BDPP* are underlined; Scheme 3.8} as the major product (greater than 80 % yield by ^{1}H NMR spectroscopy). Highly soluble **17** was isolated from hexamethyldisiloxane in low yield. This compound is thermally robust, showing no signs of decomposition after days in benzene at 80 °C, despite the presence of a β-hydrogen-containing tertiary alkyl group (Th-CMe_2Ar') in the BDPP* ligand.

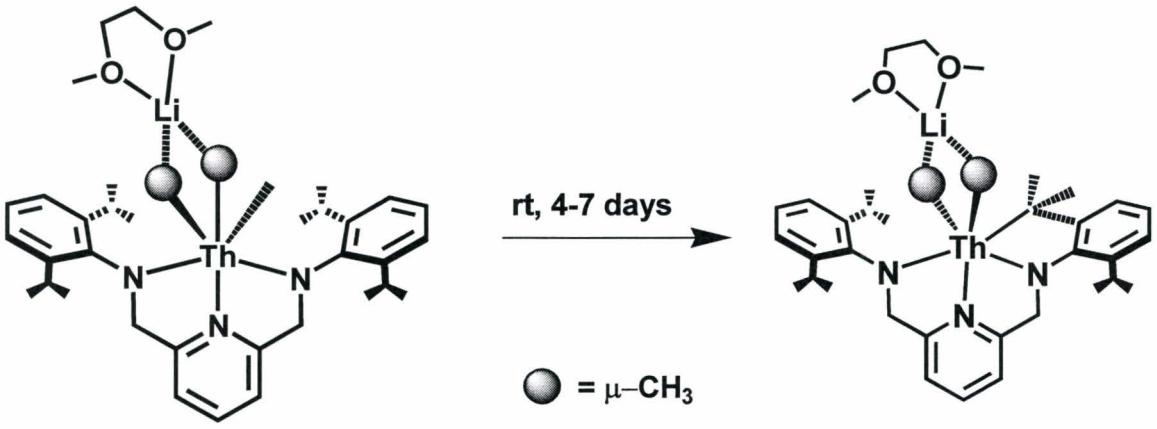

Scheme 3.8: Thermal decomposition of trimethyl 'ate' complex 16, producing metalated complex 17.

In the ^{1}H NMR spectrum of **17**, two different methyl groups are observed at –0.09 and –0.32 ppm, with corresponding signals at 53.0 and 41.4 ppm in the ^{13}C NMR spectrum. The metalated carbon atom (Th*C*Me$_2$Ar′) lies at 73.6 ppm in the ^{13}C NMR spectrum, and the β-hydrogen bearing methyl groups attached to this carbon give rise to singlets at 2.39 and 1.22 ppm in the ^{1}H NMR spectrum. The three different isopropyl-C*H* protons observed at 4.03, 3.94 and 3.79 ppm and the overall high degree of complexity in the ^{1}H NMR are consistent with a molecule that exhibits both top-bottom and side-side asymmetry (Figure 3.4).

Complex **17** is the product of ligand metallation at the central carbon in an isopropyl group of the [BDPP] ligand. Metallation of *N*-2,6-diisopropylphenyl groups is commonly observed in early transition metal and *f*-element chemistry, but typically occurs at an isopropyl methyl group. Examples of isopropyl methyne metallation are rare, but have been reported for [(BDPP)Lu(AlMe$_4$)][148] and [(nacnac)(X)Ti=CHBu] (X = Cl Br, OTf, BH$_4$, CH$_2$SiMe$_3$).[182]

X-ray quality crystals of **17•0.5hexane** (Figure 3.8) were grown from a toluene solution layered with hexanes at –30 °C. The solid state structure revealed a significantly distorted octahedral geometry at thorium, and an approximately tetrahedral geometry at the lithium atom. Thorium lies in the plane formed by N(1), N(2), and N(3) which also contains C(32), one of the bridging methyl groups. The second bridging methyl group {C(33)} as well as the carbon previously belonging to the methyne group {C(7)} are found on either side of the plane of the ligand backbone. The acute C(32)–Th–C(33) angle of 80.9(4)° is primarily a consequence of $Li(dme)^+$ bridging between the two methyl groups. The constrained geometry imposed by the BDPP* ligand backbone is responsible for the acute N(1)–Th–N(2), N(2)–Th–N(3) and N(1)–Th–C(7) angles of 63.5(3)°, 63.9(3)° and 70.7(3)° respectively.

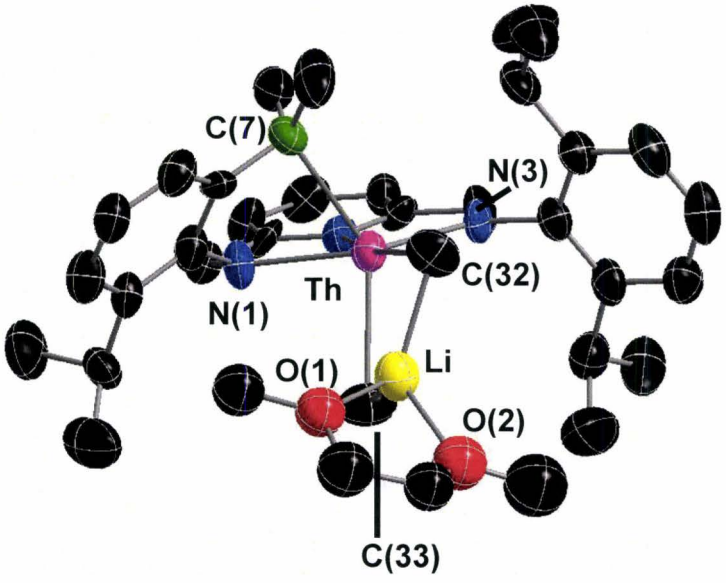

Figure 3.8: Molecular structure of [(BDPP*)Th(Me)$_2$Li(dme)]•0.5hexane (17•0.5hexane), BDPP* = 2,6-NC$_5$H$_3$(CH$_3$NAr)(CH$_2$N{C$_6$H$_3$^{i}Pr(CMe$_2$)-2,6}. Green = Metalated ^{i}Pr methine carbon {C(7)}. Thermal ellipsoids at the 50 % probability level. Hydrogen atoms and non-coordinated solvent are omitted for clarity. Only one of two orientations of the Li(dme) unit is shown.

The thorium-methyl bond distances of 2.679(13) and 2.635(12) Å are longer than Th-C(7) {2.566(12) Å} due to coordination with $Li(dme)^+$, but lie at the shorter end of the range of Th-C distances observed for bridging methyl groups in 7-coordinate [ThMe{(μ-Me)$_2$Li(tmeda)}$_3$] (2.65-2.77 Å).[36] The Th-N(1) distance of 2.298(9) Å in **17** is slightly shorter than Th-N(3) {2.350(9) Å}, likely due to the metallation of the 2,6-diisopropylphenyl substituent on N(1).

Formation of metalated complex **17** could occur through two different pathways (Figure 3.9). The first involves σ-bond metathesis between the thorium-methyl bond and the Me_2C-H bond of a 2,6-diisopropylphenyl group. The second involves α-hydrogen abstraction (of a methyl proton by a second methyl group on the metal) forming a carbene intermediate which may then undergo a metathesis reaction with the Me_2C–H bond of a 2,6-diisopropylphenyl group to yield complex **17**. In both scenarios, the same thorium complex and methane byproduct would be formed.

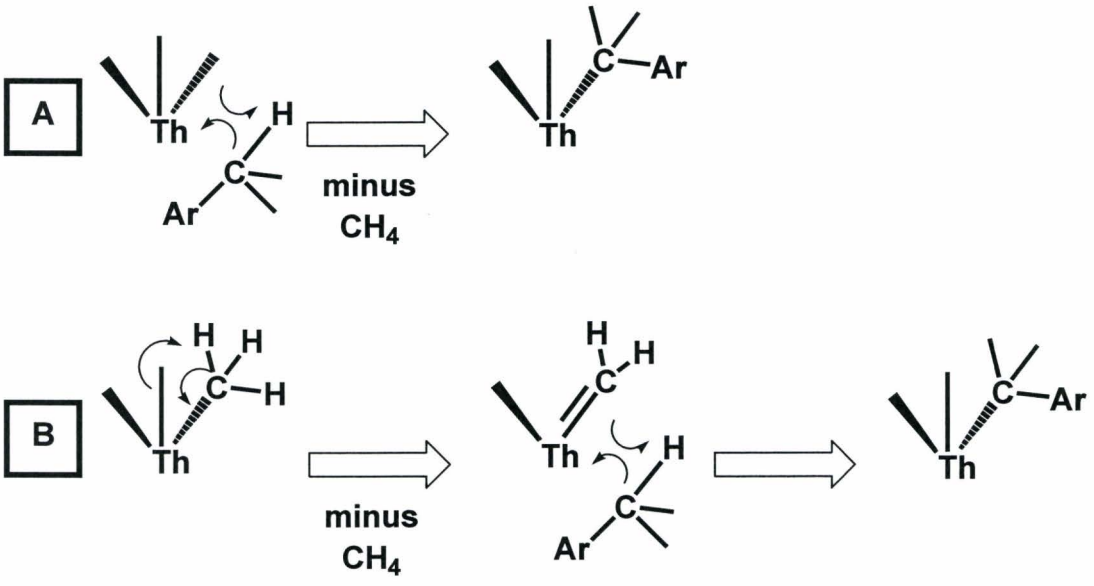

Figure 3.9: Potential pathways for the formation of complex 17 from trimethyl-ate complex 16 involving A: direct σ-bond metathesis; B: α-hydrogen abstraction to form a carbene intermediate.

As a probe to elucidate the mechanism for the formation of complex **17**, the ^{13}C and ^{2}H (D) labeled trimethyl analogue of **16**, [(BDPP)Th($^{13}CD_3$)$_3${Li(dme)}] {**16**-$^{13}C_3,d_9$} was synthesized via the reaction of [(BDPP)ThCl$_2$(dme)] (**5**) with three equivalents of Li$^{13}CD_3$/LiI. The products of the thermal decomposition of **16**-$^{13}C_3,d_9$ were monitored by ^{13}C and $^{13}C\{H\}$ NMR spectroscopy (Figure 3.10), and it was determined that the composition of the methane gas evolved from the decomposition process was $^{13}CHD_3$. The presence of this product alone is consistent with a simple σ-bond metathesis pathway, rather than a mechanism involving initial α-deuterium abstraction to produce $^{13}CD_4$.

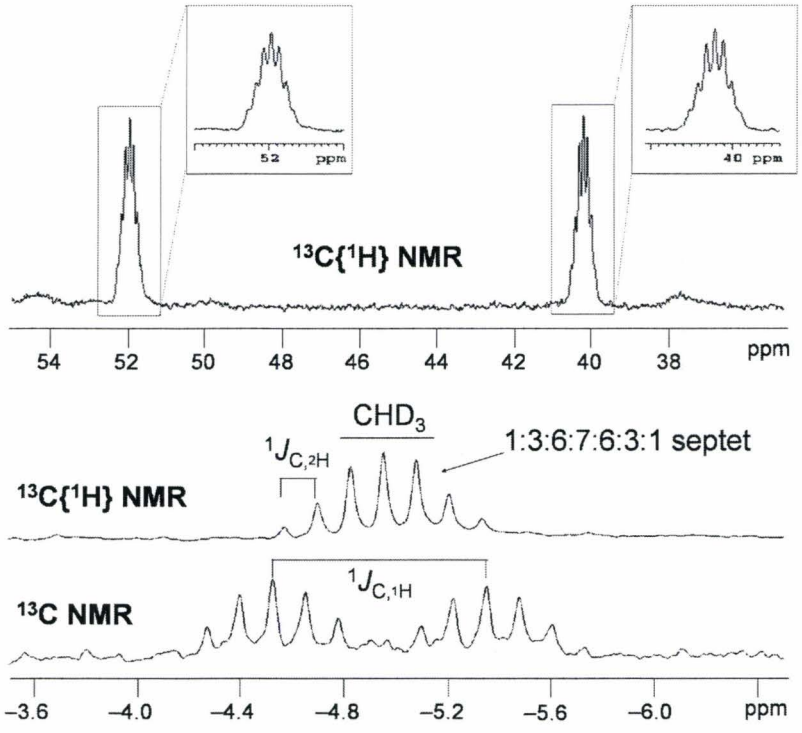

Figure 3.10: Selected regions from the ^{13}C and $^{13}C\{^1H\}$ NMR spectra of the thermal decomposition reaction of [(BDPP)Th(CD$_3$)$_3$Li(dme)] (16-$^{13}C_3$,d_9) to form [(BDPP*)Th(Me)$_2$Li(dme)] (17-$^{13}C_2$,d_6), BDPP* = 2,6-NC$_5$H$_3$(CH$_3$NAr)(CH$_2$N{C$_6$H$_3$^{i}Pr(CMe$_2$)-2,6}.

The elusive [(BDPP)ThMe$_2$] (**18**) was finally isolated via the reaction of two equivalents of BDDP trimethyl-ate complex **16** with one equivalent of [BDPP] dichloride **5** in 81 % yield (Scheme 3.9). The ^1H and ^{13}C NMR spectra of **18** are indicative of a highly symmetric molecule containing a single set of C*H*Me$_2$, CH_2 and Th–CH_3 environments (^1H NMR δ 0.01 ppm; ^{13}C NMR δ 82.5 ppm). The single set of signals observed in the NMR spectra persists upon cooling to –80 °C. This behavior is analogous to that observed for [BDPP] di-*n*-butyl complex **14**.

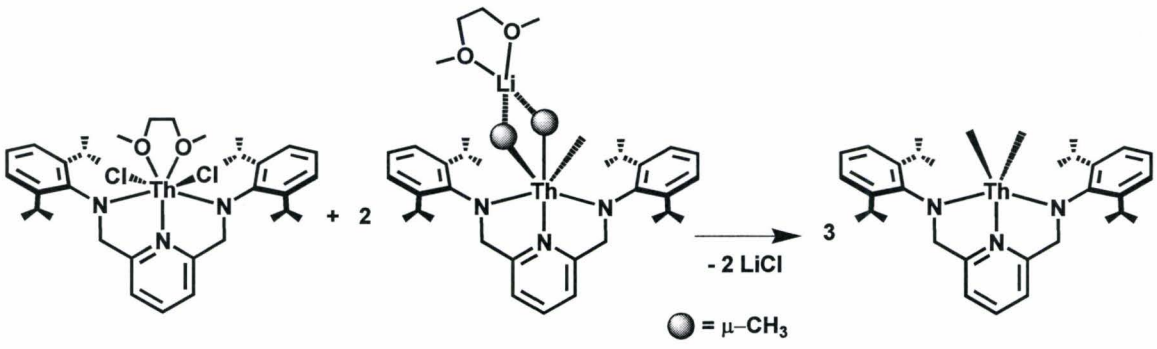

Scheme 3.9: Synthesis of [(BDPP)ThMe$_2$] (18).

While the organothorium [BDPP] complexes, [(BDPP)Th(CH_2SiMe_3)$_2$] (**9**), [(BDPP)Th(CH_2Ph)$_2$] (**13**) and [(BDPP)Th(*n*Bu)$_2$] (**14**) rival or exceeded the thermal stability of their bis-pentamethyl-cyclopentadienyl counterparts, dimethyl complex **18** is entirely decomposed to yield several unidentified products after two hours at room temperature. This behavior is in clear contrast to that of [Cp*$_2$ThMe$_2$], which is *more* stable than the CH_2SiMe_3 and CH_2Ph cyclopentadienyl analogues, being only 50 % decomposed after one week at 100 °C.[90] The thermal instability found in β-hydrogen free complex **18** is also unusual in light of the stability of the β-hydrogen containing *n*-butyl analogue (**14**). However, monitoring the decomposition of *in-situ* generated [(BDPP)Th($^{13}CD_3$)$_2$] by ^{13}C and $^{13}C\{^1H\}$ NMR spectroscopy shows the formation of only $H^{13}CD_3$ and no sign of $^{13}CD_4$, again consistent with a direct σ-bond metathesis mechanism for methane elimination. This reactivity highlights a pronounced dependence of thermal stability on the degree of steric hinderance at the metal center.

3.2.5 – Halide Exchange in the Reactions of [BDPP] and [XA_2] Dichloride Complexes with MeMgBr

Attempts to methylate dichloride **5** with methyl magnesium bromide (2 equivalents), a milder source of CH_3^-, resulted in conversion to a new product with broad ^{1}H NMR signals and CH_3 groups integrating to approximately two methyl ligands per [BDPP] ancillary. Performing this reaction in toluene and layering with hexanes at –30 ^{o}C resulted in the formation of a large (~5 x 5 x 3 mm) single X-ray quality crystal of the unexpected tetrametallic complex [{Th(BDPP)Br(μ-Br)$_2$Mg(μ-Me)(OEt$_2$)}$_2$]•2toluene (**19•2toluene**, Scheme 10).

Structural analysis showed that exchange of thorium-chloride ligands for bromides had occurred along with the formation of an adduct between the resulting [(BDPP)ThBr$_2$] moiety and MeMgBr(OEt$_2$). The complex is then tetrametallic due to methyl groups bridging between MeMgBr(OEt$_2$) moieties. This process must require the reaction of **5** with three equivalents of MeMgBr, releasing two equivalents of MeMgCl, in addition to the formation of 0.5 equivalents of **19** (Scheme 3.10**,** Figure 3.11)**.**

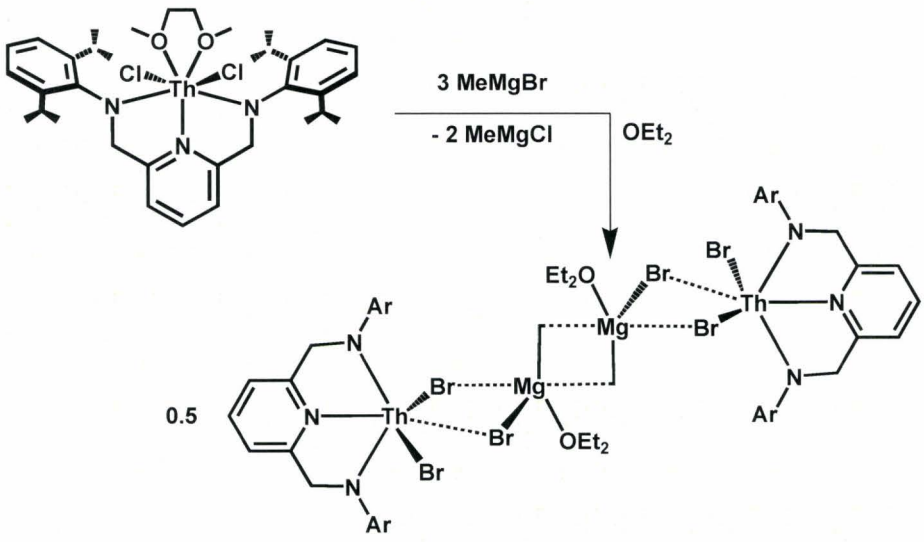

Ar = 2,6-diisopropylphenyl

Scheme 3.10: Synthesis of tetrametallic [{Th(BDPP)Br(μ-Br)$_2$Mg(μ-Me)(OEt$_2$)}$_2$] (19), with the number of equivalents of MeMgBr adjusted to those required for a balanced reaction.

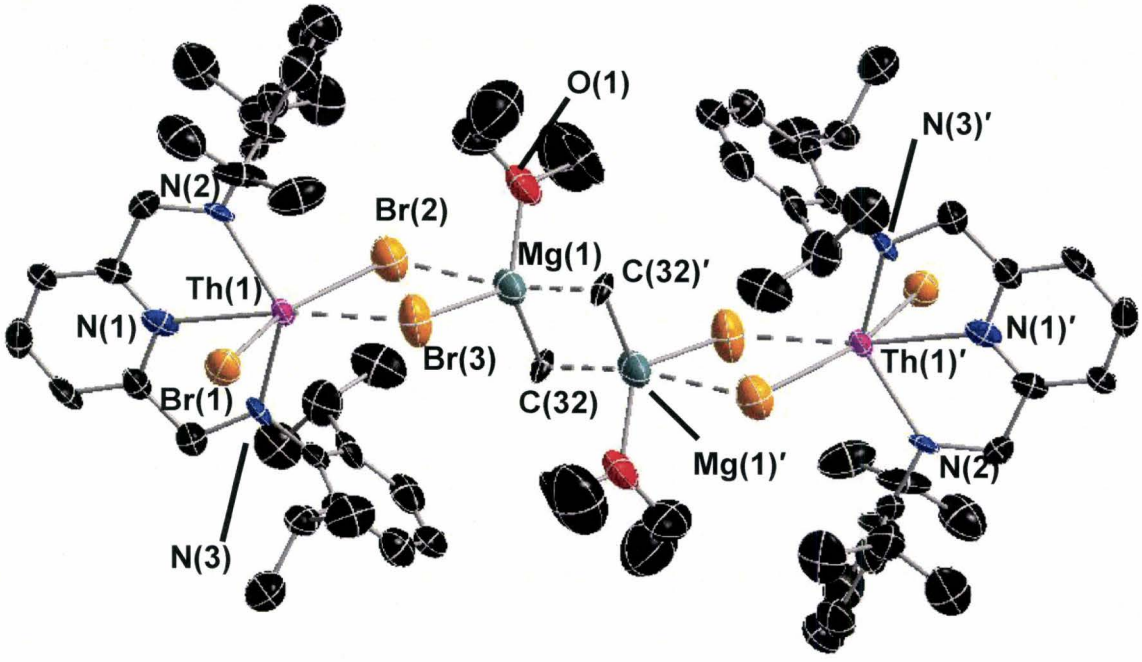

Figure 3.11: Molecular structure of tetrametallic [{Th(BDPP)Br(μ-Br)$_2$Mg(μ-Me)(OEt$_2$)}$_2$]•2toluene (19•2toluene). Thermal ellipsoids at the 50 % probability level. Hydrogen atoms and toluene solvent are omitted for clarity.

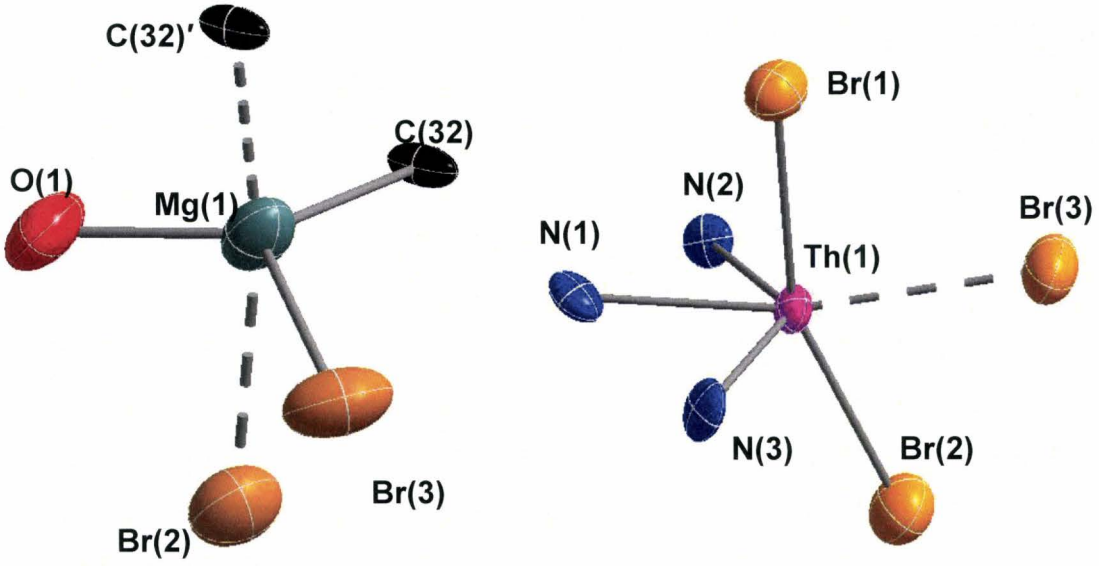

Figure 3.12: (Left) The distorted trigonal bipyramidal coordination environment of magnesium in complex 19; (Right) The highly distorted octahedral coordination environment of thorium in complex 19.

The Mg–C–Mg angles in **19** are acute {77.5(4)°}, but are typical for sterically uncluttered complexes containing a Mg(μ-alkyl)$_2$Mg core, for example [{Mg(μ-Me)$_2$}$_n$] (75°),[183] [({Mg(μ-Np)$_2$}$_3$Mg(μ-Br)$_2$)$_n$] (74.1 and 74.9°),[184] [{Br$_2$Mg(μ-Me)}$_2$]$^{2-}$ (73.7°)[185] and [{(κ^3-MeN{(CH$_2$)$_2$NMe$_2$}$_2$)Mg(μ-Me)}$_2$]$^{2+}$ (80.8 and 80.3°).[186] The asymmetry of the Mg(μ-Me)$_2$Mg core in **19** {Mg–C = 2.18(1) and 2.35(1) Å} is also not uncommon; while [{Mg(μ-Me)$_2$}$_n$] and [{Br$_2$Mg(μ-Me)}$_2$]$^{2-}$ adopt much more symmetrical structures (Mg–C = 2.24 Å in the former; Mg–C = 2.26 and 2.28 Å in the latter),[183,185] Mg–C bond distances from 2.23 to 2.34 Å were observed in [{(κ^3-MeN{(CH$_2$)$_2$NMe$_2$}$_2$)Mg(μ-Me)}$_2$]$^{2+}$,[186] and Mg–C distances from 2.20 to 2.42 Å were observed in [({Mg(μ-Np)$_2$}$_3$Mg(μ-Br)$_2$)$_n$].[184] The long Mg–C distances and acute Mg–C–Mg angle in **19** are

consistent with a 3 centre – 2 electron interaction, and confirm that the atoms bridging between Mg(1) and Mg(1') are carbon, not oxygen. For comparison, Mg–O distances and Mg–O–Mg angles are 1.94-1.99 Å and 103–106°, respectively, in the three crystallographically characterized μ_2-hydroxy magnesium complexes; [{(κ^3-$Tp^{Ar,Me}$)Mg(μ-OH)}$_2$] (Ar = *p*-*t*BuC_6H_4), [{(nacnac)Mg(THF)(μ-OH)}$_2$] and [Mg_4(THF)$_4$(OMes)$_6$(μ-OH)(μ_4-OH)].[187]

A trigonal bipyramidal geometry is observed about the magnesium centers, with C(32)', Mg(1) and Br(2) {C(32)'–Mg(1)–Br(2) = 171.3(9)°} forming the primary axis, and O(1), Br(3) and C(32) lying in the perpendicular plane. A slight distortion from an ideal trigonal bipyramidal geometry is evident, with the magnesium center laying 0.240 Å above the plane formed by O(1), Br(3) and C(32), and angles between the principal axis and in-plane atoms ranging from 80.7(4)° to 102.2(4)°. The Mg–Br(3) distance in **19** {2.534(5) Å} is similar to those observed in dinuclear [{LMgEt(μ-Br)}$_2$] complexes (2.56 Å for L = NEt_3 and 2.58 Å for L = O*i*Pr_2)[188] and in [(THF){($Me_3Si)_3$C}Mg(μ-Br)$_2$Li(THF)$_2$] (2.52 and 2.55 Å).[189] By contrast, at 2.917(6) Å, Mg–Br(2) is extremely long. A similar bonding situation was observed in the weakly bound dimer [{(*t*BuCN){($Me_3Si)_2$HC}Mg(μ-Br)}$_2$], with Mg–Br distances of 2.56 and 2.93 Å.[190]

The six coordinate Th metal centers have a highly distorted octahedral structure with N–Th–Br angles of 118.79°, 164.99° and 82.87° to the bridging bromide ligand {Br(3)} trans to the pyridine nitrogen. All other N–Th–Br angles are approximately 90° with the exception of N(1)–Th(1)–Br(2) which is 118.8(2)°. Of the three Th–Br bond lengths, Th–Br(1) and Th–Br(2) are very similar {2.856(2) and 2.884(2) Å, respectively},

even though Br(1) is terminal while Br(2) bridges between thorium and magnesium. These bond distances are in the usual range for thorium bromide complexes (2.8–2.9 Å).[84,86,160,191] However, the Th–Br bond lengths for the two bridging bromides vary significantly, with Th(1)–Br(2) being noticeably shorter than Th(1)–Br(3) {2.8848(19) Å versus 3.0065(19) Å, respectively}. Based on these bond lengths, the structure can be viewed as two molecules of (BDPP)$ThBr_2$ interacting with a central Grignard core, itself composed of two trigonal planar $MeMgBr(OEt_2)$ units linked by Mg–C–Mg bridges.

Formation of tetrametallic complex **19** is surprising given the relative strength of a Th–Cl (489 $kJmol^{-1}$) versus Th–Br (364 $kJmol^{-1}$) bond, especially when considering that Mg–Cl and Mg–Br bond strengths are so similar (327.6 and 327.2 $kJmol^{-1}$ respectively).[3] It has been reported however that there is increased ether solvent stabilization of RMgCl over analogous RMgBr compounds, which may provide some of the driving force for the production of MeMgCl and formation of the tetrametallic complex.[192] Note that reaction of dichloride **5** with two equivalents of MeMgBr followed by addition of 1,4-dioxane, did not result in the elimination of MgX_2(dioxane) {X = Cl or Br}, and formation of the corresponding methyl compound, **18**; instead, a very complex mixture of products resulted (these products do not match those formed by thermal decomposition of **18**; *vide supra*).

In actinide chemistry, a recent example of halide exchange is the reaction of $[\{O(SiMe_2NtBu)_2\}UCl_2]_2$ with MeMgBr, which resulted in the formation of $[\{O(SiMe_2NtBu)_2\}UBr_{1.46}Cl_{0.54}]_2$. By contrast, $[\{O(SiMe_2NtBu)_2\}UCl_2]_2$ reacted with $(C_3H_5)MgBr$ to give the expected diallyl complex, and $[\{O(SiMe_2N^tBu)_2\}UCl(Cp^*)]$

reacted with MeMgBr to give the anticipated methyl complex.[137] These reactions illustrate the extent to which Grignard reactivity (alkylation versus halide exchange) is influenced by subtle changes in the nature of the Grignard reagent and the d- or f-block halide complex. Another example of halide exchange in actinide chemistry is the reaction of [Cp*$_2$ThCl(η^2-*t*BuNSPh)] with MeMgBr to form [Cp*$_2$ThBr(η^2-*t*BuNSPh)].[137] Halide redistribution reactivity has also been reported for a range of lanthanide and group 3 complexes. A particularly notable example of halide exchange with a range of different aryl Grignard reagents was observed for [(P_2N_2)YCl]$_2$ [P_2N_2 = PhP($CH_2SiMe_2NSiMe_2CH_2$)$_2$PPh]. In this case, reaction with PhMgBr, *p*-tolylMgBr or *p*-biphenylMgBr gave exactly the same mixture of products: the dinuclear dichloride, the mixed chloride/bromide and the dibromide.[193]

The only other d- or f-block Grignard adduct is [Cp*(COT)Th(μ-Cl)$_2$Mg(CH_2*t*Bu)(THF)], formed via the reaction of [Cp*(COT)ThCl(THF)] with *t*BuCH$_2$MgCl.[108] However, adduct formation *and* halide exchange has only been observed in **19**. As such, complex **19** provides direct insight into the type of intermediates responsible for halide exchange. Complex **19** also highlights the potential compatibility of magnesium alkyls with metal halides; both bridging and terminal. That said, given the unavoidable presence of $MgBr_2$ in solutions of MeMgBr as a consequence of the Schlenk equilibrium (although the equilibrium lies mostly to the side of MeMgBr in OEt_2),[194] it is conceivable that halide exchange could take place via adducts with $MgBr_2$, in addition to adducts with MeMgBr.

Table 3.2: Crystallographic data collection and refinement parameters and selected bond distances for complexes 17, 19•2toluene and 20

	17[a]	**19•2toluene**[b]	**20**[b]
Formula	$C_{40}H_{62}LiN_3O_2Th$	$C_{100}H_{138}Br_6Mg_2N_6O_2Th_2$	$C_{61}H_{87}MgN_2O_3$
Fw	855.91	2448.32	920.64
Cryst. Syst.	Monoclinic	Triclinic	Monoclinic
Space Group	C2/*c*	P-1	P2(1)/*n*
a(Å)	34.258(7)	11.4202(7)	11.6044(6)
b(Å)	14.286(3)	12.7908(7)	26.1839(14)
c(Å)	17.419(4)	20.5770(12)	18.7407(10)
α(deg)	90	89.661(4)	90
β(deg)	102.922(4)	74.299(3)	94.9530(10)
γ(deg)	90	65.391(3)	90
Volume($Å^3$)	8309(3)	2611.1(3)	5673.1(5)
Z	8	1	4
Density(calcd; mg/m^3)	1.368	1.557	1.078
μ(mm^{-1})	3.622	5.199	0.075
F(000)	3456	1210	2012
Cryst size (mm^3)	0.13 x 0.10 x 0.03	0.21 x 0.19 x 0.10	0.50 x 0.50 x 0.20
θ range for collection(deg)	1.87 to 25.00	1.76 to 25.00	1.90 to 25.00
No. of reflns. collected	41676	19115	59016
No. of indep. reflns.	7306	9151	9977
Completeness to θ_{max}	99.9 %	99.4 %	99.9 %
Transmn. ratio	0.698	0.78	0.831
GOF on F^2	1.023	1.394	1.862
Final R_1 [$I > 2\sigma(I)$]	R1 = 0.0626 wR2 = 0.1184	R1 = 0.0854 wR2 = 0.1416	R1 = 0.0826 wR2 = 0.2758
R indices (all data)	R1 = 0.1446 wR2 = 0.1502	R1 = 0.1444 wR2 = 0.1538	R1 = 0.0999 wR2 = 0.2933
$M–N_{amido}$ (M = Th or Mg)	2.298(9), 2.350(9)	2.259(9), 2.266(9)	2.049(2), 2.062(2)
$M–C_{metalated}$	2.566(12),	n.a.	n.a.
$M–CH_3$	2.635(12), 2.679(13)	2.186(11), 2.321(12)	n.a.
$M–O_{xanthene}$	n.a.	n.a.	2.0796(18)
$M–N_{pyridine}$	2.614(9)	2.488(11)	n.a.
$M–O_{dme}$	n.a.	n.a.	2.091(2), 2.093(2)

[a]For **17**: *T* = 173(2) K, wavelength = 0.71073 Å, absorption correction = numerical, and refinement method = full-matrix least-squares on F^2. [b]For **19•2toluene** and **20**: *T* = 173(2) K, wavelength = 0.71073 Å, absorption correction = semiempirical from equivalents, and refinement method = full-matrix least-squares on F^2.

The analogous reaction of MeMgBr with [XA_2] dichloride **6** resulted in a similarly broad ^{1}H NMR spectrum containing a single broad methyl peak integrating to approximately 6 protons. Despite repeated attempts, X-ray quality crystals of products formed in this reaction were not obtained.

3.2.6 – Transfer of the [XA_2] Ligand from Thorium to Magnesium

During the synthesis of [(XA_2)Th(CH_2Ph)$_2$] **12** using $PhCH_2MgCl$ (*vide supra*) considerable quantities (20-50 %) of a second compound were formed if the Grignard reagent was added at –78 °C and the reaction was after a short time allowed to warm to room temperature. The identity of this compound was determined to be [(XA_2)Mg(dme)] (**20**) by ^{1}H and ^{13}C NMR spectroscopy as well as X-ray diffraction (*vide infra*). Surprisingly, this compound does not form in detectable quantities if the addition of the Grignard reagent to [(XA_2)ThCl_2(dme)] (**6**) is performed at room temperature or if the temperature of the reaction mixture is maintained at 0 °C for several hours after initial addition at –78 °C. These differences in reactivity are difficult to explain, but could involve shifts in the Schlenk equilibrium (equation 3.1) due to precipitation of $MgCl_2$ at low temperature.[192]

$$2\ RMgCl \rightleftharpoons MgR_2 + MgCl_2 \qquad (3.1)$$

The ^{1}H NMR spectrum of magnesium complex **20** in d_8-toluene is unremarkable, with signals consistent with a highly symmetric C_{2v} structure. The single dme molecule displays proton signals at δ 2.58 and 2.78 ppm for OCH_3 and OCH_2 integrating to 6 and 4

respectively. The presence of a single methyne septet at 3.55 ppm is indicative of a molecule with top-bottom and side-side symmetry in solution.

Single crystals of [(XA_2)Mg(dme)]•hexane•toluene (**20•hexane•toluene**) suitable for X-ray diffraction were grown from a toluene/hexane mixture at –30 °C. The geometry at the five-coordinate magnesium atom may best be described as distorted square pyramidal {N(1)–Mg–O(1) = 78.06(8)°; O(1)–Mg–O(3) = 97.20(9)°; N(1)–Mg–O(2) = 103.50(9)°; Figure 3.13, top}, with Mg–N bond distances of 2.049(2) and 2.062(2) Å. An $Mg–O_{xanthene}$ distance of 2.0791(18) Å is observed, which is similar to the bond lengths between the magnesium atom and the dme oxygen atoms {$Mg–O_{dme}$ = 2.091(2), 2.093(2) Å}. The single dme molecule is coordinated through one oxygen atom in the equatorial plane, while the other occupies an apical position. The 2,6-diisopropylphenyl groups are positioned to create a large open pocket for the dme molecule above the molecule, while providing steric protection to the 'open' side of the metal {C(33)•••C(42) = 7.510 Å; C(30)•••C(45) = 4.965 Å}. One of the most notable features of this structure is the deviation of the xanthene ligand back-bone towards a butterfly conformation {N(1)–Th–N(2) = 141.71(9)°; Figure 3.13, bottom}; a trait that is often observed in neutral xanthene diphosphine complexes (see Section 2.1.4) but has not been encountered in [XA_2] actinide chemistry.

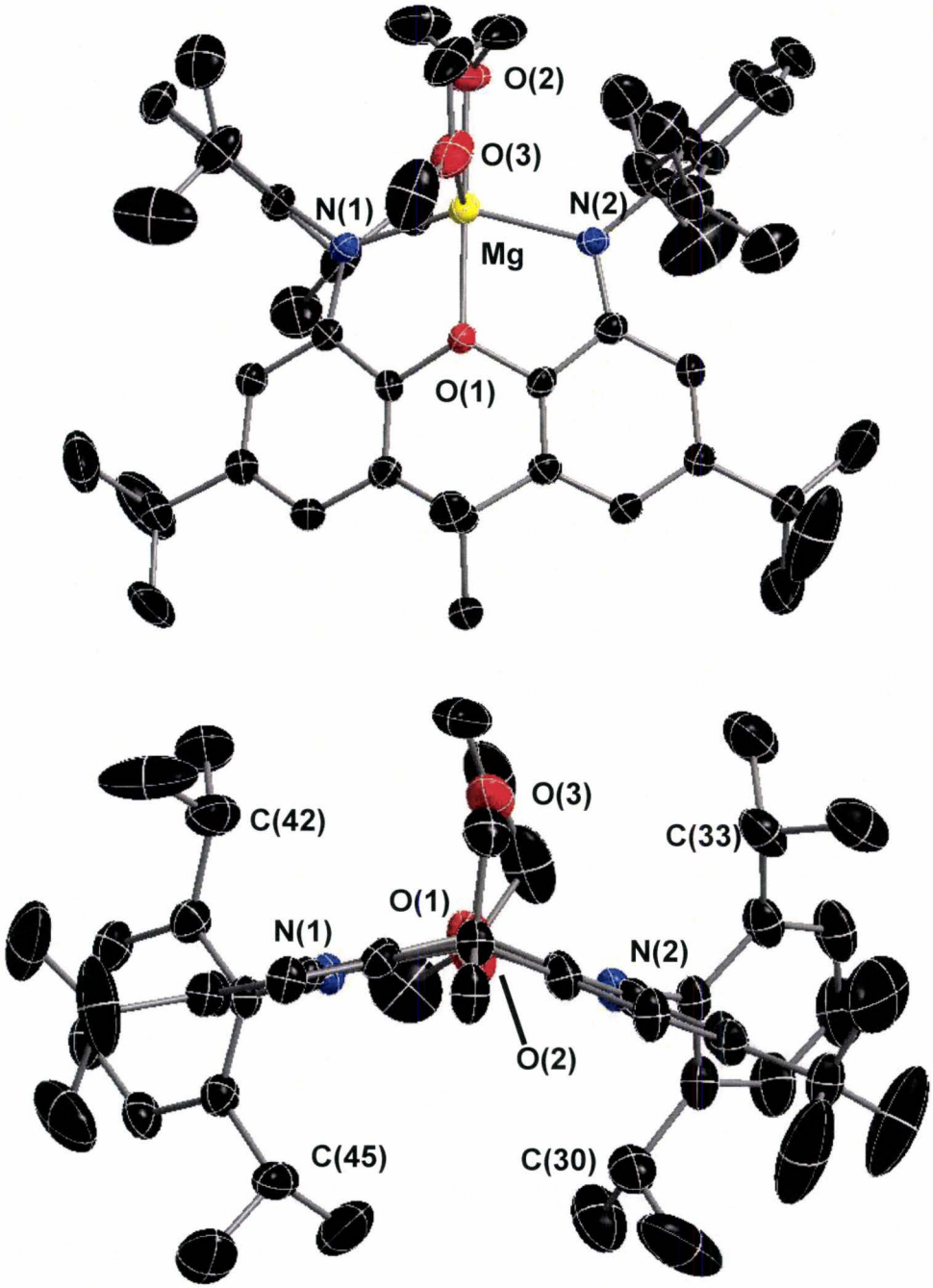

Figure 3.13: Molecular structure of [(XA$_2$)Mg(dme)]•hexane•toluene (20•hexane•toluene). Thermal ellipsoids at the 50 % probability level. Hydrogen atoms and non-coordinated solvent are omitted for clarity.

Recent examples of ancillary ligand transfer from an f-block element to magnesium are the reactions of [(nacnac)$LaBr_2(THF)_2$] and [(nacnac)La(THF)(μ-Cl)$_3$LaCl(nacnac)] [nacnac = *N*,*N*-bis(2,6-diisopropylphenyl)-β-diketiminate] with RMgCl (R = Me or allyl) to form [(nacnac)MgR(THF)] and [$LaX_3(THF)_n$] (X = Cl or Br).[195] The yttrium complex [$(PNP)_2Y(\mu\text{-}Cl)]_2$ [PNP = $N(SiMe_2CH_2PMe_2)_2$] also undergoes ligand transfer to yield [$(PNP)Y(C_3H_5)(\mu\text{-}Cl)]_2$ and [$Mg(PNP)_2$] when treated with $(C_3H_5)MgCl$ or $Mg(C_3H_5)_2$(dioxane).[196]

3.3 – Conclusions

In summary, a family of well-defined, neutral thorium dialkyl compounds (R = CH_2SiMe_3, CH_2Ph, *n*Bu and Me) supported by the [BDPP] and [XA_2] ligands has been developed. The trimethyl 'ate' complex [(BDPP)$ThMe_3${Li(dme)}] (**16**) was also prepared. The CH_2SiMe_3, CH_2Ph and *n*Bu derivatives demonstrate excellent thermal stability, in some cases rivaling or exceeding that of their bis(pentamethylcyclopentadienyl) analogues. The thermal stability of the di-*n*-butyl complexes **14** and **15** is remarkable given the presence of β-hydrogen atoms. By contrast, the dimethyl complex [(BDPP)$ThMe_2$] (**18**) and the trimethyl 'ate' complex **16** exhibit low thermal stability, highlighting the extent to which thermal stability in these complexes is controlled by the steric environment at the metal. Thermal decomposition in complex **16** occurs by ligand metallation via a straightforward σ-bond metathesis pathway. The decomposition of complexes [(L)$Th(R)_2$] {L = [BDPP], R = CH_2SiMe_3 (**9**),

CH_2Ph (**13**); L = $[XA_2]$, R = CH_2SiMe_3 (**10**), CH_2Ph (**12**)} results in the release of tetramethylsilane or toluene and precipitation of insoluble thorium-containing byproducts.

The more sterically encumbered CH_2SiMe_3 and CH_2Ph complexes exhibit fluxional behavior on the NMR time scale due to exchange of the in-plane and axial hydrocarbyl groups. The CH_2SiMe_3 complexes also exhibit an equilibrium between products, engaging in α-agostic interactions to a greater or lesser extent depending on temperature, with more agostic products favored at lower temperatures.

In contrast to the clean reactivity of chloride precursors **5** and **6** with alkyllithium reagents, reactions with Grignard reagents (MeMgBr or $PhCH_2MgCl$) resulted, under certain conditions, in halide exchange and adduct formation, or ancillary ligand transfer to magnesium. The formation of $[\{Th(BDPP)Br(\mu\text{-}Br)_2Mg(\mu\text{-}Me)(OEt_2)\}_2]$ (**19**) provides insight into the type of intermediates likely involved in undesired halide exchange reactions between d- or f-element halide complexes and Grignard reagents.

Chapter 4:

Cationic Organothorium Complexes and a Thorium Dication

4.1 – Introduction to Chapter 4

4.1.1 – Insertion Reactivity and Ethylene Polymerization

Insertion reactions are one of the fundamental types of organometallic reaction. They are also one of the basic steps in many prominent catalytic processes such as olefin polymerization, hydroamination and hydrogenation.[197-199] Insertion reactions involve migration of a coordinated unsaturated ligand (*e.g.* C_2H_4, C_2R_2 or CO) into an adjacent M–X bond to produce a new ligand in which bonds have been formed between the unsaturated ligand fragment, M and X. The two most common types of insertion reactions are referred to as 1,1- or 1,2-insertion, depending whether the metal and migrated ligand end up on the same or adjacent carbon atoms (Scheme 4.1).

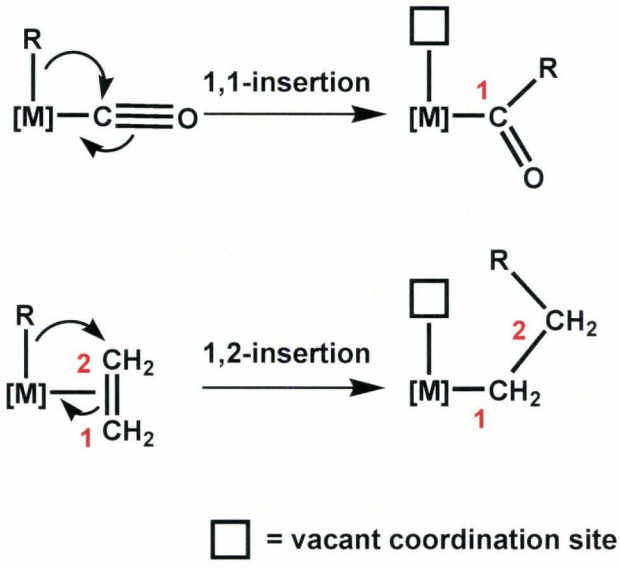

Scheme 4.1: (top) 1,1-insertion involving an alkyl group and CO, (bottom) 1,2-insertion involving an alkyl group and ethylene.

Catalytic cycles involving insertion reactions rely on binding of an unsaturated substrate in a vacant coordination site on the active catalyst, prior to the insertion step. For example, in early transition metal ethylene polymerization, an ethylene molecule must first coordinate to the metal center, where it undergoes 1,2-insertion with the alkyl group present on the metal, becoming part of the growing polymer chain (Scheme 4.2). This cycle is repeated until a chain termination event is encountered.[200]

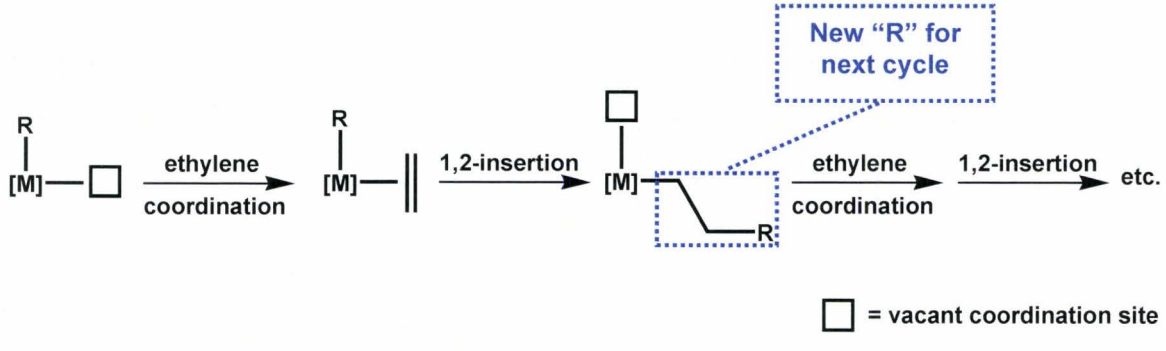

Scheme 4.2: A generic Cossee-Arlman mechanism for ethylene polymerization.

Cationic d^0-transition metal and lanthanide alkyl complexes are well established as the active species in olefin polymerization catalysis.[201] Examples of typical catalysts for olefin polymerization include carbocyclic ligand based $[Cp^*_2ZrMe][A]$, $[Cp^*(MeInd)TiMe][A]$ (MeInd = 1-methylindenyl), and $[\{SiMe_2(C_5Me_4)(N\textit{t}Bu)\}Mme][A]$ (M = Zr or Ti),[202] as well as non-carbocyclic complexes such as $[(R_3PN)_2TiMe][A]$ and $[\{CH_2(CH_2NAr)_2\}]TiMe][A]$,[203] where A is a weakly coordinating anion (*vide infra*). Polymerization catalysts of the predominantly trivalent group 3 and lanthanide metals have also been a subject of intense recent investigation, and high activities have been achieved for neutral, monocationic and dicationic alkyl complexes bearing both carbocyclic and non-carbocyclic ancillaries.[202]

Coordinatively unsaturated group 4, group 3 and lanthanide complexes with a d^0 configuration are well-suited for insertion-based polymerization due to their highly electrophilic nature, which aids greatly in the insertion step and promotes initial binding of alkene substrates, despite the unavailability of d- or f-electrons for π-back donation. The absence of d- or f-electrons on the metal available for back-donation into a β-C-H σ* orbital also results in complexes that are highly resistant β-H elimination; a potentially very important pathway for chain termination in olefin polymerization.[204]

While neutral dialkyl complexes have been reported to effect olefin polymerization,[197] highly active catalysts are typically prepared by abstraction of an alkyl group from a polyalkyl precursor to form a cationic species. Such species are particularly reactive due to increased electrophilicity and decreased coordinative saturation, relative to a neutral polyalkyl precursor complex.

4.1.2 – Cationic Alkyl Complex Formation

4.1.2.1 – Reaction with Methylaluminoxane (MAO)

One of the pivotal events in the development and wide scale implementation of olefin polymerization in industry involved the discovery that the combination of early transition metal metallocenes with methylaluminoxane (MAO; partially hydrolyzed trimethylaluminum), is capable of producing highly active catalytic systems for the polymerization of olefins.[205] Among the advantages of olefin polymerizations processes involving MAO activation is the potential for often robust and readily synthesized metallocene dichloride complexes to be used as pre-catalysts, bypassing the need to isolate air-sensitive metallocene alkyl compounds. MAO therefore serves both as an alkylating agent and a Lewis acid for alkyl group abstraction (Figure 4.1).

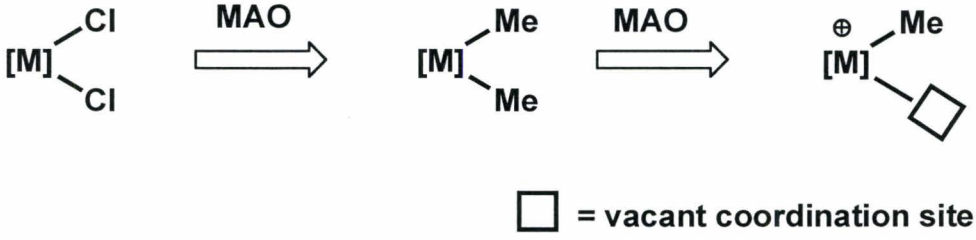

Figure 4.1: Metallocene activation roles performed by MAO.

While activation of metallocenes with MAO has been shown to be useful for the production of highly active olefin polymerization catalysts, the procedure is not without its flaws. The partial hydrolysis of trimethylaluminum is difficult to control, and often results in batches of MAO that differ greatly in composition and molecular weight,[206] which can lead to substantial variations in olefin polymerization catalyst activity.[207]

Another notable challenge pertaining to MAO co-catalyst usage is the poorly-defined structure of this compound. The difficulty in establishing the structure of MAO arises from its heterogeneity, and to date, a complete picture of the chemical structure and function of this co-catalyst has remained elusive.[208]

Furthermore, only a small amount of MAO is capable of behaving as an activator, typically requiring the use of a huge (*e.g.* 1000-fold) excess of the co-catalyst relative to a transition metal pre-catalyst. This is not only problematic from a financial and environmental perspective, but also greatly hinders mechanistic studies relating to olefin polymerization reactivity.

4.1.2.2 – Alternative Reagents for Alkyl Complex Formation

The desire to confirm the nature of the active species in olefin polymerization was largely responsible for the exploration of Lewis acid activators other than MAO for cationic alkyl complex synthesis. The goal of this area of research was the isolation and characterization of active species analogous to those presumed to be involved in MAO activated catalytic processes.

It was discovered that highly Lewis acidic boranes[205] such as tris(pentaflurophenyl)borane,[209] $B(C_6F_5)_3$, and acidic ammonium salts or trityl salts paired with a bulky 'non-coordinating' anion, such as $[PhNMe_2H][B(C_6F_5)_4]$ or $[Ph_3C][B(C_6F_5)_4]$,[123,210-212] were capable of producing active catalysts for polymerization when combined with transition metal polyalkyl complexes.[213] It is important to note that these boron-based activators are incapable of reacting with metal dichlorides to form

active species for polymerization, making the synthesis and isolation of highly reactive polyalkyl metal precursors a requirement to enable this approach.

The greatest advantage of using discrete molecules as activators is the ability to directly examine the nature of the resulting cationic complexes.[211,212] For example, the influence of supporting ligands and activators on catalyst structure, stability and reactivity can now be closely examined. However, it is important to note that while metal cations synthesized through the use of boron based activators are often discrete and isolable, they are highly air and moisture sensitive, and require rigorously anhydrous techniques for their study and utilization.[214]

4.1.2.2.1 – Reaction with Tris(pentaflurophenyl)borane

One of the most commonly employed boron based activators is tris(pentafluorophenyl)borane, $B(C_6F_5)_3$. Reaction of this perfluorinated triaryl borane with alkyl metal complexes results in a competitive binding interaction between the metal center and the borane for the abstracted alkyl group (Scheme 4.3). The resultant species generally has a greatly elongated M–C bond, with the alkyl group strongly associated to the boron atom.[215]

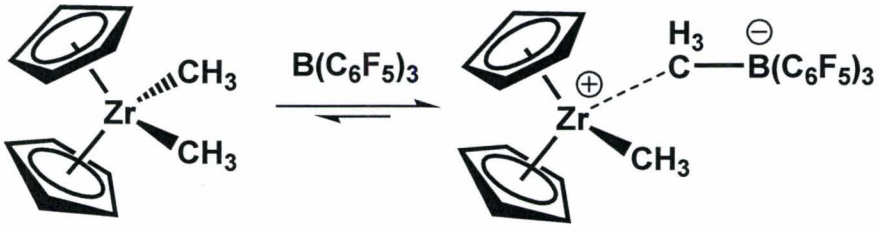

Scheme 4.3: Activation of $[Cp_2ZrMe_2]$ by tris(pentafluorophenyl)borane.

4.1.2.2.2 – Reaction with Diphenylanilinium and Trityl Salts of Tetrakis(pentafluorophenyl)borate

An alternative to the use of tris(pentafluorophenyl)borane for alkyl abstraction (pre-catalyst activation) involves the use of ammonium or trityl borate salts. With these reagents competition between the metal center and the Lewis acid activator for the alkyl group does not occur. Instead, these borate salts operate by completely eliminating the abstracted alkyl group as a reaction byproduct.

The two most common borate salts for pre-catalyst activation are trityl tetrakis(pentafluorophenyl)borate[212] $\{[Ph_3C][B(C_6F_5)_4]\}$ and dimethyl anilinium tetrakis(pentafluorophenyl)borate $\{[PhNMe_2H][B(C_6F_5)_4]\}$. In the former, the cationic trityl group acts as an alkyl abstraction agent similar to $B(C_6F_5)_3$. However, alkyl abstraction by $[Ph_3C]^+$ is irreversible and the tetrakis(pentafluorophenyl)borate anion becomes associated with the cationic metal center (Scheme 4.4). In the latter activator, the dimethylanilinium cation is a source of a single proton capable of reacting with an alkyl group on the metal center, eliminating R–H and the bulky, commonly non-coordinating byproduct dimethylaniline (Scheme 4.4). This method for alkyl group abstraction is also irreversible. The use of a borate salt, unlike tris(pentafluorophenyl)borane activation, does not result in metal stabilization through sharing of the alkyl group, and coordination of the neutral reaction byproducts (HR, NMe_2Ph or Ph_3CR) is not generally observed.[216] Instead, the cationic metal center typically interacts weakly with the $B(C_6F_5)_4^-$ counterion via long C–F•••M contacts. However, while $[B(C_6F_5)_4]^-$ based activators have proven to be highly effective for olefin

polymerization, the resulting complexes often suffer from poor solubility in hydrocarbons, poor thermal stability, and lack of crystallinity.[217]

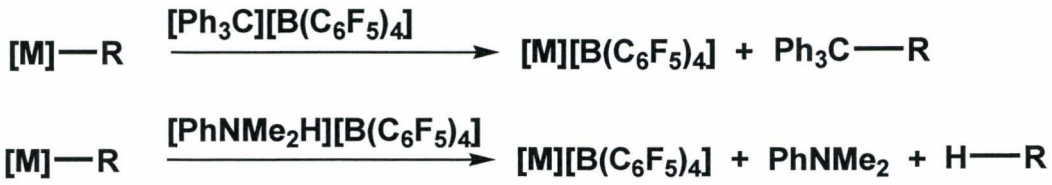

Scheme 4.4: Metal alkyl abstraction using $[Ph_3C][B(C_6F_5)_4]$ (top) and $[PhNMe_2H][B(C_6F_5)_4]$ (bottom).

4.1.3 – Actinide Olefin Polymerization Catalysts and Chapter Content

In contrast to group 3, group 4, and lanthanide catalysts for olefin polymerization, catalysts based on thorium or uranium are rare, and non-carbocyclic systems have yet to be developed. The only isolated base-free mononuclear actinide alkyl cation that has been reported to be active for ethylene polymerization is $[Cp^*_2ThMe][A]$ (A = a non-coordinating borate anion). Cationic thorium and uranium hydrocarbyl complexes are discussed in detail in Section 1.2.2.7 (*vide supra*).[51] The focus of this chapter is the synthesis of cationic thorium(IV) complexes via the reaction of neutral thorium dialkyl [BDPP] and $[XA_2]$ complexes with $B(C_6F_5)_3$ and $[Ph_3C][B(C_6F_5)_4]$.

4.2 – Results and Discussion

4.2.1 – Monocationic $[(XA_2)Th(CH_2Ph)][PhCH_2B(C_6F_5)_3]$

Slow addition of $[XA_2]$ dibenzyl complex **12** to one equivalent of $B(C_6F_5)_3$ in hexanes resulted in the immediate precipitation of $[(XA_2)Th(CH_2Ph)][PhCH_2B(C_6F_5)_3]$ (**21**, Scheme 4.5) as a bright yellow solid in 95 % yield. Despite numerous attempts, X-ray quality crystals of **21** could not be obtained. However, the nature of monocation **21** was established by NMR spectroscopy and elemental analysis.

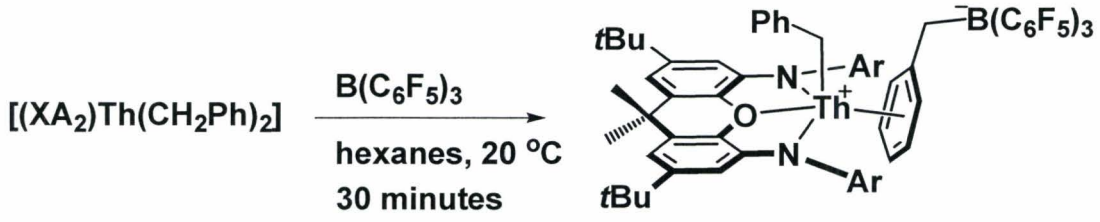

Scheme 4.5: Synthesis of monocationic $[(XA_2)Th(CH_2Ph)][PhCH_2B(C_6F_5)_3]$ (21).

At –50 °C in d_8-toluene, complex **21** shows Th–CH_2 signals at 2.40 ppm in the ^{1}H NMR spectrum and 93.1 ppm in the ^{13}C NMR spectrum. The *ipso*-ThCH_2*Ph* signals are observed at 144.5 ppm in the ^{13}C NMR spectrum. On the anion's side, BCH_2*Ph* signals are observed at 6.52 (*ortho*), 5.98 (*meta*) and 6.56 (*para*) ppm in the ^{1}H NMR spectrum, with B$CH_2C_6H_5$ and *ipso*-BCH_2*Ph* at 35.9 and 162.9 ppm respectively. The benzyl group on thorium is η^1-coordinated based on a $^1J_{C\text{-}H}$ value of 119 Hz for ThCH_2Ph.[218]

Solution NMR data for **21** between 50 and –90 °C are consistent with a C_s-symmetric complex lacking top-bottom symmetry. These data, as well as the high solubility of **21**, indicate tight ion pairing, presumably through π-coordination of the anion. Evidence for this coordination mode is provided by the 3.93 ppm chemical shift difference between the *para* and *meta* B-C_6F_5 resonances ($\Delta\delta_{m-p}$) in the ^{19}F NMR spectrum. The value of $\Delta\delta_{m-p}$ is a reliable probe for coordination of $[RB(C_6F_5)_3]^-$ (R = Me, CH_2Ph) to cationic metals; values of $\Delta\delta_{m-p}$ in the range of 3 to 6 ppm are indicative of anion coordination, while values lower than 3 ppm correspond to non-coordination of the anion.[219] The low frequency position of the *m*-BCH_2*Ph* protons (5.98 ppm) and the shift of the *ipso*-BCH_2*Ph* carbon signal (162.9 ppm) to significantly higher frequency than the "free" anion (148.2 ppm) also provide evidence to indicate tight ion pairing. Furthermore, through-space coupling between the *o*- and *m*-BCH_2*Ph* protons and one of the $CHMe_2$ groups was observed by 2D-ROESY NMR spectroscopy.

4.2.2 – Synthesis and Properties of Monocationic $[(XA_2)Th(CH_2SiMe_3)(\eta^6\text{-}C_6H_6)][B(C_6F_5)_4]$

4.2.2.1 – Synthesis and *In-situ* NMR Characterization

Reaction of a 1.5 mM solution of $[XA_2]$ dialkyl complex **10** in benzene with one equivalent of $[Ph_3C][B(C_6F_5)_4]$ resulted in the formation of several organic byproducts and a new organometallic compound over a period of 48 hours. The reaction of **10** with

two equivalents of $[Ph_3C][B(C_6F_5)_4]$ is considerably faster, resulting in complete consumption of the dialkyl precursor in just three hours, and formation of the same organometallic product. The organic byproducts formed in these reactions gave rise to NMR signals which are also be obtained by the reaction of $[Ph_3C][B(C_6F_5)_4]$ or Ph_3CCl with $LiCH_2SiMe_3$. The formation of multiple products in these reactions is surprising given that a single product ($Ph_3CCH_2SiMe_3$) would ordinarily be expected. However, similar observations have been made in the reactions of titanium trimethylsilylmethyl complexes with $[Ph_3C][B(C_6F_5)_4]$, and between Ph_3CCl with $LiCH_2SiMe_3$; the Mountford group identified these products as Ph_3CH and two isomers of $Ph_3CCH_2SiMe_3$.[220]

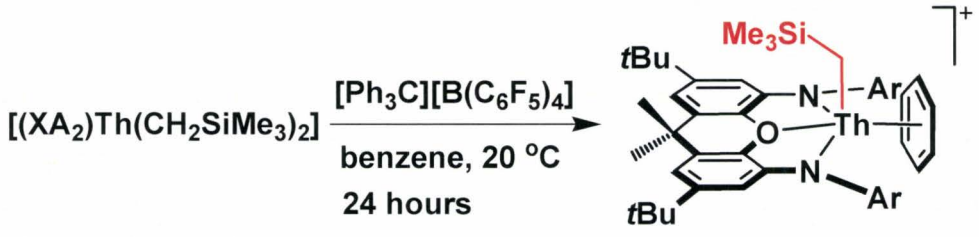

Scheme 4.6: Synthesis of monocationic $[(XA_2)Th(CH_2SiMe_3)(\eta^6\text{-}C_6H_6)][B(C_6F_4)_4]$ (22).

The ^1H and ^{13}C NMR spectra of **22** gave evidence for the formation of a thorium(IV) alkyl cation as the organometallic product, with Th-CH_2 signals for a single remaining alkyl group at δ 0.24 and 85.5 ppm in the ^1H and ^{13}C NMR spectra, respectively. The spectra also correspond with a complex that exhibits top-bottom asymmetry through the observation of two different CMe_2 and CHMe$_2$ environments.

4.2.2.2 – Solid-State Structure of $[(XA_2)Th(CH_2SiMe_3)(\eta^6\text{-}C_6H_6)][B(C_6F_5)_4]$

Unambiguous characterization of the reaction product was obtained by performing the reaction of **10** with $[Ph_3C][B(C_6F_5)_4]$ at higher concentrations (~15 mM in benzene). This resulted in the precipitation of an orange-brown oil that upon layering with hexanes at 20 °C yielded yellow crystals growing within the oil and protruding into the hexane solvent. ^{1}H NMR spectroscopy showed that this product is identical to that observed under more dilute conditions. While the oily coating on the crystals prevented successful investigation by elemental analysis, X-ray crystallography revealed the formation of a non-carbocyclic thorium alkyl cation by trimethylsilylmethyl group abstraction. However, rather than formation of a coordinatively unsaturated species stabilized through weak metal-tetrakis(pentafluorophenyl)borate anion interactions, a solvent-separated ion pair, $[(XA_2)Th(CH_2SiMe_3)(\eta^6\text{-}C_6H_6)][B(C_6F_5)_4]$ (**22**, Figure 4.2) was observed as a result of η^6-benzene coordination. In addition to being the first structurally characterized non-cyclopentadienyl thorium alkyl cation, complex **22** is a rare example of an arene solvent-coordinated alkyl cation (*vide infra*) and is the first example of this type of complex for an f-block metal.

In the solid-state structure of **22**, the $[XA_2]$ ligand is bound to thorium via slightly shorter Th–N and Th–O bonds than in neutral complex **10**, with Th–N distances of 2.278(3) and 2.288(3) Å versus 2.292(4) and 2.312(4) Å in **22**, and a Th–O distance of 2.496(5) Å versus 2.534(3) Å in **10**. The CH_2SiMe_3 group is bound in an apical position above the plane of the ligand with a Th–C(48)–Si angle of 131.0(2)°, which strongly suggests the presence of an α-agostic Th–H–C interaction (cf., 127.6(3)° and 126.8(3)° in

complex **10** in which both alkyl groups engage in temperature-dependant α-agostic Th–H–C interactions). However, the $ThCH_2$ signal in the ^{13}C NMR spectrum of **22** was extremely broad, preventing the measurement of a $^{1}J_{C\text{-}H}$ coupling constant. Benzene is approximately η^6-coordinated in the plane of the ligand, with Th–C bond distances in the range of 3.18 - 3.31 Å, and a distance of 2.95 Å from thorium to the centroid of the ring.

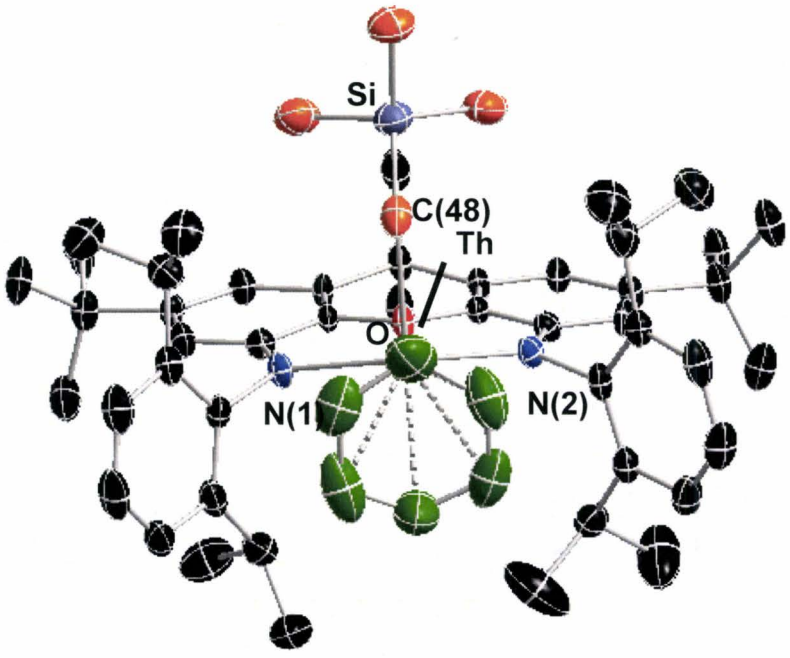

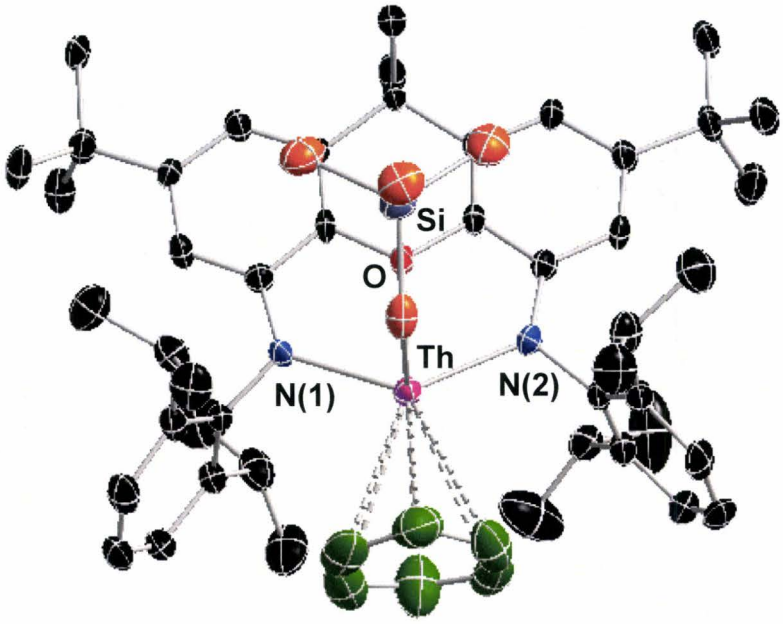

Figure 4.2: Molecular structure of $[(XA_2)Th(CH_2SiMe_3)(\eta^6\text{-}C_6H_6)][B(C_6F_5)_4]$•benzene (22•benzene). Thermal ellipsoids at the 50 % probability level. Hydrogen atoms, the borate anion and non-coordinated benzene solvent are omitted for clarity. Coordinated benzene carbon atoms in green and trimethylsilylmethyl carbons in orange.

4.2.2.3 – Detailed NMR Characterization of $[(XA_2)Th(CH_2SiMe_3)(\eta^6\text{-}C_6H_5R)][B(C_6F_5)_4]$

While neutral complex **10** does not react with PMe_3, cationic complex **22** reacted rapidly with PMe_3 to precipitate a poorly soluble brown oil, presumably $[(XA_2)Th(CH_2SiMe_3)(PMe_3)_x][B(C_6F_5)_4]$. Attempts to investigate the exact nature of the oil by dissolving it in THF resulted in decomposition to form $H_2[XA_2]$. The unequivocal absence of protic impurities in the d_8-THF was confirmed by obtaining a ^1H NMR spectrum of $LiCH_2SiMe_3$ in the same solvent used.

Reaction of cation **22** with pyridine, 4-(dimethylamino)pyridine, Et_3PO or $PhNMe_2$ also resulted in decomposition, and addition of THF resulted in polymerization of the solvent. However, the compound is stable under vacuum and may be redissolved without decomposition in bromobenzene. In the ^1H NMR spectrum of **22** in C_6D_5Br, all benzene signals were unfortunately obscured by the $[XA_2]$, $Ph_3CCH_2SiMe_3$ isomers, Ph_3CH, Ph_3C^+ (2 equivalents used for the preparation of **22**) and residual proteo-solvent signals.

Detailed NMR characterization of the $[(XA_2)Th(CH_2SiMe_3)(\eta^6\text{-arene})]^+$ cation was finally achieved by conducting the reaction of dialkyl **10** with two equivalents of $[Ph_3C][B(C_6F_5)_4]$ in toluene, which after three hours resulted in formation of the related cationic species $[(XA_2)Th(CH_2SiMe_3)(\eta^6\text{-toluene})][B(C_6F_5)_4]$ (**23**). Subsequent evaporation to dryness *in vacuo* and redissolution of complex **23** (with six equivalents of toluene remaining) in C_6D_5Br allowed observation of both free and coordinated toluene in the ^1H NMR spectrum at 20 °C, confirming that the coordinated toluene molecule in **23** is strongly bound in solution, and does not undergo rapid exchange with free toluene on the NMR timescale or undergo substitution by C_6D_5Br. Addition of 10 equivalents of toluene (C_7H_8) to a solution of benzene coordinated **22** in C_6D_6 similarly did not result in the appearance of signals for coordinated toluene in the ^1H NMR spectrum. Analogous behavior has been reported for certain d^0 π-aryl complexes, including $[Cp''MMe_2(\eta^6\text{-toluene})][MeB(C_6F_5)_3]$ (M = Ti, Zr, or Hf; Cp″ = 1,3-bis(trimethylsilyl)cyclopentadienyl; *vide infra*).[221] However, an EXSY NMR spectrum of **23** revealed that exchange of free and coordinated toluene, and loss of top-bottom asymmetry (cross peaks between C*H*Me_2

signals), does occur on a longer time scale. A small $^{1}J_{C\text{-}H}$ coupling constant of 104 Hz for ThCH_2 is also indicative of the presence of Th–H–C α-agostic interactions in **23**; an observation consistent with the unusually large Th–C–Si angle in the solid state structure of benzene-coordinated cation **22**.

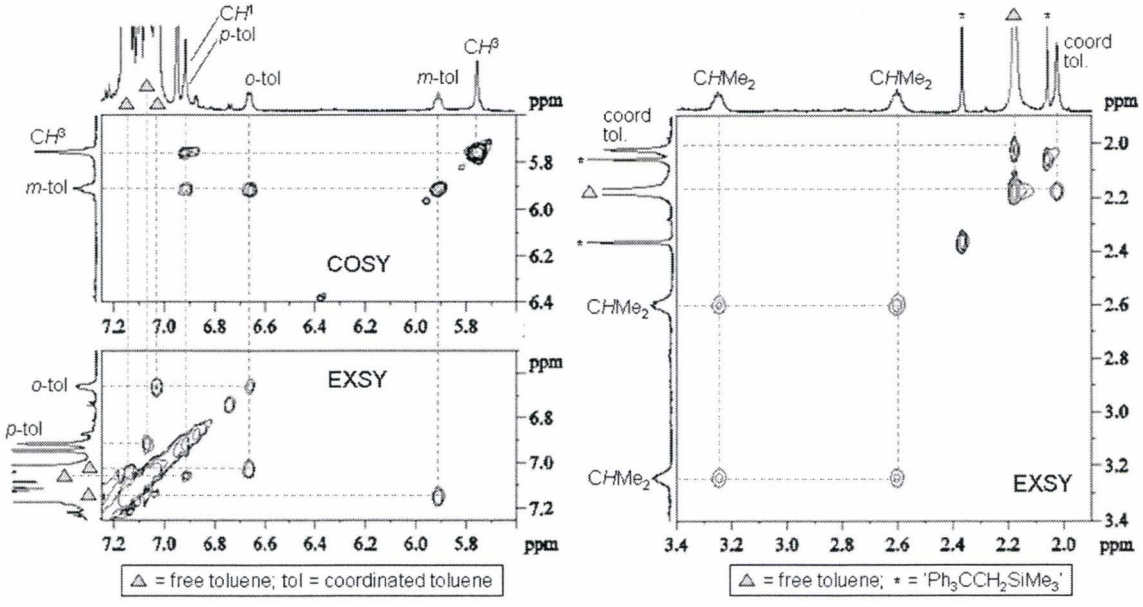

Figure 4.3: Selected regions of the ^{1}H-^{1}H COSY and EXSY (τ_m 0.5 s) NMR spectra for 23 with 6 equivalents of toluene in C_6D_5Br at 20 °C (sample generated in situ from the reaction of 10 with 2 equivalents of $[Ph_3C][B(C_6F_5)_4]$ in toluene, followed by evaporation to dryness *in vacuo* and redissolution in C_6D_5Br).

Table 4.1: Crystallographic data collection and refinement parameters and selected bond distances for monocationic and dicationic complexes 22•2benzene and 27

	22•2benzene	**27**
Formula	$C_{63}H_{85}$	$C_{127}H_{121}B_2F_{30}N_2OTh$
fw	1825.51	2514.92
Cryst. Syst.	Orthorhombic	Triclinic
Space group	Pca2(1)	P-1
a(Å)	26.721(6)	13.8360(16)
b(Å)	15.842(5)	16.6177(19)
c(Å)	19.271(6)	25.570(3)
α(deg)	90	76.793(2)
β(deg)	90	87.806(3)
γ(deg)	90	89.678(2)
Volume($Å^3$)	8158(4)	5719.5(11)
Z	4	2
Density(calcd; mg/m^3)	1.486	1.460
μ(mm^{-1})	1.935	1.405
F(000)	3672	2550
Cryst size (mm^3)	0.50 x 0.50 x 0.01	0.20 x 0.20 x 0.02
θ range for collection(deg)	1.49 to 27.16°	1.64 to 27.53°
No. of reflns. collected	92468	71694
No. of indep. reflns.	15797	25890
Completeness to θ_{max}	99.2 %	98.3 %
Max. and min. transmn.	0.9809 and 0.4445	1.000 and 0.842
GOF on F^2	1.036	0.970
Final R_1 [$I > 2\sigma(I)$]	R1 = 0.0313	R1 = 0.0722
	wR2 = 0.0572	wR2 = 0.1341
R indices (all data)	R1 = 0.0674	R1 = 0.1586
	wR2 = 0.0673	wR2 = 0.1653
Th–N_{amido}	2.278(3), 2.28(3)	2.317(6), 2.322(5)
Th–O	2.496(3)	2.403(4)
Th–C_{alkyl}	2.434(5)	n.a.
Th–C_{arene}	3.179 – 3.310	2.901 – 3.281
		2.937 – 3.257

For **22•2benzene** and **27**: *T* = 173(2) K, wavelength = 0.71073 Å, absorption correction = semiempirical from equivalents, and refinement method = full-matrix least-squares on F^2.

4.2.3 – Synthesis and Properties of Monocationic $[(XA_2)Th(\eta^2\text{-}CH_2Ph)(\eta^6\text{-}C_7H_8)][B(C_6F_5)_4]$

In a reaction analogous to the synthesis of complex **22**, treatment of $[(XA_2)Th(CH_2Ph)_2]$ (**12**) with one equivalent of $[Ph_3C][B(C_6F_5)_4]$ in benzene or toluene resulted in the slow formation of one equivalent of Ph_3CCH_2Ph per equivalent of **12** consumed and precipitation of an orange-brown oil. Unlike the oil formed in the reaction of **10** with $[Ph_3C][B(C_6F_5)_4]$, this oil was insoluble in benzene, toluene, OEt_2 and bromobenzene, and polymerized THF, which precluded characterization by solution NMR spectroscopy. Deposition of the oil formed during the reaction as a film on the walls of the reaction vessel also prevented direct NMR spectroscopy of the oil using an NMR insert. Furthermore, reaction of the oil with PMe_3 did not result in the formation of a more soluble product, and attempted dissolution of the presumed PMe_3-coordinated product in d_8-THF resulted in decomposition to release $H_2[XA_2]$. However, for the oil deposited in toluene, layering with hexanes provided yellow crystals growing within the oil and protruding out into the solvent. X-ray diffraction of the crystals (Table 4.1) revealed the second example of an organothorium cation existing as an arene solvent-separated ion pair: $[(XA_2)Th(\eta^2\text{-}CH_2Ph)(\eta^6\text{-}C_7H_8)][B(C_6F_5)_4]$ (**24**, Figure 4.4).

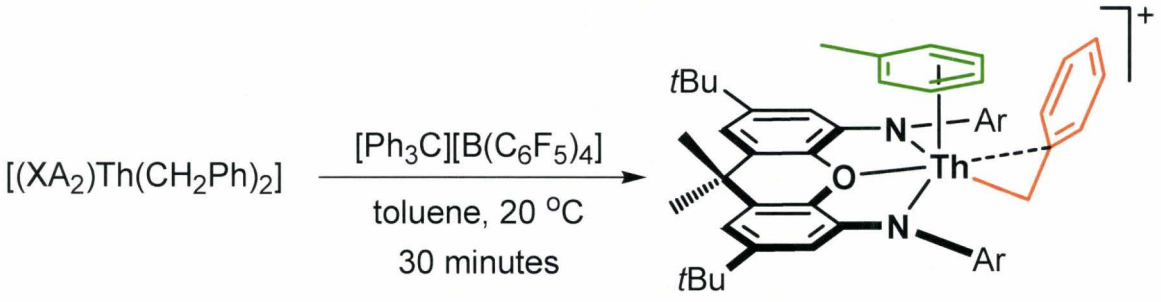

Scheme 4.7: Synthesis of monocationic $[(XA_2)Th(\eta^2\text{-}CH_2Ph)(\eta^6\text{-}C_7H_8)][B(C_6F_5)_4]$ (24).

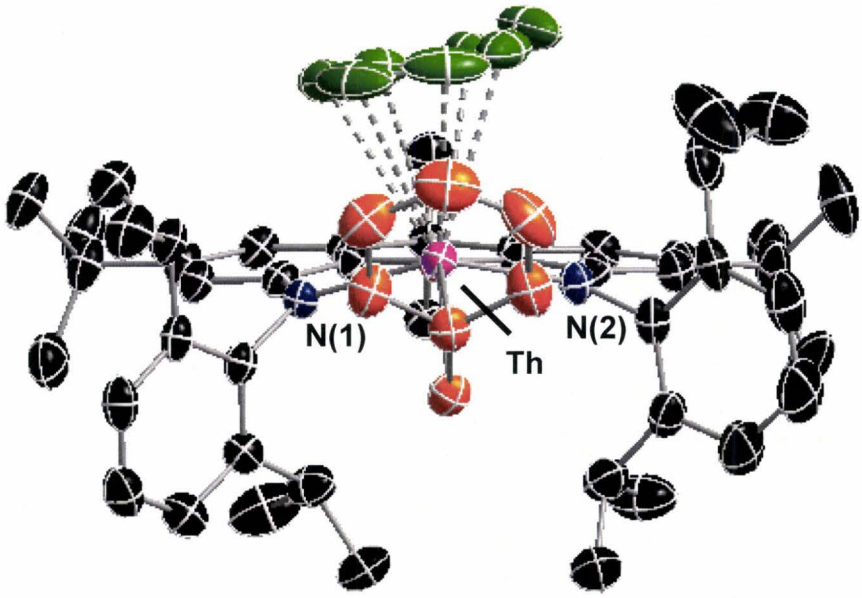

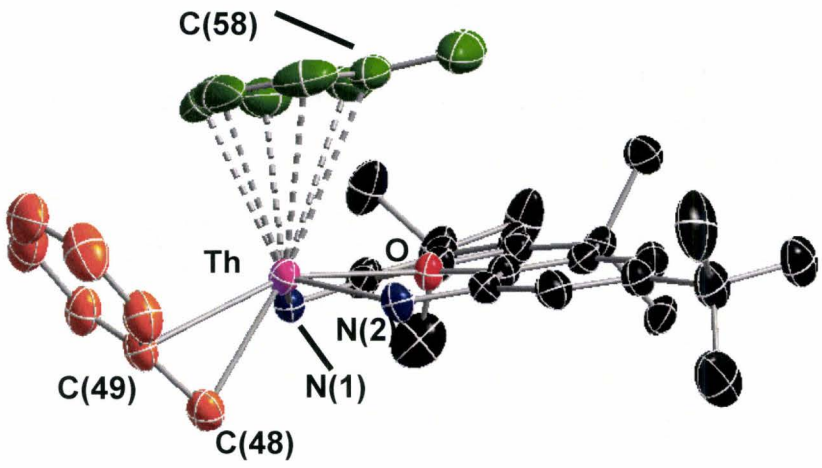

Figure 4.4: Molecular structure of $[(XA_2)Th(\eta^2\text{-}CH_2Ph)(\eta^6\text{-}C_6H_5Me)][B(C_6F_5)_4]$•2toluene (24•2toluene). Thermal ellipsoids at the 50 % probability level. In both views, hydrogen atoms, the borate anion and non-coordinated toluene solvent are omitted for clarity. In the second view (bottom), *N*-aryl groups are also omitted for clarity. Coordinated toluene carbon atoms in green and benzyl carbon atoms in orange.

The solid state structure of cationic benzyl complex **24** shares many similarities with that of **22**. However, in **24**, the arene occupies an apical position and the anionic R group (η^2-CH_2Ph) is bound in the plane of the $[XA_2]$ ligand. The arene is also less symmetrically bound to the metal in **24**, with Th-C distances increasing from 3.06 to 3.44 Å toward the most sterically hindered methyl-substituted position {C(58)}. It is therefore possible that toluene in **24** may be more accurately described as η^4- or η^5-coordinated. However, η^6-bonding cannot be excluded on the basis of the observed Th–C distances, which lie within the sum of the van der Waals radii for thorium and carbon (~3.60 Å).[7, 222] In addition, the Th–ring centroid distance of 2.94 Å is almost identical to that observed in complex **22**.

Similarly to complex **22**, a reduction in the Th–N and Th–O bond distances is observed relative to the corresponding neutral precursor, with Th–N distances of 2.314(3) and 2.320(3) Å in **24** versus 2.318(2) – 2.339(3) Å in **12** and a Th–O distance of 2.455(3) Å versus 2.526(2) and 2.519(2) Å in **12** (note: the two sets of Th–N and Th–O bond lengths listed for dibenzyl **12** correspond to the two distinct molecules in the unit cell). In complex **24** shortening of the Th–O bond distance relative to that in neutral dibenzyl precursor **12** is particularly pronounced, perhaps as a result of η^2-benzyl coordination in the plane of the [XA_2] ligand, which positions the metal further above the NON-plane and back toward the xanthene backbone of the ligand (evident by the displacement of thorium from the NON-plane by 0.724 Å in **24** versus 0.469 Å in **22**).

The current observations of arene solvent coordination, even in the presence of a polyhapto-coordinating benzyl ligand (in **24**), further highlight the extent to which metal-arene interactions become favorable in the chemistry of more sterically open non-carbocyclic alkyl thorium cations.

4.2.4 – Comparison of [$(XA_2)Th(CH_2SiMe_3)(\eta^6\text{-}C_6H_6)$][$B(C_6F_5)_4$] and [$(XA_2)Th(CH_2SiMe_3)(\eta^6\text{-}C_7H_8)$][$B(C_6F_5)_4$] with Literature Examples of Arene Solvent-Separated Ion Pairs

While contact ion pairs (CIPs) such as [Cp^*_2ZrMe][$MeB(C_6F_5)_3$] have been studied in detail, and solvent separated ion pairs (SSIPs) involving strong donor solvents are common {*e.g.*, [$Cp^*_2ZrMe(THF)$][$MeB(C_6F_5)_3$]},[205] SSIPs involving weakly coordinated arene solvents are rare, and their impact on olefin polymerization activity and

selectivity is not well understood. McConville *et al.* invoked a species of the form $[\{CH_2(CH_2NAr)_2\}TiR(\eta^6\text{-toluene})]^+$ (Ar = Xyl or $C_6H_3{}^iPr_2$-2,6) to explain greatly reduced polymerization activities observed in the presence of small amounts of toluene.[223] In addition, Piers *et al.* reported the synthesis of $[(nacnac^{Me2})ScMe(\eta^6\text{-}C_6R_6)][B(C_6F_5)_4]$ (C_6R_6 = bromobenzene, benzene, toluene, *p*-xylene, or mesitylene), and while $[(nacnac^{Me2})ScMe(\eta^6\text{-}C_6H_3Me_3\text{-}1,3,5)][B(C_6F_5)_4]$ is an active ethylene polymerization catalyst in bromobenzene, it shows negligible activity in more strongly-donating toluene.[224] Other d^0 arene solvent coordinated alkyl complexes are $[Cp''MR_2(\eta^6\text{-toluene})][RB(C_6F_5)_3]$ {M = Zr, R – Me; M = Hf, R = Me or Et; Cp'' = 1,3-$C_5H_3(SiMe_3)_2$} in which the arene is tightly coordinated,[221] $[Cp^*MMe_2(\eta^6\text{-}C_6R_6)][MeB(C_6F_5)_3]$ (M = Ti, C_6R_6 = toluene or mesitylene; M = Zr, C_6R_6 = benzene, toluene, *p*-xylene, *m*-xylene, mesitylene, styrene, anisole) in which the arene is particularly labile for M = Ti,[225] and $[\{\kappa^1N\text{-}t\text{BuNSiMe}_2(\eta^5,\eta^1C\text{-}C_5Me_3CH_2)\}Ti(\eta^6\text{-toluene})][B(C_6F_5)_4]$ in which the arene is only weakly bound.[179]

4.2.5 – Comparison of $[(XA_2)Th(CH_2SiMe_3)(\eta^6\text{-}C_6H_6)][B(C_6F_5)_4]$ and $[(XA_2)Th(\eta^2\text{-}CH_2Ph)(\eta^6\text{-}C_7H_8)][B(C_6F_5)_4]$ with Other Arene-coordinated Actinide Complexes

Other structurally characterized actinide(IV) complexes containing a bound neutral arene are $[\{(C_6Me_6)UCl_2\}_2(\mu\text{-Cl})_3][AlCl_4]$ and $[\{(C_6Me_6)UCl_2(\mu\text{-Cl})_3\}_2UCl_2]$ reported by Cotton *et al.*, with $U\text{–}C_{mean}$ bond distances of 2.92 and 2.94 Å respectively.[226] To allow meaningful comparison with **22** and **24**, the $M\text{–}C_{mean}$ distances can be adjusted to take into account the larger ionic radius of thorium(IV) {0.94 Å} relative to

uranium(IV) {0.89 Å}.[7] In addition, some indication of the extent to which the increased steric presence and electron density associated with a C_6Me_6 ring, relative to a C_6H_6 ring, affects M–C_{mean} bond distances can be assessed with reference to $[(C_6R_6)U^{III}(AlCl_4)_3]$; only small variations in the U–C_{mean} distances are observed for C_6R_6 = benzene, toluene and mesitylene (2.92, 2.94 and 2.93 Å respecitively).[227] Similarly, Sm–C_{mean} distances in $[(\eta^6\text{-}C_6R_6)Sm^{III}(AlCl_4)_3]$ vary from 2.91 to 2.88 Å for C_6R_6 = benzene, *m*-xylene and mesitylene.[227] Based on these data, it appears that much stronger actinide-arene bonding is observed in Cotton's C_6Me_6 complexes.[226] The longer Th–C distances of 3.263 and 3.240 Å in **22** and **24**, respectively, are likely the result of very significant steric hindrance in the $[XA_2]$ and [BDPP] complexes, perhaps combined with the general trend toward reduced covalency in complexes of thorium, relative to uranium.[90]

4.2.6 – Dinuclear $[(BDPP)Th(\eta^2\text{-}CH_2Ph)(\mu\text{-}\eta^1\text{:}\eta^6\text{-}CH_2Ph)Th(\eta^1\text{-}CH_2Ph)(BDPP)][B(C_6F_5)_4]$

In contrast to the reactions of neutral $[(XA_2)Th(CH_2SiMe_3)_2]$ (**10**) and $[(XA_2)Th(CH_2Ph)_2]$ (**12**) with $[Ph_3C][B(C_6F_5)_4]$, which formed only mononuclear products, addition of less than one equivalent of $[Ph_3C][B(C_6F_5)_4]$ to solutions of $[(BDPP)Th(CH_2Ph)_2]$ (**13**) in benzene resulted in precipitation of an orange-brown oil, which upon layering with hexanes at 20 °C yielded crystals of dinuclear $[(BDPP)Th(\eta^2\text{-}CH_2Ph)(\mu\text{-}\eta^1\text{:}\eta^6\text{-}CH_2Ph)Th(\eta^1\text{-}CH_2Ph)(BDPP)][B(C_6F_5)_4]$ (**25**, Figure 4.5).

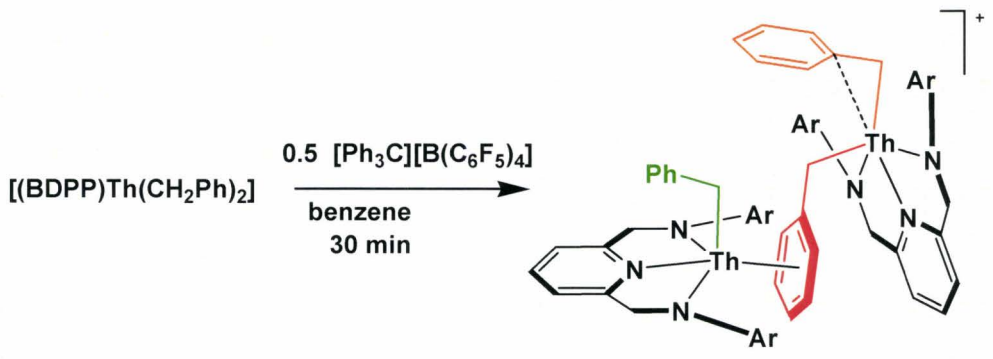

Scheme 4.8: Synthesis of dinuclear [(BDPP)Th(η^2-CH_2Ph)(μ-η^1:η^6-CH_2Ph)Th(η^1-CH_2Ph)(BDPP)][$B(C_6F_5)_4$] (25).

Complex **25** is composed of a cationic [(BDPP)Th(η^1-CH_2Ph)]$^+$ fragment coordinated via an η^6-interaction to the benzyl group of a molecule of the neutral starting material [(BDPP)Th(CH_2Ph)$_2$] (**13**). In more detail, the metal center {Th(2)} in the cationic fragment of **25** is η^1-coordinated to a benzyl substituent in an axial position, and in the plane of the ligand, is η^6-coordinated to the benzyl group of a molecule of the neutral starting material **13**. By contrast, the metal center {Th(1)} in the coordinated molecule of **25** is η^2-coordinated to a benzyl group in the plane of the ligand, and η^1-coordinated to the bridging benzyl ligand, which occupies an axial position.

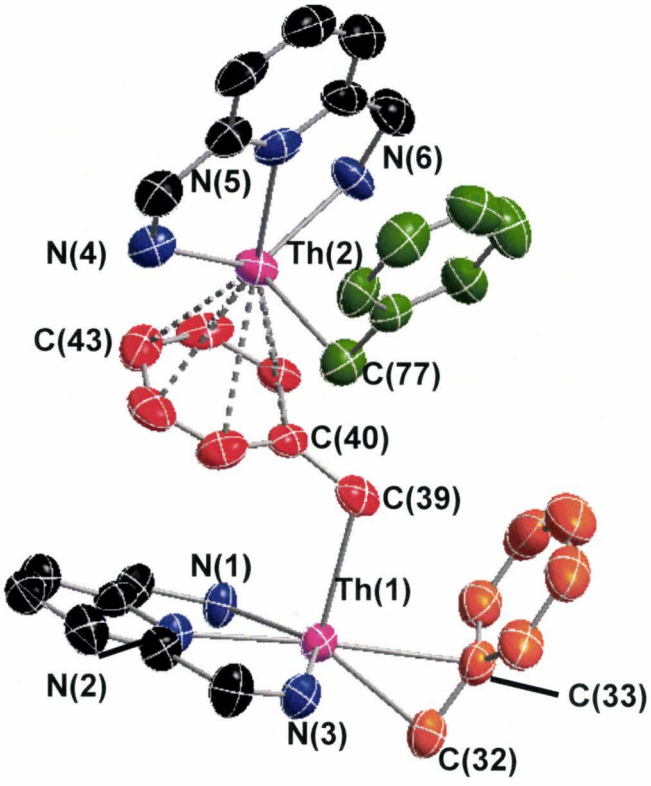

Figure 4.5: Molecular structure of [(BDPP)Th(η^2-CH_2Ph)(μ-η^1:η^6-CH_2Ph)Th(η^1-CH_2Ph)(BDPP)][$B(C_6F_5)_4$]•0.75hexane•0.55benzene (25•0.75hexane•0.55benzene). Thermal ellipsoids at the 50 % probability level. The borate anion, 2,6-diisopropylphenyl groups, hydrogen atoms and solvent are omitted for clarity. The "neutral moiety" non-bridging benzyl group is colored orange, the bridging benzyl group is colored red and "cationic moiety" benzyl group is colored green.

The arrangement of the ligands in the cationic portion of **25** is more similar to that in the trimethylsilylmethyl cation **22**, than η^6-benzyl cation **24**; that is, the alkyl group (η^1-benzyl in **25**) does not lie in the plane of the ligand, but rather occupies an apical site. However, while benzene is bound quite symmetrically in complex **22**, the Th–C_{ring} distances in **25** vary from 2.97(1) to 3.35(1) Å, increasing toward the more sterically hindered *ipso*-carbon{C(40)} of the μ-η^1:η^6-benzyl ligand. A similar variation in Th–C_{ring}

distances was observed in toluene-coordinated cation **24**. The presence of significant steric hinderance at the arene coordinated cationic thorium center is particularly evident from the degree of twisting in the 2,6-diisopropylphenyl rings of the [BDPP] ligand on Th(2), resulting in C(59)•••C(71) and C(62)•••C(74) distances of 4.37 and 8.31 Å respectively.

Crystallographically characterized complexes containing a μ-η^1:η^n-benzyl bridging interaction similar to that in **25** have not been previously reported in f-block or early transition metal (groups 3-5) chemistry, and to the best of our knowledge, such complexes do not exist for any metal. Observation of this unusual coordination mode in **25** again illustrates the propensity of cationic non-carbocyclic thorium complexes to engage in π-arene coordination. The strong tendency towards π-arene bonding in this chemistry may also be related to increased covalency in actinide-ligand bonding, relative to the lanthanide-ligand bonding, and the potential for f-orbital involvement in bonding. However, it is perhaps unexpected that a π-interaction between the cationic fragment and a molecule of neutral **13** is preferred over an η^6-interaction with benzene, which was present in vast excess as the reaction and crystallization solvent. This preference is likely due to the more electron rich nature of metal-benzyl groups, relative to benzene, in part as a result of delocalization of negative charge into the ring. The presence of a more effective interaction between the cationic fragment of **25** and the benzyl group of a molecule of **13**, relative to an interaction with a neutral arene, is supported by a Th–ring centroid distance of 2.79 Å, as compared to 2.95 and 2.94 Å in **22** and **24** respectively.

Table 4.2: Crystallographic data collection and refinement parameters and selected bond distances for cationic complexes 24•toluene and 25•0.75hexane•0.55benzene

	24•2toluene	**25•0.75hexane•0.55benzene**
Formula	$C_{97}H_{89}BF_{20}N_2OTh$	$C_{144.8}H_{116.8}BF_{20}N_6Th_2$
fw	1921.55	2435.43
Cryst. Syst.	Monoclinic	Monoclinic
Space group	C2/c	P2(1)/n
a(Å)	47.788(3)	12.8654(6)
b(Å)	14.0800(8)	15.9543(8)
c(Å)	27.0268(15)	53.790(3)
α(deg)	90	90
β(deg)	121.8730(10)	91.4000(10)
γ(deg)	90	90
Volume(Å^3)	16540.0(16)	11037.5(9)
Z	8	4
Density(calcd; mg/m^3)	1.543	1.466
μ(mm^{-1})	1.900	2.774
F(000)	7744	4850
Cryst size (mm^3)	0.45 x 0.40 x 0.05	0.50 x 0.12 x 0.08
θ range for collection(deg)	1.44 to 27.58°	1.48 to 26.53°
No. of reflns. collected	89440	129031
No. of indep. reflns.	19101	22842
Completeness to θ_{max}	99.7 %	99.6 %
Max. and min. transmn.	1.00 and 0.77	1.000 and 0.549
GOF on F^2	0.981	1.255
Final R_1 [$I > 2\sigma(I)$]	R1 = 0.0396	R1 = 0.0957
	wR2 = 0.0912	wR2 = 0.2158
R indices (all data)	R1 = 0.0636	R1 = 0.1455
	wR2 = 0.0984	wR2 = 0.2377
Th–N_{amido}	2.317(3), 2.321(3)	Th(1): 2.276(8), 2.290(9)
		Th(2): 2.266(9), 2.300(10)
Th–C	2.482(4)	Th(1): 2.562(12), 2.617(11)
		Th(2): 2.504(11)
Th–C_{ipso}	2.727(4)	Th(1): 2.820(12)
Th–N_{py}	n.a.	Th(1): 2.550(9)
		Th(2): 2.524(9)
Th–O	2.454(2)	n.a.

For **24•2toluene** and **25•0.75hexane•0.55benzene**: T = 173(2) K, wavelength = 0.71073 Å, absorption correction = semiempirical from equivalents, and refinement method = full-matrix least-squares on F^2.

Direct investigation of the organometallic products formed in the reaction of complex **13** with $[Ph_3C][B(C_6F_5)_4]$ was prevented by their insolubility in benzene, toluene, OEt_2 or bromobenzene, and polymerization of THF. However, the reaction could be probed indirectly by monitoring the disappearance of **13** and the formation of Ph_3CCH_2Ph by ^1H NMR spectroscopy in the presence of $O(SiMe_3)_2$ as an internal standard. The reaction of **13** with half an equivalent of $[Ph_3C][B(C_6F_5)_4]$ was complete after 30 minutes at 20 °C, whereupon no further change in the amount of starting materials was observed. This reaction resulted in consumption of 0.7 equivalents of **13** and release of 0.5 equivalents of Ph_3CCH_2Ph, consistent with the formation of a 0.3:0.2:0.3 mixture of unreacted **13**, **25**, and a mononuclear cation (Scheme 4.9). This mononuclear cation is presumed to have the composition of $[(BDPP)Th(CH_2Ph)(benzene)][B(C_6F_5)_4]$ (**26**) by analogy with cations **22** and **24**. The formation of a 0.3:0.2:0.3 mixture of **13**, **25** and **26** was also confirmed by the addition of ten equivalents of PMe_3 to the reaction mixture, which resulted in liberation of 0.2 equivalents of soluble **13** back into solution. In contrast, addition of ten equivalents of toluene to mixtures containing dinuclear **25** did not release any observable amounts of **13**. However, conducting the reaction of **13** with one equivalent of $[Ph_3C][B(C_6F_5)_4]$ resulted in an approximately 1:1 ratio of **13** consumed to Ph_3CCH_2Ph produced, consistent with the precipitation of mononuclear **26** as the major product.

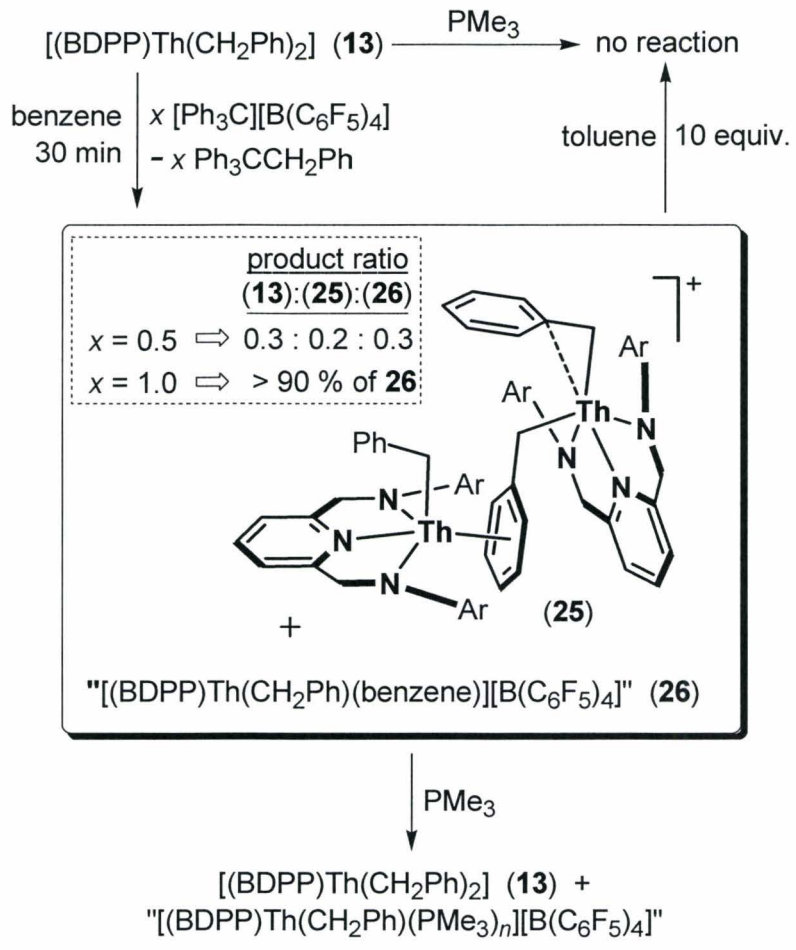

Scheme 4.9: Synthesis and reactivity of [(BDPP)Th(η^2-CH_2Ph)(μ-η^1:η^6-CH_2Ph)Th(η^1-CH_2Ph)(BDPP)][$B(C_6F_5)_4$] (25).

In contrast to reactions of neutral [BDPP] dibenzyl **13** with [Ph_3C][$B(C_6F_5)_4$], monitoring the reaction of [(XA_2)Th(CH_2Ph)$_2$] (**12**) with half an equivalent of [Ph_3C][$B(C_6F_5)_4$] and subsequent addition of PMe_3 by ^{1}H NMR spectroscopy did not provide any evidence for the formation of a dinuclear complex analogous to **25**. The greater accessibility of a dinuclear complex with the [BDPP] ligand relative to the [XA_2]

ligand, is likely a consequence of the less sterically bulky and more flexible backbone of the [BDPP] ligand.

4.2.7 – Synthesis and Properties of Dicationic $[(XA_2)Th][PhCH_2B(C_6F_5)_3]_2$

Slow diffusion of a hexane solution of $B(C_6F_5)_3$ into a toluene solution of monocation **21** at –30 °C resulted in the precipitation of a bright orange crystals. Solution NMR spectroscopic studies on this product were not possible due to insolubility in solvents with which it did not react, such as toluene, benzene, and bromobenzene. The complex was however identified as dicationic $[(XA_2)Th][PhCH_2B(C_6F_5)_3]_2$ (**27**, Scheme 4.6) by X-ray crystallography (Table 4.1) and elemental analysis. The only other structurally characterized organoactinide dications are $[(COT)U(hmpa)_3][BPh_4]_2$ and $[Cp^*_2U(NCMe)_5][X]_2$ (X = I, OTf or BPh_4).[129, 228]

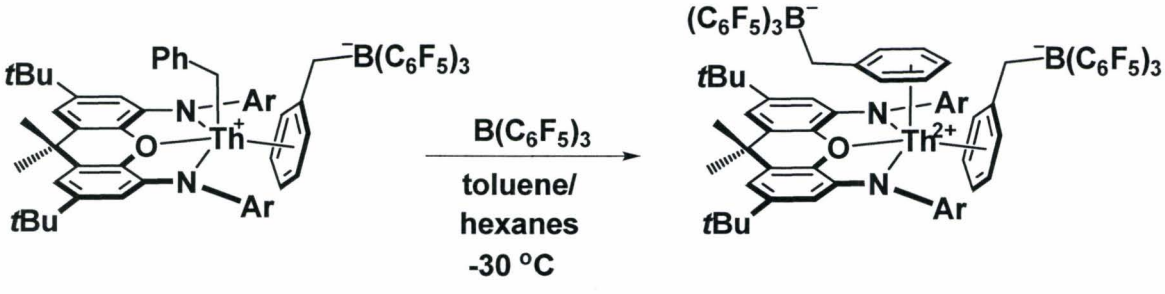

Scheme 4.10: Synthesis of dicationic $[(XA_2)Th][PhCH_2B(C_6F_5)_3]_2$ (27).

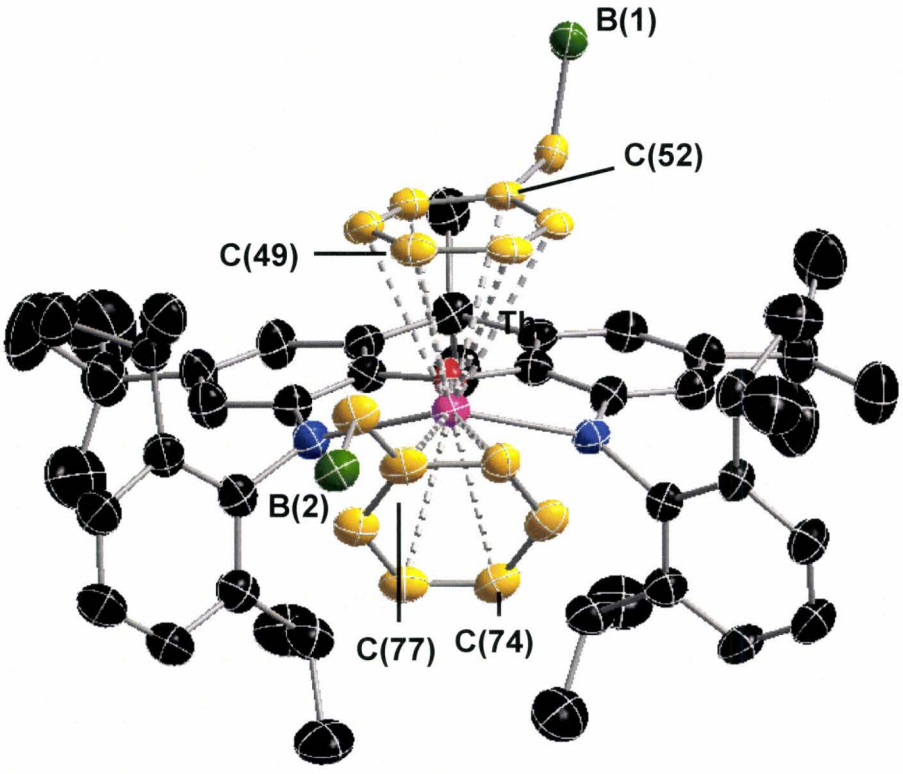

Figure 4.6: Molecular structure of dicationic $[(XA_2)Th][[PhCH_2B(C_6F_5)_3]_2$•3toluene•2hexanes (27•3toluene•2hexanes). Thermal ellipsoids at the 50 % probability level. Perfluorinated aryl groups, hydrogen atoms and solvent molecules are omitted for clarity.

The $[XA_2]$ backbone in dication **27** is approximately planar and the benzyl borate anions are π-coordinated to thorium both in the ligand plane and in the apical site, with Th–C(X) bond distances increasing in order of C(X) = C_{para} < C_{meta} < C_{ortho} < C_{ipso} and ranging from 2.900(7) to 3.280(7) and 2.937(6) to 3.257(7) Å for the borate anions in the ligand plane and apical site respectively. To minimize unfavorable steric interactions between the benzylborate anions and the ligand isopropyl groups, the thorium atom resides 0.908(6) Å above the plane defined by the NON-donor atoms, and the 2,6-diisopropylphenyl groups are rotated to give C(30)•••C(45) and C(33)•••C(42) distances

of 4.139(12) and 8.531(11) Å respectively. Thorium–nitrogen distances in dication **27** {2.317(6), 2.322(5) Å} are extremely similar to monocationic $[(XA_2)Th(CH_2Ph)(\eta^6\text{-toluene})][B(C_6F_5)_4]$ {2.317(3), 2.321(3) Å} and neutral $[(XA_2)Th(CH_2Ph)_2]$ {2.318(2), 2.332(2) Å}, consistent with the very high rigidity of the $[XA_2]$ ligand framework. However, Th–O bond distances increase in the order of $[(XA_2)Th][PhCH_2B(C_6F_5)_3]_2$ < $[(XA_2)Th(CH_2Ph)(\eta^6\text{-toluene})][B(C_6F_5)_4]$ < $[(XA_2)Th(CH_2Ph)_2]$ {Th-O: 2.403(4) < 2.454(2) < 2.5263(2) Å}, highlighting some degree of flexibility available to $[XA_2]$ to stabilize metal centers of varying electron deficiency.

Interestingly, reaction of $[(XA_2)Th(CH_2Ph)_2]$ with two equivalents of $[Ph_3C][B(C_6F_5)_4]$ rather than two equivalents of $B(C_6F_5)_3$ resulted in liberation of two equivalents of Ph_3CCH_2Ph, suggesting the formation of an as-yet unidentified dicationic species. Analogous behavior was observed in the reaction of two equivalents of $[Ph_3C][B(C_6F_5)_4]$ with dibenzyl complex $[(BDPP)Th(CH_2Ph)_2]$ (**13**), but not with bis-trimethylsilylmethyl complexes **9** and **10**.

Double alkyl, aryl or hydride abstraction has rarely been observed in d- or f-element chemistry,[129,229-232] and the resulting dications are typically stabilized by additional Lewis base (O-, N- or P-donor) coordination. The only other "Lewis base-free" dications that are formed by an analogous method are $[(t\text{Bu}_3\text{PN})_2\text{Ti}][X]_2$,[230] $[(\text{nacnac})\text{Sc}]X_2$,[231] and $[(C_5H_4CMe_2Ph)_2Zr]X_2$,[232] where X is the $MeB(C_6F_5)_3$ anion, and $[LSc(CH_2SiMe_3)][B(C_6F_5)_4]_2$ generated *in situ*, and characterized by NMR spectroscopy {L = 1,1,1-tris[(*S*)-4-isopropyloxazolinyl]ethane}[233] or suggested on the basis of extremely high 1-hexene polymerization activity (L= 1,4,7-trithiacyclononane).[234]

4.3 Conclusions

In summary, use of the rigid, dianionic [XA_2] and [BDPP] ligands has allowed the synthesis and characterization of the first non-cyclopentadienyl thorium alkyl cations and a rare thorium dication. All complexes were prepared by alkyl abstraction from dialkyl precursors using $B(C_6F_5)_3$ or $[Ph_3C][B(C_6F_5)_4]$, and were investigated in solution by NMR spectroscopy and/or in the solid state by X-ray crystallography. Some of these cations (**22**, **23** and **24)** are rare examples of arene solvent-separated ion pairs, dinuclear **25** is a unique μ-η^1:η^6-CH_2Ph bridged complex, and mononuclear **21** and dicationic **27** exist as tight contact ion pairs. The structures of these complexes highlight an extremely strong preference for π-arene coordination in highly electrophilic and sterically open non-carbocyclic actinide alkyl cations.

Chapter 5:

The Future of [XA_2] and [BDPP] Supported Neutral and Cationic Organoactinide Complexes in Olefin Polymerization, Hydroamination Catalysis and the Preparation of Thorium Hydride Complexes

5.1 – Introduction to Chapter 5

The advances in the chemistry of non-carbocyclic organoactinide complexes described in this dissertation present an opportunity for the study of these new systems as catalysts for industrially relevant transformations. Two areas of catalytic reactivity are of particular interest: olefin polymerization and hydroamination catalysis. Also of interest is the potential for our non-carbocyclic thorium systems to stabilize highly reactive terminal and/or bridging hydride complexes. Preliminary exploration of catalytic reactivity, attempted synthesis of thorium hydride complexes, and proposed future directions in these areas are described in this chapter.

5.2 – Preliminary Results

5.2.1 – Metal Catalyzed Olefin Polymerization

Polyolefins, the generic name for synthetic polymers based on ethylene, propylene and α-olefins, are produced in quantities upwards of 70 billion kilograms *per anum*, and are the most common synthetic materials used world-wide.[235] While polyolefins were

originally synthesized for commercial use through high-pressure radical polymerization processes,[236] the development of Ziegler-Natta type polymerization catalysts shifted the focus of research in this area towards the use of metal catalysts.[237] The development and evolution of homogeneous, single-site olefin polymerization catalysts has been explored since, and has recently experienced a renaissance, becoming a focus of intense study in the last two decades. Advances in this field have resulted in the development of specialized catalyst precursors and co-catalysts that grant a large degree of control over polymer molecular weight and microstructure.

For more detailed discussion of the relevant organometallic reactions involved in metal-catalyzed olefin polymerization, see Section 4.1.1.

5.2.1.1 – Neutral Thorium Dibenzyl and Bis-trimethylsilylmethyl Complex Reactivity with Ethylene

The neutral thorium bis-trimethylsilylmethyl and dibenzyl complexes **9**, **10**, **12** and **13** in toluene (~0.5 mM) were exposed to 1 atm of ethylene at 20 to 110 °C. In each case, no polymer formation was observed, even after extended periods of time (several days). This result is perhaps unsurprising, given the much greater effectiveness of cationic metal alkyl complexes for olefin polymerization relative to neutral polyalkyl derivatives. However, coordination of thorium to arene solvent (observed for cationic alkyl complexes; Chapter 4) could also have a detrimental effect on olefin polymerization activity.

To circumvent this potential obstacle, dibenzyl compounds **12** and **13,** and bis-trimethylsilylmethyl compounds **9** and **10** were exposed to 1 atm of ethylene as suspensions or solutions in hexanes (only **12** dissolved fully in hexanes). For the dibenzyl compounds, polyethylene formation was not observed at temperatures up to 70 °C. However, both the [BDPP] and [XA_2] bis-trimethylsilylmethyl complexes **9** and **10** showed polymerization upon reaction with ethylene gas at 70 °C for 24 hours; polymer was precipitated after quenching the reaction with methanol.

A summary of the reactivity of neutral thorium alkyl and benzyl complexes for ethylene polymerization in hexanes can be found in Table 5.1. Differences in reactivity of the bis-trimethylsilylmethyl and dibenzyl complexes may be due to polyhapto coordination of the benzyl groups (observed in solution and the solid state; Section 3.2.2), sterically saturating the coordination sphere of the metal and precluding ethylene coordination.

Table 5.1: Summary of preliminary ethylene polymerization reactivity for [(L)Th(R)$_2$] {L = [BDPP], [XA$_2$]; R = CH$_2$Ph, CH$_2$SiMe$_3$} in hexanes*

Complex	[complex] / mM	t / hr	Temp. / °C	Polymer Formation
[(BDPP)Th(CH$_2$Ph)$_2$]	0.574	36	22	No
[(BDPP)Th(CH$_2$Ph)$_2$]	0.574	36	70	No
[(XA$_2$)Th(CH$_2$Ph)$_2$]	0.461	36	22	No
[(XA$_2$)Th(CH$_2$Ph)$_2$]	0.461	36	70	No
[(BDPP)Th(CH$_2$SiMe$_3$)$_2$]	0.580	36	22	No
[(BDPP)Th(CH$_2$SiMe$_3$)$_2$]	0.580	36	70	Yes
[(XA$_2$)Th(CH$_2$SiMe$_3$)$_2$]	0.464	36	22	No
[(XA$_2$)Th(CH$_2$SiMe$_3$)$_2$]	0.464	36	70	Yes

Reaction conditions: All reactions were performed under a static atmosphere of ethylene. The complexes were placed in 20 mL of solvent, and freeze-pumped three times prior to the introduction of ethylene. *All complexes are largely insoluble in hexanes and were reacted as suspensions, with the exception of [(XA$_2$)Th(CH$_2$Ph)$_2$] which is soluble. Note: although [(XA$_2$)Th(CH$_2$Ph$_2$)$_2$] is the only compound fully soluble at room temperature; [(XA$_2$)Th(CH$_2$SiMe$_3$)$_2$] is noticeably more soluble at increased temperatures.

5.2.1.2 – Reactivity of Monocationic Thorium Complexes with Ethylene

5.2.1.2.1 – Cationic Thorium Alkyl Complexes Generated In-Situ in Arene Solvents

It was expected that the cationic nature of complexes **21** – **27** would result in a net increase in reactivity towards ethylene compared to neutral precursor complexes **9**, **10**, **12** and **13**. However, solutions of [(XA$_2$)Th(CH$_2$SiMe$_3$)(η^6-C$_6$H$_6$)][B(C$_6$F$_5$)$_4$] (**22**) or suspensions of [(XA$_2$)Th][η^6-PhCH$_2$B(C$_6$F$_5$)$_4$]$_2$ (**27**) in benzene or toluene, as well as complexes [(XA$_2$)Th(η^2-CH$_2$Ph)(η^6-C$_6$H$_5$Me)][B(C$_6$F$_5$)$_4$] (**24**), [(BDPP)Th(η^2-CH$_2$Ph)(μ-η^1:η^6-CH$_2$Ph)Th(η^1-CH$_2$Ph)(BDPP)][B(C$_6$F$_5$)$_4$] (**25**), and [(BDPP)Th(CH$_2$Ph)(benzene)]-[B(C$_6$F$_5$)$_4$] (**26**) generated as oils by the addition of one or half an equivalent of

$[Ph_3C][B(C_6F_5)_4]$ to their respective neutral dialkyl precursors in benzene or toluene, did not polymerize ethylene at 1 atm (20-70 °C). These observations highlight the significant potential for olefin polymerization activity in more sterically open non-cyclopentadienyl thorium alkyl cations to be diminished or negated by arene (solvent, neutral dibenzyl precursor, or benzylborate anion) coordination. The negative effects of π-arene coordination can be explained on the basis of hindered access of olefin monomers to the metal center, as well as the greatly reduced solubility of many solvent-separated ion pairs, relative to contact ion pairs.

5.2.1.2.2 – Reactions of $[(XA_2)ThR_2]$ (R = CH_2Ph or CH_2SiMe_3) with $B(C_6F_5)_3$ in Hexanes

Non-aromatic solvents were investigated for ethylene polymerization reactions involving cationic organoactinide complexes. These reactions were performed as follows: Hexane was added *in vacuo* to a mixture of a neutral $[(XA_2)ThR_2]$ (R = CH_2Ph, CH_2SiMe_3) complex and $B(C_6F_5)_3$, and after a 10 minute mixing time, 1 atm of ethylene was introduced. At room temperature, neither complex showed any activity for ethylene polymerization, even after 24 hours. Increasing the temperature to 70 °C also had no effect on the reactivity of $[(XA_2)Th(CH_2Ph)_2]$ activated with $B(C_6F_5)_3$. However, at 70 °C, a significant increase in ethylene polymerization activity was observed for $[(XA_2)Th(CH_2SiMe_3)_2]/B(C_6F_5)_3$; considerable polymer precipitation was observed after 36 hours. The observed increase in activity at higher temperatures indicates substantial thermal stability of the catalytic species, and may be due to improved catalyst solubility at

higher temperatures in addition to the direct effects of increased reaction temperature. In stark contrast to the observed catalytic activity of the *in situ* generated [XA_2] based cations formed in hexanes, complexes of the [BDPP] ligand showed no sign of polymerization activity under identical conditions.

5.2.1.2.3 – Reactions of [$(XA_2)ThR_2$] (R = CH_2Ph or CH_2SiMe_3) with [Ph_3C][$B(C_6F_5)_4$] in Hexanes

Ethylene polymerization reactions using [$(XA_2)Th(CH_2Ph)_2$] (**12**) and [$(XA_2)Th(CH_2SiMe_3)_2$] (**10**) in combination with [Ph_3C][$B(C_6F_5)_4$] resulted in polymer formation at room temperature, with the latter catalyst/co-catalyst combination being considerably more active, as evidenced by the complete solidification of the reaction mixture by precipitated polyethylene after 16 hours. Low thermal stability of the cationic active species is likely responsible for the decrease in polymerization activity observed for [$(XA_2)Th(CH_2Ph)_2$]/[Ph_3C][$B(C_6F_5)_4$] and [$(XA_2)Th(CH_2SiMe_3)_2$]/[Ph_3C][$B(C_6F_5)_4$] upon raising the temperature from 20 to 70 °C. By contrast, the polymerization activity of [$(XA_2)Th(CH_2SiMe_3)_2$]/$B(C_6F_5)_3$ increased at higher temperature. The lower thermal stability of cationic alkyl complexes paired with the $B(C_6F_5)_4^-$ anion, relative to an $RB(C_6F_5)_3^-$ (R = alkyl or benzyl) anion is well documented and stems from less effective cation-anion interactions in $B(C_6F_5)_4^-$ complexes.

However, at temperatures where a particular alkyl cation is stable paired with either a $RB(C_6F_5)_3^-$ or a $B(C_6F_5)_4^-$ anion, less effective cation-anion interactions in the latter complexes typically result in higher catalyst activities. This trend is clearly

observed when comparing the room temperature catalytic activities of $[(XA_2)Th(CH_2SiMe_3)][Me_3SiCH_2B(C_6F_5)_3]$ with $[(XA_2)Th(CH_2SiMe_3)][B(C_6F_5)_4]$, and $[(XA_2)Th(CH_2Ph)][PhCH_2B(C_6F_5)_3]$ with $[(XA_2)Th(CH_2Ph)][B(C_6F_5)_4]$.

Table 5.2: Summary of preliminary ethylene polymerization reactions using $[(XA_2)Th(R)_2]$ {R = CH_2Ph, CH_2SiMe_3} in combination with $B(C_6F_5)_3$ or $[Ph_3C][B(C_6F_5)_4]$ in hexanes

Complex[a]	[complex][b] / mM	t / hr	Temp. / °C	Amount of Polymer Formed
$[(XA_2)Th(CH_2Ph)][RB(C_6F_5)_3]$	0.5	36	22	None
$[(XA_2)Th(CH_2Ph)][RB(C_6F_5)_3]$	0.5	36	70	None
$[(XA_2)Th(CH_2SiMe_3)][RB(C_6F_5)_3]$	0.5	36	22	None
$[(XA_2)Th(CH_2SiMe_3)][RB(C_6F_5)_3]$	0.5	36	70	Large amount
$[(XA_2)Th(CH_2Ph)][B(C_6F_5)_4]$	0.5	36	22	Small amount
$[(XA_2)Th(CH_2Ph)][B(C_6F_5)_4]$	0.5	36	70	None
$[(XA_2)Th(CH_2SiMe_3)][B(C_6F_5)_4]$	0.5	36	22	Large amount
$[(XA_2)Th(CH_2SiMe_3)][B(C_6F_5)_4]$	0.5	36	70	Moderate amount

Reaction conditions: All reactions were performed under a static atmosphere of ethylene. The neutral complexes and activators were placed in roundbottom flasks and approximately 20 mL of hexanes were transferred *in vacuo*. Ten minutes of mixing time was allowed prior to the introduction of ethylene. Resulting cationic complexes precipitated as residues on the bottom of the flask. R = CH_2SiMe_3 or CH_2Ph; [a]Catalyst structure proposed based on reactivity observed in aromatic solvents and general literature precedent. [b]Values of concentration are approximate and assume complete solubility, which is not the case.

5.2.1.3 – Future Directions in Olefin Polymerization

The preliminary reactions of both the neutral and cationic thorium alkyl complexes discussed above show notable potential. However, industrial scale reactions are often performed at pressures of up to 75 atm and temperatures greater than 160 °C. Further studies should therefore endeavor to probe catalytic activity under a wider range of temperatures and pressures, with careful control of temperature, cation concentration in solution, stirring rate and reaction time. Investigation of different solvents to increase

catalyst solubility, and characterization of the resulting polymers (molecular weight and polydispersity) by gel-permeation chromatography (GPC) and differential scanning calorimetry (DSC) should also be performed.

The propensity of the thorium complexes in this work to engage in ethylene polymerization may also benefit from systematic modification of the steric environment around the metal center. Increased ligand steric demands in the form of larger *N*-Ar groups (*e.g.* 2,4,6-tri-*tert*-butyl-phenyl) could potentially be used to simultaneously discourage strong π-arene interactions between the thorium center and arene solvents, and increase complex thermal stability. A thorough and quantitative study of the polymerization activities of established and new [XA_2] and [BDPP] systems, complete with polymer property investigation is then likely to prove profitable. Furthermore, use of alternative trityl borate salts, such as $[Ph_3C][B(C_6F_4Si^iPr_3\text{-}p)_4]$[51] may lead to catalysts with increased solubility in solvents of low polarity, leading to more uniform polymer properties.

5.2.2 – Intramolecular and Intermolecular Hydroamination

Hydroamination is an atom economical process that results in the direct addition of amines to carbon-carbon double and triple bonds, the importance of which lies primarily in the production of biologically active nitrogen-containing organic molecules.[238] This process may be performed intramolecularly on substrates that contain both an amine and a carbon-carbon multiple bond (aminoalkenes/aminoalkynes) or

intermolecularly between an amine and a multiple bond containing substrate (for examples, see Scheme 5.1).

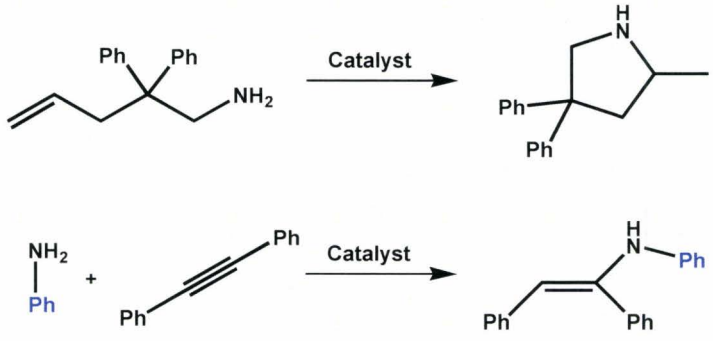

Scheme 5.1: Examples of (top) intramolecular hydroamination of 2,2-diphenyl-4-pentenyl amine and (bottom) intermolecular hydroamination of aniline and diphenylacetylene.

5.2.2.1 – Intramolecular Versus Intermolecular Hydroamination

Both inter- and intramolecular hydroamination reactions suffer from a high activation barrier for the direct addition of amines across C-C multiple bonds due to the electrostatic repulsion between the nitrogen lone pair and the electron-rich π-bond. However, intramolecular hydroamination processes enjoy substantial entropic advantages over intermolecular processes. The negative entropy of the reaction for intermolecular processes is responsible for decelerated reaction rates at the higher temperatures necessary to overcome the initial activation barrier.[102] The overall effect is greatly increased reaction times and decreased activity for catalysts systems in intermolecular hydroamination when compared to intramolecular hydroamination.[199]

5.2.2.2 – Lanthanide and Actinide Hydroamination Catalysts

In intramolecular hydroamination reactions, rare earth and actinide catalysts, such as $[(L)_2Y\{N(SiMe_3)_2\}(THF)]$ {L = *N*-2,6-diisopropylphenyl(naphthyl)amidate},[239] $[(Cp^*)_2LnR]$ {R = H or $CH(SiMe_3)_2$}[240] and $[(CGC)Th(NMe_2)_2]$ {CGC = $Me_2Si(C_5Me_4)(N\textit{t}Bu)$}[52] undergo initial protonolysis by the amine group of the aminoalkene to generate amido complexes.[198,199] The turnover limiting step is then insertion of the alkene into the metal-nitrogen bond, which is followed by protonolysis of the resulting metal-carbon bond by an aminoalkene molecule to regenerate the catalytically active amido complex (Figure 5.1). In general, alkene hydroamination rates for the lanthanides increase with larger Ln^{3+} ionic radius (La > Sm > Lu) and more open supporting ligation [e.g. $Et_2SiCp(C_5Me_4)$ > $Me_2Si(C_5Me_4)_2$ > Cp^*_2).[199]

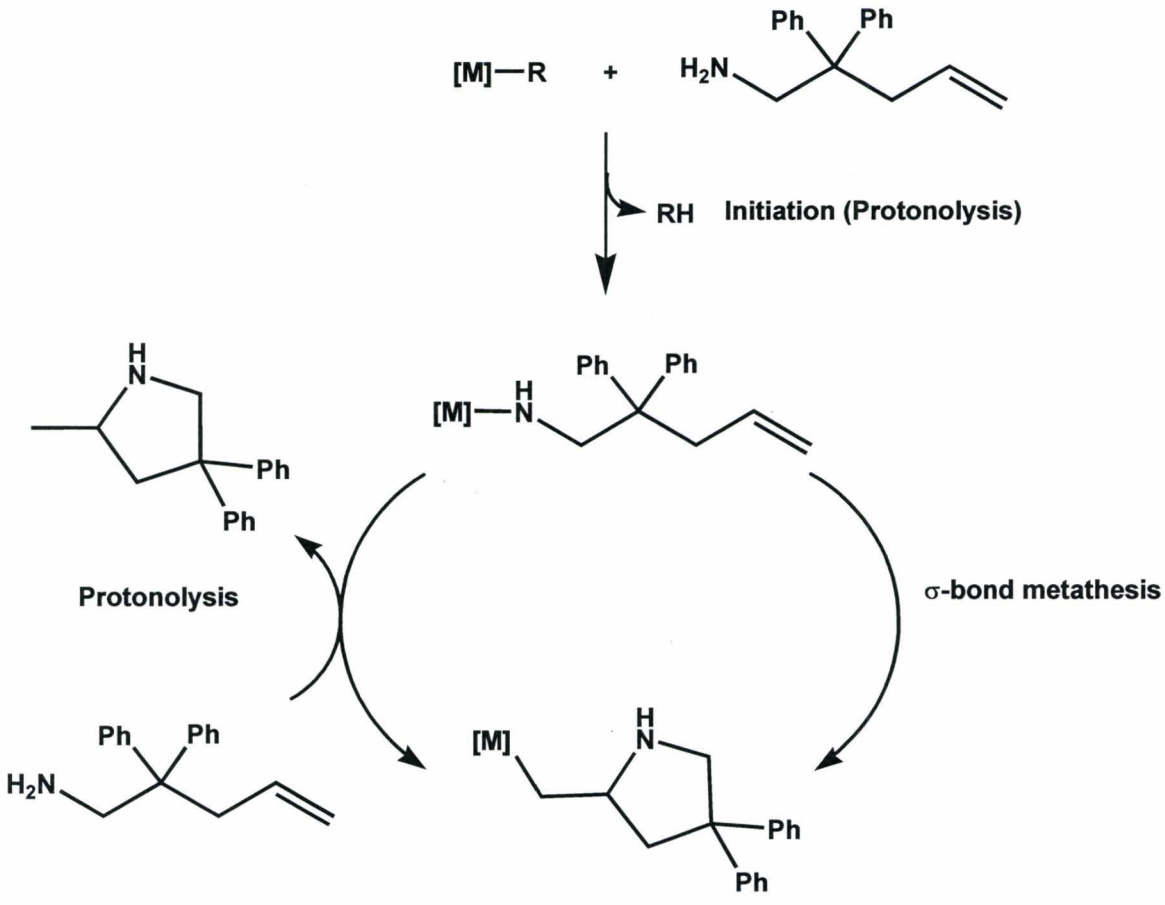

Figure 5.1: Simplified catalytic cycle for lanthanide or actinide-mediated hydroamination of aminoalkenes. [M] = Lanthanide or actinide complex; R = alkyl or amido.

5.2.2.3 – Early Transition metal Hydroamination Catalysts

Dialkyl titanium and zirconium alkene hydroamination catalysts are in many cases thought to proceed via a different mechanism to the lanthanide and actinide catalysts, involving the formation of a metal-*imido* species (Figure 5.2).[241] In this mechanism, the crucial step is a formal [2 + 2] cycloaddition of the imido species with the alkene, which is followed by protonation to regenerate the catalyst and to release the hydroamination product.[242]

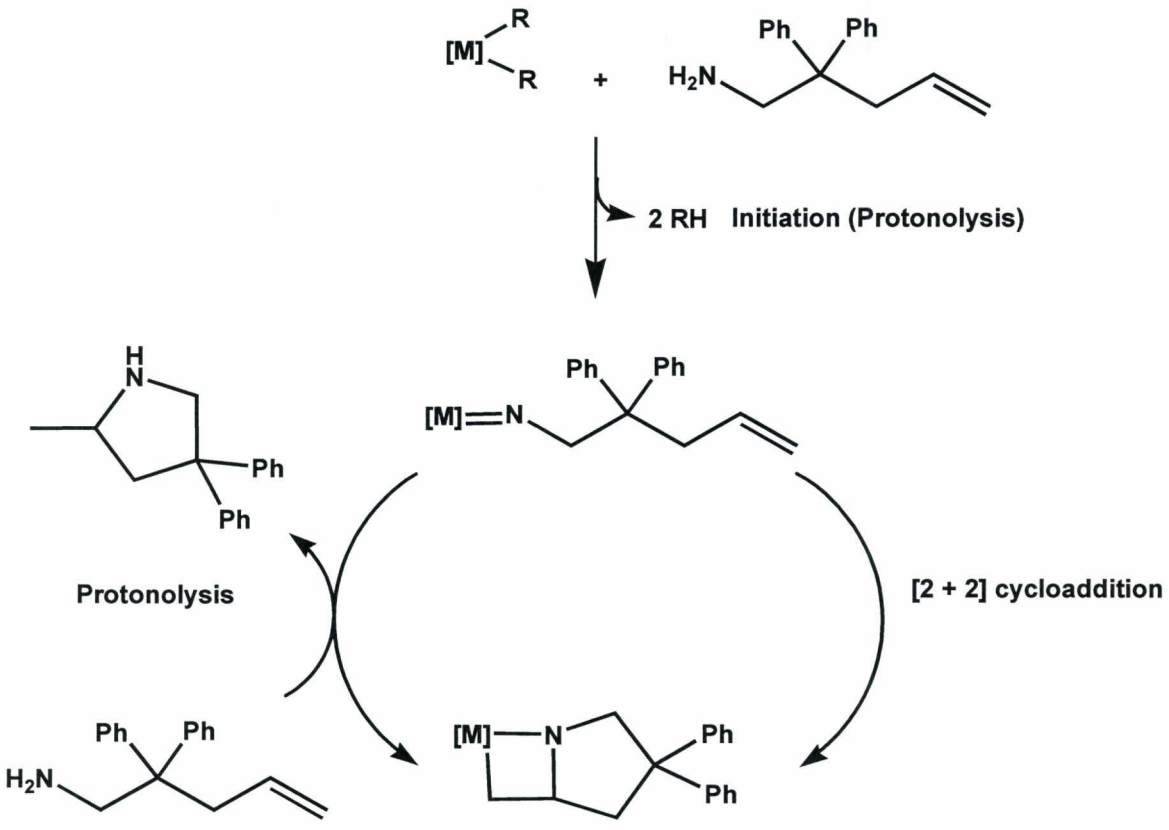

Figure 5.2: Simplified catalytic cycle for early transition metal-mediated hydroamination of aminoalkenes. [M] = Ti or Zr complex.

5.2.2.3 – Late Transition Metal Hydroamination Catalysts

Late transition metals, including iridium,[243] rhodium,[244,245] nickel,[246] palladium,[247,248] platinum[249] and ruthenium[250] have been employed as catalysts for hydroamination. In contrast to early transition metal, lanthanide and actinide catalysts, late transition metal hydroamination catalysts undergo oxidative addition of an amine substrate to generate an amido complex as the initial step in the catalytic cycle (Figure

5.3). Oxidative addition is followed by olefin insertion, and the cycle is concluded by a reductive elimination step that yields the hydroamination product.

Late transition metal catalysts offer greater polar functional group tolerance than their early transition metal counterparts. However, the reductive elimination step in the catalytic cycle often only proceeds under acidic conditions that are incompatible with the presence of free amines.[238] Many late transition metal catalysts also suffer from short catalyst lifetimes due to catalyst poisoning by the aminoalkene or aminoalkyne substrates, and reduced reactivity leading to long reaction times and an inability to catalyze hydroamination with more challenging substrates (*vide infra*).[245, 246, 248, 251]

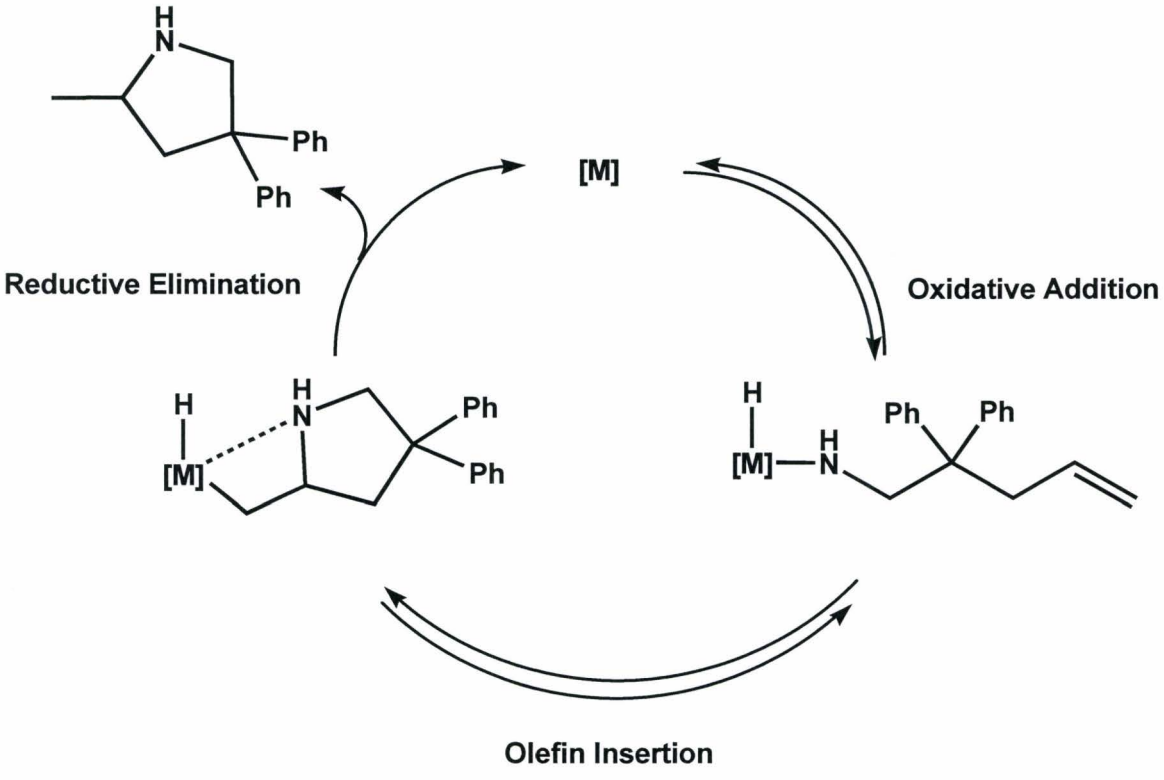

Figure 5.3: Simplified catalytic cycle for late transition metal mediated hydroamination of aminoalkenes. [M] = Late transition metal complex.

5.2.2.4 – Substrates for Intramolecular Hydroamination of Alkenes

A wide range of substrates have been utilized to challenge the ability of metal catalysts to perform inter and intramolecular hydroamination reactions. While a comprehensive list of hydroamination substrates examined is beyond the scope of this introduction, several commonly employed intramolecular hydroamination substrates are presented in Figure 5.4 arranged in order of increasing resistance towards catalytic transformation.

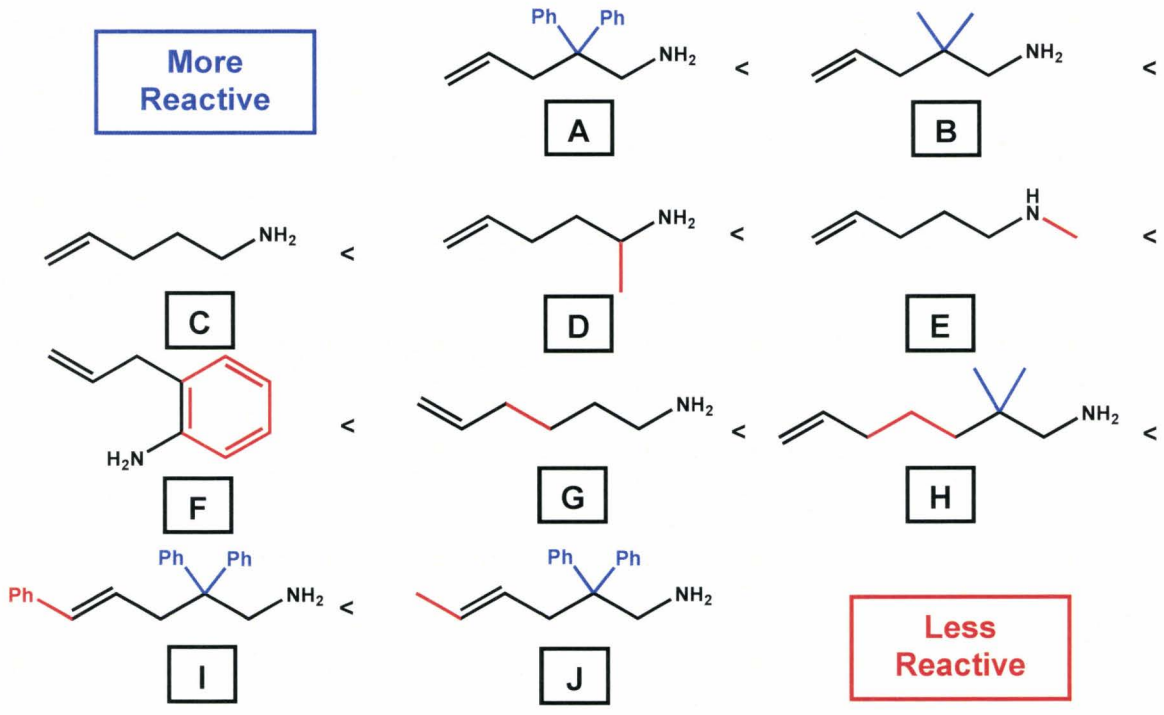

Figure 5.4: Commonly studied substrates for intramolecular hydroamination catalysis by early transition metal, lanthanide and actinide catalysts. Substrates A-J are arranged in order of increasing resistance towards catalytic transformation. Highlighted sections of each substrate indicate structural differences from C, leading to increased (blue) or decreased (red) hydroamination reactivity.

Substrates **A** and **B** are the most readily cyclized aminoalkenes due to a presumed favorable cyclic 5-membered transition state at the metal center during the olefin insertion step. By contrast, longer chain substrates requiring a 6- or 7-membered cyclic transition state (**G** and **H**) are considerably less reactive. The *gem dialkyl effect*[252] invoked by the presence of geminal diaryl or dialkyl substituents (in this case on the β-carbon) also aids the hydroamination process, and is evident by the lower reactivity of unsubstituted substrate **C** in comparison to substrates **A** or **B**.

Increased steric demands in close proximity to the metal center in the rate determining step for substrates **D**, **E**, **I** and **J** as well as substrate conformational rigidity in **F** present further challenges to hydroamination catalysts. Within this group of substrates the most challenging hydroamination reactions involve internal alkenes (**I** and **J**), resulting in considerable steric congestion around the metal center. However, electronic effects are also important, since phenyl-substituted **I** is more reactive than methyl-substituted **J**.

5.2.2.5 – Intramolecular and Intermolecular Hydroamination by Neutral Thorium Dialkyl Complexes

Preliminary reactivity studies of neutral [(BDPP)Th(CH_2SiMe_3)$_2$] towards intramolecular hydroamination show highly promising results. Addition of 100 equivalents of 2,2-diphenyl-4-pentenylamine to a toluene solution of [(BDPP)Th(CH_2SiMe_3)$_2$] resulted in almost complete conversion to the cyclized product (Scheme 5.1, top) in under 5 minutes at room temperature. This activity is greater than

that observed for most common metallocene based group 4 catalysts and is comparable to the most active lanthanide hydroamination catalysts.[238]

In contrast to intramolecular hydroamination catalysis, intermolecular catalysis by [BDPP] or [XA_2] based systems has shown a lack of success. Preliminary reactivity in this area has been explored using neutral bis-trimethylsilylmethyl dialkyl complexes [(L)Th(CH_2SiMe_3)$_2$] {L = [BDPP] (**9**), [XA_2] (**10**)} in the presence of phenyl aniline ($PhNH_2$) and styrene or diphenyl acetylene (see Scheme 5.1, bottom). However, in both cases, no sign of catalytic reactivity was observed up to temperatures of 80 °C.

Stoichiometric reactions between diphenylacetylene and phenyl aniline individually with the neutral dialkyl complexes **9** and **10** were performed. Addition of two equivalents of diphenylacetylene to [(L)Th(CH_2SiMe_3)$_2$] {L = [BDPP], [XA_2]} in toluene at room temperature resulted in no reaction, even at temperatures of 80 °C. A lack of coordination with diphenylacetylene is unsurprising on both steric and electronic grounds; less sterically demanding dme solvent does not coordinate to neutral dialkyl complexes **9** and **10**, and thorium(IV) lacks d- or f-electrons for π-backdonation to the alkyne. However, deprotonation of phenyl aniline was clearly observed upon addition of two equivalents this reagent to [(XA_2)Th(CH_2SiMe_3)$_2$] in toluene, giving rise to bis-amido complex [(XA_2)Th($NHPh$)$_2$]•$O(SiMe_3)_2$ {**28•O(SiMe$_3$)$_2$**, Scheme 5.2}, which was isolated in 78 % yield. Complex **28** exhibits a ^{1}H NMR signal at 5.21 ppm for Th-N*H* proton and signals at 6.97, 6.23 and 6.58 ppm, respectively, for the *ortho*, *meta* and *para* NH*Ph* protons. A single septet corresponding to the methyne (C*H*Me_2) proton at 3.43 ppm and pair of doublets for the isopropyl methyl (CH*Me*$_2$) groups at 1.07 and 1.17 ppm

are consistent with a C_{2v} symmetric complex in solution, and lowering the temperature to –80 °C did not result in any change in the ^1H NMR spectrum.

Imido complex formation by intramolecular elimination of $PhNH_2$ from **28** could not be achieved at room temperature or upon heating in a sealed vessel for days at 80 °C. Formation of an imido complex by reaction of **10** with one equivalent of $PhNH_2$ was also unsuccessful, leading only to a 1:1 mixture of the starting complex (**10**) and bis-amido complex (**28**).

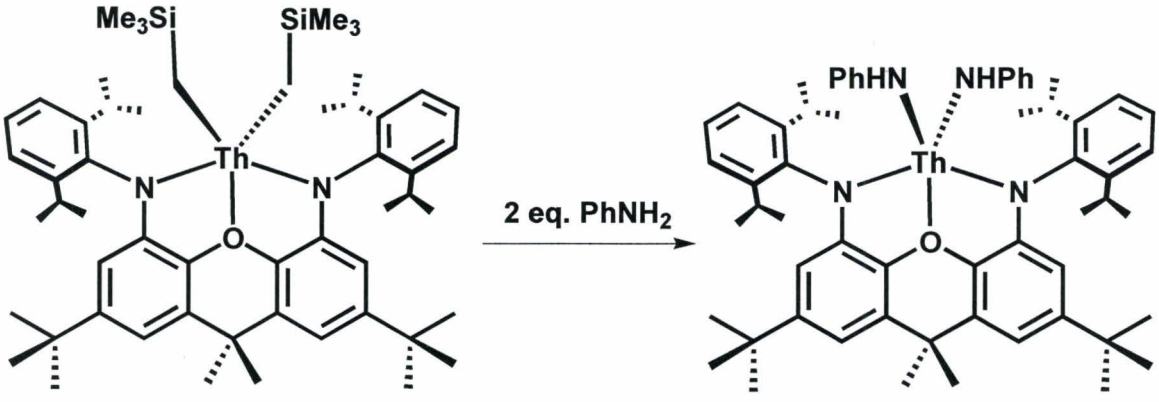

Scheme 5.2: Synthesis of bis-amido complex $[(XA_2)Th(NHPh)_2]\bullet O(SiMe_3)_2$ {28•$O(SiMe_3)_2$}.

5.2.2.6 – Future Directions in Hydroamination

The preliminary studies of intramolecular hydroamination catalysis by neutral [BDPP] and $[XA_2]$ alkyl complexes show promising results and are worthy of further study. In particular, given the high activity of $[(BDPP)Th(CH_2SiMe_3)_2]$ for hydroamination of 2,2-diphenyl-4-pentenylamine, the limit of reactivity of this catalyst

with more challenging substrates such as unsubstituted, sterically congested, strained or internal aminoalkenes (Figure 5.4) is of particular interest.

This work could be further extended to the intramolecular hydroamination of alkyne substrates, and systematic ligand modification may be beneficial to achieve optimal complex performance. The ease of synthetic modification at the periphery of [BDPP] and [XA_2] ligands is likely to be a great asset in this work.

5.2.3 – Non-carbocyclic Ancillaries for the Formation of Thorium Hydride Complexes

5.2.3.1 – Introduction to Hydride Complex Synthesis and Actinide Hydride Complexes

In comparison to transition metal hydride complexes which have been thoroughly studied and reviewed,[253,254] lanthanide hydride complexes are more scarce, and actinide hydride complexes are extremely limited, especially in the absence of cyclopentadienyl ligands (see Section 1.2.2.6). Hydride complexes may be synthesized through a variety of methods, the most common of which involves direct hydrogenation of a metal alkyl precursor with hydrogen gas or a hydrosilane (e.g. $PhSiH_3$). However, reaction between a metal halide precursor and a reactive metal hydride, such as $LiAlH_4$, $MHBEt_3$ (M = Li, Na, K) or $NaAlH_2(OCH_2CH_2OCH_3)_2$ (Vitride)[106,116] may also be employed. In transition metal chemistry, β-H elimination from a β-H containing alkyl complex is also a common pathway to metal hydride complexes. However, as discussed in Section 1.2.2.5, β-H

elimination is much less favorable in actinide chemistry, and to date, only one example of a 5f-element hydride formed via β-hydrogen elimination from an alkyl precursor has been reported; UV-irradiation of [$(Cp)_3Th$*i*Pr] formed Cp_3Th with elimination of propane and propene. A hydride intermediate is implied in this reactivity, but was not isolated or detected spectroscopically.[25]

The simplest hydride complexes of thorium and uranium are their binary hydrides, ThH_2, Th_4H_{15}, and UH_3, which can be obtained from the reaction of the respective metals with hydrogen gas.[255] However, the lack of solubility of these polymeric compounds severely limits their potential reactivity, and prompts the development of more complex ancillary ligand-supported hydride complexes.

Actinide hydride complexes are capable of participating in several reaction types which include stoichiometric addition reactions to carbon-carbon[109] and carbon-oxygen[109,110,256] multiple bonds, and σ-bond metathesis reactions with alcohol,[102] thiol,[64] hydroxide,[257] and other small molecules.[25,256] More importantly, actinide hydride compounds such as $[(Cp^*)AnH_2]_2$ (An = Th, U), are capable of catalyzing the hydrogenation reactions of alkenes (1-hexene, propylene), alkynes (diphenylacetylene), and even arenes (benzene, toluene, *p*-xylene, naphthalene).[17] Furthermore, insertion of CO into metal hydride bonds is favored in actinide chemistry due to increased M–C bond strengths and a M–O interaction in the resulting formyl (M–CHO) complexes.[258]

With all of the above in mind, it would be of great general interest to investigate the ability of non-carbocyclic ligands {[BDPP] and $[XA_2]$} to stabilize highly reactive thorium hydride compounds.

5.2.3.2 – Reaction of [(BDPP)Th(X)$_2$(dme)$_y$] (X = CH_2SiMe_3, y = 0; X = Cl, y = 1) Relevant to Hydride Complex Synthesis

Our initial foray into the area of actinide hydride complex formation began with the exposure of [(BDPP)Th(CH_2SiMe_3)$_2$] (**9**) to approximately 4 atm of hydrogen (1 atm of hydrogen was introduced to a degassed J-Young tube containing **9** in C_6D_6 at –196 °C before sealing and warming to room temperature). The reaction was then monitored over a period of 14 days.

Consumption of [(BDPP)Th(CH_2SiMe_3)$_2$] was complete after two days at room temperature with ~1.5 equivalents of $SiMe_4$ produced and one additional $SiMe_3$ peak (presumably a new $ThCH_2SiMe_3$ signal) at 0.1 ppm. The spectrum of the reaction mixture showed signals consistent with the presence of two considerably different products in solution with an approximate ratio of 1:1 (Figure 5.5). The first product (product A) has lost top-bottom symmetry, giving rise to two sets of doublets for the back-bone CH_2 group (5.47 and 4.89 ppm) with a large $^2J_{H\text{-}H}$ value of 20.1 Hz, and two septets due to isopropyl CHMe$_2$ signals (4.12 and 3.51 ppm). In contrast, the second product (product B) appears to be highly symmetrical, giving rise to a single set of back-bone CH_2 and isopropyl CHMe$_2$ signals in the ^{1}H NMR spectrum at 4.82 and 3.47 ppm, respectively. The symmetry of product A is consistent with a mixed alkyl/hydride complex such as [(XA_2)ThH(CH_2SiMe_3)], and integration of the new $SiMe_3$ signal at 0.1 ppm supports this assignment. The symmetry of product B is consistent with a dihydride product, and the amount of $SiMe_4$ produced matches that expected for formation of a 1:1 mixture of a hydrido/alkyl and dihydride product. The majority of thorium hydride

complexes bear cyclopentadienyl ligands, and give rise to Th–H ^{1}H NMR signals between 12.9 and 20.4 ppm (Table 1.7 in Section 1.2.2.6). However, the hydride signal for $[\{(Me_3Si)_2N\}_3ThH]$[106] was reported at 0.63 ppm; far upfield of the corresponding signals in cyclopentadienyl complexes. This literature precedent provides additional support for assignment of the sharp 1H NMR singlet at 2.73 ppm (integration 2H) in complex B as Th–H signals.[254]

After reacting for nine days (Figure 5.7), peaks corresponding to the less symmetrical product A had diminished greatly, while those corresponding to the more symmetrical product B had gained in intensity. This reactivity is further consistent with conversion of a mixed hydrido/alkyl complex to a dihydride product. The decrease in intensity of the signals corresponding to the less symmetric product also allowed closer examination of the alkyl region between 0.8 and 1.7 ppm. Beyond the two large CH*Me*$_2$ signals (doublets at 1.50 and 1.25 ppm), the most prominent feature is a new intense singlet at 1.37 ppm, integrating to 6 protons. The origin of this peak is currently unclear.

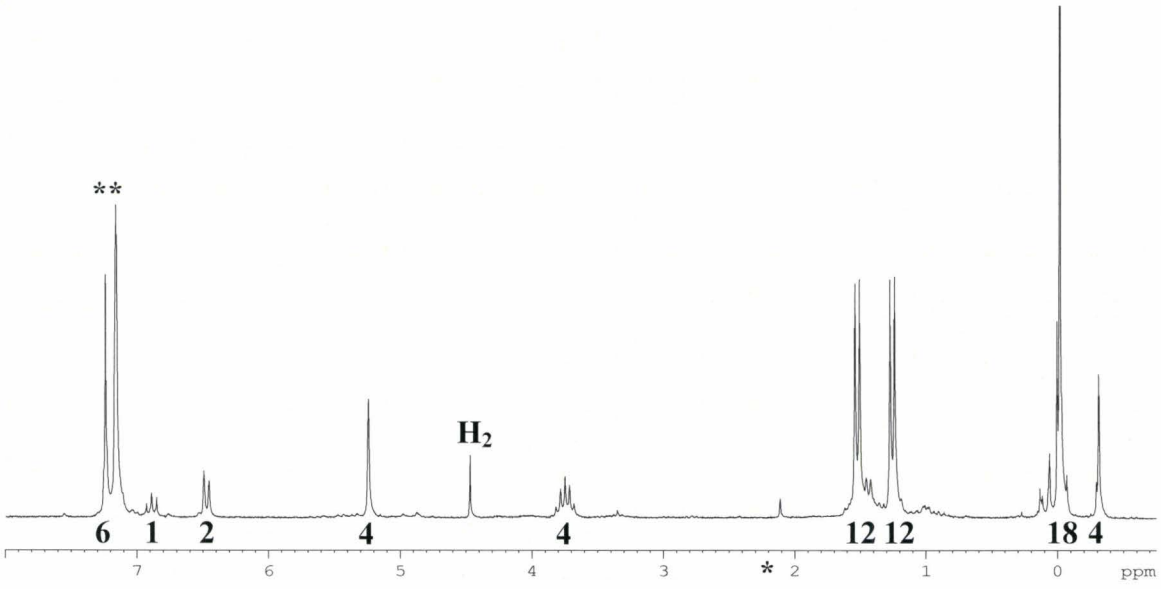

Figure 5.5: ^{1}H NMR spectrum of the reaction of [(BDPP)Th(CH$_2$SiMe$_3$)$_2$] (9) with H$_2$ after 30 minutes, in d_6-benzene. Spectrum shows the ^{1}H NMR of unreacted 9. * = toluene; ** = ^{1}H impurities in d_6-benzene.

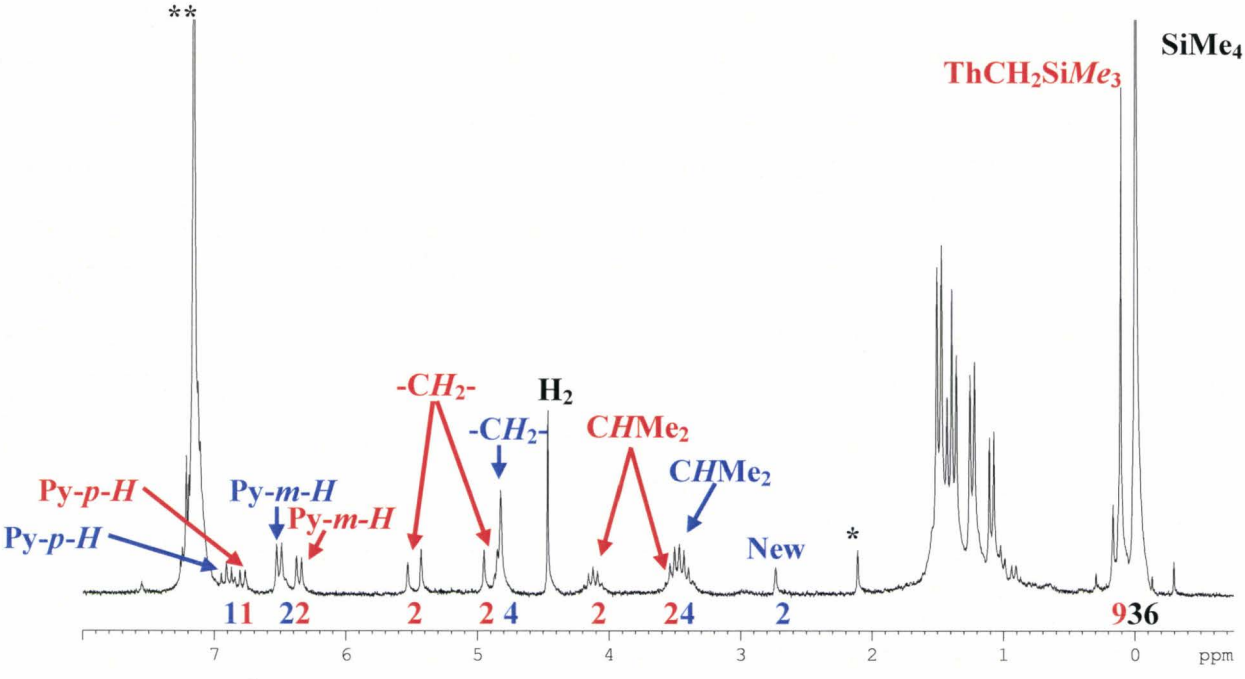

Figure 5.6: ^{1}H NMR spectrum of the reaction of [(BDPP)Th(CH$_2$SiMe$_3$)$_2$] (9) with H$_2$ after 2 days, in d_6-benzene. Red = signals proposed to arise from asymmetrical product A; Blue = signals proposed to arise from symmetrical product B. * = toluene; ** = ^{1}H impurities in d_6-benzene.

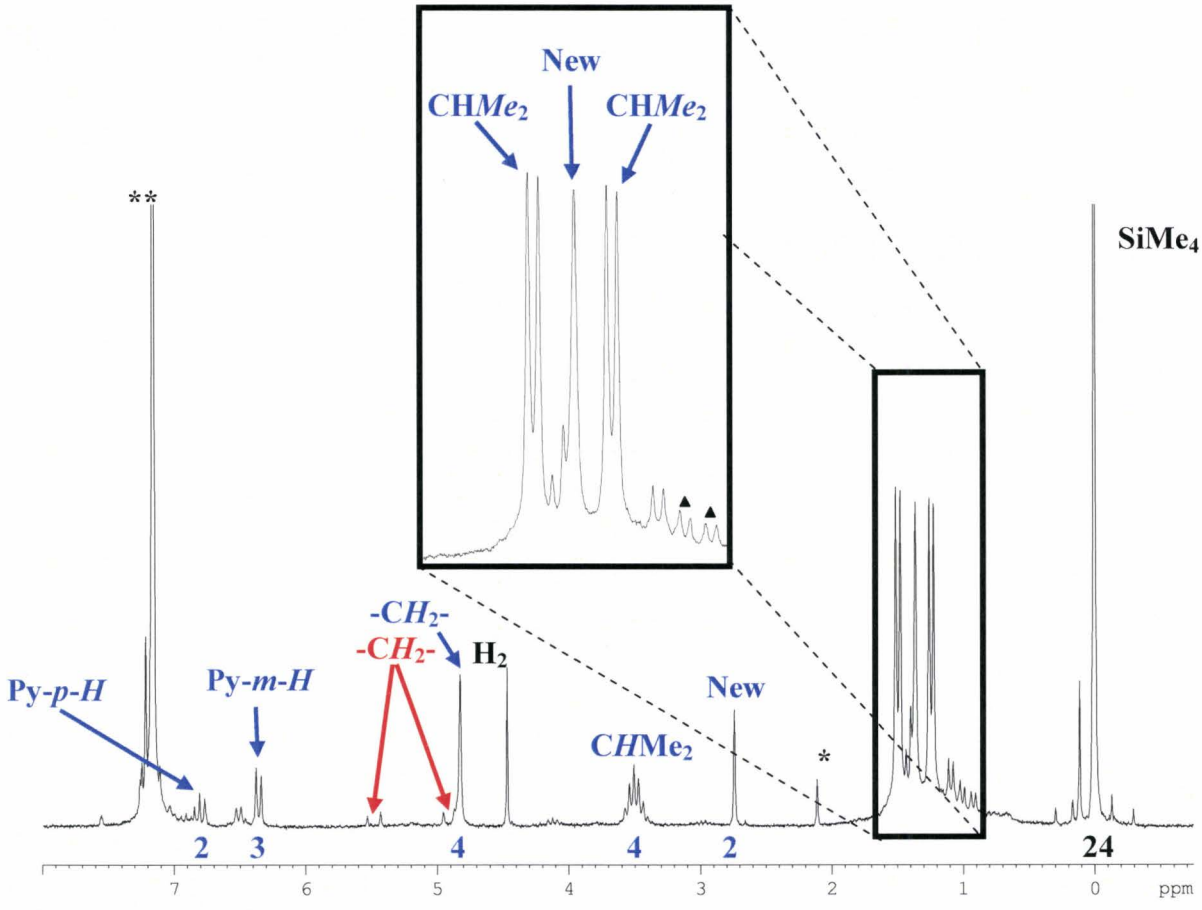

Figure 5.7: ^{1}H NMR spectrum of the reaction of [(BDPP)Th(CH_2SiMe_3)$_2$] (9) with H_2 after 9 days, in d_6-benzene. Red = signals proposed to arise from asymmetrical product; Blue = signals proposed to arise from symmetrical product. * = toluene; ** = ^{1}H impurities in d_6-benzene;▲= unknown impurities.

Unfortunately, reproduction of the reaction on larger quantities was unsuccessful. Reaction of [(BDPP)Th(CH_2SiMe_3)$_2$] with 4 atm of hydrogen gas in a reaction bomb took considerably longer to proceed than on a smaller scale, and monitoring the reaction over prolonged time periods (up to three weeks) showed the precipitation of a black, insoluble powder, and formation of a complex mixture of products in solution. Attempts to isolate

hydride complexes via the reaction of [(BDPP)$ThCl_2$(dme)] (**6**) with $LiAlH_4$, $KHB(Et)_3$ and $NaH_2Al(OCH_2CH_2OCH_3)_2$ were also unsuccessful, giving rise to intractable mixtures of products, and no reaction was observed between [(BDPP)$Th(CH_2SiMe_3)_2$] and $PhSiH_3$ (up to 5 equivalents) at 20 to 110 °C. Finally, attempted synthesis of [BDPP] hydride complexes through β-hydride elimination from [(BDPP)Th(*n*Bu)$_2$] (**14**, see Section 3.2.3) were also unsuccessful; this complex does not undergo clean decomposition using either thermal or UV-photolysis methods.

5.2.3.3 – Reactions of $[(XA_2)Th(X)_2(dme)_y]$ ($X = CH_2SiMe_3$, $y = 0$; $X = Cl$, $y = 1$) Relevant to Hydride Complex Synthesis

The reaction of $[(XA_2)Th(CH_2SiMe_3)_2]$ with hydrogen gas (4 atm) in a J-Young NMR tube was approximately 90 % complete after 14 days at room temperature. Monitoring the reaction by ^1H NMR spectroscopy over this period did not show any evidence for an intermediate complex of low symmetry. The product of the reaction appears to share one signal at 2.69 ppm that is analogous to the singlet at 2.75 ppm in the [BDPP] reaction, however, the alkyl region of the spectrum is highly congested, with substantial overlap of the xanthene *t*Bu, and $CHMe_2$ signals. Attempts at large scale synthesis and isolation of the product of this reaction also met with difficulty due to the extended reaction times required.

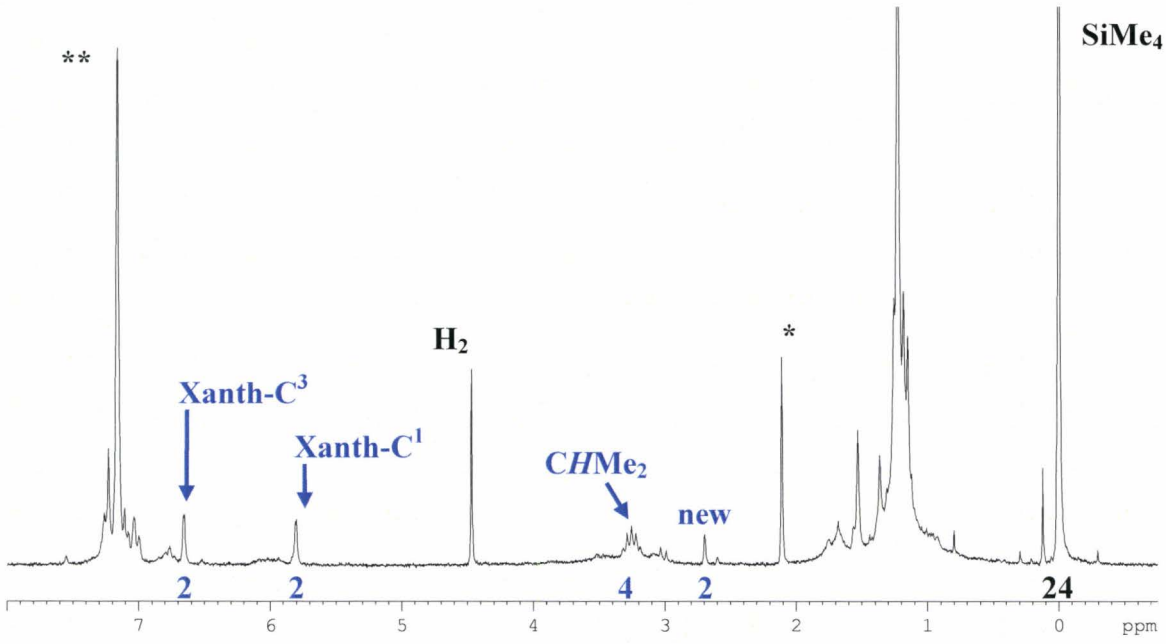

Figure 5.8: ^{1}H NMR spectrum of the reaction of [(XA$_2$)Th(CH$_2$SiMe$_3$)$_2$] (10) with H$_2$ after 14 days, in d_6-benzene. * = toluene; ** = ^{1}H impurities in d_6-benzene.

5.2.3.4 – Future Directions in Thorium Hydride Complex Formation

Long reaction times required for preparative scale reactions of dialkyl complexes [(BDPP)Th(CH$_2$SiMe)$_2$] and [(XA$_2$)Th(CH$_2$SiMe$_3$)$_2$] with hydrogen gas rendered decomposition pathways competitive with product formation. Future work in this field should include the reaction of thorium dialkyl complexes with hydrogen gas at elevated pressures to substantially decrease reaction times. Ligand modification to increase the thermal stability of the resulting hydride complexes may also prove beneficial.

5.3 – Conclusions

In conclusion, the newly developed [XA$_2$] ligand, and previously reported [BDPP] ligand have proven useful for the preparation of neutral and/or cationic complexes

capable of catalyzing ethylene polymerization and intramolecular hydroamination reactivity. Preliminary studies in ethylene polymerization showed that both neutral and cationic thorium alkyl complexes are suitable to catalyze this reaction. The propensity of the cationic alkyl thorium complexes in this work to coordinate arene solvents lead to improved catalyst performance in hexanes versus benzene or toluene, and the highest activity was observed for "$[(XA_2)Th(CH_2SiMe_3)][Me_3SiCH_2B(C_6F_5)_3]$" generated *in situ* in hexanes. However, the cationic complexes in this work are poorly soluble or insoluble in hexanes, presumably leading to lower polymerization activities than would be observed for a fully-soluble catalyst.

In the area of hydroamination, neutral [BDPP] and $[XA_2]$ dialkyl complexes demonstrate extremely high activities for the intramolecular hydroamination of 2,2-diphenyl-4-pentenylamine. However, attempts to perform intermolecular hydroamination ($PhNH_2 + C_2Ph_2$ or styrene) were unsuccessful.

Actinide hydride complex synthesis was also attempted, and both $[(BDPP)Th(CH_2SiMe_3)_2]$ and $[(XA_2)Th(CH_2SiMe_3)_2]$ react with H_2 (4 atm) over extended periods of time to produce new, as yet unidentified complexes. However, in both cases, decomposition became competitive with product formation in preparative scale reactions, preventing isolation of pure complexes. Other approaches to access thorium hydride complexes were also unsuccessful {*e.g.* using $PhSiH_3$, $LiAlH_4$, $KHB(Et)_3$ and $NaH_2Al(OCH_2CH_2OCH_3)_2$}.

Suggestions for future work in the areas of olefin polymerization, olefin hydroamination, and hydride synthesis are presented in Sections 5.2.1.3, 5.2.2.6 and

5.2.3.4 above, and include modified reaction conditions, investigations of substrate scope and reactivity, and tailoring of catalyst properties through ligand design. Furthermore, in the case of cationic complexes, investigation of alternative weakly-coordinated counterions is proposed.

Chapter 6:

Experimental Methods

6.1 – General

6.1.1 – Laboratory Equipment and Apparatus

An argon-filled MBraun UNIlab glove box was employed for the manipulation and storage of all oxygen and moisture sensitive compounds, and all thermally unstable compounds were stored in a –30 °C freezer within the glove box. Reactions were performed on a double manifold high vacuum line using standard techniques,[259] and all reaction products were thoroughly dried *in vacuo*. Commonly utilized specialty glassware includes the swivel frit assembly, J-Young NMR tubes, and thick walled flasks equipped with Teflon stopcocks. Residual oxygen and moisture was removed from the argon stream by passage through an Oxisorb-W scrubber from Matheson Gas Products.

6.1.2 – Solvents

Anhydrous 1,2-dimethoxy ethane (dme) and diethylether were purchased from Aldrich and dried further as described below. Hexanes, toluene and THF were initially dried and distilled at atmospheric pressure from CaH_2, sodium and sodium/benzophenone respectively. Unless otherwise noted, all proteo solvents were stored over an appropriate drying agent (dme, OEt_2, THF, toluene, C_6H_6 = Na/Ph_2CO; hexanes, $O(SiMe_3)_2$ = Na/Ph_2CO/tetraglyme) and introduced to reactions via vacuum transfer with condensation

at –78 °C. Deuterated solvents (ACP Chemicals) were dried over CaH_2 (CD_2Cl_2, C_6D_5Br) or Na/Ph_2CO (C_6D_6, d_8-toluene, d_8-THF).

6.1.3 – Instrumentation and details for NMR experiments

Nuclear magnetic resonance spectroscopy (^1H, $^{13}C\{^1H\}$, ^{19}F, ^{11}B, DEPT-135, COSY, HSQC, HMBC, EXSY, NOESY and ROESY experiments) was performed on Bruker AV-200 (^1H 200.106 MHz), DRX-500 (^1H 500.133 MHz, $^{13}C\{^1H\}$ 125.757 MHz, $^{11}B\{^1H\}$ 193.173 MHz, ^{19}F 470.593 MHz) and AV-600 (^1H 600.139 MHz, $^{13}C\{^1H\}$ 150.903 MHz) spectrometers. All 2D NMR experiments were performed using Bruker DRX-500 or AV-600 spectrometers. All spectra were obtained at room temperature (298K) unless otherwise specified. All ^1H NMR and ^{13}C NMR spectra were referenced relative to $SiMe_4$ through a resonance of the employed deuterated solvent or proteo impurity of the solvent; C_6D_6 (δ 7.15 ppm), C_7D_8 (δ 7.09, 7.00, 6.98, 2.09), C_6D_5Br (δ 7.30, 7.02, 6.94 ppm), d_8-THF (3.58, 1.73 ppm), CD_2Cl_2 (5.32 ppm) for ^1H NMR, and C_6D_6 (δ 128.0 ppm), C_7D_8 (δ 137.86, 129.24, 128.33, 125.49, 20.4), C_6D_5Br (δ130.9, 129.3, 126.1, 122.3 ppm), d_8-THF (67.57, 25.37 ppm), CD_2Cl_2 (54.0 ppm) for ^{13}C NMR. ^{11}B NMR spectra were referenced to an external standard of neat boron trifluoride diethyl etherate (δ 0.00 ppm). ^{19}F NMR spectra were referenced to an external standard of $CFCl_3$.

All NMR samples were prepared inside a glove box in tubes capped with rubber septa or in J-Young tubes. ^1H NMR spectra are presented in the format of chemical shift

(ppm), multiplicity, number of protons, $^{Y}J_{X\text{-}X'}$ coupling constant (where Y is the number of bonds between the coupled nuclei, X and X′ are the type of nuclei, and the coupling constant is given in Hz), and assignment.

Herein, Q = quaternary, Ar = 2,6-diisopropylphenyl, the *ipso* carbon refers to the carbon attached to nitrogen, Py and Xanth refer to the pyridine and xanthene backbones of the [BDPP] and [XA_2] ligands respectively, and CH^1 and CH^3 refer to the 1- and 3-positions of the Xanthene backbone {*para* and *ortho* respectively to the amido group in [XA_2]}. *Q* is used to indicate a quaternary carbon atom, and *Bz* is used to indicate a CH_2Ph group. Note: Xanthene quaternary carbons are not always evident in the ^{13}C NMR spectrum. All identifiable Xanth-*Q* signals are listed.

6.1.4 – Other Instrumentation and Analysis

A Fisher Scientific Ultrasonic FS-30 bath was used to sonicate reaction mixtures where indicated. Combustion elemental analyses were performed on a Thermo EA1112 CHNS/O analyzer by Dr. Steve Kornic of this department. X-ray crystallographic analyses were performed on suitable crystals coated in Paratone oil and mounted on a P4 diffractometer with a Bruker Mo rotating-anode generator and a SMART1K CCD area detector or a Bruker Mo SMART APEX2 in the McMaster Analytical X-Ray (MAX) Diffraction Facility. Full X-ray crystallographic details may be found in the individual tables for each crystal structure (see Appendix 1).

6.1.5 – NMR Tube Reactions

Unless otherwise noted, NMR tube reactions were carried out by mixing separate solutions of reagents in their corresponding deuterated solvents inside the glove box. Subsequent reagents were introduced by microsyringe through the septum at the top of the NMR tube. The contents of the tube were thoroughly shaken and unless otherwise indicated, the contents were placed in the spectrometer and monitored within 15 minutes of mixing. In reactions were gasses were employed as reagents, J-Young tubes fitted with vacuum line adapters were utilized. Upon attachment to the vacuum line, solutions were cooled to an appropriate temperature and freeze-pump-thaw cycles were used to remove all traces of Argon prior to introduction of reagent gasses.

6.1.6 – Starting Materials

$Th(NO_3)_4(H_2O)_4$ was purchased from Strem Chemicals. $SOCl_2$, $O(SiMe_3)_2$, 2,6-bis(bromomethyl)pyridine, tetraglyme, xanthone, $AlMe_3$ (2M in toluene), $Pd(OAc)_2$, $PhCH_2MgBr$ (1.0 M solution in Et_2O), NaO*t*Bu, DPEPhos [bis{2-(diphenylphosphino)phenyl}ether], NaH, KH (30 wt.% in mineral oil), $LiCH_2SiMe_3$ (1.0M in pentane), *n*BuLi (2.0M in cyclohexane),[260] Fe powder and Br_2 were purchased from Sigma-Aldrich. 2,6-diisopropylaniline was purchased from Lancaster. Prior to use, solid $LiCH_2SiMe_3$ was obtained by removal of pentane *in vacuo*, solid KH was obtained by filtration and washing with hexanes, and 2,6-diisopropylaniline was distilled from CaH_2. H_2[BDPP],[147] 4,5-dibromo-2,7-di-*tert*-butyl-9,9-dimethylxanthene,[261] were prepared by literature procedures. $ThCl_4(dme)_2$[165] was

prepared by a modified procedure (*vide infra*) based upon literature procedures. $B(C_6F_5)_3$ was purchased from Boulder Scientific and dried by repeated cycles of stirring in dimethylchlorosilane for 14 hours and sublimation. Dryness of $B(C_6F_5)_3$ was monitored post sublimation by ^{19}F NMR (peak sharpness), and was usually achieved within 1 or 2 cycles of drying. $[Ph_3C][B(C_6F_5)_4]$ was purchased from Strem and used as received. Ethylene (99.99 %) was purchased from Aldrich and used as received.

6.2 – Experimental Procedures Pertaining to Chapter 2

6.2.1 – Synthetic Procedures and Characterization

Synthesis of $ThCl_4(dme)_2$:

$Th(NO_3)_4(H_2O)_4$ (40.000 g, 94.41 mmol) was placed in a 250 mL flask. The flask was placed in a water bath and concentrated HCl (175 mL) was added slowly. The solution was refluxed under N_2, using a heating mantle for 4 days, until the evolution of yellow gas had ceased completely. The water and HCl were removed *in vacuo* at room temperature leaving behind a white solid (Note: it is extremely important that the water be removed without heating, as the resulting $ThCl_4(H_2O)_x$ undergoes significant decomposition to hydroxyl/chloro and/or oxy/chloro complexes at temperatures higher than 100 °C).[159] To this solid, $SOCl_2$ (200 mL) was added and the resulting solution was refluxed under N_2 for 3 days. The remaining $SOCl_2$ was removed *in vacuo*, and the flask was quickly detached from the reflux condenser and attached to a pre-dried swivel frit under N_2. Toluene (100 mL) was added (Note: direct vacuum transfer of toluene onto this solid was avoided as cross-transfer of any remaining $SOCl_2$ into the solvent drying

bomb would present a serious hazard) and the resulting product was sonicated for 10 minutes. The solid was collected on the frit and the mother liquors were discarded. After drying *in vacuo*, the apparatus was brought into the glove box and 31.215 g of a grey-white solid was collected. The solid was placed in a Soxhlet apparatus with a cellulose thimble, and a round bottom flask containing dme (300 mL) and set to reflux for 2 days to exchange coordinated $SOCl_2$ with dme. A brown solution and a considerable amount of solid was obtained when the Soxhlet extraction was halted. The flask was once again quickly detached from the apparatus and attached to a pre-dried swivel frit under Ar. The solid was washed three times with dme (50 mL) and twice with hexanes (100 mL) to yield $ThCl_4(dme)_2$ as a beige solid (26.750g, 48.28 mmol) in 52 % yield.

$H_2(XA_2)$ (1):

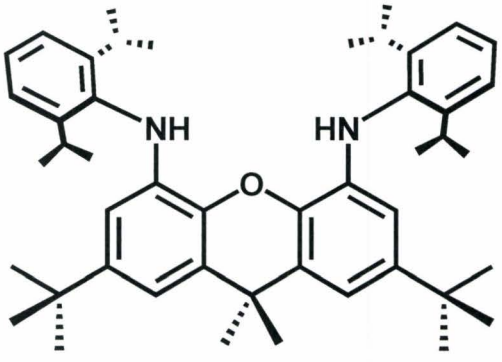

4,5-dibromo-2,7-di-*tert*-butyl-9,9-dimethylxanthene (10.00 g, 20.82 mmol), 2,6-diisopropylaniline (7.85 mL, 41.64 mmol), NaO^tBu (5.60 g, 58.30 mmol), $Pd(OAc)_2$ (40 mg, 0.21 mmol) and DPEPhos (167 mg, 0.31 mmol) in toluene (150 mL) were heated to 100 °C for 16 hours. The reaction mixture was then quenched with water, extracted into toluene (3 x 50 mL), dried over $MgSO_4$ and concentrated to approximately 30 mL.

Recrystallization from a hot ethanol/toluene (10:1) solution gave **1** as a white solid (12.02 g, 17.86 mmol) in 86 % yield. **^{1}H NMR (C_6D_6, 600 MHz):** δ 7.26-7.21 (m, 6H, Ar-*H*), 6.99 (d, 2H, $^4J_{H\text{-}H}$ 1.9 Hz, C*H*^{3}), 6.51 (d, 2H, $^4J_{H\text{-}H}$ 1.9 Hz, C*H*^{1}), 5.93 (s, 2H, N*H*), 3.47 (sept, 4H, $^3J_{H\text{-}H}$ 6.9 Hz, C*H*Me$_2$), 1.98 (s, 18H, C*Me*$_3$), 1.68 (s, 6H, C*Me*$_2$), 1.18 (d, 12H, $^3J_{H\text{-}H}$ 6.9 Hz, CH*Me*$_2$), 1.14 (d, 12H, $^3J_{H\text{-}H}$ 6.9 Hz, CH*Me*$_2$). **^{13}C{^{1}H} NMR (C_6D_6, 125 MHz):** δ 147.8 (Ar-*C*$_{ipso}$), 146.1, 136.4, 135.9 (Xanth-*Q*), 136.2 (Ar-*C*$_{ortho}$), 129.4 (Ar-*C*$_{para}$), 124.3 (Ar-*C*$_{meta}$), 111.9 (*C*H^3), 108.1 (*C*H^1), 35.1 (*C*Me$_2$), 34.8 (*C*Me$_3$), 32.9 (C*Me*$_2$), 31.7 (C*Me*$_3$), 28.7 (*C*HMe$_2$), 24.7, 23.5 (CH*Me*$_2$). Anal. Calcd. for $C_{47}H_{64}N_2O$: C, 83.88; H, 9.58; N, 4.16. Found: C, 83.91; H, 9.64; N, 4.00 %.

$K_2(dme)_2[XA_2]$ (2):

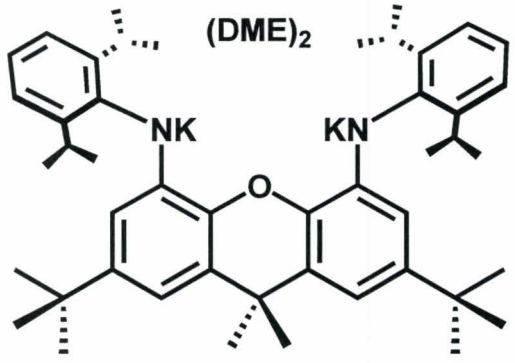

KH (0.120 g, 3.00 mmol) and $H_2[XA_2]$ (0.750 g, 1.11 mmol) in dme (60 mL) were stirred at room temperature for 5 h. The solution was filtered to remove excess KH. Solvent was removed *in vacuo* and hexamethyldisiloxane (30 mL) was added, followed by sonication. The solution was cooled to –78 °C and filtered on a pre-cooled frit to obtain 0.756 g (0.81 mmol, 73 %) of **2** as a white solid. **^{1}H NMR (C_6D_6, 600 MHz):** δ 7.29 (d, 4H, $^3J_{H\text{-}H}$ 7.5 Hz, Ar-*H*$_{meta}$), 7.14 (t, 2H, $^3J_{H\text{-}H}$ 7.5 Hz, Ar-*H*$_{para}$), 6.57 (d, 2H, $^4J_{H\text{-}H}$

2.0 Hz, C*H*^{3}), 6.18 (d, 2H, $^4J_{H\text{-}H}$ 2.0 Hz, C*H*^{1}), 3.00 (sept, 4H, $^3J_{H\text{-}H}$ 6.9 Hz, C*H*Me$_2$), 2.97 (s, 8H, OC*H*$_2$), 2.83 (s, 12H, OC*H*$_3$), 1.90 (s, 6H, C*Me*$_2$), 1.40 (s, 18H, C*Me*$_3$), 1.29 (d, 12H, $^3J_{H\text{-}H}$ 6.8 Hz, CH*Me*), 1.16 (d, 12H, $^3J_{H\text{-}H}$ 7.0 Hz, CH*Me*). **^{13}C{^{1}H} NMR (C$_6$D$_6$, 125 MHz):** δ 154.1 (Ar-*C*$_{ipso}$), 149.2 (Ar-*C*$_{ortho}$), 147.7, 143.0, 138.6, 132.9 (Xanth-*Q*), 124.3 (Ar-*C*$_{para}$), 120.6 (Ar-*C*$_{meta}$), 109.1 (*C*H^1), 100.8 (*C*H^3), 71.7 (O*C*H$_2$), 58.7 (O*Me*), 36.4 (*C*Me$_2$), 35.6 (C*Me*$_3$), 32.8 (*C*Me$_3$), 31.2 (C*Me*$_2$), 28.7 (*C*HMe$_2$), 25.5, 24.8 (CH*Me*$_2$). Anal. Calcd. for $C_{55}H_{82}N_2O_5K_2$: C, 71.07; H, 8.89; N, 3.01. Found: C, 71.16; H, 8.86; N, 3.10 %.

Na$_2$[XA$_2$] (3):

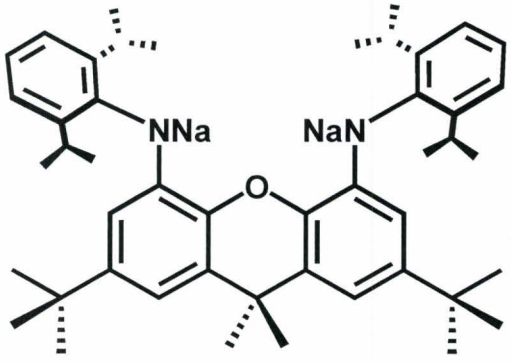

NaH (0.100 g, 4.17 mmol) and H$_2$[XA$_2$] (0.700 g, 1.04 mmol) were refluxed in toluene (60 mL) for 2-12 days.* The solution was then filtered to remove excess NaH, solvent was removed *in vacuo*, and hexamethyldisiloxane (30 mL) was added. Sonication and filtration gave 0.555 g (0.866 mmol, 84 %) of **3** as a white solid. **^{1}H NMR (C$_6$D$_6$, 600 MHz):** δ 7.28 (d, 4H, $^3J_{H\text{-}H}$ 7.7 Hz, Ar-*H*$_{meta}$), 7.19 (t, 2H, $^3J_{H\text{-}H}$ 7.6 Hz, Ar-*H*$_{para}$), 6.67 (d, 2H, $^4J_{H\text{-}H}$ 2.0 Hz, C*H*^{3}), 6.34 (d, 2H, $^4J_{H\text{-}H}$ 2.0 Hz, C*H*^{1}), 2.98 (sept, 4H, $^3J_{H\text{-}H}$ 6.9 Hz, C*H*Me$_2$), 1.81 (s, 6H, C*Me*$_2$), 1.35 (s, 18H, C*Me*$_3$), 1.29 (d, 12H, $^3J_{H\text{-}H}$ 6.8 Hz, CH*Me*$_2$), 0.99 (d, 12H, $^3J_{H\text{-}H}$ 7.1 Hz, CH*Me*$_2$). **^{13}C{^{1}H} NMR (C$_6$D$_6$, 125 MHz):** δ 151.8,

148.8, 146.2, 133.0 (Xanth-*Q*), 137.4 (Ar-C_{ipso}), 128.6 (Ar-C_{ortho}), 125.0 (Ar-C_{meta}), 121.2 (Ar-C_{para}), 109.4 (CH^3), 101.2 (CH^1), 35.8 (CMe_2), 34.4 (CMe_3), 31.4 (CMe_3), 28.3 (CMe_2), 27.7 ($CHMe_2$), 24.0, 23.4 ($CHMe_2$). Anal. Calcd. for $C_{47}H_{62}N_2Na_2O$: C, 78.73; H, 8.72; N, 3.91. Found: C, 79.09; H, 8.65; N, 3.96 %. * The reaction time was not reproducible. Typically, no reaction was observed for days but once the reaction began, it took less than 24 hours to reach completion

Li_2[BDPP] (4):

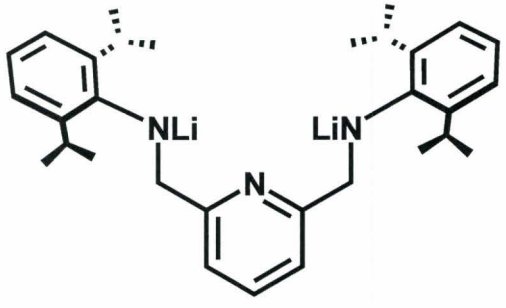

2.0 M ^{n}BuLi in cyclohexane (2.20 mL, 4.37 mmol) was added dropwise to 2,6-bis(2,6-diisopropylanilinomethyl)pyridine (1.00 g, 2.19 mmol) in hexanes (30 mL) at –78 °C. After stirring at –78 °C for 5 min. the solution was warmed to –45 °C for 5 min to give a yellow/brown solution with large amounts of yellow precipitate. The mixture was then re-cooled to –78 °C and filtered quickly on a pre-cooled frit to provide **4** as a yellow solid (0.898 g, 1.91 mmol) in 87 % yield. **^{1}H NMR (d_8-THF,* –30 °C, 500 MHz):** δ 7.58 (t, 1H, $^3J_{H\text{-}H}$ 7.3 Hz, Py-CH_{para}), 7.44 (d, 2H, $^3J_{H\text{-}H}$ 7.3 Hz, Py-CH_{meta}), 6.71 (d, 4H, $^3J_{H\text{-}H}$ 7.3 Hz, Ar-H_{meta}), 6.23 (t, 2H, $^3J_{H\text{-}H}$ 7.3 Hz, Ar-H_{para}), 4.78 (s, 4H, NCH_2), 3.73 (sept, $^3J_{H\text{-}H}$ 6.9 Hz, CHMe$_2$), 1.11 (d, 24H, $^3J_{H\text{-}H}$ 6.7 Hz, CHMe_2). **^{13}C{^{1}H} NMR (d_8-THF, –30°C,**

125 MHz): δ 166.4 (Py-C_{ortho}), 160.1 (Ar-C_{ipso}), 138.5 (Ar-C_{ortho}), 133.0 (Py-C_{para}), 120.8 (Ar-C_{meta}), 115.9 (Py-C_{meta}), 110.2 (Ar-C_{para}), 62.4 (NCH_2), 25.5 ($CHMe_2$), 21.0 ($CHMe_2$). Anal. Calcd. for $C_{31}H_{41}N_3Li_2$: C, 79.29; H, 8.80; N 8.95. Found: C, 79.15; H, 9.21; N, 8.49 %. * Li_2[BDPP] (**4**) shows similar thermal stability in both benzene and THF (extensive decomposition in minutes at room temperature), and is considerably less stable in toluene (decomposition occurs rapidly even at –30 °C). The thermal decomposition of **4** in benzene is not clean and a mixture of unidentified air-sensitive products is formed.

[(BDPP)$ThCl_2$(dme)] (5):

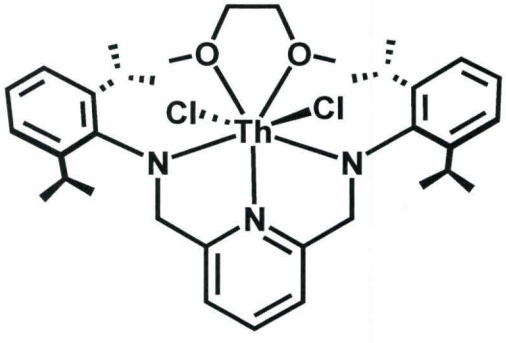

Method A. $ThCl_4(dme)_2$ (0.600 g, 1.08 mmol) and $LiCH_2SiMe_3$ (0.204 g, 2.17 mmol) in toluene (60 mL) were stirred for 1 h at –78 °C followed by 1 h at 0 °C. A solution of 2,6-bis(2,6-diisopropylanilinomethyl)pyridine (0.620 g, 1.35 mmol) in toluene (10 mL) was then added dropwise. The solution was allowed to warm to room temperature over ca. 2 hours, stirred for an additional 12 h, and then filtered to remove lithium salts. Solvent was removed *in vacuo*, and hexanes (30 mL) were added, followed by sonication and filtration to give **5** as a white solid (0.781 g, 0.92 mmol) in 85 % yield. **Method B.** $ThCl_4(dme)_2$

(0.140 g, 0.25 mmol) in benzene (10 mL) was placed in an ice-water bath (the majority of the solution did not freeze, despite the 6 °C freezing point of benzene). A solution of Li_2[BDPP] (**4**) (0.119 g, 0.25 mmol) in benzene (5 mL) was added dropwise (over 1-2 min). The solution was stirred for one hour, followed by filtration and removal of solvent *in vacuo*. Hexanes (10 mL) were added, followed by sonication and filtration to give **5** as a white solid (0.109 g, 0.13 mmol) in 51 % yield. **^{1}H NMR (C_6D_5Br, 600 MHz):** δ 7.24 (t, 1H, $^3J_{H\text{-}H}$ 7.6 Hz, Py-CH_{para}), 7.17 (br. m, 6H, Ar-*H*), 6.85 (d, 2H, $^3J_{H\text{-}H}$ 7.6 Hz, Py-C*H*), 5.27 (s, 4H, NCH_2), 4.19 (sept, $^3J_{H\text{-}H}$ 6.7 Hz, C*H*Me$_2$), 3.42 (s, 2H, OCH_2), 2.38 (s, 3H, OCH_3), 1.42, 1.15 (d, 24H, $^3J_{H\text{-}H}$ 6.7 Hz, CH*Me*$_2$). **^{13}C{^{1}H} NMR (C_6D_6, 125 MHz):** δ 165.0 (Py-C_{ortho}), 148.1 (Ar-C_{ipso}), 147.6 (Ar-C_{ortho}), 137.4 (Py-C_{para}), 125.3 (Ar-C_{meta}), 116.8 (Py-C_{meta}), 124.2 (Ar-C_{para}), 70.6 (NCH$_2$), 27.8 (*C*HMe$_2$), 27.0, 24.3 (CH*Me*$_2$). Anal. Calcd. for $C_{35}H_{51}Cl_2N_3O_2Th$: C, 49.53; H, 6.06; N 4.95. Found: C, 49.85; H, 6.35; N, 4.37 %.

[(XA_2)$ThCl_2$(dme)] (6):

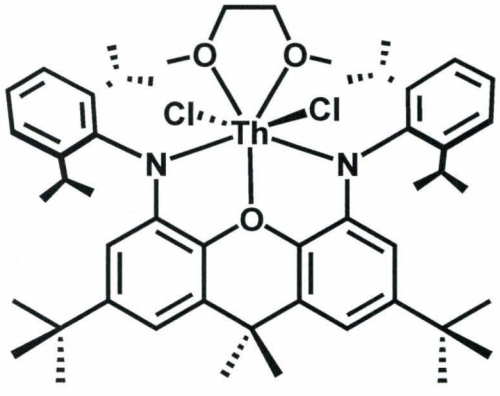

$ThCl_4(dme)_2$ (0.416 g, 0.75 mmol) and $K_2(dme)_2[XA_2]$ (**2**) (0.700 g, 0.75 mmol) in toluene (60 mL) were stirred for 16 h at 100°C. The solution was cooled to room temperature, filtered and the solvent was removed *in vacuo.* Hexanes (30 mL) were added, followed by sonication and filtration to give **6** as a white solid (0.378 g, 0.36 mmol) in 59 % yield. **^{1}H NMR (C_6D_6, 600 MHz):** δ 7.31 (m, 4H, $^3J_{H-H}$ 7.5 Hz, Ar-*H*), 7.25 (m, 2H, $^3J_{H-H}$ 7.5 Hz, Ar-*H*), 6.85 (d, 2H, $^4J_{H-H}$ 1.8 Hz, C*H*^{3}), 5.89 (d, 2H, $^4J_{H-H}$ 1.8 Hz, C*H*^{1}), 4.06 (sept, 4H, $^3J_{H-H}$ 6.8 Hz, C*H*Me$_2$), 3.04 (s, 4H, OC*H*$_2$), 2.25 (s, 6H, OC*H*$_3$), 1.70 (s, 6H, C*Me*$_2$), 1.47 (d, 12H, $^3J_{H-H}$ 6.7 Hz, CH*Me*$_2$), 1.25 (s, 18H, C*Me*$_3$), 1.09 (d, 12H, $^3J_{H-H}$ 6.9 Hz, CH*Me*$_2$). **^{13}C{^{1}H} NMR (C_6D_6, 125 MHz):** δ 149.4 (Ar-*C*$_{ortho}$), 147.1, 145.9, 141.3 (Xanth-*Q*), 142.0 (Ar-*C*$_{ipso}$), 127.3 (Ar-*C*$_{para}$), 125.4 (Ar-*C*$_{meta}$), 111.7 (*C*H^1), 111.4 (*C*H^3), 71.0 (O*C*H$_2$), 61.3 (O*Me*), 34.9 (*C*Me$_3$), 34.1 (*C*Me$_2$), 33.8 (C*Me*$_2$), 31.7 (C*Me*$_3$), 28.1 (*C*HMe$_2$), 27.2, 24.8 (CH*Me*$_2$). Anal. Calcd. for $C_{51}H_{72}Cl_2N_2O_3Th$: C, 57.57; H, 6.82; N, 2.63. Found: C, 57.76; H, 6.89; N, 2.49 %.

[(BDPP)Th(NEt$_2$)$_2$] (7).

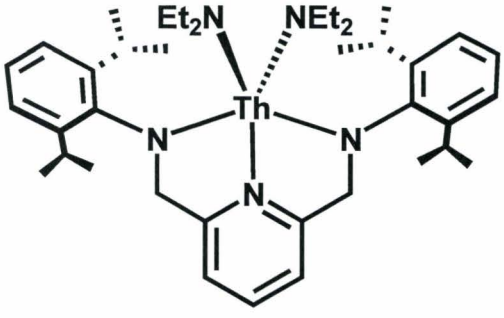

[(BDPP)ThCl$_2$(dme)] (**5**) (0.250 g, 0.29 mmol) and LiNEt$_2$ (0.047 g, 0.59 mmol) in toluene (25 mL) were stirred at room temperature for 1 hour. The solution was filtered

and toluene was removed *in vacuo*. Hexamethyldisiloxane (10 mL) was added and the mixture was sonicated. Collection of the resulting solid through filtration produced **7** as an off-white solid (0.154 g, 0.185 mmol) in 64 % yield. **^{1}H NMR (C_6D_6, 600 MHz):** δ 7.26 (d, 4H, $^3J_{H\text{-}H}$ 7.2 Hz, Ar-H_{meta}), 7.20 (t, 2H, $^3J_{H\text{-}H}$ 6.8 Hz, Ar-H_{para}), 6.92 (t, 1H, $^3J_{H\text{-}H}$ 7.5 Hz, Py-CH_{para}), 6.52 (d, 2H, $^3J_{H\text{-}H}$ 7.7 Hz, Py-CH_{meta}), 5.17 (s, 4H, CH_2NAr), 3.70 (sept, 4H, $^3J_{H\text{-}H}$ 6.9 Hz, CHMe$_2$), 3.00 (q, 8H, $^3J_{H\text{-}H}$ 6.8 Hz, NCH_2CH$_3$), 1.42 (d, 12H, $^3J_{H\text{-}H}$ 7.0 Hz, CHMe_2), 1.30 (d, 12H, $^3J_{H\text{-}H}$ 6.8 Hz, CHMe_2), 0.87 (t, 12H, $^3J_{H\text{-}H}$ 6.8 Hz, NCH$_2$CH_3). **^{13}C{^{1}H} NMR (C_6D_6, 125 MHz):** δ 165.6 (Py-C_{ortho}), 148.0 (Ar-C_{ortho}), 147.6 (Ar-C_{ipso}), 137.4 (Py-C_{para}), 124.3 (Ar-C_{meta}), 124.9 (Ar-C_{para}), 117.1 (Py-C_{meta}), 68.3 (*C*H$_2$NAr), 40.7 (NCH_2CH$_3$), 28.3 (*C*HMe$_2$), 26.7, 25.3 (CHMe_2), 15.9 (NCH$_2$CH_3). Anal. Calcd. for $C_{39}H_{61}N_5Th$: C, 56.30 H, 7.39; N, 8.42. Found: C, 55.94; H, 7.56; N, 7.77 %.

[Th(BDPP)$_2$] (8):

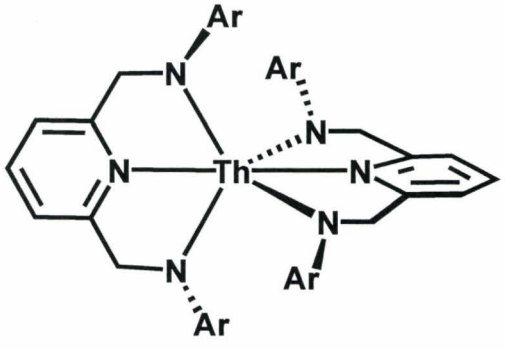

Method A. [(BDPP)Th(CH$_2$SiMe$_3$)$_2$] (**9**) (0.200 g, 0.23 mmol) and 2,6-bis(2,6-diisopropylanilinomethyl) pyridine (0.106 g, 0.23 mmol) in benzene (15 mL) were heated at 100 °C for 24 hours in a sealed flask. Upon cooling, the reaction mixture was filtered

and the solvent was reduced to ca. 1 mL *in vacuo*. Addition of hexamethyldisiloxane (10 mL) and sonication afforded **8** as a pale greenish yellow solid (0.097 g, 0.085 mmol) in 37 % isolated yield. **Method B.** $ThCl_4(dme)_2$ (0.100 g, 0.18 mmol) and Li_2BDPP (0.170 g, 0.36 mmol) in benzene (15 mL) were stirred at 0 °C for one hour (the majority of the solution did not freeze, despite the 6 °C freezing point of pure benzene). The reaction mixture was then warmed to room temperature, filtered, and the solvent was removed *in vacuo*. Addition of hexanes (5 mL) and sonication gave a brown solid, which was collected by filtration and washed with hexanes several times. Recrystallization by cooling a hot, concentrated toluene solution of **8** to –30 °C afforded the product as a pale greenish yellow solid (0.109 g, 0.095 mmol) in 26 % isolated yield. **^{1}H NMR (C_6D_6, 600 MHz):** δ 7.10 (m, 12H, Ar-*H*), 6.81 (t, 2H, $^3J_{H\text{-}H}$ 7.7 Hz, Py-CH_{para}), 6.48 (d, 4H, $^3J_{H\text{-}H}$ 7.7 Hz, Py-CH_{meta}), 4.87 (s, 8H, NCH_2), 3.00 (sept, 8H, $^3J_{H\text{-}H}$ 6.5 Hz, C*H*Me$_2$), 1.01 (d, 24H, $^3J_{H\text{-}H}$ 6.5 Hz, CHMe_2), 0.97 (d, 24H, $^3J_{H\text{-}H}$ 6.6 Hz, CHMe_2). **^{13}C{^{1}H} NMR (CD_2Cl_2, 125 MHz):** δ 167.5 (Py-C_{ortho}), 156.1 (Ar-C_{ortho}), 146.2 (Ar-C_{ipso}), 138.0 (Py-C_{meta}), 123.9 (Ar-CH_{meta}), 123.4 (Ar-C_{para}), 117.5 (Py-C_{para}), 68.0 (NCH_2), 29.5 (*C*HMe$_2$), 27.7, 24.1 (CHMe_2). Anal. Calcd. for $C_{62}H_{82}N_6Th$: C, 65.13; H, 7.23; N, 7.35. Found: C, 65.22; H, 7.36; N, 7.02 %.

6.3 – Experimental Procedures Pertaining to Chapter 3

6.3.1 – Synthetic Procedures and Characterization

[(BDPP)Th(CH_2SiMe_3)$_2$] (9):

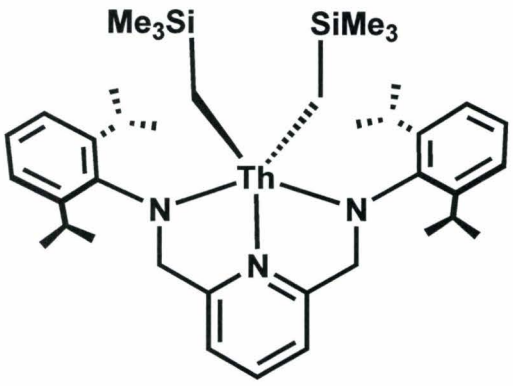

Method A. $ThCl_4(dme)_2$ (0.750 g, 1.35 mmol) and $LiCH_2SiMe_3$ (0.510 g, 5.41 mmol) in toluene (60 mL) were stirred for 1 h at –78 °C followed by 1 h at 0 °C. The cloudy, colourless solution was then re-cooled to –78 °C and a solution of 2,6-bis(2,6-diisopropylanilinomethyl)pyridine (0.620 g, 1.35 mmol) in toluene (10 mL) was added dropwise. The solution was allowed to warm to room temperature over ca. 2 hours, stirred for an additional 12 h, and then filtered to remove lithium salts. Solvent was removed *in vacuo* and hexamethyldisiloxane (30 mL) was added, followed by sonication and filtration to afford **9** as an off-white solid (0.949 g, 1.10 mmol) in 82 % yield. **Method B.** [(BDPP)$ThCl_2$(dme)] (**5**) (0.150 g, 0.18 mmol) and $LiCH_2SiMe_3$ (0.033 g, 0.35 mmol) in toluene (15 mL) were stirred for 30 minutes at room temperature. The solution was filtered and solvent was removed *in vacuo*. Hexamethyldisiloxane (10 mL) was added, followed by sonication and filtration to afford **9** as an off-white solid (0.106 g, 0.12 mmol) in 68 % yield. **^{1}H NMR (C_6D_6):** δ 7.24 (m, 6H, Ar-C*H*), 6.90 (t, 1H, $^3J_{H\text{-}H}$ 7.7 Hz, Py-CH_{para}), 6.49 (d, 2H, $^3J_{H\text{-}H}$ 7.7 Hz, Py-CH_{meta}), 5.24 (s, 4H, NCH_2), 3.75 (sept, 4H, $^3J_{H\text{-}H}$ 6.8 Hz, C*H*Me$_2$), 1.52 (d, 12H, $^3J_{H\text{-}H}$ 6.8 Hz, CH*Me*$_2$), 1.26 (d, 12H, $^3J_{H\text{-}H}$ 6.8 Hz, CH*Me*$_2$), –0.02 (s, 18H, Si*Me*$_3$), –0.32 (s, 4H, ThCH_2). **^{13}C{^{1}H} NMR (C_6D_6, 125 MHz):**

δ 164.8 (Py-C_{ortho}), 148.1 (Ar-C_{ipso}), 141.9 (Ar-C_{ortho}), 138.4 (Py-C_{para}), 126.8 (Ar-C_{meta}), 125.0 (Ar-C_{para}), 117.8 (Py-C_{meta}), 89.9 (ThCH_2), 68.7 (NCH_2), 28.7 ($CHMe_2$), 27.3, 24.9 (CHMe_2), 3.8 (SiMe_3). Anal. Calcd. for $C_{39}H_{63}N_3Si_2Th$: C, 54.33; H, 7.37; N, 4.87. Found: C, 54.10; H, 7.35; N, 4.69 %.

[(XA_2)Th(CH_2SiMe_3)$_2$] (10):

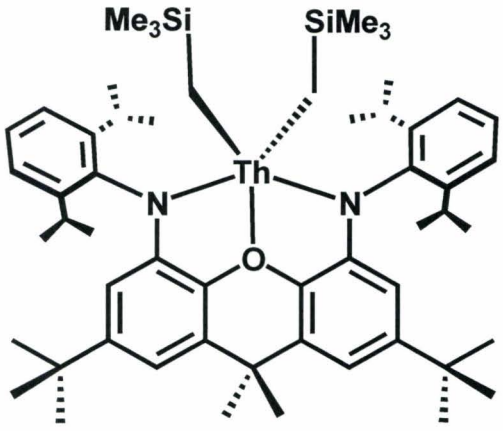

Method A. Complex **10** was prepared in a similar fashion to **9** (method A) using 0.750 g (1.35 mmol) of $ThCl_4(dme)_2$, 0.510 g (5.41 mmol) of $LiCH_2SiMe_3$ and 0.909 g (1.35 mmol) of $H_2[XA_2]$ (**1**). However, the crude filtered product was sonicated in hexanes (20 mL) before filtration to give 0.710 g of **10** as a white solid (0.711g, 0.66 mmol) in 49 % yield. **Method B.** Complex **10** was prepared in a similar fashion to **9** (method B) using [(XA_2)ThCl_2(dme)] (**6**) (0.250 g, 0.25 mmol) and $LiCH_2SiMe_3$ (0.048 g, 0.51 mmol). However, the crude filtered product was sonicated in hexanes (10 mL) before filtration to afford **10** as a white solid (0.175 g, 0.16 mmol) in 65 % yield. **^{1}H NMR (d_8-toluene, 600 MHz):** δ 7.26 (m, 6H, Ar-*H*), 6.77 (d, 2H, $^4J_{H\text{-}H}$ 1.5 Hz, CH^3), 6.00 (d, 2H, $^4J_{H\text{-}H}$ 1.5 Hz, CH^1), 3.54 (sept, 4H, $^3J_{H\text{-}H}$ 7.0 Hz, C*H*Me_2), 1.66 (s, 6H, CMe_2), 1.40 (d, 12H, $^3J_{H\text{-}H}$ 7.0

Hz, CH*Me*$_2$), 1.16 (d, 12H, $^3J_{H\text{-}H}$ 7.0 Hz, CH*Me*$_2$), 0.03 (s, 18H, Si*Me*$_3$), –0.17 (s, 4H, ThC*H*$_2$). **^{13}C{^{1}H} NMR (*d*$_8$-toluene, 125 MHz):** δ 146.2 (Ar-*C*$_{ortho}$), 148.8, 148.5 (Xanth-*Q*), 142.6 (Ar-*C*$_{ipso}$), 130.3 (Ar-*C*$_{para}$), 129.7 (Ar-*C*$_{meta}$), 110.7 (*C*H^1), 110.9 (*C*H^3), 35.6 (*C*Me$_3$), 35.5 (*C*Me$_2$), 31.4 (C*Me*$_2$), 32.1 (C*Me*$_3$), 29.5 (*C*HMe$_2$), 26.8, 25.5 (CH*Me*$_2$), 3.4 (Si*Me*$_3$). **Note:** ThCH_2 was not observed at room temperature but was observed at +50 or –80 °C (see main text). Anal. Calcd. for $C_{55}H_{84}N_2OSi_2Th$: C, 61.31 H, 7.86; N, 2.60. Found: C, 61.41; H, 8.06; N, 2.37 %.

[(BDPP)Th(CH$_2$SiMe$_3$)$_2$] (11):

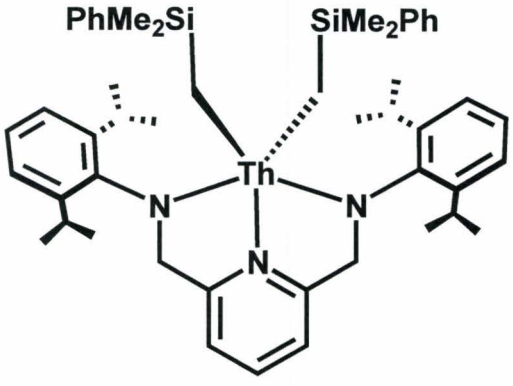

ThCl$_4$(dme)$_2$ (0.100 g, 0.18 mmol) and LiCH$_2$SiMe$_2$Ph (0.113 g, 0.72 mmol) in toluene (20 mL) were stirred for 1 h at –78 °C followed by 1 h at 0 °C. The cloudy, colourless solution was then re-cooled to –78 °C and a solution of 2,6-bis(2,6-diisopropylanilinomethyl)pyridine (0.082 g, 0.18 mmol) in toluene (3 mL) was added dropwise. The solution was allowed to warm to room temperature over ca. 2 hours, stirred for an additional 12 h, and then filtered to remove lithium salts. Solvent was removed *in vacuo* and hexamethyldisiloxane (30 mL) was added, followed by sonication and filtration to afford **11** as an off-white solid (0.138 g, 0.14 mmol) in 78 % yield. **^{1}H NMR**

(C_6D_6): δ 7.46 (d, 4H, $^3J_{H\text{-}H}$ 8.0 Hz, $SiMe_2Ph_{ortho}$), 7.21 (m, 12H, Ar-$H_{meta/para}$, $SiMe_2Ph_{meta/para}$), 6.94 (t, 1H, $^3J_{H\text{-}H}$ 7.8 Hz, Py-CH_{para}), 6.50 (d, 2H, $^3J_{H\text{-}H}$ 7.8 Hz, Py-CH_{meta}), 5.16 (s, 4H, NCH_2), 3.60 (sept, 4H, $^3J_{H\text{-}H}$ 7.0 Hz, CHMe$_2$), 1.45 (d, 12H, $^3J_{H\text{-}H}$ 7.0 Hz, CHMe_2), 1.18 (d, 12H, $^3J_{H\text{-}H}$ 6.9 Hz, CHMe_2), 0.15 (s, 12H, SiMe_3), –0.22 (s, 4H, ThCH_2). **$^{13}C\{^1H\}$ NMR (C_6D_6, 125 MHz):** δ 164.2 (Py-C_{ortho}), 147.4 (Ar-C_{ipso}), 145.3 (Ph-C_{ipso}), 140.9 (Ar-C_{ortho}), 137.6 (Py-C_{para}), 132.9 (Ph-C_{ortho}), 127.1, 127.5, 126.1, 124.3 (Ar-$C_{meta/para}$, Ph-$C_{meta/para}$), 117.0 (Py-C_{meta}), 86.3 (ThCH_2), 67.7 (NCH_2), 28.0 ($CHMe_2$), 26.6, 24.0 (CHMe_2), 1.3 (SiMe_2).

[(XA_2)Th($CH_2Ph)_2$] (12):

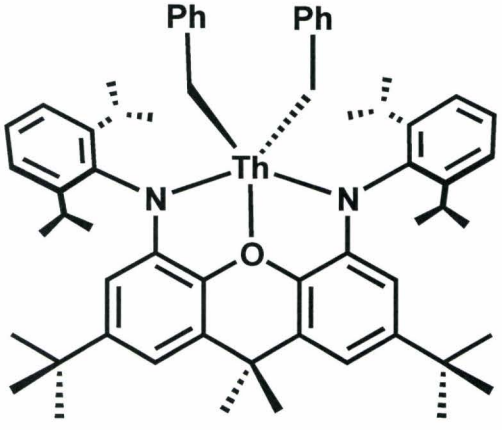

A 1.0 M solution of $PhCH_2MgBr$ in OEt_2 (1.21 mL, 1.21 mmol) was added dropwise to a –78 °C solution of [(XA_2)ThCl_2(dme)] (**6**) (0.600 g, 0.61 mmol) in toluene (30 mL), and then allowed to warm to room temperature over 3 hours. The solvent was removed *in vacuo* and hexanes (30 mL) was added. The solution was then filtered and evaporated to dryness *in vacuo* to yield **12** as a yellow solid (0.659 g, 0.37 mmol) in 56 % yield. X-Ray quality crystals were grown by cooling a concentrated solution of **12** in

hexanes from room temperature to –30 °C. **^{1}H NMR (C_6D_6, 600 MHz, 50 °C):** δ 7.26 (br. s, 6H, Ar-*H*), 7.02 (br. s, 4H, Th*Bz*$_{meta}$), 6.80 (br. s, 2H, C*H*^{1}), 6.65 (br. s, 2H, Th*Bz*$_{para}$), 6.01 (br. s, 2H, C*H*^{3}), 3.42 (sept, 4H, $^{3}J_{H\text{-}H}$ 6.4 Hz, C*H*Me$_2$), 1.69 (s, 6H, C*Me*$_2$), 1.35 (br. d, 12H, $^{3}J_{H\text{-}H}$ 5.7 Hz, CH*Me*$_2$), 1.31 (s, 4H, ThC*H*$_2$), 1.20 (s, 18H, C*Me*$_3$), 1.09 (br. s, 12H, CH*Me*$_2$). **^{13}C{^{1}H} NMR (C_6D_6, 151 MHz, 50 °C):** δ 148.8 (Th*Bz*$_{ipso}$, Ar-*C*$_{ortho}$), 148.0, 145.7, 141.8 (Xanth-*Q*), 136.5 (Ar-*C*$_{ipso}$), 131.0 (broad s, Th*Bz*$_{meta}$), 129.4 (C^{6}) 127.9 (*Ar*-C$_{para}$), 125.1, 125.0 (Th*Bz*$_{ortho}$, Ar-C$_{meta}$), 121.9 (broad s, Th*Bz*$_{para}$), 111.0 (*C*H^{3}), 110.8 (*C*H^{1}), 35.0 (*C*Me$_3$), 34.9 (*C*Me$_2$), 32.2 (C*Me*$_2$), 31.7 (C*Me*$_3$), 29.5 (*C*HMe$_2$), 26.7, 24.1 (2 x CH*Me*$_2$). **^{1}H NMR (*d*$_8$-toluene, 500 MHz, –40 °C):** δ 7.20 (broad m, 4H, Ar-*H*$_{para}$, Ar-*H*$_{meta}$), 7.14 (broad m, 4H, Ar-*H*$_{meta}$, Th*Bz*$_{meta}$ B), 7.07 (s, 2H, Th*Bz*$_{ortho}$ A), 7.00 (s, 2H, Th*Bz*$_{meta}$ A), 6.85 (t, Th*Bz*$_{para}$ B), 6.84 (s, 2H, C*H*^{1}), 6.56 (t, $^{3}J_{H\text{-}H}$ 6.9 Hz, Th*Bz*$_{para}$ A), 6.08 (s, 2H, C*H*^{3}), 5.32 (d, 2H, $^{3}J_{H\text{-}H}$ 6.7 Hz, Th*Bz*$_{ortho}$ B), 3.45, 3.16 (sept, 2 x 2H, $^{3}J_{H\text{-}H}$ 6.9 Hz, C*H*Me$_2$), 1.79, 1.57 (s, 2 x 3H, C*Me*$_2$), 1.34 (s, 2H, ThC*H*$_2$ B), 1.30, 1.29, 1.11, 1.05 (d, 4 x 6H, $^{3}J_{H\text{-}H}$ 6.9 Hz, CH*Me*$_2$), 1.26 (s, 2H, ThC*H*$_2$ A), 1.22 (s, 18H, C*Me*$_3$). **^{13}C{^{1}H} NMR (*d*$_8$-toluene, 126 MHz, –40 °C):** δ 149.3 (Th*Bz*$_{ipso}$ A & Ar-*C*$_{ortho}$), 147.7, 147.6 (Ar-*C*$_{ortho}$, Xanth-*Q*), 145.5 (Xanth-*Q*), 144.2 (Th*Bz*$_{ipso}$ B), 142.2 (Xanth-*Q*), 134.2 (Ar-*C*$_{ipso}$), 133.3 (Ar-*C*$_{meta}$), 129.3 (Xanth-*Q*), 128.7 (Th*Bz*$_{meta}$ A), 127.9 (Ar-*C*$_{meta}$), 124.8 (Ar-*C*$_{para}$, Th*Bz*$_{ortho}$ A & Th*Bz*$_{meta}$ B), 124.3 (Th*Bz*$_{ortho}$ B), 123.0 (Th*Bz*$_{para}$ B), 120.6 (Th*Bz*$_{para}$ A), 110.5 (*C*H^{3}), 109.9 (*C*H^{1}), 93.4 (Th*C*H$_2$ B) 90.9 (Th*C*H$_2$ A), 35.7, 26.5 (2 x C*Me*$_2$), 34.9, 34.8 (*C*Me$_3$ & *C*Me$_2$), 31.5 (C*Me*$_3$), 30.0, 29.0 (2 x *C*HMe$_2$), 26.7 (2 x CH*Me*$_2$), 23.7, 23.6 (2 x CH*Me*$_2$). ^{13}C NMR (*d*$_8$-toluene, 126 MHz, –40 °C): δ 93.4 (t, $^{1}J_{C\text{-}H}$ 139 Hz, Th*C*H$_2$ B) 90.9 (t, $^{1}J_{C\text{-}H}$ 120 Hz,

ThCH_2 A). Anal. Calcd. for $C_{61}H_{76}N_2OTh$: C, 67.51; H, 7.06; N, 2.56. Found: C, 67.84; H, 7.31; N, 2.58 %. **Note:** ThCH_2 A = η^1-coordinated; ThCH_2 B = η^2 or η^3-coordinated. Assignments of hapticity are based on $^1J_{C\text{-}H}$ values for ThCH_2Ph. Lower frequency shifts for the MCH_2Ph and *ipso*-MCH_2*Ph* carbon resonances in ^{13}C NMR spectra have also been cited as evidence of η^2-benzyl coordination.[179, 181]

[(BDPP)Th(CH_2Ph)$_2$] (13):

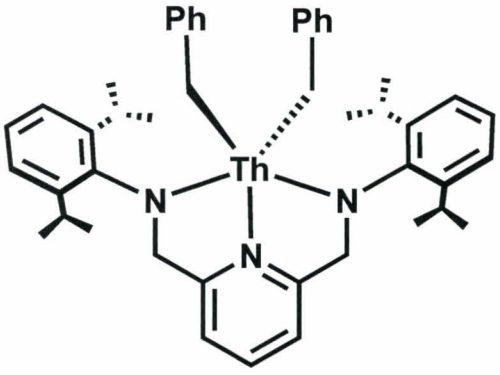

A 1.0 M solution of PhCH_2MgCl in OEt_2 (0.41 mL, 0.41 mmol) was added dropwise to a –78 °C solution of [(BDPP)ThCl_2(dme)] (**5**) (175 mg, 0.21 mmol) in toluene (15 mL), before warming to room temperature over 3 hours. The mixture was then filtered to remove insoluble salts and the mother liquors were evaporated to dryness *in vacuo*. Hexanes (30 mL) was added, followed by sonication and filtration to collect **13** as a yellow solid (120 mg, 0.14 mmol) in 67 % yield. X-Ray quality crystals of **13** were obtained by layering a toluene solution of **13** with hexanes at –30 °C. **^{1}H NMR (C_7D_8, 500 MHz, –35 °C):** δ 7.22 (m, 6H, Ar-H_{meta}, Ar-H_{para}, ThBz_{meta} A), 7.12 (br, s, 2H, *Ar-m*), 6.96 (br, s, 2H, ThBz_{ortho} B), 6.80 (app. t, $^3J_{H\text{-}H}$ 7.8 Hz, 2H, ThBz_{meta} B), 6.78 (t, $^3J_{H\text{-}H}$ 8.2 Hz, 1H, Py-CH_{para}), 6.74 (t, $^3J_{H\text{-}H}$ 6.4 Hz, 1H, ThBz_{para} A), 6.32 (d, 2H, $^3J_{H\text{-}H}$ 8.1 Hz , Py-

C*H*$_{meta}$), 6.22 (t, 1H, $^{3}J_{H\text{-}H}$ 7.8 Hz, Th*Bz*$_{para}$ B), 5.47 (d, 2H, $^{3}J_{H\text{-}H}$ 7.6 Hz, Th*Bz*$_{ortho}$ A), 5.07, 4.83 (d, 2 x 2H, $^{2}J_{H\text{-}H}$ 19 Hz, Py-C*H*$_2$), 3.88, 3.47 (septet, 2 x 2H, $^{3}J_{H\text{-}H}$ 7.2 Hz, C*H*Me$_2$), 1.49, 1.41, 1.33, 1.07 (d, 4 x 6H, $^{3}J_{H\text{-}H}$ 7.2 Hz, CH*Me*$_2$), 1.45 (s, 2H, ThC*H*$_2$ A), 1.15 (s, 2H, ThC*H*$_2$ B). **^{13}C{^{1}H} NMR (C$_7$D$_8$, 125 MHz, –35 °C):** δ 164.3 (Py-*C*$_{ortho}$), 150.0 (Th*Bz*$_{ipso}$ B), 149.7, 147.7 (Ar-*C*$_{ortho}$), 145.8 (Th*Bz*$_{ipso}$ A), 141.8 (Ar-*C*$_{ipso}$), 132.4, 126.3 (Ar-C$_{para}$, Th*Bz*$_{meta}$ A), 124.3 (Th*Bz*$_{ortho}$ B), 124.0, 123.8 (2 x Ar-*C*$_{meta}$), 123.5 (Th*Bz*$_{ortho}$ A), 121.3 (Th*Bz*$_{para}$ A), 118.8 (Th*Bz*$_{para}$ B), 117.2 (Py-*C*$_{meta}$), 116.3 (Py-*C*$_{para}$), 89.6 (Th*C*H$_2$ A), 78.5 (Th*C*H$_2$ B), 67.5 (N*C*H$_2$), 30.0 , 28.2 (*C*HMe$_2$), 28.03, 27.73, 23.44, 22.78 (CH*Me*$_2$). Anal. Calcd. for C$_{45}$H$_{55}$N$_3$Th: C, 62.13; H, 6.37; N, 4.83. Found: C, 61.91; H, 6.94; N, 4.90 %.

[(BDPP)Th(*n*Bu)$_2$] (14):

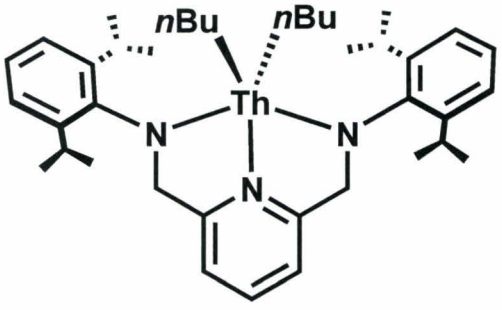

1.6 M *n*BuLi in hexane (0.368 mL, 0.59 mmol) was added dropwise to [(BDPP)ThCl$_2$(dme)] (**5**) (0.250 g, 0.29 mmol) in toluene (25 mL) at room temperature. The solution was stirred for 30 minutes, filtered, and the solvent removed *in vacuo*. Hexamethyldisiloxane (10 mL) was added, followed by sonication (1 hour) and filtration to give **14** as an off-white solid (0.133 g, 0.17 mmol) in 57 % yield. **^{1}H NMR (C$_6$D$_6$, 500 MHz):** δ 7.20 (app s, 6H, Ar-C*H*), 6.91 (t, 1H, $^{3}J_{H\text{-}H}$ 7.6 Hz, Py-C*H*$_{para}$), 6.5 (d, 2H, $^{3}J_{H\text{-}H}$

7.6 Hz, Py-CH_{meta}), 5.19 (s, 4H, NCH_2), 3.77 (sept, 4H, $^3J_{H\text{-}H}$ 6.6 Hz, CHMe$_2$), 1.49 (d, 12H, $^3J_{H\text{-}H}$ 6.6 Hz, CHMe_2), 1.49 (app. d, 2H, ThCH$_2$CH_2), 1.29 (app. d, 2H, ThCH$_2$CH$_2$CH_2), 1.26 (d, 12H, $^3J_{H\text{-}H}$ 6.6 Hz, CHMe_2), 0.87 (t, 6H, $^3J_{H\text{-}H}$ 6.6 Hz, ThCH$_2$CH$_2$CH$_2$CH_3), 0.35 (d, 2H, $^3J_{H\text{-}H}$ 7.9 Hz, ThCH_2). **^{13}C{^{1}H}NMR (C_6D_6, 125 MHz):** δ 165.12 (Py-C_{ortho}), 148.54 (Ar-C_{ipso}), 142.42 (Ar-C_{ortho}), 126.16, 124.43 (Ar-C_{para}, Ar-C_{meta}), 137.95 (Py-C_{para}), 117.67 (Py-C_{meta}), 87.73 (ThCH$_2$), 68.39 (NCH$_2$), 28.65 (CHMe$_2$), 27.35, 24.93 (CHMe_2), 28.54 (ThCH$_2$$CH_2$), 29.40 (ThCH$_2CH_2$$CH_2$), 14.60 (ThCH$_2CH_2CH_2$$CH_3$). Anal. Calcd. for $C_{39}H_{59}N_3Th$: C, 58.41; H, 7.42; N, 5.24. Found: C, 58.07; H, 7.04; N, 5.20 %.

[(XA$_2$)Th(*n*Bu)$_2$] (15):

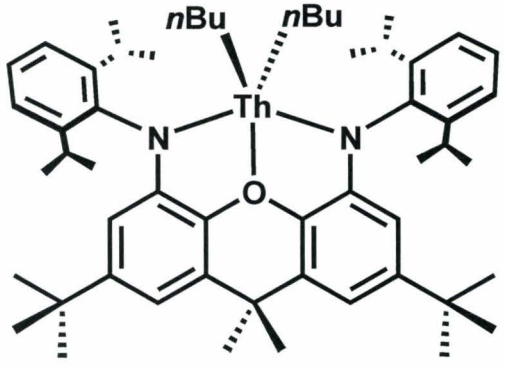

1.6 M *n*BuLi in hexane (0.176 mL, 0.28 mmol) was added dropwise to [(XA$_2$)ThCl$_2$(dme)] (**6**) (0.150 g, 0.14 mmol) in toluene (25 mL) at room temperature. The solution was stirred for 30 minutes, filtered, and the solvent removed *in vacuo*. Hexamethyldisiloxane (10 mL) was added, followed by sonication (1 hour) and filtration to give **15** as an off-white solid (0.049 g, 0.05 mmol) in 35 % yield. **^{1}H NMR (C_6D_6, 600 MHz):** δ 7.24 (app. s, 6H, Ar-CH), 6.80 (app. s, 2H, $^4J_{H\text{-}H}$ 2.1 Hz, CH^1), 6.13 (app. s, 2H,

$^4J_{H\text{-}H}$ 7.9 Hz, CH^3), 3.59 (sept, 4H, $^3J_{H\text{-}H}$ 7.0 Hz, CHMe$_2$), 1.63 (s, 6H, CMe_2) 1.71 (app. t, 2H, ThCH$_2$CH_2), 1.37 (d, 12H, $^3J_{H\text{-}H}$ 7.1 Hz, CHMe_2), 1.29 (app. d, 2H, ThCH$_2$CH$_2$CH_2), 1.16 (d, 12H, $^3J_{H\text{-}H}$ 7.1 Hz, CHMe_2), 0.83 (t, 6H, $^3J_{H\text{-}H}$ 6.6 Hz, ThCH$_2$CH$_2$CH$_2$CH_3), 0.45 (d, 2H, $^3J_{H\text{-}H}$ 7.8 Hz, ThCH_2). **^{13}C{^{1}H} NMR (C_6D_6, 125 MHz):** δ 146.0 (Ar-C_{ortho}), 148.3, 135.4, 129.9 (Xanth-Q), 141.8 (Ar-C_{ipso}), 128.4, 127.9 (Ar-$CH_{meta/para}$), 110.0 (CH^1), 109.9 (CH^3), 95.6 (ThCH$_2$), 35.1 (CMe$_3$), 35.0 (CMe$_2$), 31.4 (CMe_2), 31.8 (CMe_3), 29.2 (CHMe$_2$), 26.3, 25.1 (CHMe_2), 28.8 (ThCH$_2$CH$_2$), 29.8 (ThCH$_2$CH$_2$CH$_2$), 14.60 (ThCH$_2$CH$_2$CH$_2$CH$_3$). Anal. Calcd. for $C_{55}H_{80}N_2$)Th: C, 64.94; H, 7.93; N, 2.75. Found: C, 63.98; H, 7.33; N, 2.38 %.

[(BDPP)ThMe$_3$][Li(dme)] (16):

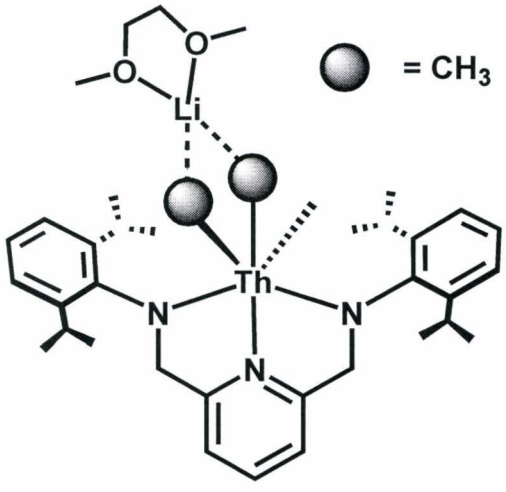

[(BDPP)ThCl$_2$(dme)] (**5**) (0.750 g, 0.88 mmol) and MeLi (0.058 g, 2.65 mmol) in toluene (25 mL) were stirred for 15 minutes at room temperature. The solution was filtered and the solvent was removed *in vacuo*. Hexamethyldisiloxane (10 mL) was added, followed by sonication and filtration to give **16** as an off-white solid (0.482 g, 0.65

mmol) in 74 % yield. **^{1}H NMR (C_6D_6, 500 MHz):** δ 7.27 (d, 4H, $^3J_{H\text{-}H}$ 7.6 Hz, Ar-CH_{meta}), 7.13 (t, 1H, $^3J_{H\text{-}H}$ 7.3 Hz, Ar-CH_{para}), 6.99 (t, 1H, $^3J_{H\text{-}H}$ 7.9 Hz, Py-CH_{para}), 6.63 (d, 2H, $^3J_{H\text{-}H}$ 7.9 Hz, Py-CH_{meta}), 5.39 (s, 4H, NCH_2), 4.20 (m, 4H, $^3J_{H\text{-}H}$ 6.3 Hz, CHMe$_2$), 1.59, 1.35 (d, 12H, $^3J_{H\text{-}H}$ 6.6 Hz, CHMe_2), 0.02 (s, 9H, ThMe_3). **^{13}C{^{1}H} NMR (C_6D_6, 125 MHz):** δ 166.0 (Py-C_{ortho}), 148.1 (Ar-C_{ortho}), 137.0 (Py-C_{para}), 124.9, 124.9 (Ar-C_{meta}, Ar-C_{para}), 69.9 (OCH_2), 68.1 (NCH_2), 58.7 (OCH_3), 56.3 (ThMe_3), 28.1 (CHMe$_2$), 27.9, 24.8 (CHMe_2). Anal. Calcd. for $C_{38}H_{60}LiN_3O_2Th$: C, 55.00; H, 7.29; N, 5.06. Found: C, 55.67; H, 7.29; N, 4.80 %.

[(BDPP*)Th(μ-Me$_2$)Li(dme)] (17):

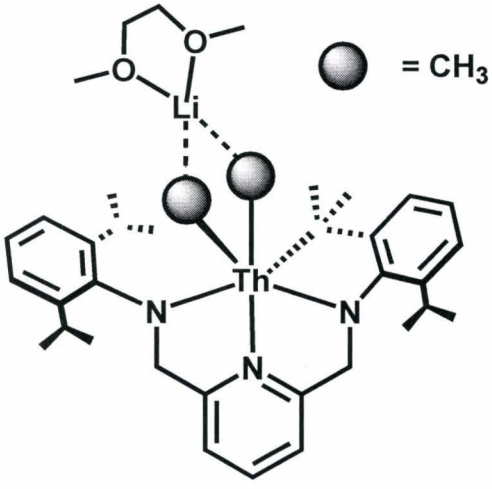

[(BDPP)ThMe$_3$][Li(dme)] (**16**) (0.100 g, 0.14 mmol) in toluene (10 mL) was stirred for 4 days at room temperature. The solution was filtered and the solvent removed *in vacuo*. Hexamethyldisiloxane (10 mL) was added, followed by sonication and filtration to give **17** as a brown solid (0.22 g, 0.03 mmol) in 20 % yield. ^{1}H NMR (C_6D_6, 500 MHz): δ 7.35-7.25 (app. m, 6H, Ar-C$H_{meta/para}$), 6.89 (t, 1H, $^3J_{H\text{-}H}$ 7.5 Hz, Py-CH_{para}),

6.58 (d, 2H, $^{3}J_{H\text{-}H}$ 7.5 Hz, Py-C*H*$_{meta}$), 5.95 (d, 1H, $^{2}J_{H\text{-}H}$ 19.7 Hz, NC*H*$_2$), 5.32 (app s, 2H, NC*H*$_2$), 4.78 (d, 1H, $^{2}J_{H\text{-}H}$ 19.6 Hz, NC*H*$_2$), 4.03 (sept, 1H, $^{3}J_{H\text{-}H}$ 6.6 Hz, C*H*Me$_2$), 3.94 (sept, 1H, $^{3}J_{H\text{-}H}$ 6.8 Hz, C*H*Me$_2$), 3.79 (sept, 1H, $^{3}J_{H\text{-}H}$ 6.6 Hz, C*H*Me$_2$), 2.52 (s, 6H, OC*H*$_3$), 2.39 (br s, 7H, OC*H*$_2$ and ThC*Me*$_2$Ar), 1.71 (d, 3H, $^{3}J_{H\text{-}H}$ 6.7 Hz, CH*Me*$_2$), 1.61 (d, 3H, $^{3}J_{H\text{-}H}$ 6.8 Hz, CH*Me*$_2$), 1.50 (d, 3H, $^{3}J_{H\text{-}H}$ 6.7 Hz, CH*Me*$_2$), 1.41 (d, 3H, $^{3}J_{H\text{-}H}$ 5.9 Hz, CH*Me*$_2$), 1.39 (d, 3H, $^{3}J_{H\text{-}H}$ 6.0 Hz, CH*Me*$_2$), 1.35 (d, 3H, $^{3}J_{H\text{-}H}$ 6.5 Hz, CH*Me*$_2$), 1.22 (s, 3H, ThC*Me*$_2$Ar), -0.09 (s, 3H, Th*Me*$_2$), -0.32 (s, 3H, Th*Me*$_2$). $^{13}C\{^{1}H\}$ NMR (C_6D_6, 125 MHz): δ 168.45 (Py-*C*$_{ortho}$), 165.57 (Py-*C*$_{ortho}$), 148.13, 147.89, 147.41, 146.94, 146.77 (Ar-*C*$_{ipso}$), 136.59 (Py-*C*$_{para}$), 168.45 (Py-*C*$_{ortho}$), 124.57, 124.22, 124.05, 123.10, 118.74, 117.08 (Ar-*C*$_{para}$, Ar-*C*$_{meta}$), 116.86 (Py-*C*$_{meta}$), 73.61 (Th*C*Me$_2$Ar), 116.86 (Py-*C*$_{meta}$), 70.19 (N*C*H$_2$), 69.68 (O*C*H$_2$), 67.93 (N*C*H$_2$), 58.96 (O*C*H$_3$), 53.00, 41.44 (Th*Me*$_2$), 30.16, 28.63, 27.83 (*C*HMe$_2$), 27.57, 26.90, 26.31, 25.73, 24.80, 24.79 (CH*Me*$_2$), 27.29, 23.09 (ThC*Me*$_2$Ar). Anal. Calcd. for $C_{37}H_{54}LiN_3O_2Th$: C, 54.74; H, 6.70; N, 5.18. Found: C, 54.51; H, 6.26; N, 4.94 %.

[(BDPP)ThMe$_2$] (18):

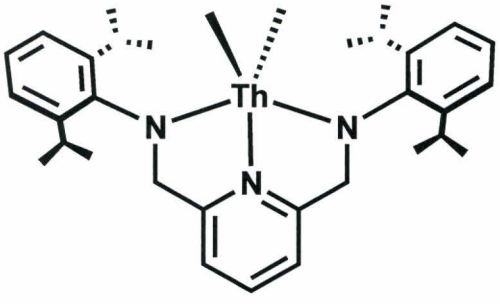

[(BDPP)$ThCl_2$(dme)] (**5**) (0.115 g, 0.14 mmol) and [(BDPP)$ThMe_3$][Li(dme)] (**16**) (0.200 g, 0.27 mmol) in toluene (15 mL) were stirred for 5 minutes at room temperature. The solution was cooled to 0 °C, filtered, and the solvent was removed *in vacuo*. Hexamethyldisiloxane (10 mL) was added, followed by intermittent sonication and cooling to –78 °C, to give **18** after filtration as an off-white solid (0.238 g, 0.33 mmol) in 81 % yield. **^{1}H NMR (C_7D_8, –25 °C, 500 MHz):** δ 7.19 (app s, 6H, Ar-C*H*), 6.82 (t, 1H, $^3J_{H\text{-}H}$ 7.7 Hz, Py-CH_{para}), 6.37 (d, 2H, $^3J_{H\text{-}H}$ 7.7 Hz, Py-CH_{meta}), 5.12 (s, 4H, NCH_2), 3.75 (br s, 4H, C*H*Me_2), 1.47, 1.23 (br s, 12H, CHMe_2), 0.01 (s, 6H, ThMe_2). **^{13}C{^{1}H}NMR (C_7D_8, –25 °C, 125 MHz):** δ 164.6 (Py-C_{ortho}), 148.0 (Ar-C_{ortho}), 126.0, 125.0 (Ar-C_{para}, Ar-C_{meta}), 117.1 (Py-C_{para}), 82.7 (ThMe_2), 68.2 (NCH_2), 28.1 (*C*HMe_2), 27.3, 24.3 (CHMe_2). **Note:** Acquisition of elemental analysis data was not possible due to thermal instability.

[(XA_2)Mg(dme)] (20):

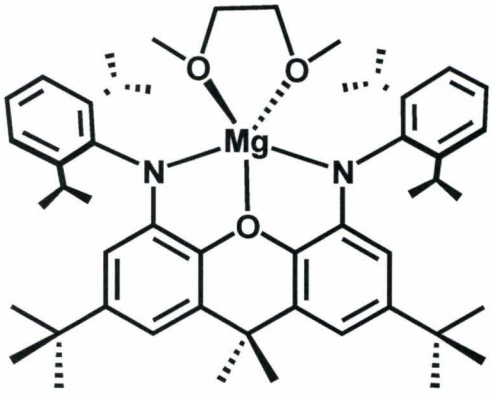

H_2[XA_2] (0.121 g, 0.18 mmol) and $ThCl_4$(dme)$_2$ (0.100 g, 0.18 mmol) were placed in toluene (10 mL). 1.0 M BzMgCl in Et_2O (0.360 mL, 0.36 mmol) was added dropwise

to the solution. After 1 hour, the solution was filtered and solvent was removed *in vacuo* to give **20** as a bright yellow solid (0.098 g, 0.124 mmol) in 69 % yield. **Note:** Although thorium is not incorporated in the reaction product, the addition of $ThCl_4(dme)_2$ was requires in order to obtain a high yield of **20**. **^{1}H (C_6D_6, 600 MHz):** δ 7.27 (d, 4H, $^3J_{H\text{-}H}$ 7.5 Hz, Ar-H_{meta}), 7.20 (t, 2H, $^3J_{H\text{-}H}$ 7.4 Hz, Ar-H_{para}), 6.62 (d, 2H, $^4J_{H\text{-}H}$ 1.7 Hz, CH^3), 6.24 (d, 2H, $^4J_{H\text{-}H}$ 1.7 Hz, CH^1), 3.55 (sept, 4H, $^3J_{H\text{-}H}$ 6.8 Hz, CHMe$_2$), 2.79 (s, 6H, OMe), 2.58 (s, 4H, OCH_2), 1.70 (s, 6H, CMe_2), 1.27 (d, 12H, $^3J_{H\text{-}H}$ 6.7 Hz, CHMe_2), 1.12 (d, 12H, $^3J_{H\text{-}H}$ 6.7 Hz, CHMe_2). **^{13}C{^{1}H} NMR (C_6D_6, 125 MHz):** δ 148.8 (Ar-C_{ortho}), 148.2, 147.0, 132.1 (Xanth-Q), 146.1 (Ar-C_{ipso}), 123.5 (Ar-C_{para}), 123.8 (Ar-C_{meta}), 109.1 (CH^1), 103.0(CH^3), 69.4 (OCH_2), 59.9 (OMe), 36.5 (CMe$_2$), 35.1 (CMe$_3$), 28.8 (CMe_2), 32.0 (CMe_3), 28.2 (CHMe$_2$), 26.0, 24.4 (CHMe_2). Anal. Calcd. for: $C_{51}H_{72}MgN_2O_3$: C, 77.99; H, 9.24; N, 3.57. Found: C, 78.43; H, 9.71; N, 3.48 %.

6.4 – Experimental Procedures Pertaining to Chapter 4

6.4.1 – Synthetic Procedures and Characterization

[(XA_2)Th(CH_2Ph)][$B(C_6F_5)_3(CH_2Ph)$] (21):

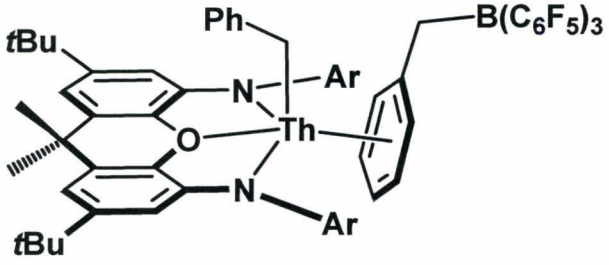

A –30 °C solution of [[(XA$_2$)Th(CH$_2$Ph)$_2$] (**12**) (0.100 g, 0.092 mmol) in hexanes (5 mL) was added dropwise to a –30 °C solution of B(C$_6$F$_5$)$_3$ (0.047 g, 0.092 mmol) in hexanes (2 mL). The reaction mixture was allowed to settle in the glove box freezer overnight before the mother liquors were removed, and the solid was washed with hexanes (3 x 2 mL). Residual solvent was then removed *in vacuo* to afford **21** as a yellow-orange solid (0.138 g, 0.88 mmol) in 95 % yield. Complex **21** is stable for days at room temperature under an inert atmosphere, both in solution and as a solid. However, rapid thermal decomposition was observed at temperatures above 60 °C. **^{1}H NMR (C$_6$D$_6$, 600 MHz):** δ 7.31 (t, 2H, $^3J_{H\text{-}H}$ 7.5 Hz, Ar-*H$_{para}$*), 7.23 (d, 4H, $^3J_{H\text{-}H}$ 7.5 Hz, Ar-*H$_{meta}$*), 6.87 (m, 4H, Th*Bz$_{ortho}$*, Th*Bz$_{meta}$*), 6.77 (d, 2H, $^4J_{H\text{-}H}$ 1.5 Hz, C*H*^{1}), 6.56 (br. m, 2H, Th*Bz$_{para}$*, B*Bz$_{para}$*), 6.52 (d, 2H, $^3J_{H\text{-}H}$ 6.5 Hz, B*Bz$_{ortho}$*), 5.98 (t, 2H, $^3J_{H\text{-}H}$ 6.5 Hz, B*Bz$_{para}$*), 5.76 (d, 2H, $^4J_{H\text{-}H}$ 1.5 Hz, C*H*^{3}), 3.25 (broad s, 2H, BC*H*$_2$), 3.00, 2.59 (sept, 2 x 2H, $^3J_{H\text{-}H}$ 7 Hz, C*H*Me$_2$), 2.40 (sharp s, 2H, ThC*H*$_2$), 1.52, 1.40 (s, 2 x 3H, C*Me*$_2$), 1.29, 1.14, 0.98, 0.76 (d, 4 x 6H, $^3J_{H\text{-}H}$ 6.9 Hz, CH*Me*$_2$), 1.08 (s, 18H, C*Me*$_3$). **^{13}C{^{1}H} NMR (C$_6$D$_6$, 151 MHz):** δ 162.9 (B*Bz$_{ipso}$*), 148.5, 143.2, 140.6, 128.7 (Xanth-*Q*), 148.0 (broad d, *J* 240 Hz, *ortho*- or *meta*-*C*$_6$F$_5$), 148.0, 145.4 (2 x Ar-*C$_{ortho}$*), 144.5 (Th*Bz$_{ipso}$*), 138.3 (broad d, *J* ~230 Hz, *para*-*C*$_6$F$_5$), 136.7 (broad d, *J* ~240 Hz, *ortho*- or *meta*-*C*$_6$F$_5$), 136.0 (Ar-*C$_{ipso}$*), 134.8 (B*Bz$_{meta}$*), 134.0 (B*Bz$_{ortho}$*), 129.15 (Ar-*C$_{para}$*), 128.3 (Th*Bz$_{meta}$*), 126.8 (B*Bz$_{para}$*), 125.4 (Th*Bz$_{ortho}$*), 125.2, 125.1 (2 x Ar-*C$_{meta}$*), 122.4 (Th*Bz$_{para}$*), 112.3 (*C*H^1), 110.4 (*C*H^3), 93.1 (ThCH$_2$), 35.9 (broad s, BCH$_2$), 34.2 (*C*Me$_3$), 33.8 (*C*Me$_2$), 33.6, 28.4 (2 x C*Me*$_2$), 30.6 (C*Me*$_3$), 29.7, 28.3 (2 x *C*HMe$_2$), 26.0, 24.7, 24.6, 22.9 (4 x CH*Me*$_2$). **^{13}C NMR (C$_6$D$_6$, 151 MHz):** δ 92.09 (t, $^1J_{C\text{-}H}$ 119 Hz, ThCH$_2$). **^{11}B NMR (C$_6$D$_6$, 193**

MHz): δ –11.62. **^{19}F NMR (C_6D_6, 471 MHz):** δ –128.93 (d, *J* 20 Hz, F_{ortho}), –160.40 (t, $^3J_{F\text{-}F}$ 20 Hz, F_{para}), –164.34 (app. t, $^3J_{F\text{-}F}$ 20 Hz, F_{meta}). Anal. Calcd. For $C_{79}H_{77}BF_{15}N_2OTh$: C, 59.37; H, 4.86; N, 1.75. Found: C, 59.33; H, 5.01; N, 1.57 %.

$[(XA_2)Th(CH_2SiMe_3)(\eta^6\text{-}C_6H_6)][B(C_6F_5)_4]$, (22):

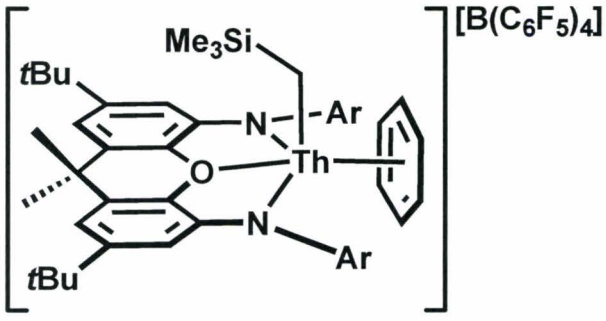

Method A: A solution of $[Ph_3C][B(C_6F_5)_4]$ (150 mg, 0.162 mmol) in benzene (10 mL) was added dropwise to a solution of $[(XA_2)Th(CH_2SiMe_3)_2]$ (**9**) (175 mg, 0.162 mmol) in benzene (10 mL) at room temperature. The mixture was stirred for 15 minutes, and then allowed to settle. The orange mother liquors were then decanted to leave an orange-brown oil, which was washed with hexanes (10 mL), layered with hexanes (10 mL), and then stored at 20 °C for several days to yield X-ray quality crystals of **22**·C_6H_6 growing within and at the surface of the oil. Note: Crystals of **22** were always coated with oil, which prevented elemental analysis. **Method B:** A solution of $[Ph_3C][B(C_6F_5)_4]$ (17 mg, 0.019 mmol) in C_6D_6 (3 mL) was added dropwise to a solution of $[(XA_2)Th(CH_2SiMe_3)_2]$ (**9**) (10 mg, 0.009 mmol) in C_6D_6 (3 mL) at room temperature. The solution was stirred for 16 hours prior to investigation by ^{1}H, ^{13}C and 2D NMR spectroscopy. **^{1}H NMR (C_6D_6, 600 MHz, 20 °C):** δ 7.42 (t, 2H, $^3J_{H\text{-}H}$ 7.5 Hz, Ar-CH_{para}), 7.27, 7.25 (app. t, 2 x 2H, $^3J_{H\text{-}H}$ 6.9

Hz, Ar-C*H*$_{meta}$), 6.82 (d, 2H $^4J_{H\text{-}H}$ 1.9 Hz, C*H*^{1}), 5.82 (d, 2H, $^4J_{H\text{-}H}$ 1.9 Hz, C*H*^{3}), 3.25, 2.50 (septet, 2 x 2H, $^3J_{H\text{-}H}$ 6.9 Hz, C*H*Me$_2$), 1.61, 1.46 (s, 2 x 3H, C*Me*$_2$) 1.28, 1.13, 1.03, 0.86 (d, 4 x 6H, $^3J_{H\text{-}H}$ 7.1 Hz, CH*Me*$_2$), 1.07 (s, 18H, C*Me*$_3$), 0.25 (s, 2H, ThC*H*$_2$), –0.13 (s, 9H, Si*Me*$_3$). **^{13}C{^{1}H} NMR (C$_6$D$_6$, 150 MHz, 20 °C):** δ 149.6, 147.5 (Ar-*C*$_{ortho}$), 145.0, 142.4, 129.6 (Xanth-*Q*), 133.1 (Ar-*C*$_{ipso}$), 131.2 (Ar-C$_{para}$), 126.6, 126.1 (2 x Ar-*C*$_{meta}$), 113.2 (*C*H^1), 110.6 (*C*H^3), 85.5 (Th-*C*H$_2$), 35.2, 27.2 (C*Me*$_2$), 35.0 (*C*Me$_3$), 33.9 (*C*Me$_2$), 31.3 (C*Me*$_3$), 27.6 , 25.5 (*C*HMe$_2$), 27.9, 25.6, 25.1, 23.7 (CH*Me*$_2$), 2.9 (SiMe$_3$).

[(XA$_2$)Th(CH$_2$SiMe$_3$)(η^6-toluene)][B(C$_6$F$_5$)$_4$] (23).

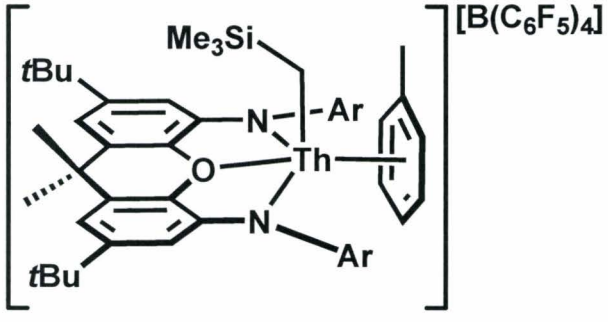

A solution of [Ph$_3$C][B(C$_6$F$_5$)$_4$] (17 mg, 0.019 mmol) in toluene (3 mL) was added dropwise to a solution of [(XA$_2$)Th(CH$_2$SiMe$_3$)$_2$] (**9**) (10 mg, 0.009 mmol) in toluene (3 mL) at room temperature. The solution was stirred for 3 hours and then evaporated to dryness in vacuo. The resulting oil was dissolved in d_5-bromobenzene. **^{1}H NMR (C$_6$D$_5$Br, 600 MHz, 20 °C):** δ 7.46 (t, 2H, $^3J_{H\text{-}H}$ 7.6 Hz, Ar-*C*$_{para}$), 7.38, 7.30 (broad d, 2 x 2H, Ar-*C*$_{meta}$), 6.92 (s, 2H, C*H*^{1}), 6.92 (m, 1H, *Ph*Me$_{para}$), 6.67 (d, 2H, $^3J_{H\text{-}H}$ 6.8 Hz, *Ph*Me$_{ortho}$), 5.91 (app t, 2H, $^3J_{H\text{-}H}$ 6.8 Hz, *Ph*Me$_{meta}$), 5.76 (s, 2H, C*H*^{3}), 3.24, 2.60 (septet, 2 x 2H, $^3J_{H\text{-}H}$ 6.9 Hz, C*H*Me$_2$), 2.02 (s, 3H, Ph*Me*), 1.70, 1.67 (s, 2 x 3H, C*Me*$_2$), 1.32,

1.18, 1.10, 0.86 (d, 4 x 6H, $^{3}J_{H\text{-}H}$ 6.9 Hz, CH*Me*$_2$), 1.11 (s, 18H, C*Me*$_3$), 0.06 (s, 2H, ThC*H*$_2$), –0.16 (s, 9H, Si*Me*$_3$). **^{13}C{^{1}H} NMR (C_6D_5Br, 150 MHz, 20 °C):** δ 149.5, 142.1, 129.3 (Xanth-*Q*), 149.1, 147.5 (Ar-*C*$_{ortho}$), 135.0 (*Ph*Me$_{ortho}$), 134.5 (*Ph*Me$_{meta}$), 132.9 (Ar-*C*$_{ipso}$), 130.7 (Ar-*C*$_{para}$), 127.7 (*Ph*Me$_{para}$), 126.2, 125.5 (2 x Ar-*C*$_{meta}$), 125.4 (*Ph*Me$_{ipso}$), 113.2 (*C*H^{1}), 110.2 (*C*H^{3}), 90.5 (Th-*CH*$_2$, $^{1}J_{C,H}$ 104 Hz), 35.2, 27.5 (C*Me*$_2$), 34.8 (*C*Me$_3$), 34.5 (*C*Me$_2$), 31.2 (C*Me*$_3$), 29.8, 27.4 (*C*HMe$_2$), 27.1, 25.4, 25.3, 23.5 (CH*Me*$_2$), 21.4 (Ph*Me*) 2.7 (SiMe$_3$).

[(XA$_2$)Th(CH$_2$Ph)(η^6-toluene)][B(C$_6$F$_5$)$_4$], (24).

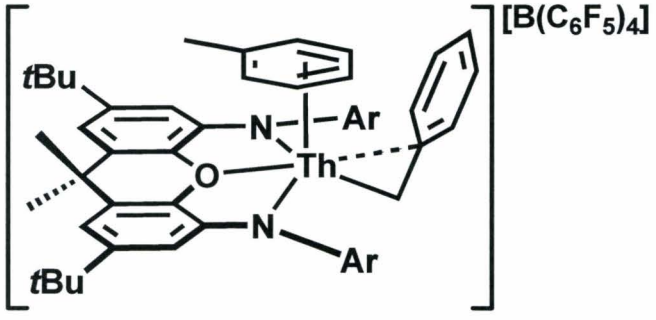

A solution of [Ph$_3$C][B(C$_6$F$_5$)$_4$] (150 mg, 0.162 mmol) in toluene (10 mL) was added dropwise to a solution of [(XA$_2$)Th(CH$_2$Ph)$_2$] (**12**) (175 mg, 0.162 mmol) in toluene (10 mL) at room temperature. The mixture was stirred for 15 minutes, and then allowed to settle. The light orange mother liquors were decanted to leave an orange-brown oil, which was washed with hexanes (10 mL), layered with hexanes (10 mL) and stored at 20 °C for several days to yield X-ray quality crystals of **24**·2C$_7$H$_8$ growing within and at the surface of the oil. Extremely air-sensitive **24** was always obtained as an oil, or as crystals coated with oil, and was insoluble in solvents with which it did not

react. This precluded elemental analysis or solution NMR spectroscopy, and as a result, direct characterization of **24** was limited to single crystal X-ray crystallography.

[(BDPP)Th(η^2-CH_2Ph)(μ-η^1:η^6-CH_2Ph)Th(η^1-CH_2Ph)(BDPP)][$B(C_6F_5)_4$] (25)

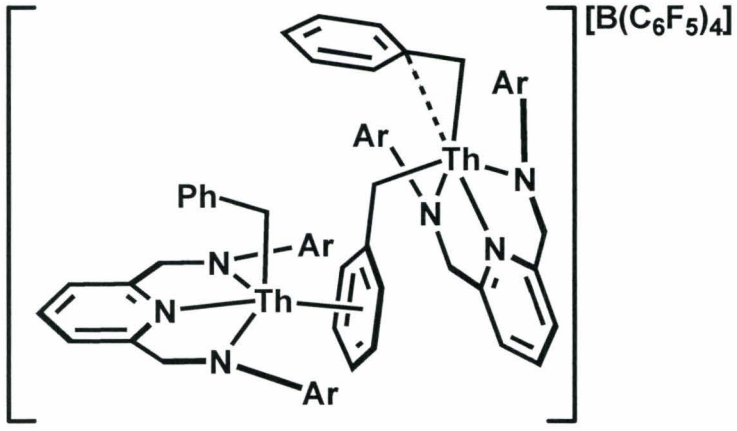

A solution of [Ph_3C][$B(C_6F_5)_4$] (150 mg, 0.162 mmol) in benzene (10 mL) was added dropwise to a solution of [(BDPP)Th(CH_2Ph)$_2$] (**13**) (141 mg, 0.162 mmol) in benzene (10 mL) at room temperature. The mixture was stirred for 15 minutes, and then allowed to settle. The light orange mother liquors were then decanted to leave an orange-brown oil, which was washed with hexane (10 mL) and then layered with hexanes (10 mL) and stored at 20 °C for several days to yield several X-ray quality crystals of **25**·0.75hexane·0.55benzene growing within and at the surface of the oil. These crystals were obtained in low yield (the formation of **25** was presumably due to a slight deficiency in the mount of [Ph_3C][$B(C_6F_5)_4$] added), and were coated with oil, which precluded elemental analysis. In addition, all products formed in the reactions of **13** with [Ph_3C][$B(C_6F_5)_4$] are insoluble in solvents with which they do not react, which prevented

observation of **25** by solution NMR spectroscopy. As a result, direct characterization of **25** was limited to single crystal X-ray crystallography.

$[(XA_2)Th][B(C_6F_5)_3(CH_2Ph)]_2$ (27):

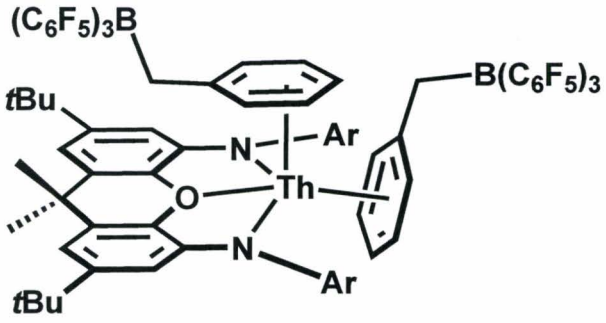

A –30 °C solution of $[(XA_2)Th(CH_2Ph)][PhCH_2B(C_6F_5)_3]$ (**21**) (0.035 g, 0.022 mmol) in toluene (2 mL) was layered with a solution of $B(C_6F_5)_3$ (0.012 g, 0.022 mmol) in hexanes (1 mL) and allowed to slowly diffuse overnight at –30 °C. The mother liquors were carefully decanted away from the resulting orange crystals, which were then washed with toluene (3 x 2 mL) and hexanes (3 x 2 mL). Removal of residual solvent *in vacuo* afforded **27** as an orange solid (0.029 g, 0.013 mmol) in 63 % yield. X-ray quality crystals were obtained using the method outlined above. Solution ^{1}H, ^{13}C, ^{11}B and ^{19}F NMR spectra were not obtained due to reaction of **27** with THF, 1,2-dimethoxyethane or bromobenzene, and the insolubility of **27** in less reactive solvents such as benzene, toluene and α,α,α-trifluorotoluene. Anal. Calcd. For $C_{97}H_{76}B_2F_{30}N_2OTh$: C, 55.23; H, 3.63; N, 1.33. Found: C, 55.70; H, 3.77; N, 1.53 %.

6.5 – Experimental Procedures Pertaining to Chapter 5

6.5.1 – Synthesis Procedures and Characterization

[(XA$_2$)Th(NHPh)$_2$]•O(SiMe$_3$)$_2$ {28•O(SiMe$_3$)$_2$}:

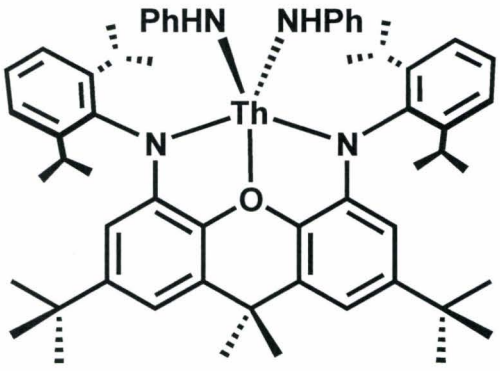

Aniline (0.051 mL, 0.557 mmol) was added dropwise to a solution of [(XA$_2$)Th(CH$_2$SiMe$_3$)$_2$] (**10**) (0.300 g, 0.278 mmol) in toluene (30 mL) at room temperature. After 30 minutes, the solvent was removed *in vacuo* and O(SiMe$_3$)$_2$ (30 mL) was added. The solution was then sonicated, filtered and evaporated to dryness *in vacuo* to yield **28•O(SiMe$_3$)$_2$** as an off-white solid (0.236 g, 0.217 mmol) in 78 % yield. **^{1}H NMR (C$_6$D$_6$, 600 MHz):** δ 7.29 (t, 2H, $^3J_{H\text{-}H}$ 6.2 Hz, Ar-C*H*$_{para}$), 7.26 (d, 4H, $^3J_{H\text{-}H}$ 6.2 Hz, Ar-C*H*$_{meta}$), 6.97 (t, 4H, $^3J_{H\text{-}H}$ 7.6 Hz, NH*Ph*$_{meta}$), 6.87 (d, 2H, $^4J_{H\text{-}H}$ 2 Hz, C*H*^{1}), 6.58 (t, 2H, $^3J_{H\text{-}H}$ 7.7 Hz, NH*Ph*$_{para}$), 6.23 (d, 4H, $^3J_{H\text{-}H}$ 7.6 Hz, NH*Ph*$_{ortho}$), 6.14 (s, 2H, $^4J_{H\text{-}H}$ 2.1 Hz, C*H*^{3}), 5.21 (s, 2H, N*H*Ph), 3.43 (sept, 4H, $^3J_{H\text{-}H}$ 7 Hz, C*H*Me$_2$), 1.68 (s, 6H, C*Me*$_2$), 1.23 (s, 18H, C*Me*$_3$), 1.17 (d, 12H, $^3J_{H\text{-}H}$ 6.9 Hz, CH*Me*$_2$), 1.07 (d, 12H, $^3J_{H\text{-}H}$ 6.8 Hz, CH*Me*$_2$). **^{13}C{^{1}H} NMR (C$_6$D$_6$, 151 MHz):** δ 153.1 (NH*Ph*$_{ipso}$), 149.1, 148.9 (Xanth-*Q*), 134.5 (Ar-*C*$_{ipso}$), 129.4 (NH*Ph*$_{meta}$), 128.6 (Ar-*C*$_{para}$), 125.7 (Ar-*C*$_{meta}$), 117.9

(NH*Ph*$_{para}$), 116.4 (NH*Ph*$_{ortho}$), 109.6 (*C*^{1}, *C*^{3}), 35.3 (*C*Me$_2$), 35.0 (*C*Me$_3$), 31.7 (C*Me*$_3$), 31.1 (C*Me*$_2$), 29.2 (*C*HMe$_2$), 26.1 (CH*Me*$_2$), 24.7 (CH*Me*$_2$). Anal. Calcd. for $C_{65}H_{92}N_4O_2Si_2Th$ {**28•O(SiMe$_3$)$_2$**}: C, 62.47; H, 7.42; N, 4.48. Found: C, 62.67; H, 7.38; N, 4.37 %.

References

(1) Clark, D. L.; Hobart, D. E.; Neu, M. P. *Chem. Rev.* **1995,** *95*, 25.

(2) Caley, E. R. *Isis* **1948,** *38*, 190.

(3) Hammond, C. R., The Elements in *CRC Handbook of Chemistry and Physics*. 90th ed. Lide, D. R. Ed.; 2009; p. 4-1

(4) Hahn, O.; Strassmann, F. *Naturwissenschaften* **1939,** *27*, 11.

(5) Seaborg, G. T.; Goffman, J. W.; Stoughton, R. W. *Phys. Rev.* **1947,** *71*, 378.

(6) Slater, J. C. *J. Chem. Phys.* **1964,** *41*, 3199.

(7) Shannon, R. D. *Acta Crystallogr., Sect. A* **1976,** *32*, 751.

(8) (a) Pepper, M.; Bursten, B. E. *Chem. Rev.* **1991,** *91*, 719. (b) Korobkov, I.; Gambarotta, S.; Yap, G. P. A.; Thompson, L.; Hay, P. J. *Organometallics* **2001,** *20*, 5440.

(9) Marks, T. J. *Science* **1982,** *217*, 989.

(10) Lam, O. P.; Anthon, C.; Meyer, K. *Dalton Trans.* **2009**, 9677.

(11) Ciliberto, E.; Condorelli, G.; Fagan, P. J.; Manriquez, J. M.; Fragala, I.; Marks, T. J. *J. Am. Chem. Soc.* **1981,** *103*, 4755.

(12) (a) Clark, J. P.; Green, J. C. *J. Chem. Soc. Dalton Trans.* **1977**, 505. (b) Rosch, N.; Streitwieser, A. *J. Organomet. Chem.* **1978,** *145*, 195.

(13) Chang, A. H. H.; Pitzer, R. M. *J. Am. Chem. Soc.* **1989,** *111*, 2500.

(14) Gaunt, A. J.; Reilly, S. D.; Enriquez, A. E.; Scott, B. L.; Ibers, J. A.; Sekar, P.; Ingram, K. I. M.; Kaltsoyannis, N.; Neu, M. P. *Inorg. Chem.* **2008,** *47*, 29.

(15) Roger, M.; Belkhiri, L.; Arliguie, T.; Thuery, P.; Boucekkine, A.; Ephritikhine, M. *Organometallics* **2008,** *27*, 33.

(16) (a) Iwasaki, M. *J. Nucl. Mater.* **1968,** *22*, 216. (b) Iwasaki, M. *J. Inorg. Nucl. Chem.* **1964,** *26*, 1853. (c) Labaton, V. Y. *J. Inorg. Nucl. Chem.* **1958,** *10*, 86. (d) McNamara, B. K.; Scheele, R.; Kozelisky, A.; Edwards, M. *J. Nucl. Mater.* **2009,** *394*, 166.

(17) Ephritikhine, M. *Chem. Rev.* **1997,** *97*, 2193.

(18) Maldivi, P.; Petit, L.; Adamo, C.; Vetere, V. *C. R. Chim.* **2007,** *10*, 888.

(19) Jensen, M. P.; Bond, A. H. *J. Am. Chem. Soc.* **2002,** *124*, 9870.

(20) Nash, K. L.; Madic, C.; Mathur, J. N.; Lacquement, J., Actinide Separation Science and Technology. In *The Chemistry of the Transactinide Elements*, 3rd ed.; Morss, L. R.; Fuger, J., Eds. Springer: Dordrecht, 2006; Vol. 4, 2622.

(21) Burns, C. J.; Bursten, B. E. *Comments Inorg. Chem.* **1989,** *9*, 61.

(22) (a) Pauling, L. *J. Am. Chem. Soc.* **1932,** *54*, 3570, (b) Silberberg, M., Between the Extremes: Electronegativity and Bond Polarity. In *Chemistry; The Molecular Nature of Matter and Change*, 3rd ed.; McGraw-Hill: New York, USA., 2003; 344.

(23) Cotton, S., Organometallic Chemistry of the Actinides. In *Lanthanide and Actinide Chemistry*, 1st ed.; Woollins, D.; Crabtree, R. H.; Atwood, D.; Meyer, G., Eds. John Wiley & Sons Ltd.: West Sussex, England, 2006; Vol. 1, 209.

(24) Kanellakopulos, B.; Dornberger, E.; Baumgartner, T. *Inorg. Nucl. Chem. Lett.* **1974,** *10*, 155.

(25) Kalina, D. G.; Marks, T. J.; Wachter, W. A. *J. Am. Chem. Soc.* **1977,** *99*, 3877.

(26) Bruno, J. W.; Kalina, D. G.; Mintz, E. A.; Marks, T. J. *J. Am. Chem. Soc.* **1982,** *104*, 1860.

(27) Blake, P. C.; Lappert, M. F.; Atwood, J. L.; Zhang, H. M. *J. Chem. Soc. Chem. Commun.* **1986**, 1148.

(28) Parry, J. S.; Cloke, F. G. N.; Goles, S. J.; Hursthouse, M. B. *J. Am. Chem. Soc.* **1999,** *121*, 6867.

(29) Bursten, B. E.; Strittmatter, R. J. *J. Am. Chem. Soc.* **1991,** *113*, 552.

(30) Kot, W. K.; Shalimoff, G. V.; Edelstein, N.; Edelman, M. A.; Lappert, M. F. *J. Am. Chem. Soc.* **1988,** *110*, 986.

(31) Korobkov, I.; Gambarotta, S.; Yap, G. P. A. *Angew. Chem. Int. Ed.* **2003,** *42*, 814.

(32) (a) Scherer, O. J.; Werner, B.; Heckmann, G.; Wolmershauser, G. *Angew. Chem. Int. Ed.* **1991**, 553. (b) Scherer, O. J.; Schultze, J.; Wolmershauser, G. *J. Organomet. Chem.* **1994,** *484*, C5.

(33) Gilman, H. *Adv. Organomet. Chem.* **1968,** *7*, 33.

(34) (a) Marks, T. J. *Prog. Inorg. Chem.* **1979,** *25*, 224. (b) Marks, T. J.; Ernst, R. D., Chapter 21. In *Comprehensive Organometallic Chemistry*, 1st ed.; Wilkinson, G.; Stone, F. G. A.; Abel, E. W., Eds. Pergamon Press: Oxford, England, 1982; Chapter 21. (b) Gilman, H.; Jones, R. G.; Bindschadler, E.; Blume, D.; Karmas, G.; Martin, G. A.; Nobis, J. F.; Thirtle, J. R.; Yale, H. L.; Yoeman, F. A. *J. Am. Chem. Soc.* **1956,** *78*, 2790.

(35) Sigurdson, E. R.; Wilkinson, G. *J. Chem. Soc. Dalton Trans.* **1977**, 812.

(36) Lauke, H.; Swepston, P. J.; Marks, T. J. *J. Am. Chem. Soc.* **1984,** *106*, 6841.

(37) Bucaille, A.; Le Borgne, T.; Ephritikhine, M.; Daran, J. C. *Organometallics* **2000,** *19*, 4912.

(38) Fortier, S.; Melot, B. C.; Wu, G.; Hayton, T. W. *Journal of the American Chemical Society* **2009,** *131*, 15512.

(39) Köhler, E.; Brüser, W.; Thiele, K.-H. *J. Organomet. Chem.* **1974,** *76*, 235.

(40) Eisen, M. S.; Marks, T. J. *J. Am. Chem. Soc.* **1992,** *114*, 10358.

(41) Edwards, P. G.; Andersen, R. A.; Zalkin, A. *J. Am. Chem. Soc.* **1981,** *103*, 7792.

(42) Edwards, P. G.; Andersen, R. A.; Zalkin, A. *Organometallics* **1984,** *3*, 293.

(43) Thiele, K. H.; Opitz, R.; Kohler, E. *Z. Anorg. Allg. Chem.* **1977,** *435*, 45.

(44) Wilke, G.; Bogdanovic, B.; Hardt, P.; Keim, W.; Kroner, M.; Oberkirch, W.; Tanaka, K.; Walter, D. *Angew. Chem. Int. Ed.* **1966**, 151.

(45) Carlson, C. N.; Hanusa, T. P.; Brennessel, W. W. *J. Am. Chem. Soc.* **2004,** *126*, 10550.

(46) Vanderhooft, J. C.; Ernst, R. D. *J. Organomet. Chem.* **1982,** *233*, 313.

(47) Brunelli, M.; Perego, G.; Lugli, G.; Mazzei, A. *J. Chem. Soc. Dalton Trans.* **1979**, 861.

(48) Brunelli, M.; Lugli, G. *J. Magn. Reson.* **1973,** *9*, 247.

(49) Marks, T. J.; Day, V. W., Actinide Hydrocarbyl and Hydride Chemistry. In *Fundamental and Technological Aspects of Organo-f-Element Chemistry; Nato Science Series C.*, 1st ed.; Marks, T. J.; Fragala, I., Eds. Reidel Publishing Company: Dordrecht, 1985; Vol. 155, 115.

(50) (a) Takats, J., Organoactinide Complexes Containing Classical Ligands. In *Fundamental and Technological Aspects of Organo-f-Element Chemistry; Nato Science Series C*, 1st ed.; Marks, T. J.; Fragala, I., Eds. Reidel Publishing Company: Dordrecht, 1985; Vol 155, 159. (b) Evans, W. J. *J. Organomet. Chem.* **2002,** *647*, 2. (c) Golden, J. T.; Kazul'kin, D. N.; Scott, B. L.; Voskoboynikov, A. Z.; Burns, C. J. *Organometallics* **2003,** *22*, 3971. (d) Baudry, D.; Bulot, E.; Ephritikhine, M. *J. Chem. Soc. Chem. Commun.* **1989**, 1316.

(51) Jia, L.; Yang, X. M.; Stern, C. L.; Marks, T. J. *Organometallics* **1997,** *16*, 842.

(52) Stubbert, B. D.; Stern, C. L.; Marks, T. J. *Organometallics* **2003,** *22*, 4836.

(53) Fendrick, C. M.; Schertz, L. D.; Day, V. W.; Marks, T. J. *Organometallics* **1988,** *7*, 1828.

(54) Cendrowski-Guillaume, S. M.; Nierlich, M.; Ephritikhine, M. *J. Organomet. Chem.* **2002,** *643*, 209.

(55) Seyferth, D. *Organometallics* **2004,** *23*, 3562.

(56) Xie, Z. *Coord. Chem. Rev.* **2002,** *231*, 23.

(57) Baudry, D.; Bulot, E.; Charpin, P.; Ephritikhine, M.; Lance, M.; Nierlich, M.; Vigner, J. *J. Organomet. Chem.* **1989,** *371*, 155.

(58) (a) Arliguie, T.; Lance, M.; Nierlich, M.; Vigner, J.; Ephritikhine, M. *J. Chem. Soc. Chem. Commun.* **1995**, 183. (b) Arliguie, T.; Lance, M.; Nierlich, M.; Ephritikhine, M. *J. Chem. Soc. Dalton Trans.* **1997**, 2501.

(59) Wilkinson, G.; Birmingham, J. M. *J. Am. Chem. Soc.* **1954,** *76*, 6210.

(60) Reynolds, L. T.; Wilkinson, G. *J. Inorg. Nucl. Chem.* **1956,** *2*, 246.

(61) Marks, T. J.; Seyam, A. M. *Inorg. Synth.* **1976,** *26*, 147.

(62) Anderson, M. L.; Crisler, L. R. *J. Organomet. Chem.* **1969,** *17*, 345.

(63) (a) Goffart, J.; Gilbert, B.; Duyckaerts, G. *Inorg. Nucl. Chem. Lett.* **1977,** *13*, 186. (b) Arduini, A. L.; Edelstein, N. M.; Jamerson, J. D.; Reynolds, J. G.; Schmid, K.; Takats, J. *Inorg. Chem.* **1981,** *20*, 2470. (c) Paolucci, G.; Rossetto, R.; Zanella, R.; Fischer, R. D. *J. Organomet. Chem.* **1985,** *284*, 213. (d) DeRidder, D. J. A.; Apostolidis, C.; Rebizant, J.; Kanellakopulos, B.; Maier, R. *Acta Crystallogr. Sect C.* **1996,** *52*, 1436. (e) Brandi, G.; Brunelli, M.; Lugli, G.; Mazzei, A. *Inorg. Chim. Acta* **1973,** *7*, 319. (f) Calderazzo, F. *Pure Appl. Chem.* **1973,** *33*, 453. (g) Gabala, A. E.; Tsutsui, M. *J. Am. Chem. Soc.* **1973,** *95*, 91.

(64) Leverd, P. C.; Ephritikhine, M.; Lance, M.; Vigner, J.; Nierlich, M. *J. Organomet. Chem.* **1996,** *507*, 229.

(65) Marks, T. J.; Seyam, A. M.; Kolb, J. R. *J. Am. Chem. Soc.* **1973,** *95*, 5529.

(66) Tsutsui, M.; Ely, N.; Gebala, A. *Inorg. Chem.* **1975,** *14*, 78.

(67) Halstead, G. W.; Baker, E. C.; Raymond, K. N. *J. Am. Chem. Soc.* **1975,** *97*, 3049.

(68) Burns, C. J.; Eisen, M. S., Organoactinide Chemistry: Synthesis and Characterization. In *The Chemistry of the Actinide and Transactinide Elements*, 3rd ed.; Morss, L. R.; Edelstein, N. M.; Fuger, J.; Katz, J. J., Eds. Springer Publishing: Dordrecht, 2006; Vol. 5, 2799.

(69) Blake, P. C.; Edelman, M. A.; Hitchcock, P. B.; Hu, J.; Lappert, M. F.; Tian, S.; Muller, G.; Atwood, J. L.; Zhang, H. M. *J. Organomet. Chem.* **1998,** *551*, 261.

(70) Wong, C. H.; Yesn, T. M.; Lee, T. Y. *Acta Crystallogr.* **1965,** *18*, 340.

(71) Spirlet, M. R.; Rebizant, J.; Apostolidis, C.; Andreti, G. D.; Kanellakopulos, B. *Acta Crystallogr. Sect. C.* **1989,** *112*, 116.

(72) Rebizant, J.; Spirlet, M. R.; Apostolidis, C.; Vandenbossche, G.; Kanellakopulos, B. *Acta Crystallogr. Sect C.* **1991,** *47*, 864.

(73) Leong, J.; Hodgson, K. O.; Raymond, K. N. *Inorg. Chem.* **1973,** *12*, 1329.

(74) Fischer, E. O.; Treiber, A. *Naturforsch* **1962,** *17b*, 276.

(75) Fischer, E. O.; Hristidue, Y. *Naturforsch* **1962,** *17b*, 275.

(76) Baumgärtner, F.; Fischer, E. O.; Kanellakopulos, B.; Laubereau, P. *Angew. Chem. Int. Ed.* **1969**, 202.

(77) Baumgärtner, F.; Fischer, E. O.; Kanellakopulos, B.; Laubereau, P. *Angew. Chem. Int. Ed.* **1968**, 634.

(78) (a) Burns, J. H.; Laubereau, P. *Inorg. Chem.* **1971,** *10*, 2789. (b) Laubereau, P.; Ganguly, L.; Burns, J. H.; Benjamin, B. M.; Atwood, J. L.; Selbin, J. *Inorg. Chem.* **1971,** *10*, 2274.

(79) Doretti, L.; Zanella, P.; Faraglia, G.; Faleschini, S. *J. Organomet. Chem.* **1972,** *43*, 339.

(80) (a) Bagnall, K. W.; Edwards, J. *J. Organomet. Chem.* **1974,** *80*, C14. (b) Bagnall, K. W.; Edwards, J.; Tempest, A. C. *J. Chem. Soc. Dalton Trans.* **1978**, 295. (c) Bombieri, G.; Depaoli, G.; Delpra, A.; Bagnall, K. W. *Inorg. Nucl. Chem. Lett.* **1978,** *14*, 359. (d) Lemarechal, J. F.; Villiers, C.; Charpin, P.; Lance, M.; Nierlich, M.; Vigner, J.; Ephritikhine, M. *J. Chem. Soc. Chem. Commun.* **1989**, 308.

(81) Ernst, R. D.; Kennelly, W. J.; Day, C. S.; Day, V. W.; Marks, T. J. *J. Am. Chem. Soc.* **1979,** *101*, 2656.

(82) (a) Goffart, J.; Meunier-Piret, J.; Duyckaerts, G. *Inorg. Nucl. Chem. Lett.* **1980,** *16*, 233. (b) Meunier-Piret, J.; Declercq, J. P.; German, G.; van Meersche, M. *Bull. Soc. Chim. Belg.* **1980,** *89*, 212.

(83) Edelman, M. A.; Lappert, M. F. *Inorg. Chim. Acta* **1987,** *139*, 185.

(84) Edelman, M. A.; Hitchcock, P. B.; Hu, J.; Lappert, M. F. *New J. Chem.* **1995,** *19*, 481.

(85) Mintz, E. A.; Moloy, K. G.; Marks, T. J.; Day, V. W. *J. Am. Chem. Soc.* **1982,** *104*, 4962.

(86) Butcher, R. J.; Clark, D. L.; Grumbine, S. K.; Scott, B. L.; Watkin, J. G. *Organometallics* **1996,** *15*, 1488.

(87) Cymbaluk, T. H.; Ernst, R. E.; Day, V. W. *Organometallics* **1983,** *2*, 963.

(88) Kanellakopulos, B.; Aderhold, C.; Dornberger, E. *J. Organomet. Chem.* **1974,** *66*, 447.

(89) Zalkin, A.; Brennan, J. G.; Andersen, R. A. *Acta Crystallogr. Sect. C.* **1987,** *43*, 418.

(90) Manriquez, J. M.; Fagan, P. J.; Marks, T. J. *J. Am. Chem. Soc.* **1978,** *100*, 3939.

(91) Fagan, P. J.; Manriquez, J. M.; Vollmer, S. H.; Day, C. S.; Day, V. W.; Marks, T. J. *J. Am. Chem. Soc.* **1981,** *103*, 2206.

(92) (a) Spirlet, M. R.; Rebizant, J.; Apostolidis, C.; Kanellakopulos, B. *Acta Crystallogr. Sect. C* **1992,** *48*, 2135. (b) Rabinovich, D.; Schimek, G. L.;

Pennington, W. T.; Nielsen, J. B.; Abney, K. D. *Acta Crystallogr. Sect. C.* **1997,** *53*, 1794. (c) Rabinovich, D.; Bott, S. G.; Nielsen, J. B.; Abney, K. D. *Inorg. Chim. Acta* **1998,** *274*, 232.

(93) (a) Blake, P. C.; Lappert, M. F.; Taylor, R. G.; Atwood, J. L.; Hunter, W. E.; Zhang, H. M. *J. Chem. Soc. Dalton Trans.* **1995**, 3335. (b) Lukens, W. W. J.; Beshouri, S. M.; Stuart, A. L.; Andersen, R. A. *Organometallics* **1999,** *18*, 1235.

(94) Dash, A. K.; Gourevich, I.; Wang, J. Q.; Wang, J. X.; Kapon, M.; Eisen, M. S. *Organometallics* **2001,** *20*, 5084.

(95) (a) Erker, G.; Muhlenbernd, T.; Benn, R.; Rufinska, A. *Organometallics* **1986,** *5*, 402. (b) Smith, G. M.; Suzuki, H.; Sonnenberger, D. C.; Day, V. W.; Marks, T. J. *Organometallics* **1986,** *5*, 549.

(96) Marks, T. J.; Wachter, W. A. *J. Am. Chem. Soc.* **1976,** *98*, 703.

(97) Clark, D. L.; Grumbine, S. K.; Scott, B. L.; Watkin, J. G. *Organometallics* **1996,** *15*, 949.

(98) Butcher, R. J.; Clark, D. L.; Grumbine, S. K.; Scott, B. L.; Watkin, J. G. *Organometallics* **1996,** *19*, 2560.

(99) Bruno, J. W.; Smith, G. M.; Marks, T. J.; Fair, C. K.; Schultz, A. J.; Williams, J. M. *J. Am. Chem. Soc.* **1986,** *108*, 40.

(100) Porter, R. M.; Danopoulos, A. A. *Polyhedron* **2006,** *25*, 859.

(101) Manriquez, J. M.; Fagan, P. J.; Marks, T. J. *J. Am. Chem. Soc.* **1981,** *103*, 6650.

(102) Bruno, J. W.; Marks, T. J.; Morss, L. R. *J. Am. Chem. Soc.* **1983,** *105*, 6824.

(103) (a) Halpern, J. *Acc. Chem. Res.* **1982,** *15*, 238. (b) Connor, J. A.; Zafarani-Moattar, M. T.; Bickerton, J.; Saied, N. I.; Suradi, S.; Carson, R.; Takhin, G. A.; Skinner, H. A. *Organometallics* **1982,** *1*, 1166.

(104) Dias, A. R.; Salema, M. S.; Simoes, J. A. M. *Organometallics* **1982,** *1*, 971.

(105) Broach, R. W.; Schultz, A. J.; Williams, J. M.; Brown, G. M.; Manriquez, J. M.; Fagan, P. J.; Marks, T. J. *Science* **1979,** *203*, 172.

(106) Turner, H. W.; Simpson, S. J.; Andersen, R. A. *J. Am. Chem. Soc.* **1979,** *101*, 2782.

(107) Clark, D. L.; Grumbine, S. K.; Scott, B. L.; Watkin, J. G. *J. Am. Chem. Soc.* **1995,** *117*, 9089.

(108) Gilbert, T. M.; Ryan, R. R.; Sattelberger, A. P. *Organometallics* **1989,** *8*, 857.

(109) Fagan, P. J.; Manriquez, J. M.; Maatta, E. A.; Seyam, A. M.; Marks, T. J. *J. Am. Chem. Soc.* **1981,** *103*, 6650.

(110) Moloy, K. G.; Marks, T. J. *J. Am. Chem. Soc.* **1984,** *106*, 7051.

(111) Lin, Z. R.; Marks, T. J. *J. Am. Chem. Soc.* **1987,** *109*, 7979.

(112) Lin, Z.; Marks, T. J. *J. Am. Chem. Soc.* **1990,** *112*, 5515.

(113) Bruno, J. W.; Stecher, H. A.; Morss, L. R.; Sonnenberger, D. C.; Marks, T. J. *J. Am. Chem. Soc.* **1986,** *108*, 7275.

(114) Yang, X. M.; King, W. A.; Sabat, M.; Marks, T. J. *Organometallics* **1993,** *12*, 4254.

(115) Berthet, J. C.; Lemarechal, J. F.; Ephritikhine, M. *J. Chem. Soc. Chem. Commun.* **1991**, 360.

(116) Jemine, X.; Goffart, J.; Ephritikhine, M.; Fuger, J. *J. Organomet. Chem.* **1993,** *448*, 95.

(117) Baudry, D.; Dormond, A.; Hafid, A. *New J. Chem.* **1993,** *17*, 465.

(118) Gradoz, P.; Boisson, C.; Baudry, D.; Lance, M.; Nierlich, M.; Vigner, J.; Ephritikhine, M. *J. Chem. Soc. Chem. Commun.* **1992**, 1720.

(119) (a) Lemarechal, J. F.; Villiers, C.; Charpin, P.; Lance, M.; Nierlich, M.; Vigner, J.; Ephritikhine, M. *J. Chem. Soc. Chem. Commun.* **1992**, 1720. (b) Berthet, J. C.; Villiers, C.; Lemarechal, J. F.; Delavaux-Nicot, B.; Lance, M.; Nierlich, M.; Vigner, J.; Ephritikhine, M. *J. Organomet. Chem.* **1992,** *440*, 53.

(120) Jia, L.; Yang, X. M.; Stern, C. L.; Marks, T. J. *Organometallics* **1997,** *16*, 842.

(121) (a) Chen, Y. X.; Stern, C. L.; Yang, S. T.; Marks, T. J. *J. Am. Chem. Soc.* **1996,** *118*, 12451, (b) Lin, Z.; Lemarechal, J. F.; Sabat, M.; Marks, T. J. *J. Am. Chem. Soc.* **1987,** *109*, 4127, (c) Chen, Y. X.; Metz, M. V.; Li, L. T.; Stern, C. L.; Marks, T. J. *J. Am. Chem. Soc.* **1998,** *120*, 6287, (d) Evans, W. J.; Nyce, G. W.; Ziller, J. W. *Organometallics* **2001,** *20*, 5489.

(122) Jia, L.; Yang, X. M.; Stern, C. E.; Marks, T. J. *Organometallics* **1994,** *13*, 3755.

(123) Yang, X. M.; Stern, C. L.; Marks, T. J. *Organometallics* **1991,** *10*, 840.

(124) (a) Marks, T. J.; Jia, L.; Yang, X. M. U.S. Patent 5,477,895, 1995. (b) Marks, T. J.; Chen, Y.-X. U.S. Patent 6,229,034 B1, 2001. (c) Marks, T. J.; Chen, Y.-X. U.S. Patent 6,403,732 B2, 2002.

(125) Campbell, R. E. J.; The Dow Chemical Co. U.S. Patent 4,665,046, 1987.

(126) (a) Marks, T. J. *Acc. Chem. Res.* **1992,** *25*, 57. (b) Finch, W. C.; Gillespie, R. D.; Hedden, D.; Marks, T. J. *J. Am. Chem. Soc.* **1990,** *112*, 6221. (c) Hedden, D.; Marks, T. J. *J. Am. Chem. Soc.* **1988,** *110*, 1647. (d) Toscano, P. J.; Marks, T. J. *J. Am. Chem. Soc.* **1985,** *107*, 653. (e) He, M. Y.; Xiong, G. X.; Toscano, P. J.; Burwell, R. L.; Marks, T. J. *J. Am. Chem. Soc.* **1985,** *107*, 641.

(127) Evans, W. J.; Kozimor, S. A.; Ziller, J. W. *Organometallics* **2005,** *24*, 3407.

(128) Monreal, M. J.; Diaconescu, P. L. *Organometallics* **2008,** *27*, 1702.

(129) Cendrowski-Guillaume, S. M.; Lance, M.; Nierlich, M.; Ephritikhine, M. *Organometallics* **2000,** *19*, 3257.

(130) Moisan, L.; Le Borgne, T.; Villiers, C.; Thuery, P.; Ephritikhine, M. *C. R. Chim.* **2007,** *10*, 883.

(131) Lin, Z.; Lemarechal, J. F.; Sabat, M.; Marks, T. J. *J. Am. Chem. Soc.* **1978,** *109*, 4127.

(132) Dash, A. K.; Wang, J. X.; Berthet, J. C.; Ephritikhine, M.; Eisen, M. S. *J. Organomet. Chem.* **2000,** *604*, 83.

(133) (a) Baudin, C.; Ephritikhine, M. *J. Organomet. Chem.* **1989,** *364*, C1. (b) Baudin, C.; Baudry, D.; Ephritikhine, M.; Lance, M.; Navaza, A.; Nierlich, M.; Vigner, J. *J. Organomet. Chem.* **1991,** *415*, 59. (c) Korobkov, I.; Arunachalampillai, A.; Gambarotta, S. *Organometallics* **2004,** *23*, 6248.

(134) Beshouri, S. M.; Fanwick, P. E.; Rothwell, I. P.; Huffman, C. J. *Organometallics* **1987,** *6*, 2498.

(135) Wedler, M.; Knowsel, F.; Edelmann, F. T.; Behrens, U. *Chem. Ber.* **1992,** *125*, 1313.

(136) Domingos, A.; Marques, N.; Dematos, A. P.; Santos, I.; Silva, M. *Organometallics* **1994,** *13*, 654.

(137) Jantunen, K. C.; Batchelor, R. J.; Leznoff, D. B. *Organometallics* **2004,** *23*, 2186.

(138) Jantunen, K. C.; Haftbaradaran, F.; Katz, M. J.; Batchelor, R. J.; Schatte, G.; Leznoff, D. B. *Dalton Trans.* **2005**, 3083.

(139) Piers, W. E.; Emslie, D. J. H. *Coord. Chem. Rev.* **2002,** *233*, 131.

(140) (a) McGeachin, S. G. *Can. J. Chem.* **1968,** *46*, 1903. (b) Kim, W.-K.; Fevola, M. J.; Liable-Sands, L.; Rheingold, A. L.; Theopold, K. H. *Organometallics* **1998,** *17*, 4541.

(141) Hitchcock, P. B.; Lappert, M. F.; Liu, D. S. *J. Organomet. Chem.* **1995,** *488*, 241.

(142) Wright, R. J.; Power, P. P.; Scott, B. L.; Kiplinger, J. L. *Organometallics* **2004,** *23*, 4801.

(143) Campello, M. P. C.; Calhorda, M. J.; Domingos, A.; Galvao, A. M.; Leal, J. P.; de Matos, A. P.; Santos, I. *J. Organomet. Chem.* **1997,** *538*, 223.

(144) Bourget-Merle, L.; Lappert, M. F.; Severn, J. R. *Chem. Rev.* **2002,** *102*, 3031.

(145) Guerin, F.; McConville, D. H. *Organometallics* **1995,** *14*, 3154.

(146) (a) Guerin, F.; McConville, D. H.; Vittal, J. J.; Yap, G. A. P. *Organometallics* **1998,** *17*, 5172. (b) Guerin, F.; McConville, D. H.; Vittal, J. J.; Yap, G. A. P. *Organometallics* **1998,** *17*, 1290. (c) Guerin, F.; McConville, D. H.; Payne, N. C.

Organometallics **1996,** *15*, 5085. (d) Estler, F.; Eickerling, G.; Herdtweck, E.; Anwander, R. *Organometallics* **2003,** *22*, 1212.

(147) Guerin, F.; McConville, D. H.; Vittal, J. J. *Organometallics* **1996,** *15*, 5586.

(148) Zimmermann, M.; Estler, F.; Herdtweck, E.; Tornroos, K. W.; Anwander, R. *Organometallics* **2007,** *26*, 6029.

(149) (a) Black, D. G.; Swenson, D. C.; Jordan, R. F.; Rogers, R. D. *Organometallics* **1995,** *14*, 3539. (b) Woodman, P. R.; Alcock, N. W.; Munslow, I. J.; Sanders, C. J.; Scott, P. *Dalton Trans.* **2000**, 3340. (c) Emslie, D. J. H.; Piers, W. E.; Parvez, M. *Dalton Trans.* **2003**, 2615.

(150) Tsurugi, H.; Matsuo, Y.; Yamagata, T.; Mashima, K. *Organometallics* **2004,** *23*, 2797.

(151) Hunter, W. E.; Harncir, D. C.; Bynum, V.; Pentilla, R. A.; Atwood, J. L. *Organometallics* **1995,** *14*, 789.

(152) Lauher, J. W.; Hoffmann, R. *J. Am. Chem. Soc.* **1976,** *98*, 1729.

(153) Kamer, P. C. J.; van Leeuwen, P. W. N. M.; Reek, J. N. H. *Acc. Chem. Res.* **2001,** *34*, 895.

(154) (a) Kranenburg, M.; van der Burgt, Y. E. M.; Kamer, P. C. J.; van Leeuwen, P. W. N. M.; Goubitz, K.; Fraanje, J. *Organometallics* **1995,** *14*, 3081. (b) Mora, G.; Deschamps, B.; van Zutphen, S.; Le Goff, X. F.; Ricard, L.; Le Floch, P. *Organometallics* **2007,** *26*, 1846.

(155) Sandee, A. J.; van der Veen, L. A.; Reek, J. N. H.; Kamer, P. C. J.; Lutz, M.; Spek, A. L.; van Leeuwen, P. W. N. M. *Angew. Chem. Int. Ed.* **1999**, 3231.

(156) Zuideveld, M. A.; Swennenhuis, B. H. G.; Boele, M. D. K.; Guari, Y.; van Strijdonck, G. P. F.; Reek, J. N. H.; Kamer, P. C. J.; Goubitz, K.; Fraanje, J.; Lutz, M.; Spek, A. L.; van Leeuwen, P. W. N. M. *Dalton Trans.* **2002**, 2308.

(157) Turculet, L.; McDonald, R. *Organometallics* **2007,** *26*, 6821.

(158) Wilson, D. J.; Sebastian, A.; Cloke, F. G. N.; Avent, A. G.; Hitchcock, P. B. *Inorg. Chim. Acta* **2003,** *345*, 89.

(159) Thorium. In *Gmelin Handbook of Inorganic and Organometallic Chemistry*, 8th ed.; Springer-Verlag: Berlin, Germany, 1993; Vol C4, 65.

(160) Rabinovich, D.; Scott, B. L.; Nielsen, J. B.; Abney, K. D. *J. Chem. Crystallogr.* **1999,** *29*, 243.

(161) Korobkov, I.; Gambarotta, S.; Yap, G. P. A. *Angew. Chem. Int. Ed.* **2003,** *42*, 4958.

(162) Barton, R. J.; Dabeka, R. W.; Shengzhi, H.; Mihichuk, L. M.; Pizzey, M.; Robertson, B. E.; Wallace, W. J. *Acta Crystallogr. Sect. C* **1983,** *39*, 714.

(163) Clark, D. L.; Watkin, J. G. *Inorg. Chem.* **1993,** *32*, 1766.

(164) Berg, J. M.; Clark, D. L.; Huffman, J. C.; Morris, D. E.; Sattelberger, A. P.; Streib, W. E.; Vandersluys, W. G.; Watkin, J. G. *J. Am. Chem. Soc.* **1992,** *114*, 10811.

(165) Athimoolam, A.; Gambarotta, S.; Korobkov, I. *Organometallics* **2005,** *24*, 1996.

(166) Barnhart, D. M.; Clark, D. L.; Grumbine, S. K.; Watkin, J. G. *Inorg. Chem.* **1995,** *34*, 1695.

(167) (a) Hitchcock, P. B.; Hu, J.; Lappert, M. F.; Tian, S. *J. Organomet. Chem.* **1997,** *536*, 473. (b) Domingos, A.; Marcalo, J.; Santos, I.; de Matos, A. P. *Polyhedron* **1990,** *9*, 1645. (c) Wedler, M.; Knosel, F.; Noltemeyer, M.; Edelman, F. T.; Behrens, U. *J. Organomet. Chem.* **1990,** *388*, 21.

(168) Mishin, V. Y.; Sidorenko, G. V.; Suglobov, D. N. *Radiokhimiya* **1986,** *28*, 293.

(169) Lugli, G.; Marconi, W.; Mazzei, A.; Paladino, N.; Pedretti, U. *Inorg. Chim. Acta* **1969,** *3*, 253.

(170) Kohler, E.; Bruser, W.; Thiele, K. H. *J. Organomet. Chem.* **1974,** *76*, 235.

(171) (a) Aizenberg, M.; Turculet, L.; Davis, W. M.; Schattenmann, F.; Schrock, R. R. *Organometallics* **1998,** *17*, 4795. (b) Cameron, T. M.; Gordon, J. C.; Michalczyk, R.; Scott, B. L. *Chem. Commun.* **2003**, 2282. (c) Reardon, D.; Conan, F.; Gambarotta, S.; Yap, G.; Wang, Q. Y. *J. Am. Chem. Soc.* **1999,** *121*, 9318.

(172) Fendrick, C. M.; Mintz, E. A.; Schertz, L. D.; Marks, T. J.; Day, V. W. *Organometallics* **1984,** *3*, 819.

(173) Zalkin, A.; Templeton, D. H.; Levanda, C.; Streitwieser, A. *Inorg. Chem.* **1980,** *19*, 2560.

(174) Straub, T.; Haskel, A.; Neyroud, T. G.; Kapon, M.; Botoshansky, M.; Eisen, M. S. *Organometallics* **2001,** *20*, 5017.

(175) (a) Ohff, A.; Kosse, O.; Baumann, W.; Tillack, A.; Kempe, R.; Gorls, H.; Burlakov, V. V.; Rosenthal, U. *J. Am. Chem. Soc.* **1995,** *117*, 10399. (b) Peulecke, N.; Ohff, A.; Kosse, P.; Tillack, A.; Spannenberg, A.; Kempe, R.; Baumann, W.; Burlakov, V. V.; Rosenthal, U. *Chem. Eur. J.* **1998,** *4*, 1852.

(176) (a) Brookhart, M.; Green, M. L. H.; Wong, L.-L. *Prog. Inorg. Chem.* **1988,** *36*, 1. (b) Scherer, W.; McGrady, G. S. *Angew. Chem. Int. Ed.* **2004**, 1782.

(177) Jaffart, J.; Cole, M. L.; Etienne, M.; Reinhold, M.; McGrady, J. E.; Maseras, F. *Dalton Trans.* **2003**, 4057.

(178) Fryzuk, M. D.; Johnson, S. A.; Rettig, S. J. *J. Am. Chem. Soc.* **2001,** *123*, 1602.

(179) Chen, Y. X.; Marks, T. J. *Organometallics* **1997,** *16*, 3649.

(180) Horton, A. D.; de With, J. *Organometallics* **1997,** *16*, 5424.

(181) Pellecchia, C.; Immirzi, A.; Grassi, A.; Zambelli, A. *Organometallics* **1993,** *12*, 4473.

(182) (a) Basuli, F.; Bailey, B. C.; Watson, L. A.; Tomaszewski, J.; Huffman, J. C.; Mindiola, D. J. *Organometallics* **2005,** *24*, 1886. (b) Basuli, F.; Bailey, B. C.; Huffman, J. C.; Mindiola, D. J. *Organometallics* **2005,** *24*, 3321.

(183) Weiss, E. *J. Organomet. Chem.* **1964,** *2*, 314.

(184) Markies, P. R.; Schat, G.; Akkerman, O. S.; Bickelhaupt, F.; Smeets, W. J. J.; Duisenberg, A. J. M.; Spek, A. L. *J. Organomet. Chem.* **1989,** *375*, 11.

(185) Vestergren, M.; Erikson, J.; Hakanson, M. *J. Organomet. Chem.* **2003,** *681*, 215.

(186) Viebrock, H.; Abeln, D.; Weiss, E. *Zeitsch. Natur. Section B* **1994,** *49*, 89.

(187) Teng, W. J.; Guino, -O. M.; Hitzbleck, J.; Englich, U.; Ruhlandt-Senge, K. *Inorg. Chem.* **2006,** *45*, 9531.

(188) (a) Toney, J. H.; Stucky, G. D. *Chem. Commun.* **1967**, 1168. (b) Spek, A. L.; Voorberge, P.; Schat, G.; Blomberg, C.; Bickelhaupt, F. *J. Organomet. Chem.* **1974,** *77*, 147.

(189) Butrus, N. H.; Eaborn, C.; Elkheli, M. N. A.; Hitchcock, P. B.; Smith, J. D.; Sullivan, A. C.; Tavakkoli, K. *Dalton Trans.* **1988**, 381.

(190) Caro, C. F.; Hitchcock, P. B.; Lappert, M. F.; Layh, M. *Chem. Commun.* **1998**, 1297.

(191) (a) Clark, D. L.; Frankcom, T. M.; Miller, M. M.; Watkin, J. G. *Inorg. Chem.* **1992,** *31*, 1628. (b) Rabinovich, D.; Chamberlin, R. M.; Scott, B. L.; Nielsen, J. B.; Abney, K. D. *Inorg. Chem.* **1997,** *36*, 4216. (c) Rabinovich, D.; Schimek, G. L.; Pennington, W. T.; Nielsen, J. B.; Abney, K. D. *Acta Crystallogr. Section C.* **1997,** *54*, 1794. (d) Aldaher, A. G. M.; Bagnall, K. W.; Benetollo, F.; Polo, A.; Bombieri, G. *J. Less-Common Met.* **1986,** *122*, 167.

(192) Tammiku-Taul, J.; Burk, P.; Tuulmets, A. *J. Phys. Chem.* **2004,** *108*, 133.

(193) (a) Fryzuk, M. D.; Jafarpour, L.; Kerton, F. M.; Love, J. B.; Patrick, B. O.; Rettig, S. J. *Organometallics* **2001,** *20*, 1387. (b) Erker, G.; Zwettler, R.; Kruger, C.; Hylakryspin, I.; Gleiter, R. *Organometallics* **1990,** *9*, 524. (c) Fryzuk, M. D.; Duval, P. B.; Rettig, S. J. *Can. J. Chem.* **2001,** *79*, 536, (d) Dohring, A.; Jensen, V. R.; Jolly, P. W.; Thiel, W.; Weber, J. C. *Organometallics* **2001,** *20*, 2234. (e) Liu, Y.; Zhong, Z.; Nakajima, K.; Takahashi, T. *J. Org. Chem.* **2002,** *67*, 7451. (f) Kirillov, E.; Lehmann, C. W.; Razavi, A.; Carpentier, J.-F. *Organometallics* **2004,** *23*, 2768. (g) Sugiyama, H.; Gambarotta, S.; Yap, G. P. A.; Wilson, D. R.; Thiele, S. K. H. *Organometallics* **2004,** *23*, 5054. (h) Klamo, S. B.; Wendt, O. F.; Henling, L. M.; Day, M. W.; Bercaw, J. E. *Organometallics* **2007,** *26*, 3018.

(i) Gaess, D.; Harms, K.; Pokoj, M.; Stolz, W.; Sundermeyer, J. R. *Inorg. Chem.* **2007,** *46*, 6688.

(194) The Chemistry of Organomagnesium Compounds. In *The Patai Series: The Chemistry of Functional Groups*, Rappoport, Z.; Mark, I., Eds. John Wiley & Sons: Chichester, England, 2008.

(195) (a) Sanchez-Barba, L. F.; Hughes, D. L.; Humphrey, S. M.; Bochmann, M. *Organometallics* **2006,** *25*, 1012. (b) Bambirra, S.; Perazzolo, F.; Boot, S. J.; Sciarone, T. J. J.; Meetsma, A.; Hessen, B. *Organometallics* **2008,** *27*, 704.

(196) (a) Fryzuk, M. D.; Haddad, T. S.; Rettig, S. J. *Organometallics* **1992,** *11*, 2967. (b) Evans, L. T. J.; Coles, M. P.; Cloke, F. G. N.; Hitchcock, P. B. *Dalton Trans.* **2007**, 2707.

(197) Hou, Z. M.; Wakatsuki, Y. *Coord. Chem. Rev.* **2002,** *231*, 1.

(198) Molander, G. A.; Romero, J. A. C. *Chem. Rev.* **2002,** *102*, 2161.

(199) Hong, S.; Marks, T. J. *Acc. Chem. Res.* **2004,** *37*, 673.

(200) (a) Cossee, P. *J. Catal.* **1964,** *3*, 80, (b) Arlman, E. J.; Cossee, P. *J. Catal.* **1964,** *3*, 99.

(201) Coates, G. W. *Chem. Rev.* **2000,** *100*, 1223.

(202) (a) Alt, H. G.; Koppl, A. *Chem. Rev.* **2000,** *100*, 1205. (b) McKnight, A. L.; Waymouth, R. M. *Chem. Rev.* **1998,** *98*, 2587.

(203) Gibson, V. C.; Spitzmesser, S. K. *Chem. Rev.* **2002,** *103*, 283.

(204) Labinger, J. A.; Hart, D. W.; Seibert, W. E.; Schwartz, J. *J. Am. Chem. Soc.* **1975,** *97*, 3851.

(205) Chen, E. Y. X.; Marks, T. J. *Chem. Rev.* **2000,** *100*, 1391.

(206) Reddy, S. S.; Sivaram, S. *Prog. Polym. Sci.* **1995,** *20*, 309.

(207) (a) Reddy, S. S.; Radhakrishnan, K.; Sivaram, S. *Polym. Bull.* **1996,** *36*, 165, (b) Sinn, H. *Macromol. Symp.* **1995,** *97*, 27.

(208) (a) Zurek, E.; Ziegler, T. *Organometallics* **2001,** *21*, 83. (b) Zurek, E.; Ziegler, T. *Inorg. Chem.* **2001,** *40*, 3279. (c) Zurek, E.; Woo, T. K.; Firman, T. K.; Ziegler, T. *Inorg. Chem.* **2000,** *40*, 361. (d) Thorn-Csanyi, E.; Dehmel, J.; Halle, O.; Sciborski, W. *Macromol. Chem. Phys.* **1994,** *195*, 3017. (e) Harlan, C. J.; Bott, S. G.; Barron, A. R. *J. Am. Chem. Soc.* **1995,** *117*, 6465. (f) Babushkin, D. E.; Semikoleova, N. V.; Zakharov, V. A.; Talsi, E. P. *Macromol. Chem. Phys.* **2000,** *201*, 558. (g) Ystenes, M.; Eilertsen, J. L.; Liu, J.; Ott, M.; Rytter, E.; Stovneng, J. A. *J. Polym. Sci.* **2000,** *38*, 3106. (h) Imhoff, D. W.; Simeral, L. S.; Sangokoya, S. A.; Peel, J. H. *Organometallics* **1998,** *17*, 1941.

(209) (a) Massey, A. G.; Park, A. J. *J. Organomet. Chem.* **1964,** *2*, 245. (b) Massey, A. G.; Park, A. J. *J. Organomet. Chem.* **1966,** *5*, 218.

(210) Yang, X.; Stern, C. L.; Marks, T. J. *J. Am. Chem. Soc.* **1991,** *113*, 3623.

(211) Yang, X. M.; Stern, C. L.; Marks, T. J. *J. Am. Chem. Soc.* **1994,** *116*, 10015.

(212) Chien, J. C. W.; Tsai, W. M.; Rausch, M. D. *J. Am. Chem. Soc.* **1991,** *113*, 8570.

(213) (a) Ewen, J. A. *J. Am. Chem. Soc.* **1984,** *106*, 6355. (b) Ewen, J. A.; Haspeslagh, L.; Atwood, J. L.; Zhang, H. M. *J. Am. Chem. Soc.* **1987,** *109*, 6544. (c) Ewen, J. A.; Jones, R. L.; Razavi, A.; Ferrara, J. D. *J. Am. Chem. Soc.* **1988,** *110*, 6255.

(214) Pedeutour, J.-N.; Radhakrishnan, K.; Cramail, H.; Deffieux, A. *Macromol. Rapid Commun.* **2001,** *22*, 1095.

(215) Piers, W. E.; Chivers, T. *Chem. Soc. Rev.* **1997,** *26*, 345.

(216) Casey, C. P.; Carepenetti, D. W. *J. Organomet. Chem.* **2002,** *642*, 120.

(217) Jia, L.; Yang, X.; Ishihara, A.; Marks, T. J. *Organometallics* **1995,** *14*, 3135.

(218) Pellecchia, C.; Immirzi, A.; Pappalardo, D.; Peluso, A. *Organometallics* **1994,** *13*, 3773.

(219) Horton, A. D. *Organometallics* **1996,** *15*, 2675.

(220) Bolton, P. D.; Clot, E.; Adams, N.; Dubberley, S. R.; Cowley, A. R.; Mountford, P. *Organometallics* **2006,** *25*, 2806.

(221) Lancaster, S. J.; Robinson, O. B.; Bochmann, M.; Coles, S. J.; Hursthouse, M. B. *Organometallics* **1995,** *14*, 2456.

(222) Bondi, A. *J. Phys. Chem.* **1964,** *68*, 441.

(223) (a) Scollard, J. D.; McConville, D. H. *J. Am. Chem. Soc.* **1996,** *118*, 10008. (b) Scollard, J. D.; McConville, D. H.; Payne, N. C.; Vittal, J. J. *Macromolecules* **1996,** *29*, 5241.

(224) (a) Hayes, P. G.; Piers, W. E.; Parvez, M. *J. Am. Chem. Soc.* **2003,** *125*, 5622. (b) Hayes, P. G.; Piers, W. E.; Parvez, M. *Chem. Eur. J.* **2007,** *13*, 2632.

(225) (a) Wang, Q.; Quyoum, R.; Gillis, D. J.; Tudoret, M.-J.; Jeremic, D.; Hunter, B. K.; Baird, M. C. *Organometallics* **1996,** *15*, 693. (b) Gillis, D. J.; Quyoum, R.; Tudoret, M.-J.; Wang, Q.; Jeremic, D.; Roszak, A. W.; Baird, M. C.

Organometallics **1996,** *15*, 3600. (c) Gillis, D. J.; Tudoret, M. J.; Baird, M. C. *J. Am. Chem. Soc.* **1993,** *115*, 2543.

(226) (a) Campbell, G. C.; Cotton, F. A.; Haw, J. F.; Schwotzer, W. *Organometallics* **1986,** *5*, 274. (b) Cotton, F. A.; Schwotzer, W. *Organometallics* **1985,** *4*, 942. (c) Cotton, F. A.; Schwotzer, W.; Simpson, C. Q. *Angew. Chem. Int. Ed.* **1986**, 637.

(227) (a) Cotton, F. A.; Schwotzer, W. *Organometallics* **1987,** *6*, 1275. (b) Cesari, M.; Pedretti, U.; Zazzetta, A.; Lugli, G.; Marconi, W. *Inorg. Chim. Acta* **1971,** *5*, 439. (c) Garbar, A. V.; Leonov, M. R.; Zakharov, L. N.; Struchkov, Y. T. *Russ. Chem. Bull.* **1996,** *45*, 451.

(228) (a) Maynadie, J.; Berthet, J. C.; Thuery, P.; Ephritikhine, M. *J. Am. Chem. Soc.* **2006,** *128*, 1082. (b) Maynadie, J.; Berthet, J. C.; Thuery, P.; Ephritikhine, M. *Organometallics* **2006,** *25*, 5603.

(229) (a) Bosch, B. E.; Erker, G.; Frohlich, R.; Meyer, O. *Organometallics* **1997,** *16*, 5449. (b) Arndt, S.; Spaniol, T. P.; Okuda, J. *Angew. Chem. Int. Ed.* **2003**, 5075. (c) Elvidge, B. R.; Arndt, S.; Zeimentz, P. M.; Spaniol, T. P.; Okuda, J. *Inorg. Chem.* **2005,** *44*, 6777. (d) Bambirra, S.; Meetsma, A.; Hessen, B. *Organometallics* **2006,** *25*, 3454. (e) Arndt, S.; Okuda, J. *Adv. Synth. Catal.* **2005,** *347*, 339.

(230) Guerin, F.; Stephan, D. W. *Angew. Chem. Int. Ed.* **2000,** *39*, 1298.

(231) Hayes, P. G.; Piers, W. E.; McDonald, R. *J. Am. Chem. Soc.* **2002,** *124*, 2132.

(232) Green, M. L. H.; Sassmannshausen, J. *Chem. Commun.* **1999**, 115.

(233) Ward, B. D.; Bellemin-Laponnaz, S.; Gade, L. H. *Angew. Chem. Int. Ed.* **2005,** *44*, 1668.

(234) Tredget, C. S.; Bonnet, F.; Cowley, A. R.; Mountford, P. *Chem. Commun.* **2005**, 3301.

(235) Hustad, P. D. *Science* **2009,** *325*, 704.

(236) Fawcett, E. W.; Gibson, R. O.; Perrin, M. W.; Patton, J. G.; Williams, E. G. Patent 471,590, 1937.

(237) (a) Ziegler, K.; Holzkamp, E.; Breil, H.; Martin, H. *Angew. Chem. Int. Ed.* **1955**, 426. (b) Natta, G. J. *J. Am. Chem. Soc.* **1955,** *77*, 1708.

(238) Muller, T. E.; Beller. *Chem. Rev.* **1998,** *98*, 675.

(239) Stanlake, L. J. E.; Schafer, L. L. *Organometallics* **2009,** *28*, 3990.

(240) (a) Giardello, M. A.; Conticello, V. P.; Brard, L.; Gagne, M. R.; Marks, T. J. *J. Am. Chem. Soc.* **1994,** *116*, 10241. (b) Li, Y. W.; Marks, T. J. *J. Am. Chem. Soc.* **1996,** *118*, 9295.

(241) (a) Bexrud, J. A.; Beard, J. D.; Leitch, D. C.; Schafer, L. L. *Org. Lett.* **2005,** *7*, 1959. (b) Ackermann, L.; Bergman, R. G. *Org. Lett.* **2002,** *4*, 1475. (c) Ackermann, L.; Bergman, R. G.; Loy, R. N. *J. Am. Chem. Soc.* **2003,** *125*, 11956.

(242) Hyunseok, K.; Lee, P. H.; Livinghouse, T. *Chem. Commun.* **2005**, 5205.

(243) (a) Dorta, R.; Egli, P.; Zurcher, F.; Togni, A. *J. Am. Chem. Soc.* **1997,** *119*, 10857. (b) Casalnuovo, A. L.; Calabrese, J. C.; Milstein, D. *J. Am. Chem. Soc.* **1988,** *110*, 6738, (c) Zhao, J.; Goldman, A. S.; Hartwig, J. F. *Science* **2005,** *307*, 1080.

(244) (a) Brunet, J.-J.; Commenges, G.; Niebecker, D.; Rosenberger, L. *J. Organomet. Chem.* **1994,** *469*, 221. (b) Beller, M.; Thiel, O. R.; Trauthwein, H.; Hartung, C. G. *Chem. Eur. J.* **2000,** *6*, 2513.

(245) Utsunomiya, M.; Kuwano, R.; Kawatsura, M.; Hartwig, J. F. *J. Am. Chem. Soc.* **2003,** *125*, 5608.

(246) (a) Pawlas, J.; Nakao, Y.; Kawatsura, M.; Hartwig, J. F. *J. Am. Chem. Soc.* **2002,** *124*, 3669. (b) Fadini, L.; Togni, A. *Chem. Commun.* **2003**, 30.

(247) (a) Kawatsura, M.; Hartwig, J. F. *J. Am. Chem. Soc.* **2000,** *122*, 9546. (b) Minami, T.; Okamoto, H.; Ikeda, S.; Tanaka, R.; Ozawa, F.; Yoshifuji, M. *Angew. Chem. Int. Ed.* **2001**, 4633. (c) Minami, T.; Okamoto, H.; Ikeda, S.; Tanaka, R.; Ozawa, F.; Yoshifuji, M. *Angew. Chem. Int. Ed.* **2001**, 4501. (d) Nettekoven, U.; Hartwig, J. F. *J. Am. Chem. Soc.* **2002,** *124*, 1166.

(248) Utsunomiya, M.; Hartwig, J. F. *J. Am. Chem. Soc.* **2003,** *125*, 14286.

(249) (a) Brunet, J.-J.; Cadena, M.; Chu, N. C.; Diallo, O.; Jacob, K.; Mothes, E. *Organometallics* **2004,** *23*, 1264. (b) Bender, C. F.; Widenhoefer, R. A. *J. Am. Chem. Soc.* **2005,** *127*, 1070.

(250) (a) Utsunomiya, M.; Hartwig, J. F. *J. Am. Chem. Soc.* **2004,** *126*, 2702. (b)Takaya, J.; Hartwig, J. F. *J. Am. Chem. Soc.* **2005,** *127*, 5756.

(251) (a) Li, K. L.; Hii, K. K. *Chem. Commun.* **2003**, 1132. (b) Shimada, T.; Yamamoto, Y. *J. Am. Chem. Soc.* **2002,** *124*, 12670.

(252) (a) Beesley, R. M.; Ingold, C. K.; Thorpe, J. F. *J. Chem. Soc. Chem. Commun.* **1915,** *107*, 1080. (b) Bruice, T. C.; Pandit, U. K. *J. Am. Chem. Soc.* **1960,** *82*,

5858. (c) Ingold, C. K. *J. Chem. Soc. Chem. Commun.* **1921,** *119*, 305. (d) Jung, M. E.; Gervay, J. *J. Am. Chem. Soc.* **1991,** *113*, 324. (e) Parrill, A. L.; Dolata, D. P. *J. Mol. Struct.* **1996,** *370*, 187.

(253) Crabtree, R. H., *Comprehensive Coordination Chemistry*. Pergamon: Oxford, England, 1987; Vol. 2, p 689.

(254) (a) Hlatky, G. G.; Crabtree, R. H. *Coord. Chem. Rev.* **1985,** *65*, 1. (b) Crabtree, R. H. *Acc. Chem. Res.* **1990,** *23*, 95.

(255) Rundle, R. E. *J. Am. Chem. Soc.* **1951,** *73*, 4172.

(256) Fagan, P. J.; Moloy, K. G.; Marks, T. J. *J. Am. Chem. Soc.* **1981,** *103*, 6959.

(257) Berthet, J. C.; Ephritikhine, M.; Lance, M.; Nierlich, M.; Vigner, J. *J. Organomet. Chem.* **1993,** *460*, 47.

(258) Katahira, D. A.; Moloy, K. G.; Marks, T. J. *Organometallics* **1982,** *1*, 1723.

(259) Burger, B. J.; Bercaw, J. E., Vacuum Line Techniques for Handling Air-Sensitive Organometallic Compounds. In *Experimental Organometallic Chemistry - A Practicum in Synthesis and Characterization*, American Chemical Society: Washington, D. C., 1987; 357, 79.

(260) Burchat, A. F.; Chong, J. M.; Nielsen, N. *J. Organomet. Chem.* **1997,** *542*, 281.

(261) Nowick, J. S.; Ballester, P.; Ebmeyer, F.; Rebek, J. *J. Am. Chem. Soc.* **1990,** *112*, 8902.

Appendix 1

For complete crystallographic data tables, atomic coordinates, anisotropic displacement parameters and metrical data, see word and cif files in the attached CD. Also included are the published and accepted works arising from this thesis.